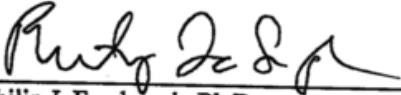


APPROVAL SHEET

Title of Dissertation: Genetic Analysis of Translational Accuracy in Mammalian Cells and Yeast

Name of Candidate: Ling Cao
Doctor of Philosophy, 2017

Dissertation and Abstract Approved: 
Philip J. Farabaugh, Ph.D.
Professor
Department of Biological Sciences

Date Approved: 11-28-17

ABSTRACT

Title of Document: GENETIC ANALYSIS OF TRANSLATIONAL ACCURACY IN MAMMALIAN CELLS AND YEAST

Ling Cao

Directed By: Dr. Philip James Farabaugh
Professor and Chair
Department of Biological Sciences

ABSTRACT

Misreading error frequency in mammalian cells during protein synthesis was reported to range from 10^{-2} to 10^{-5} error per codon. The studies reporting these error frequencies have measured several different errors by using various methods. To develop a more comprehensive understanding of translational accuracy in mammalian cells, I utilized a dual luciferase reporter system to quantify the frequency of all possible misreading events by tRNA_{UUU}^{Lys} in HEK293, *HeLa*, 22RV1 and NIH3T3 cell lines. The results showed that the pattern of misreading error frequency in these mammalian cell lines was similar but with distinct features. In addition, the difference in misreading error frequency at several error-prone codons by tRNA_{UUU}^{Lys} in mammalian cell lines did not vary as much as it did in *E. coli* and yeast. I speculate that roughly equivalent isoacceptor tRNA concentrations in mammalian cells led to this small variation in misreading frequency. In a second project, I developed a yeast *Saccharomyces cerevisiae* reporter system for errors by tRNA_{UUG}^{Gln} verifying that Gln 624 but not Gln 625 is an essential amino acid for β -galactosidase

that can be used to quantify misreading frequencies. Using this reporter system, I further tested the effects of tRNA modifications (mcm^5 and s^2 at U34, and ψ at position 38) on translational fidelity. Loss of these tRNA modifications decreased misreading frequency at some error-prone codons, suggesting that tRNA modifications do not always benefit protein translation. I have observed errors involving novel base pair mismatches in both of my projects, broadening the set of all possible misreading events.

GENETIC ANALYSIS OF TRANSLATIONAL ACCURACY IN MAMMALIAN CELLS
AND YEAST

By

Ling Cao

Dissertation submitted to the Faculty of the Graduate School of the
University of Maryland, Baltimore County, in partial fulfillment
of the requirements for the degree of
Doctor of Philosophy
2017

© Copyright by
Ling Cao
2017

Dedication

This dissertation is dedicated to my Mom, Dad and my husband, who always support and encourage me to believe in myself. Your affection and encouragement help me get such accomplishment and honor.

Acknowledgements

Thank you, Phil, for giving me the opportunity to work in the lab. Thanks for teaching me and guiding me through all these years. I have learned so much from you. Working with you is a great and valuable experience for me. Thanks for everything you have done especially for the last year of my Ph.D. Because of your patience and kindness, I was able to finish my dissertation while taking care of my new born baby.

I would like to thank my committee members, Dr. Miller, Dr. Willson, Dr. Li and Dr. Starz-Gaiano, for all your helpful and valuable comments and insight. Thank you for keeping me on the right track. Dr. Willson, thank you for all your suggestions and your cell lines. Dr. Li, thank you for teaching me techniques used in tissue cell experiment. Dr. Miller and Dr. Starz-Gaiano, thank you for all you help and being my readers.

To my lab mates, Kartik and Brooke, thank you for all your help. Brooke, thanks for helping with my experiments. Kartik, thanks for all the suggestions about my yeast projects. To my former lab mates, Arun, Monika, Nandini and Sush. Arun, thanks for being so supportive and a great friend. Nandini, Sush and Monika, thanks for teaching me many things in the lab.

To my Mom and my Dad, thank you for all your support and encouragement. Without you, I could never have such accomplishment. Thanks for being wonderful parents who taught me to trust myself, believe in hard work and never give up. You make me know that it's never too late to pursue my dream. I hope I have made you feel proud.

To my husband Chong, thank you for everything you have done since we met. I have been through so many things during these years and you are always there to support me. For me, you are more than just a husband. You are my good friend that I can share my things with you, and you are a good scientist that I can learn a lot from.

To my son Oliver, thank you for being a good baby though sometimes you barely sleep. It was hard to write this dissertation meanwhile nursing you and taking care of you. But I still love you so much. You are the best gift ever.

To my friends, Chiahua, Nusrat, Safae, Crystal, thank you for all your support. You are all ladies with strong souls. I have learned so much from all of you.

TABLE OF CONTENTS

Chapter I. INTRODUCTION	2
A. The Translational Machinery	2
1. An Overview of Errors.....	2
2. The Standard Genetic Code	3
3. Transfer RNA.....	4
4. tRNA modification.....	13
5. Ribosome	21
B. Translation initiation	38
C. Translation elongation.....	46
1. The Elongation Cycle	46
2. Maintenance of Fidelity During aa-tRNA selection	57
D. Translation Termination and Ribosome Recycling	66
1. Translation Termination.....	66
2. Ribosomal recycling	72
E. Translational errors.....	73
Chapter II. MATERIAL AND METHODS.....	82
A. Strains, Growth Conditions and Storage	82
1. Bacterial strains.....	82
2. Yeast strains	82
3. Mammalian cell lines	83
B. Transformation and transfection	84

1. Bacterial transformation.....	84
2. Yeast transformation.....	85
3. Mammalian cell transfection.....	86
C. DNA Oligonucleotides.....	87
D. Plasmids.....	87
1. Yeast Plasmids and Plasmid Constructions.....	87
2. Mammalian Plasmids and Plasmids Constructions.....	99
3. Plasmid DNA preparation and storage.....	99
E. Dual luciferase assay.....	100
1. Preparation of mammalian cell lysate.....	101
2. Dual luciferase assays.....	101
F. Beta-Glo Assay.....	102
G. Western Blotting.....	104
H. Northern dot blot analysis.....	105
I. Reverse Transcriptase Quantitative PCR.....	108
 Chapter III. AN INVESTIGATION OF THE MISREADING FREQUENCY IN DIFFERENT MAMMALIAN CELL LINES.....	 111
A. Introduction.....	111
B. Results.....	118
C. Discussion.....	154
 Chapter IV. INVESTIGATION OF MISREADING ERROR FREQUENCY BY GLUTAMINE TRANSFER RNA REPORTER SYSTEM IN YEAST <i>Saccharomyces cerevisiae</i>	 174
A. Introduction.....	174

B. Results	185
C. Discussion	207
Chapter V. LACK OF SOME tRNA MODIFICATIONS LEADS TO MORE ACCURATE PROTEIN TRANSLATION IN THE YEAST <i>Saccharomyces cerevisiae</i>	215
A. Introduction	215
B. Results	224
C. Discussion	234
Chapter VI. DISCUSSION	242
A. Discussion	242
B. Future direction	262
C. Summary	264
REFERENCES	265

LIST OF TABLES

Table I-1. The genetic code and distribution of cytoplasmic <i>S. cerevisiae</i> tRNAs	15
Table I-2. Eukaryotic initiation factors and their function	43
Table II-1. Site-directed mutagenesis oligonucleotides	88
Table II-2. RT-qPCR Oligonucleotides	93
Table II-3. Northern Dot-blot biotin labeled Oligonucleotides	93
Table II-4. DNA Sequencing Oligonucleotides	93
Table II-5. Yeast Plasmids	94
Table II-6. Site-directed mutagenesis PCR reaction mixture and amplification cycle	96
Table II-7. Mammalian Plasmids	98
Table II-8. Mammalian neomycin gene knockout plasmids	100
Table III-1. Misreading frequency by Lysine tRNA at near-cognate codons UUU	124
Table III-2. Comparison of potential error-prone codons in different cell lines	139
Table III-3. Normalized protein to qPCR expression ratio	143
Table III-4. Mutant activity relative to wild type in HEK293, HeLa, and 3T3 with and without the presence of G418	150
Table III-5. Alignment of the yeast and human ribosomal protein S23	153
Table III-6. Mutant activity relative to wild type in HEK293 cells transfected with wild type and mutant forms of RPS23	156
Table III-7. Tissue and cell type of each cell line	162
Table IV-1. All possible near-cognate mutations for <i>lacZ</i> Glutamine 624 and 625	187
Table IV-2. Misreading frequency by Gln tRNA at Q625 near-cognate codons	190

Table IV-3. Misreading frequency by Gln tRNA at Q624 near-cognate and synonymous non-cognate codons.....	194
Table IV-4. Mutant β -galactosidase activity relative to wild type by Gln tRNA.....	196
Table IV-5. The mutant β -galactosidase activity relative to wild type in the presence and absence of paromomycin	200
Table IV-6. Mutant β -galactosidase activity relative to wild type of Q624 by Gln tRNA.....	203
Table V-1. The genetic code and distribution of cytoplasmic <i>S. cerevisiae</i> tRNAs.....	216
Table V-2. Mutant form β -galactosidase activity relative to wild-type in the presence and absence of tRNA modifications.....	227
Table VI-1. All possible error-prone codons in the four mammalian cell lines	253

LIST OF FIGURES

Figure I-1. The standard genetic code	5
Figure I-2. The structure of tRNA.....	8
Figure I-3. The tRNA aminoacylation reaction.	10
Figure I-4. The tRNA identity set	12
Figure I-5. tRNA modifications and corresponding enzymes in yeast.	16
Figure I-6. Modification pathway for mcm ⁵ s ² U-containing tRNAs.	17
Figure I-7. View of the yeast ribosome.....	22
Figure I-8. The secondary structure of yeast ribosome RNA	25
Figure I-9. Intersubunit bridges.....	28
Figure I-10. Intersubunit rotation during translation.....	29
Figure I-11. Extension of r-proteins at the tRNA-binding sites on the small subunit and large subunit.....	32
Figure I-12. Conformational changes when a cognate tRNA binding.	34
Figure I-13. A cognate tRNA binding causes domain closure.....	36
Figure I-14. Near-cognate codon-anticodon mimics Watson-crick base pairing and interacts with 16S rRNA.....	37
Figure I-15. The active site of peptidyl transferase center in the 50S subunit.	39
Figure I-16. Schematic of the eukaryotic translation initiation.....	41
Figure I-17. Model of eukaryotic translation elongation pathway.	47
Figure I-18. An overview of ribosomal structure and mRNA translation.	49
Figure I-19. Peptide-bond formation on the ribosome.....	52
Figure I-20. Concerted proton-shuttle mechanism.....	54

Figure I–21. Model of the main steps of tRNA hybrid-states translocation cycle.	58
Figure I–22. Cognate, near-cognate and non-cognate codon-anticodon interaction.	59
Figure I–23. Kinetic proofreading model	62
Figure I–24. Watson-Crick-like geometry at the first and second position of codon-anticodon complex.....	67
Figure I–25. Schematic geometry of rare tautomeric states	68
Figure I–26. Model of eukaryotic translation termination and recycling pathways.	71
Figure III–1. Model of the firefly luciferase active site.....	119
Figure III–2. Near-cognate and synonymous non-cognate mutations for Lysine 529	121
Figure III–3. Mutant Fluc activities of near-cognate codons of K529 in different mammalian cell lines	123
Figure III–4. Variation in Fluc activity of K529 mutants in HEK293 cells	126
Figure III–5. Comparison of Fluc activity relative to wild type of synonymous near-cognate and non-cognate codons in HEK293 cells.....	127
Figure III–6. Mutant Fluc activity of K529 in <i>E. coli</i>	128
Figure III–7. Variation in mutant Fluc activity of K529 in yeast	131
Figure III–8. Comparison of Fluc activity relative to wild type of synonymous near-cognate and non-cognate codons in <i>HeLa</i> cells	132
Figure III–9. Comparison of Fluc activity relative to wild type of synonymous near-cognate and non-cognate codons in 22RV1 cells	134
Figure III–10. Comparison of Fluc activity relative to wild type of synonymous near-cognate and non-cognate codons in mouse 3T3 cells	135
Figure III–11. eRF1 expression level in different cell lines	140

Figure III–12. eRF3 expression level in different cell lines	141
Figure III–13. Effect of G418 on translational fidelity in HEK293 cells	145
Figure III–14. Effect of G418 on translational fidelity in <i>HeLa</i> cells	147
Figure III–15. Effect of G418 on translational fidelity in 3T3 cells	148
Figure III–16. Mutations in RPS23 only affected two near-cognate codons.....	155
Figure III–17. The pattern of tRNA misreading involves two types of base mismatches	158
Figure IV–1. A cognate tRNA binding causes domain closure	178
Figure IV–2. High residual F-luc activity of some K529 codons results from near-cognate decoding	181
Figure IV–3. Partial amino acid sequence of β -galactosidase	183
Figure IV–4. The high residual activity of some Q625 codons does not result from near-cognate decoding	188
Figure IV–5. β -galactosidase activity of Q624 near-cognate codons	192
Figure IV–6. High residual β -galactosidase activities of some Q624 codons result from near-cognate decoding	195
Figure IV–7. Aminoglycoside antibiotics increase misreading of a subset of near-cognate 624 codons	199
Figure IV–8. Mutations in <i>rps23</i> only affect β -galactosidase activities of Q624 termination codon mutants	202
Figure IV–9. Western blot of β -galactosidase of wild type and each mutant of Q624 and quantitative assay of western blot intensity	206
Figure V–1. tRNA modifications and responding enzymes in yeast	218
Figure V–2. Structure of some tRNA modifications	222

Figure V-3. Misreading frequency by Gln tRNA at near-cognate codons in the presence and absence of the formation of mcm ⁵	228
Figure V-4. Misreading frequency by Gln tRNA at near-cognate codons in the presence and absence of s ² U34 modification	230
Figure V-5. Misreading frequency by Gln tRNA at near-cognate codons in the presence and absence of pseudouridine 38 modification	232
Figure VI-1. The pattern of tRNA misreading in <i>E. coli</i> , yeast and mammalian cells	244
Figure VI-2. Geometry of canonical and rare tautomeric states	248
Figure VI-3. Illustration of the decoding principle	249
Figure VI-4. Mismatches leading to rejection of tRNA	251
Figure VI-5. Mismatches involved in mammalian cells and yeast cells	252

CHAPTER I

INTRODUCTION

Chapter I. INTRODUCTION

The genetic information is stored as DNA but is primarily expressed functionally as proteins. This expression involves two steps, transcription and translation, which are the central dogma of molecular biology. These steps must occur extremely accurately to preserve the integrity of genetic information. DNA replication and transcription happen with high fidelity because of proofreading activities that correct any incorporated wrong nucleotides. However, the maintenance of translational accuracy is more complicated.

Accurate protein translation largely depends on two processes. One is accurate aminoacylation of tRNA substrates and the other is correct decoding of the mRNA. An accurate decoding process requires selection of the correct tRNA substrate and maintenance of the correct translational reading frame. The most error-prone step in the whole central dogma seems to happen during the decoding of an mRNA sequence into protein, particularly the process of selecting a correct tRNA.

In this study, I attempt to measure a set of translational errors (misreading errors) in multiple mammalian cell lines and *Saccharomyces cerevisiae*. This study was finished in eukaryotes so most of the background information presented in the introductory chapter refers to eukaryotes.

A. The Translational Machinery

1. An Overview of Errors

During the process of transcription and translation, errors do occur in different forms. First, errors could happen during DNA replication but DNA polymerase enzymes catalyze the process with high fidelity so that errors take place at a rate of ~1 per every 100,000 nucleotides. Besides, some of the errors are corrected immediately during DNA replication by a process called proofreading,

and some are corrected after DNA replication via a process called mismatch repair. Therefore, the mutation rate was reported as low as 10^{-9} (Johnson et al., 2000). Alternatively, errors could occur during transcription. However, transcription is also a highly accurate process with an estimated error frequency of $\sim 10^{-5}$ per incorporated nucleotide (Libby & Gallant, 1991), because RNA polymerases also possess the function of proofreading that is stimulated by an incorrectly incorporated nucleotide and it subsequently removes the wrong nucleotides (Sydow & Cramer, 2009). Or errors could happen during protein translation. The ultimate amino acid sequence will be determined by the genetic information in the form of an mRNA sequence. The process of protein translation requires many components, such as genetic code, mRNA, tRNA and ribosome, and they are called the translational machinery. The process of translation is complicated and can be divided into three major steps, initiation, elongation and termination.

2. The Standard Genetic Code

A set of three nucleotides composed of a combination of adenosine (A), guanosine (G), cytidine (C) and uridine (U) was hypothesized to account for encoding 20 amino acids (Crick et al., 1961). The deciphering of the triplets is called the genetic code (Figure I-1). There are 64 codons in total, and they are displayed in a separate 'codon box.' Each codon box has four three-letter codes. Sixty-one of them are sense codons, which are recognized by aminoacyl-tRNA for decoding amino acids. Three codons, UAA, UAG, and UGA, are termination codons that are recognized by translational termination factors (Agris, 2004).

The genetic code is degenerate because the universal genetic code has 61 codons for 20 amino acids. Therefore, most amino acids are encoded by more than one codon. Eight of the codon boxes code for only one amino acid, so that they are 4-fold degenerate (Figure I-1). Other codon boxes

code for two different amino acids, which are 'split box' (e.g., asparagine and lysine, or histidine and glutamine). These amino acids have 2-fold degenerate codons. Codon boxes such as isoleucine are 3-fold degenerate. Two amino acids, methionine, and tryptophan have only one codon (Figure I-1). A series of ribosome binding assays as well as *in vitro* translation of polyribonucleotides have determined the relationship between each amino acid and its particular codon(s) (Nirenberg & Matthaei, 1961; Nirenberg & Leder, 1964; Brimacombe et al., 1965)(M. W. Nirenberg & Matthaei, 1961)(M. W. Nirenberg & Matthaei, 1961)(M. W. Nirenberg & Matthaei, 1961)(M. W. Nirenberg & Matthaei, 1961); Nirenberg et al., 1965; Nishimura et al., 1965).

3. Transfer RNA

Transfer RNAs are the fundamental molecules of translation machinery. They deliver amino acids to the ribosome to decode the genetic information based on a messenger RNA (mRNA) into a corresponding polypeptide chain (Marina V Rodnina & Wintermeyer, 2011). Such function of tRNA as an adaptor molecule makes it have a central role in translation.

a. tRNA structure

Yeast alanine tRNA was the first completely sequenced tRNA (Holley et al., 1965). Holley et al. (1965) found that the alanine tRNA is composed of 77 nucleotides (Holley et al., 1965). Now it is well known that eukaryotic tRNAs have a length of 73-90 nucleotides (nt) and adopt a secondary

		SECOND								
		U		C		A		G		
FIRST	U	UUU	Phe	UCU	Ser	UAU	Tyr	UGU	Cys	U
		UUC	Phe	UCC	Ser	UAC	Tyr	UGC	Cys	C
		UUA	Leu	UCA	Ser	UAA	Stop	UGA	Stop	A
		UUG	Leu	UCG	Ser	UAG	Stop	UGG	Trp	G
	C	CUU	Leu	CCU	Pro	CAU	His	CGU	Arg	U
		CUC	Leu	CCC	Pro	CAC	His	CGC	Arg	C
		CUA	Leu	CCA	Pro	CAA	Gln	CGA	Arg	A
		CUG	Leu	CCG	Pro	CAG	Gln	CGG	Arg	G
	A	AUU	Ile	ACU	Thr	AAU	Asn	AGU	Ser	U
		AUC	Ile	ACC	Thr	AAC	Asn	AGC	Ser	C
		AUA	Ile	ACA	Thr	AAA	Lys	AGA	Arg	A
		AUG	Met	ACG	Thr	AAG	Lys	AGG	Arg	G
	G	GUU	Val	GCU	Ala	GAU	Asp	GGU	Gly	U
		GUC	Val	GCC	Ala	GAC	Asp	GGC	Gly	C
		GUA	Val	GCA	Ala	GAA	Glu	GGA	Gly	A
		GUG	Val	GCG	Ala	GAG	Glu	GGG	Gly	G

THIRD, WOBBLE

Figure I-1. The standard genetic code

The genetic code is displayed in different boxes to show its degeneracy. The splitting boxes, which contain two different amino acids, are shown in gray. Fourfold degenerate codons are shown in yellow. Six-fold degenerate codons are shown in blue. The threefold degenerate codon of Isoleucine (Ile) is shown in green. The single codons for Met and Trp are in white color. The three termination codons are shown in red color (Agris et al., 2007).

structure (termed clover leaf) (Figure I-2). There are several domains in the tRNA secondary structure. The aminoacyl acceptor stem with a 5' phosphate end and a 3' terminal CCA sequence includes nucleotides 74 to 76. The D-arm has a modified nucleotide dihydrouridine. The anticodon arm consists of a 5 base pairs (bp) stem and 7 nucleotide loop. This loop is called the anticodon stem loop or ASL. The anticodon stem loop has a 3-nucleotide anticodon from position 34 to position 36. The variable region, starting at residue 44, can be 4-23 nucleotides (nt) long. The three-dimensional structure of tRNA is shown in Figure I-2. The figure shows a crystal structure of yeast tRNA^{Phe} (Kim et al., 1972). The tRNA folds into a 3-dimensional structure (L-shaped tertiary structure) when the acceptor stem stacks on the T stem to form one arm. Meanwhile, the D stem stacks on the anticodon stem to form another arm (Kim et al., 1972; Harry F. Noller, 2005). The area consisting of the T and the D loops at the junction of the two arms is termed the tRNA “elbow” (Figure I-2)

b. Aminoacylation and Aminoacyl-tRNAs

Each tRNA is attached to a particular amino acid. The process termed aminoacylation requires aminoacyl-tRNA synthesis enzyme.

The process of amino acids attaching to their respective tRNAs is called aminoacylation (or tRNA charging). These tRNAs are called aminoacyl-tRNAs (aa-tRNAs), which are the substrate molecules for protein translation. Aminoacyl-tRNA synthetases (ARSs) are the enzymes that are responsible for attaching an amino acid to the 3' end of a tRNA. There are twenty different AARSs. Each AARS recognizes one particular amino acid and attaches this amino acid to the correct tRNA(s). All the tRNA molecules that are charged with the same amino acid are called

isoaccepting tRNAs (Behura & Severson, 2011). There are two distinct classes of ARSs, class I

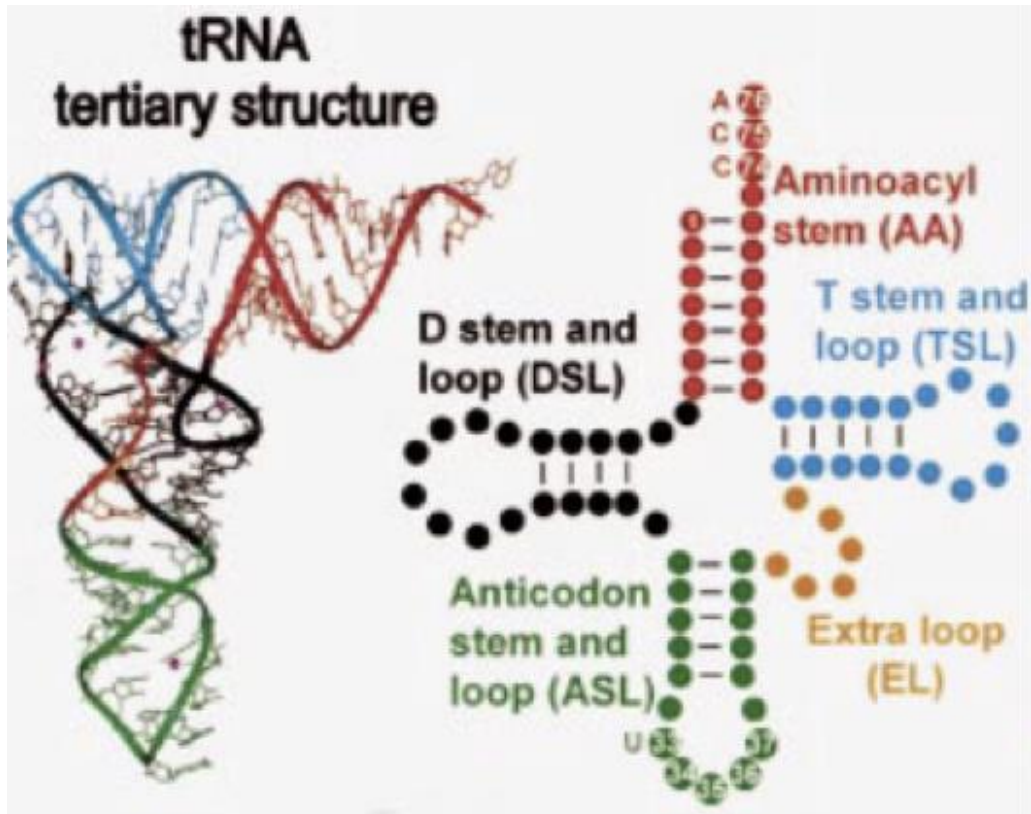


Figure I-2. The structure of tRNA.

The left is a three-dimensional structure of yeast tRNA^{Phe} and the right shows the cloverleaf secondary structure with color coded to identify the structural domains of the crystal structure. The amino acid accepting stem is in red. The dihydrouridine stem and loop domain (DSL) is in black. The anticodon stem and loop domain (ASL) is in green. The extra loop (EL) is in gold. And the ribothymidine, or TC, stem and loop (TSL) are shown in light blue (Agris, 2004)

and class II. Class I enzymes are monomeric and aminoacylate the 2' hydroxyl of the terminal adenosine of the correct tRNAs. Class II ARSs are typically dimers and tetramers and attach the amino acid to the 3' hydroxyl of the terminal adenosine of the correct tRNAs (Ibba & Soll, 2001, 2004; Abbott et al., 2014).

Typically, aminoacylation has two steps: ATP-dependent amino acid activation and transfer of the amino acid onto a tRNA (Pang et al., 2014) (Figure I-3). In the first step, the correct amino acid is attached to one molecule of ATP to form aminoacyl adenylate (aminoacyl-AMP) and inorganic pyrophosphate (Equation 1) (Figure I-3). In the next step, the amino acid is then transferred to either the 2' or 3' hydroxyl on the 3' CCA end of the corresponding tRNAs, generating the product aa-tRNA (Equation 2) (Figure I-3) (Hendrickson & Schimmel, 2003; Pang et al., 2014).

Some AARSs cannot precisely recognize the correct amino acid (cognate amino acid) only via the first step. Occasionally, a AARS will active the incorrect (non-cognate) amino acid, resulting in mischarge of the wrong amino acid onto the tRNA. AARs are responsible for selecting both tRNAs and amino acids. Therefore, AARSs play a critical role in corrective editing mechanisms to ensure the accuracy during aminoacylation.

Fersht hypothesized that besides the aminoacylation active site (synthetic site), some AARSs also have a secondary editing site (hydrolytic site). This site serves to correct errors and maintain higher specificity (Fersht, 1977). This corrective editing model is called double sieve (Fersht & Dingwall, 1979). In this double sieve model, the aminoacylation active site serves as the first sieve, the coarse sieve to exclude larger or significantly dissimilar amino acid but let smaller amino acid to go through. The second hydrolytic site serves as the fine sieve to bind to mischarged amino acid for hydrolysis, blocking the correctly charged tRNAs to release them to

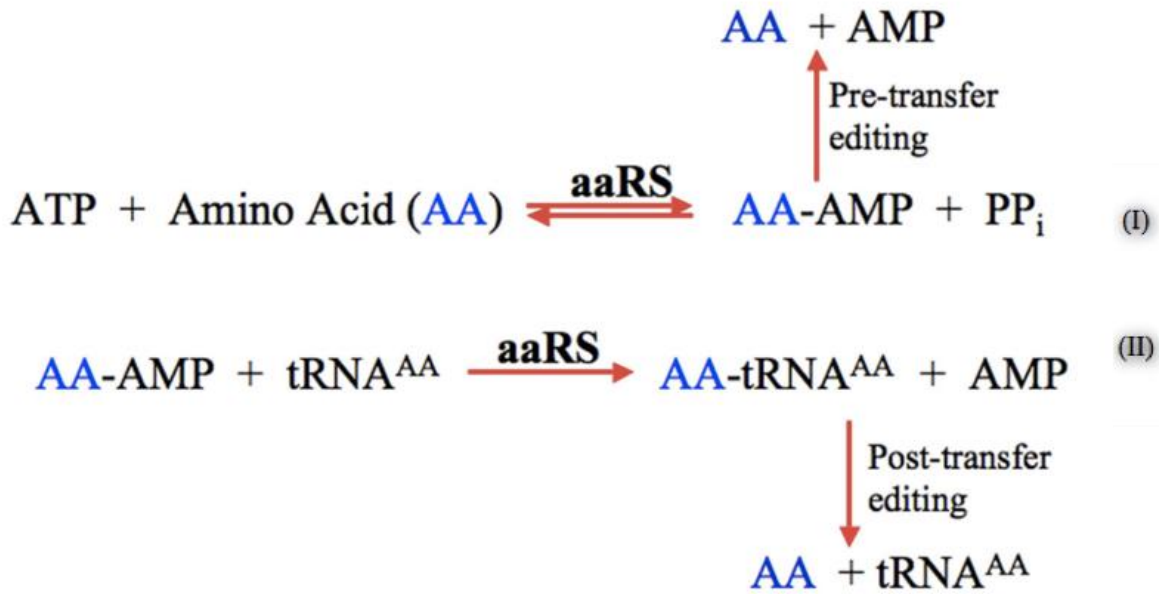


Figure I-3. The tRNA aminoacylation reaction.

Amino acid activation shows in equation (I). An amino acid (AA) is activated with ATP by its specific aminoacyl-tRNA synthetase enzyme (aaRS) to form an intermediate, aminoacyl adenylate and pyrophosphate (PP_i). An incorrect intermediate can be hydrolyzed via pre-transfer editing. After the AA is transferred to the tRNA, the reaction releases AMP and aminoacyl-tRNA (aa-tRNA) (Equation II). The wrong aa-tRNA will be hydrolyzed by post-transfer editing.

bind to elongation factors. For example, the isoleucyl-tRNA synthetase rejects valine (Val) via this double sieve model (Fersht, 1977). In the first sieve, the amino acid active site would allow smaller non-cognate amino acids to bind. Therefore, the coarse sieve would allow the formation of Ile-AMP, Val-AMP, Ile-tRNA^{Ile}, and Val-tRNA^{Ile}. The second editing site, the fine sieve, is structurally different from the synthetic site, meaning the amino acid binding pocket would be smaller. Thus, the pocket would recognize the isopropyl side chain of valine but rule out the larger isobutyl group of isoleucine. Then the second editing site would hydrolyze both Val-AMP and Val-tRNA^{Ile}, only leaving Ile-AMP and Ile-tRNA^{Ile} (Fersht, 1977; Fersht & Dingwall, 1979).

The AARSs correct aminoacylation by two pathways: pre-transfer and post-transfer of charging to the tRNA (Figure I-3) (Pang et al., 2014). Pre-transfer editing hydrolyzes the aminoacyl-adenylate to release the free amino acid and AMP (Baldwin & Berg, 1966). By comparison, post-transfer editing targets the mischarged tRNA for hydrolysis to yield free tRNA and incorrect amino acid (Figure I-3)(Eldred & Schimmel, 1972).

AARSs have either a pre-transfer editing or post-transfer editing domain as the primary editing mechanism (Fersht, 1977; Fersht & Dingwall, 1979; Englisch et al., 1986; Williams & Martinis, 2006; Martinis & Boniecki, 2010). In some cases, the AARSs possess the second editing to maintain aminoacylation fidelity in the failure of the primary editing pathway. For example, when the post-transfer editing site of *E. coli* LeuRS is abolished, the enzyme activated a pre-transfer editing pathway to maintain the overall fidelity of aminoacylation (Boniecki et al., 2008).

AARSs also recognize their correct tRNAs from a pool containing all other tRNAs via identity determinants within the tRNA (Hale et al., 1997) (Figure I-4). In most tRNAs, the most distal residues, N73, and the three anticodon nucleotides are identity determinants (Giegé et al., 1998;

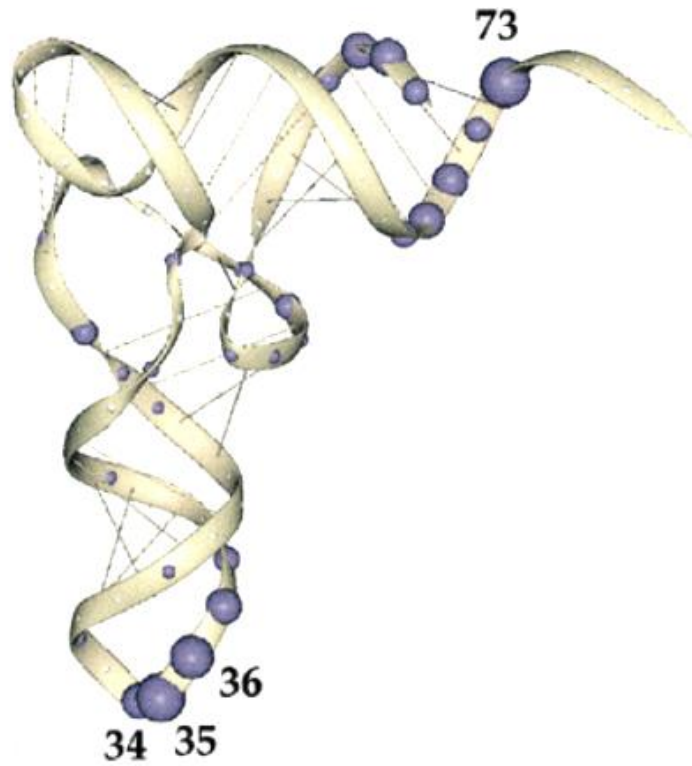


Figure I-4. The tRNA identity set

Aminoacyl-tRNA synthetase enzymes recognize particular nucleotides of their isoacceptor tRNA substrate. This is termed the tRNA identity set (Giegé et al., 1998).

Hendrickson & Schimmel, 2003). Modified nucleotides in the anticodon loop, such as L34 in tRNA^{Ile}, s⁴U34 in tRNA^{Glu}, and mnm⁵s²U34 in tRNA^{Lys}, I34 in yeast tRNA^{Ile}, also play a pivotal role in recognition by AARSs (Muramatsu et al., 1988; Senger et al., 1997; Giegé et al., 1998). In addition, anticodon stem base pairs and core positions around 21nts, including positions in the variable and D stem, are also determinants for tRNA recognition by AARSs (Nureki et al., 1994; Giegé et al., 1998; Hendrickson & Schimmel, 2003). Moreover, structural elements and sequence elements that are specific to tRNAs are also essential for AARS recognition. For example, a G3·U70 base pair in tRNAs^{Ala}, a G1·C73 base pair in tRNA^{His}, a G15·G48 base pair in tRNA^{Cys}, and the large variable loop of tRNA^{Ser} all contribute to recognition of tRNAs by their corresponding AARSs (McClain & Foss, 1988; Hou & Schimmel, 1989; Himeno et al., 1989; Himeno et al., 1990; Hou, Westhof, & Giegé, 1993).

4. tRNA modification

Posttranslational modification is a critical step for matured tRNAs. Modifications are highly conserved especially for those in the vicinity of anticodon. These modifications are essential for the decoding process.

The universal genetic code has 61 codons for 20 amino acids, and three stop codons, meaning that amino acids are encoded by more than one codon (Agris, 2004). This is termed degeneracy (El Yacoubi et al., 2012a). The 61 codons plus three stop codons are in degenerate codon family boxes (Table I-1). In these boxes, synonymous codons code for the same amino acid. There are eight unsplit boxes (all codons code for the same amino acid), five two-split boxes (the two purine-ending codons code for one amino acid and the two pyrimidine-ending codons encode for another, such as Gln/His), and three special codon boxes (Ile/Met, Tyr/Stop, and Cys/Stop Trp) (El Yacoubi

et al., 2012a) (Table I-1). In the yeast *Saccharomyces cerevisiae*, only 42 tRNAs decode 61 codons (Phizicky & Hopper, 2010). The ability of tRNA to decode more than one codon is facilitated by post-transcriptional modification of transfer RNA. Some modifications at wobble positions expand the possibility of codon-anticodon interaction and some restrict it (Agris, 2004).

Posttranscriptional modification occurs in transfer RNAs from all organisms (Björk et al., 2007). As many as 80 modifications have been reported (El Yacoubi et al., 2012). tRNA modifications can play many roles. Many modifications within the core of the tRNA play an essential role in tRNA structural stabilization; loss of these modifications can cause rapid degradation of hypomodified tRNAs (Phizicky & Alfonzo, 2010). The most diverse and complicated chemical structures are found in the anticodon stem loop or the vicinity. The two most frequently modified positions in tRNA are position 34, which is the wobble position, and position 37, which is the nucleotide next to and 3' of the anticodon (El Yacoubi et al., 2012) (Figure I-5).

a. tRNA modification pathways

Instead of uridine, 11 of 42 yeast tRNAs (26%) have modified U₃₄ with 5-carboxymethyl derivatives (xcm⁵U). The process of generating mcm⁵U and mcm⁵s²U is a very complicated pathway, which involves more than 15 gene products for mcm⁵ addition and 11 gene products for s² addition (Ranjan & Rodnina, 2016) (Figure I-6). Generation of the cm⁵U intermediate involves a complex of 13 proteins including the elongator complex (El1p-El6p), killer toxin-insensitive gene products (Ktillp-Ktil4p), suppressor of initiation of transcription (Sit4p) and associated factors (Sap185p, Sap 190p) together with acetyl-CoA. In the following step, cm⁵U is converted to mcm⁵U, in which process relies on tRNA-methyltransferase Trm9p and Trm112p as well as S-

Table I-1. The genetic code and distribution of cytoplasmic *S. cerevisiae* tRNAs

U			C			A			G				
codon	anticodon	amino acid	codon	anticodon	amino acid	codon	anticodon	amino acid	codon	anticodon	amino acid		
UUU	-	Phe	UCU	IGA	Ser	UAU	-	Tyr	UGU	-	Cys		
UUC	GmAA	Leu	UCC	-		UAC	GψA	n.a.	UGC	GCA	n.a.		
UUA	ncm⁵UmAA		UCA	ncm⁵UGA		UAA	-		UGA	-	UGG	CmCA	Trp
UUG	m ⁵ CAA		UCG	CGA		UAG	-		UGG	CmCA	Trp		
CUU	-	Leu	CCU	AGG	Pro	CAU	-		His	CGU	ICG	Arg	
CUC	GAG		CCC	-		CAC	GUG	Gln	CGC	-			
CUA	UAG		CCA	ncm⁵UGG		CAA	mcm⁵s²UUG		CGA	-			
CUG	-		CCG	-		CAG	CUG		CGG	CCG			
AUU	IAU	Ile	ACU	IGU	Thr	AAU	-		Asn	AGU	-	Ser	
AUC	-		ACC	-		AAC	GUU	Lys	AGC	GCU			
AUA	ψAψ		ACA	ncm⁵UGU		AAA	mcm⁵s²UUU		AGA	mcm⁵UCU	Arg		
AUG	CAU		ACG	CGU		AAG	CUU		AGG	CCU			
GUU	IAC	Val	GCU	IGC	Ala	GAU	-		Asp	GGU	-	Gly	
GUC	-		GCC	-		GAC	GUC	Glu	GGC	GCC			
GUA	ncm⁵UAC		GCA	ncm⁵UGC		GAA	mcm⁵s²UUC		GGA	mcm⁵UCC			
GUG	CAC		GCG	-		GAG	CUC		GGG	CCC			

The anticodon sequences of the 42 different tRNA species (1 initiator and 41 elongator tRNAs) are indicated. For anticodons with an uncharacterized RNA sequence, the primary sequence is shown. The initiator and elongator tRNA^{Met} species have identical anticodon sequences. The wobble rules suggest that an inosine (I34) residue allows pairing with U, C, and sometimes A. A tRNA with a G or its 2'-O-methyl derivative (Gm) at the wobble position should read U- and C-ending codons. Presence of a C34 residue or its 5- methyl (m⁵C) or 2'-O-methyl (Cm) variant should only allow pairing with G. The pseudouridine (C)-containing tRNA^{Ile} is presumably unable to pair with the methionine AUG codon. The anticodons containing mcm⁵U, mcm⁵s²U, ncm⁵U and ncm⁵Um derivatives are shown in bold (Johansson et al., 2008).

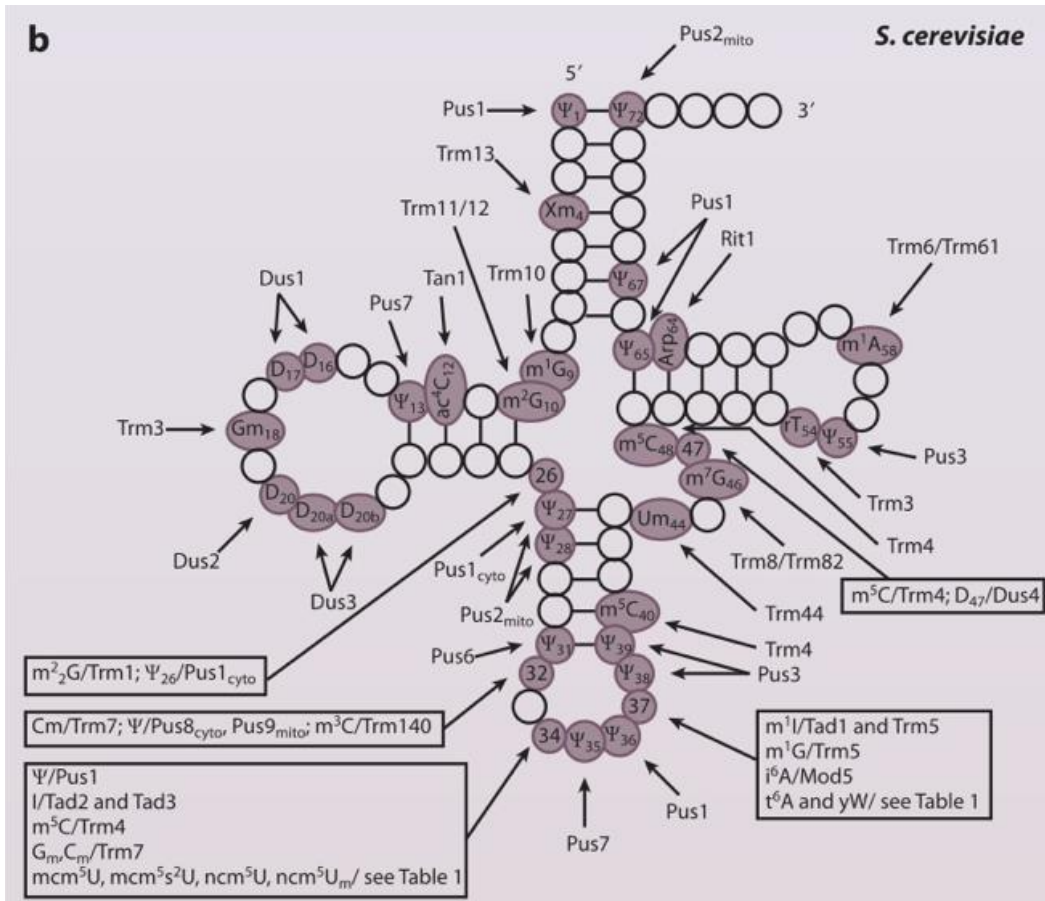


Figure I–5. tRNA modifications and corresponding enzymes in yeast.

Saccharomyces cerevisiae cytoplasmic and mitochondrial tRNAs. Corresponding accession numbers and references can be found in the SGD database (El Yacoubi et al., 2012).

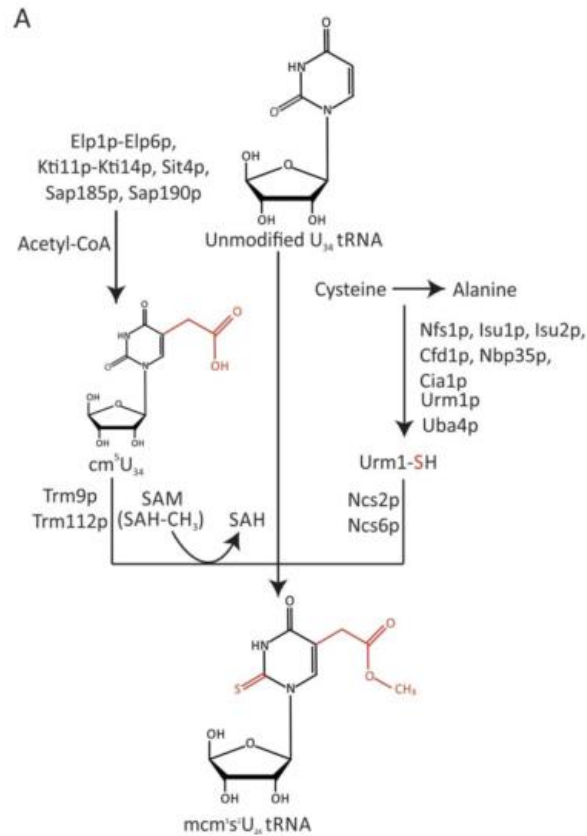


Figure I–6. Modification pathway for mcm^5s^2U -containing tRNAs.

Proteins involved in mcm^5 modification are shown on the left and proteins required for s^2 modification are shown on the right. Acetyl-CoA acts as a donor for cm^5 , and SAM as methyl donor to form mcm^5U_{34} . Cysteine acts as sulfur donor in s^2 modification. Modified side groups are shown in red (Ranjan & Rodnina, 2016)

adenosyl methionine (SAM) as the methyl donor (Karlsborn et al., 2014; L etoquart et al., 2015). Eventually, ten more proteins are required in addition of s²U. These products include ubiquitin-related modifier 1 (Urm1p) together with its activating protein, Uba4p, and other associated gene products (Leidel et al., 2009).

b. tRNA modification and decoding

Post-transcriptional modifications at the wobble positions play a pivotal role in the codon-anticodon decoding process (Agris et al., 2007). In a correct decoding process, the first and second base of the codon and the third and second base of the anticodon interact following the Watson-Crick rules (A:U, U:A, G:C, C:G). Crick proposed in his wobble hypothesis that the third base of the codon and the first base of the anticodon (wobble position) is relatively less constrained to expand tRNA recognition of codons in protein translation (Crick, 1966) so that some tRNAs can read more than one codon in decoding the 61 amino acid codons. This wobble hypothesis explains how tRNAs recognize more than one codon. The variety of hypermodified nucleotides occurring at the wobble position and position 37 of the anticodon enables the flexibility of base pairing during decoding (Gustilo et al., 2008; El Yacoubi et al., 2012). Some post-transcriptional modifications at the wobble position expand the capability of base pairing while some restrict the wobble position base-pairing (Persson, 1993). For example, inosine (I), a modified A, expands wobble position base-pairing. Adenosine would only base pair with U while inosine can recognize A, U, and C (Crick, 1966). 5-methoxycarbonylmethyl-uridine (mcm⁵U) and 5-methoxycarbonylmethyl-2-thiouridine (mcm⁵s²U) modification are thought to restrict a tRNA to only recognize A instead of A and G when the U is unmodified (Agris et al., 2007). On the other hand, carboxymethoxyuridine (cmo⁵U) expands the ability of tRNA decoding. Carboxymethoxyuridine can base pair with A, G,

and U while unmodified uridine only pairs with A and G (Björk, 1995). In addition, modifications at position 37 can indirectly affect decoding by stabilizing adjacent codon-anticodon pairing. For example, a tRNA with 2-methylthio-N6-isopentenyladenosine (ms^2i^6A37) modification at position 37 recognizes codons beginning with A; this modification is thought to stabilize the weak A1•U36 pairing. Loss of such a modification reduces the efficiency of decoding (Björk & Hagervall). Emerging evidence demonstrates that lack of some tRNA modifications can affect protein production or translational accuracy (Lyko & Tuorto, 2016; Manickam et al., 2016).

c. tRNA modification and human disease

Due to the importance of tRNA modifications in translational accuracy as well as tRNA stability (Davis, 1995; Tükenmez et al., 2015; Manickam et al., 2016), it is conceivable that loss of these modifications would have a profound influence on protein synthesis. Emerging evidence indicates that loss of tRNA modifications and the enzymes synthesizing these modifications may play critical roles in human diseases such as neurological disorders (Bednářová et al., 2017).

Yeast tRNA methyltransferase 7 (*TRM7*) encodes a methyltransferase targeting position 32 and 34 on tRNA^{Leu}, tRNA^{Phe}, and tRNA^{Trp}. The FtsJ RNA methyltransferase homolog 1 (*FTSJI*) gene has been suggested as the closest human homolog to *TRM7* (Feder et al., 2003; Towns & Begley, 2012). In humans, *FTSJI* is located on the X chromosome. Mutant forms of *FTSJI* gene have been suggested to be associated with non-syndromic X-linked mental retardation (Freude et al., 2004; Ramser et al., 2004; Takano et al., 2008). Northern blot analysis of normal human tissues showed that wild type *FTSJI* is mostly expressed in fetal brain (Freude et al., 2004). Therefore, this gene has been suggested to play an essential role in the developing brain.

Familial dysautonomia (FD) is a complicated neurological disorder that affects the autonomic and sensory nervous system (Slaugenhaupt et al., 2002). Many studies suggested that mutations in genes encoding the subunits of the Elongator complex are associated with FD (Anderson et al., 2001; Slaugenhaupt et al., 2001; Close et al., 2006). Elongator complex is required for the synthesis of 5-methoxycarbonylmethyl-2-thiouridine (mcm⁵s²U) (Huang et al., 2005; Karlsborn et al., 2014). Defects in this complex were demonstrated to show many phenotypes, which are resulting from the lack of formation of 5-methoxycarbonylmethyl-2-thiouridine (mcm⁵s²U) at the position 34 of tRNAs (Phizicky & Hopper, 2010).

The human Elongator complex is composed of IκB kinase complex-associated protein [IKBKAP (yeast Elp1p)], Stat3-interacting protein [StIP1 (yeast Elp2p)], Elongator protein 3 homolog (ELP3), ELP4, and two unidentified polypeptides (Hawkes et al., 2002). Two mutations in the human *IKBKAP* gene have been identified as causative of FD (Anderson et al., 2001; Slaugenhaupt et al., 2001). One is a single nucleotide change, leading to a truncated protein. The other mutation is a missense mutation causing an arginine to proline substitution, which was predicted to eliminate a threonine phosphorylation site in IKBKAP. Another study found a mutation changing proline to leucine in the *IKBKAP* protein (Leyne et al., 2003). Mutations of the *C. elegans* enzyme catalyzing thiolation at the wobble position (*tuc-1*), cause developmental defects in combination with mutants of ELPC1 and ELPC3 (homologs of IKAP and ELP3, respectively) (Chen et al., 2009).

Elongator has been demonstrated to affect α-tubulin acetylation in neurons suggesting that Elongator might be critical for other neurological disorders such as Huntington's, Alzheimer's, Parkinson, and amyotrophic lateral sclerosis (ALS) (Nguyen et al., 2010). Indeed, Elp3, one

subunit of the Elongator complex, is associated with amyotrophic lateral sclerosis (ALS) (Nguyen et al., 2010). The previous study showed that knockdown of Elp3 in zebrafish caused motor axonal abnormalities (Simpson et al., 2009).

All of evidence above indicates that tRNA modifications are essential in human pathologies but the answers of many questions remain unclear. What is the actual biological role of the involved tRNA modifications in these human diseases? One possibility would link tRNA modification induced diseases with protein translational fidelity because tRNA modifications have been shown to play a critical role in both fidelity and efficiency of protein translation. There was evidence of mistranslation induced protein misfolding and neuron degeneration (Lee et al., 2006). Thus, it is reasonable to speculate that the deficient tRNA modifications that caused neurological diseases might be due to translational infidelity. Given the importance of tRNA modifications in protein translation and the role in human pathologies, it is time to increase efforts on studying the molecular mechanisms of how tRNA modifications affect protein translation.

5. Ribosome

Ribosomes are large macromolecular machines in all kingdoms of life that are composed of ribosome RNA (rRNA) and ribosome proteins (Green, & Noller, 1997). The molecular weight of the ribosomes varies from 2.3 MDa in bacteria to 4.3 MDa in higher eukaryotes (Melnikov et al., 2012). All ribosomes consist of two subunits: the large subunit (LSU) (the 60s in eukaryotic and 50S in bacterial ribosome) and the small subunit (SSU) (40S in the eukaryotic and 30S in bacterial ribosome) (Spahn et al., 2001). These two individual subunits associate together to form the complete ribosome (80S in the eukaryotic and 40S in the bacterial ribosome) (Figure I-7). The two subunits carry out different roles in the translation process.

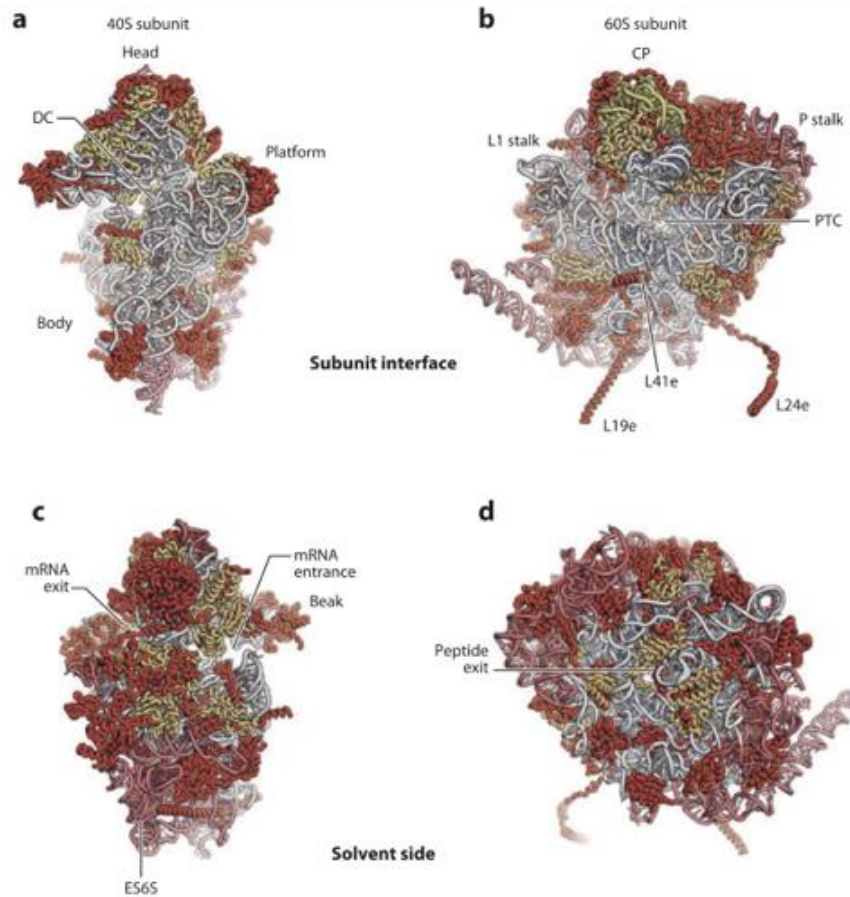


Figure I-7. View of the yeast ribosome

View from the interface (a and b) and the solvent side (c and d) of ribosomal subunits of the yeast ribosome, showing the decoding center (DC), head, body, platform, beak, and shoulder in the small subunit and the central protuberance (CP), peptidyl transferase center (PTC), L1 stalk, and P stalk in the large subunit. The common core consists of ribosomal RNA (white) and proteins (light orange); eukaryote-specific moieties are shown in red (G. Yusupova & Yusupov, 2014).

In eukaryotes, the 40S small subunit consists of a 18S rRNA and 32 different proteins. The 40S small subunit has several parts, known as 'head,' 'body,' 'platform,' 'beak' and 'shoulder' (Figure I-7). The small subunit is responsible for selecting each aminoacyl-tRNA (aa-tRNA) based on the messenger RNA sequence. Hence, the small subunit is responsible for correctly decoding the genetic information into a protein sequence. There are several functional sites on the small subunit, including the decoding center and the tRNA binding sites (A, P and E) (Rabl et al., 2011; Klinge et al., 2012; Weisser et al., 2013). Aminoacyl (A) site is the binding site for an aa-tRNA to enter the ribosome; the peptidyl (P) site is responsible for holding a tRNA attached the nascent polypeptide chain (peptidyl-tRNA); exit (E) site is the place that a deacylated tRNA leaves the ribosome. The mRNA and the three tRNA binding sites, A, P and E sites, are at the interface of the subunit with the 60S subunit. The mRNA enters through a tunnel, which is between the head and the shoulder. The 5' end of the mRNA exit site is between the head and the platform (Jenner et al., 2010). The decoding center of the small subunit is on the interface surface and portions of it are derived from three domains: the head, shoulder and the penultimate stem (Weisser et al., 2013). The 60S large subunit is composed of 5S rRNA, 5.8S rRNA, 25S-28S rRNA and 46 proteins (in yeast) or 47 (in human) ribosomal proteins (Armache et al., 2010; Behrmann et al., 2015; Khatter et al., 2015). The size of the 80S ribosome varies primarily because of insertions in four RNA expansion segments (ES) in 25S-28S rRNA (ES7L, ES15L, ES27L, and ES39L) (Armache et al., 2010). The domains of the 60S are more intertwined with each other than domains in the small subunit (Figure I-7) (Melnikov et al., 2012). The large subunit has an overall shape that looks like a crown and divides into several domains including the 'central protuberance,' 'L1-stalk' and 'P-stalk' (Figure I-7). On the eukaryotic 60S ribosomal subunit, 27 eukaryote-specific proteins, insertions and eukaryotic extensions, and several rRNA expansion segments are located on the

periphery of the large subunit. The major functional sites on the large subunit are three tRNA binding sites and the peptidyl transferase center (PTC). The three tRNA binding sites, A, P and E sites, and the peptidyl transferase center (PTC) are located on the interface side of the 60S subunit (Figure I-7) (Klinge et al., 2011; Klinge et al., 2012). The large subunit serves a different function during translation, catalyzing peptide bond formation in the peptidyl transferase center. During the formation of a peptide bond in the PTC, the nascent peptide chain is moved from a peptidyl-tRNA to an aa-tRNA to accomplish the extension of a polypeptide chain by one amino acid (discussed in detail in below) (Moore & Steitz, 2003; Polacek & Mankin, 2005; Beringer, 2008).

Most knowledge about the ribosome structure and dynamics of protein biosynthesis has been obtained from prokaryotic systems (Cate et al., 1999; Yusupov et al., 2001; Schuwirth et al., 2005). Thus, an understanding of eukaryotic ribosome structure and function is mainly derived from insights about the prokaryotic ribosome structure (Spahn et al., 2001; Anger et al., 2013). Bacterial and eukaryotic ribosomes share some common structures and functions. However, in contrast to bacterial counterparts, eukaryotic ribosomes are much larger and more complex than bacterial ribosomes. This complexity results from additional ribosome RNA (rRNA) elements, termed expansion segment, and extra ribosomal proteins (Figure I-8)(Anger et al., 2013; Chandramouli et al., 2008; Khatter et al., 2015; Klinge et al., 2012; Melnikov et al., 2012; Spahn et al., 2001).

In eukaryotes, an x-ray crystallographic study revealed that there are abundant rRNA expansion segments on the solvent side of both SSU and LSU (Ben-Shem et al., 2011). A crystal structure

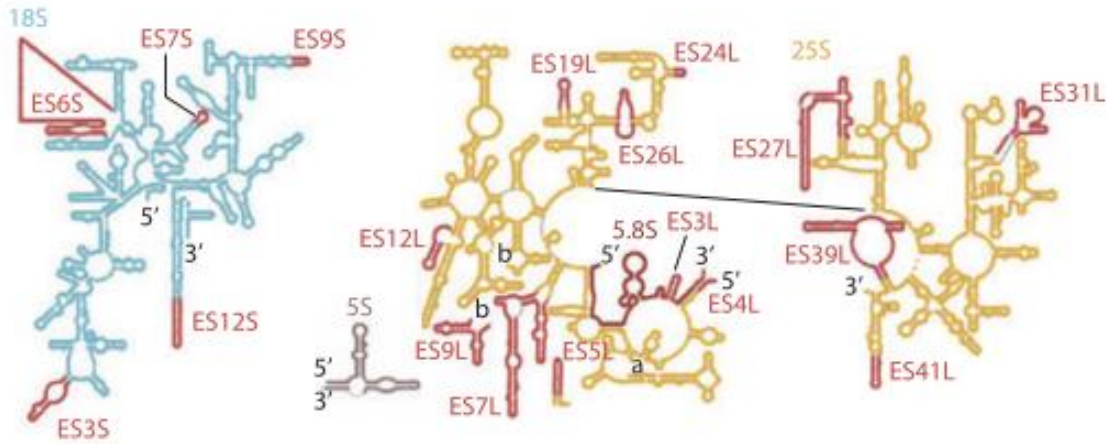


Figure I–8. The secondary structure of yeast ribosome RNA

The secondary structure of yeast ribosomal RNA, 18S, 5S, 5.8S, and 25S respectively, with expansion segments (ES), marked in red (G. Yusupova & Yusupov, 2014).

of the yeast *S. cerevisiae* ribosome at a resolution of 3.0 angstroms provides insights into the function of these eukaryote-specific expansions. Eukaryote-specific clusters, which are constituted by rRNA expansion segments, associate with eukaryote-specific proteins and protein expansion segments, extending the range of interactions between the two subunits (Ben-Shem et al., 2011). Additionally, those eukaryote-specific expansions may serve as a dock for some nonribosomal factors, such as chaperones (Beckmann et al., 2001). A very recent study revealed the role of these eukaryotic expansion segments via deleting specific eukaryotic-specific ES in yeast 25S rRNA individually (Ramesh et al., 2016). Their data suggested that 12 of the 14 deleted ES are necessary for optimal growth and are required for generating 25S rRNA, inferring that these ES play a role in ribosome biogenesis (Ramesh et al., 2016). High resolution structures of the *H. sapiens* ribosome revealed that such interactions are more complex due to ribosomal protein extensions and rRNA expansion-segments (Anger et al., 2013; Khatter et al., 2015). Such interactions have been suggested to stabilize the large expansion segments clustered on the back of the 60S subunit. The similarity between the human ribosome and the yeast *S. cerevisiae* ribosome suggests that the yeast ribosome could serve as a model to study the human ribosome.

The structures of the 30S small subunit from *Thermus thermophilus* and the 50S large subunit from the *Haloarcula marismortui* showed that ribosomes are RNA-based machines (Ban et al., 2000; Schlutzen et al., 2000). The 23S rRNA of the 50S large subunit is involved in the catalytic activity of the ribosome, and the peptidyl transferase activity (Nissen et al., 2000; Simonović & Steitz, 2009), whereas the 16S rRNA of the small subunit is responsible for the decoding, and the selection of the cognate tRNA (Carter et al., 2000). Moreover, the large subunit and the small subunit are connected by a series of bridges that are composed of rRNA-rRNA and rRNA-ribosomal protein contacts (Frank et al., 1995; Gao et al., 2003). An earlier study demonstrated that the same bridges

exist in yeast cytoplasmic ribosomes, suggesting these bridges are conserved in ribosomal structure (Spahn et al., 2001). However, due to insertion elements, additional ribosomal proteins, more complicated translation initiation and different elongation process in eukaryotes, the interaction surface between the two subunits is almost twice as large in eukaryotic ribosomes resulting from additional subunit bridges (Ben-Shem et al., 2011). These additional bridges only exist in eukaryotes, and they are termed eukaryotic-specific bridges (Figure I-9)(Spahn et al., 2001; Tibshirani et al., 2011). In prokaryotes, the subunit interface is mostly made up of rRNA (Ban et al., 2000; Cate et al., 1999; Yusupov et al., 2001). In contrast to bacteria, proteins are the primary components of eukaryote-specific bridges (Yusupov et al., 2001), which locate on the periphery of the subunit interface and the solvent side of both subunits.

Intersubunit bridges are essential elements for ribosomes because protein synthesis requires communication between the SSU and the LSU, and this communication requires the intersubunit bridges. During protein translation, the ribosome undergoes conformational changes, which are required for mRNA decoding, peptide bond formation, termination, and other processes.

These conformational rearrangements involve intersubunit rotation and a swivel movement of the head of the SSU (Figure I-10)(Chandramouli et al., 2008; Tibshirani et al., 2011; Klinge et al., 2012; Khatter et al., 2015). The bridges between the two ribosomal subunits are dynamic in composition because they change with each of the conformational rearrangements. The intersubunit bridges in eukaryotic ribosomes have been mapped using cryo-EM reconstructions

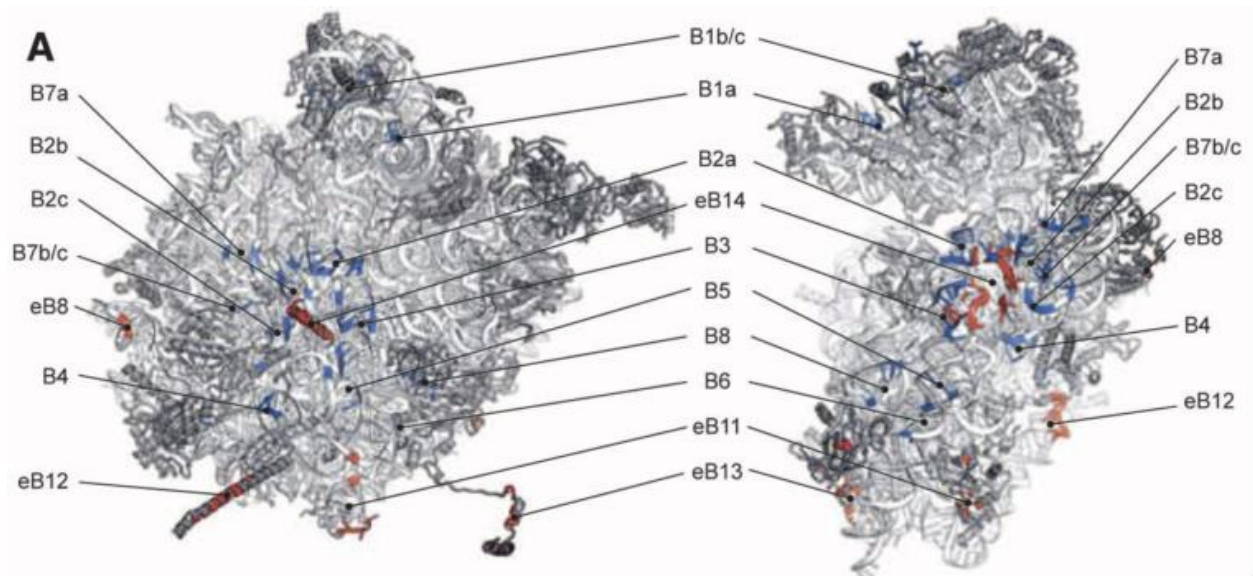


Figure I-9. Intersubunit bridges.

Interface view is showing residues forming eukaryote-specific bridges (red) and conserved ones (blue) (Ben-Shem et al., 2011).

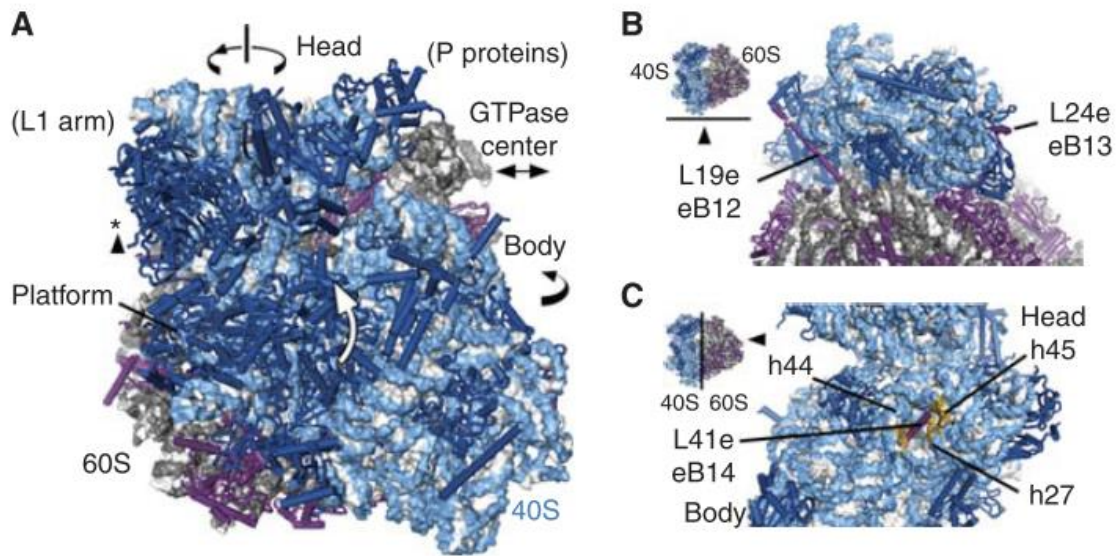


Figure I-10. Intersubunit rotation during translation.

(A) Key conformational changes in the ribosome. Rotation of the small subunit body, head domain, and opening of the mRNA- and tRNA-binding groove during mRNA and tRNA translocation (asterisk) are indicated by arrows. Closing of the small subunit body toward the large subunit during mRNA decoding is also indicated by an arrow. Dynamic regions of the large subunit (L1 arm, P proteins, and GTPase center) are labeled. (B) Eukaryotic bridges eB12 and eB13 in the yeast ribosome at the periphery of the subunits. Large subunit ribosomal proteins contributing to the bridges are marked. The view is indicated to the left. (C) Bridge eB14 in the yeast ribosome, near the pivot point of intersubunit rotation. Eukaryotic specific ribosomal protein in the large subunit L41e and 18SrRNA helices in the small subunit contributing to the bridge (gold) are indicated (Daniel N Wilson & Cate, 2012).

and X-ray crystal structures (Armache et al., 2010a, 2010b; Ben-Shem et al., 2011). Notably, more of the eukaryotic specific bridges involve long extensions from the LSU to contact the body and platform of the SSU, such as bridges eB12 and eB13 (Figure I-10) (Ben-Shem et al., 2011).

Most information about the mechanisms and dynamics of protein translation are also obtained from prokaryotic systems. In prokaryotes, the three binding sites, A, P and E sites, are located at the subunit interface. The mRNA first enters via a channel between the head and the shoulder and wraps around the neck of the 30S subunit. The 5' end of the mRNA is located between the head and the platform (Jenner et al., 2010; Yusupov et al., 2001). Since each subunit has three tRNA binding sites, the tRNAs move through the three binding sites in the two subunits in hybrid states (Rodnina et al., 2002; Dunkle et al., 2011) (discussed in detail in translation section). During elongation, an aminoacyl-tRNA (aa-tRNA) first binds to A site before its amino acid is transferred to a growing polypeptide chain (Watson, 1964). An aa-tRNA becomes a peptidyl-tRNA and moves into the peptidyl tRNA binding site, P site after the peptide chain is transferred to it (Watson, 1964). Eventually, the polypeptide chain is transferred to the following aa-tRNA from a peptidyl-tRNA, and this peptidyl-tRNA becomes deacylated, moving into an exit site, E site, before leaving the ribosome via the exit tunnel (Triana-Alonso et al., 1995; Andersen et al., 2003).

The three tRNA-binding sites on the bacterial ribosome are formed primarily of rRNA (Yusupov et al., 2001). This ribosomal RNA is highly conserved in bacterial, archaeal and eukaryotic ribosomes, suggesting that the mechanisms of the ribosome discriminating the cognate tRNA from the near- or non-cognate tRNAs are also very likely conserved (Ogle & Ramakrishnan, 2005; Demeshkina et al., 2012). Nevertheless, many ribosomal proteins occupying the tRNA binding sites play essential roles and may be responsible for the slightly different positioning of tRNAs on

the eukaryotic ribosome compared with the bacterial ribosome (Budkevich et al., 2011).

On the small subunit, a conserved loop of ribosomal protein S12 monitors the second and third positions of the codon-anticodon duplex (Ogle & Ramakrishnan, 2005). The carboxy-terminal extensions of S12 and S9/S13 stretch form globular domains, which are located on the head of the small subunit, to interact with anticodon stem loop (ASL) regions of A- and P-tRNA, respectively, whereas S7 and S11 interact with the ASL of the tRNA in the E site (Figure I-11) (Yusupov et al., 2001; Selmer et al., 2006; Jenner et al., 2010). These interactions of tRNA and the ribosome are very likely conserved in eukaryotic 80S ribosomes; however, additional interactions probably occur on the SSU involving extensions of some eukaryotic ribosomal proteins. The amino-terminal extensions of S30e and S31e reach into the A site, S25e is positioned between the P and E sites, and S1e at the E site (Figure I-11) (Armache et al., 2010b; Ben-Shem et al., 2011; Rabl et al., 2011). Additional stabilization of tRNA binding is observed through interaction between large subunit ribosomal proteins with the elbow regions of tRNAs, which are the A- and P-site tRNA, via contact with conserved ribosomal proteins L16 and L5, respectively, as well as the E-tRNA with the L1 stalk (Yusupov et al., 2001; Selmer et al., 2006; Jenner et al., 2010) (Figure I-11).

During protein translation, aa-tRNA contacts with the ribosome in at least two regions. The anticodon loop of an aa-tRNA and the mRNA interact with the decoding center (DC) on the SSU, while the 3' CCA end of the tRNA contacts the peptidyl transferase center on the LSU (Spahn et

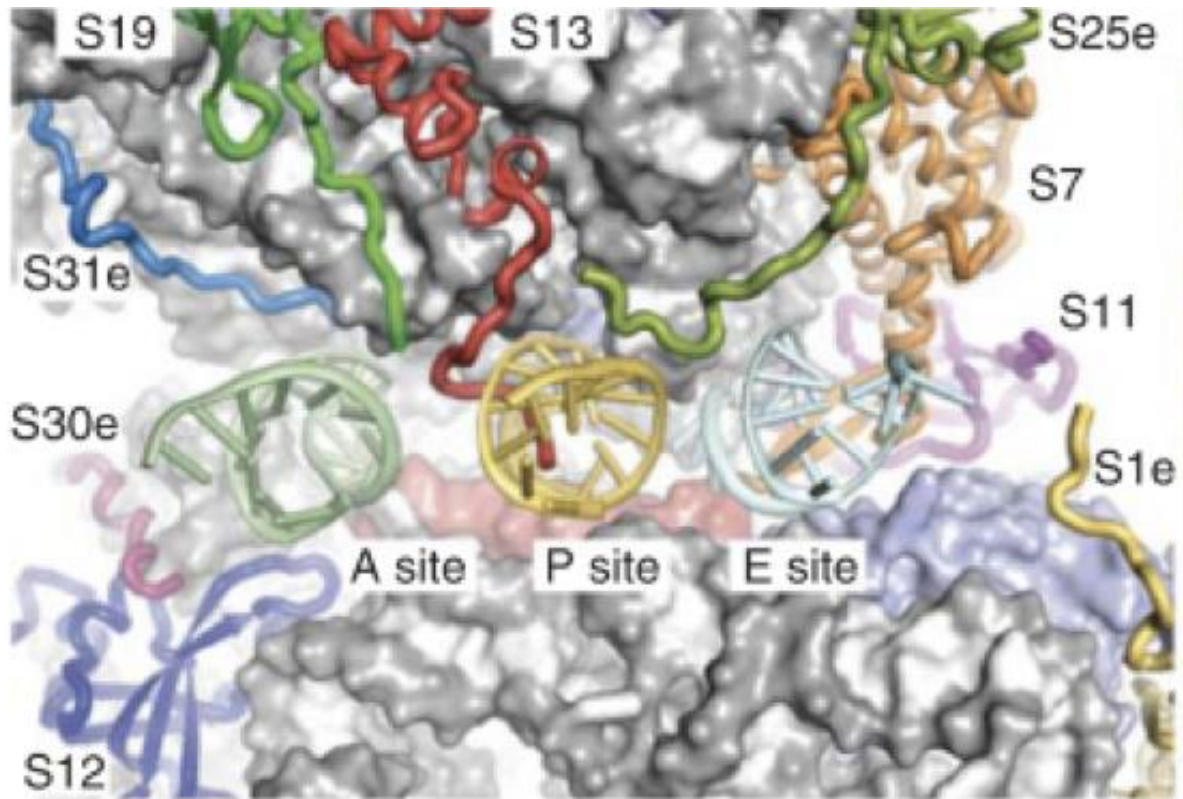


Figure I-11. Extension of r-proteins at the tRNA-binding sites on the small subunit and large subunit.

On the small subunit, a conserved loop of S12 involves in monitoring of the second and third position of the mRNA-tRNA duplex. Meanwhile the C-terminal extension of rpS19 (green) and S13 (red) approach to anticodon stem loop regions of A- and P- tRNA, respectively, whereas rpS7 (orange) and S11(purple) interacts with the anticodon stem loop of E-tRNA (Armache et al., 2010b; Rabl et al., 2011).

al., 2001). Therefore, the mechanisms of mRNA decoding and peptide bond formation are the two central interests in translation elongation by the ribosome, which make the decoding center and the peptidyl transferase center the two most important functional structure domains in the ribosome. Contacts between the tRNA and the ribosome are very well documented in prokaryotic systems (Cate et al., 1999; Carter et al., 2000; Yusupov et al., 2001). The machinery used during translation elongation has been suggested to be highly conserved in the three kingdoms of life because of the high sequence and structural conservation of the decoding center, the PTC and of the tRNA substrates. Hence, the insights of decoding and peptide bond formation obtained from the prokaryotic system are likely transferable to eukaryotic ribosomes (Rodnina et al., 2002; Ogle et al., 2003; Noller, 2006; Simonović & Steitz, 2009). Therefore, I will discuss the decoding center and PTC in detail obtained from studying in the bacterial ribosome.

One of the most important processes of translation, aa-tRNA selection, occurs in the 30S A site (discussed in detail in translation section). Emerging evidence has shown the location of the decoding center in the 30S small subunit, which is composed of parts of 16S rRNA helix 34 (h34) (including C1054), h44 (including adenines 1492, 1493 within an internal loop of h44), and h18 (including the G530 loop) (Figure I-12A) (Noller & Chaires, 1972; Prince et al., 1982; Powers & Noller, 1990; Yoshizawa, 1999). Previous studies have shown that 16S rRNA plays an essential role during the tRNA selection and the hypothesized domain closure of the 30S subunit (Figure I-12). When a cognate tRNA binds to the A site, two universally conserved bases A1493 and A1492 flip out from a position stacked within the internal loop of helix 44 (Figure I-12B). These conformational changes would monitor the interactions between the codon and the anticodon at the first two positions. Simultaneously, base G530 of helix 18 converts its conformation from

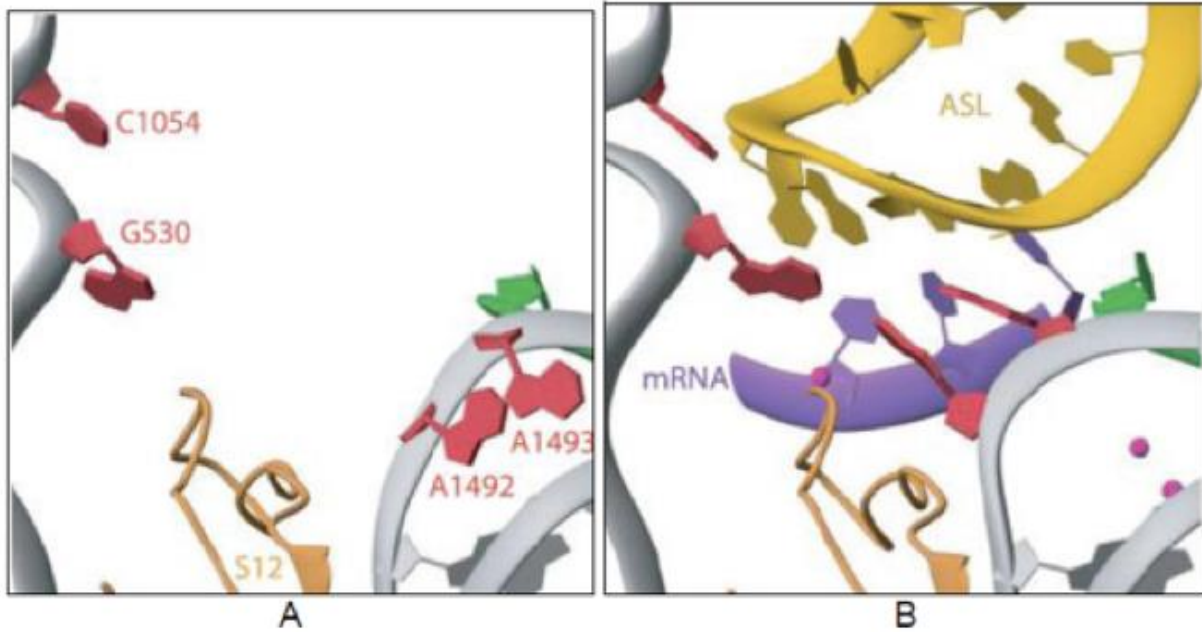


Figure I-12. Conformational changes when a cognate tRNA binds.

Decoding site of the empty A site (A) and when the codon and anticodon interact in the A site (B). Protein S12 is shown in dark yellow, 16S rRNA is in gray. Helix 33 of the 16S rRNA with C1054 is shown at upper left and 530 loop is shown at left. Helix 44 with A1492 and A1493 is shown at lower right. P site mRNA is in green, A site mRNA (right figure) is in purple, anticodon stem loop of a cognate tRNA is in light yellow, Mg²⁺ is in dark pink (Ogle et al., 2001).

syn to *anti* to monitor the second and third position (Ogle et al., 2001) (Figure I-12B). In addition to these local conformation changes, a cognate-tRNA binding induces an overall ribosome conformational change (domain closure) (Figure I-13). Domain closure involves a rotation of the head toward the shoulder and the subunit surface, and of the shoulder toward the intersubunit space and the helix44/helix27/platform region (Figure I-13). In contrast, upon binding of a near-cognate tRNA the same movement of the ribosome was not observed, suggesting that only the interaction between the ribosome and a cognate tRNA can initiate the closure of the ribosome (Ogle et al., 2002).

However, the occurrence of a cognate-tRNA specific universal ribosome conformational rearrangement for the tRNA selection is challenged. Recently, Demeshkina et al. (2012) proposed a mechanism for decoding based on six X-ray structures of the 70S ribosome, mimicking the state of binding cognate or near-cognate tRNA at the proofreading step. They found that either cognate or a near-cognate tRNA binding induces domain closure (Demeshkina et al., 2012). They suggested that the overall conformational rearrangement of the 30S small subunit forms a decoding center that forces the codon-anticodon pair in the A site to adopt a Watson-Crick conformation. They observed that when U1•G36 and G2•U35 mismatches at the first and second position in the A site, A1492, A1493, and G530 interacted with the minor groove helix in a similar way (Figure I-14). They argued that the three conserved bases A1492, A1493 and G530 are not capable of monitoring the geometry of base pair of the codon-anticodon interaction minor groove (discussed in detail in translation elongation decoding section).

In the peptidyl transferase center (PTC), the aminoacylated CCA end of the tRNA in the A site comes very close to the 3' CCA end of the tRNA in the P site for transferring the polypeptide

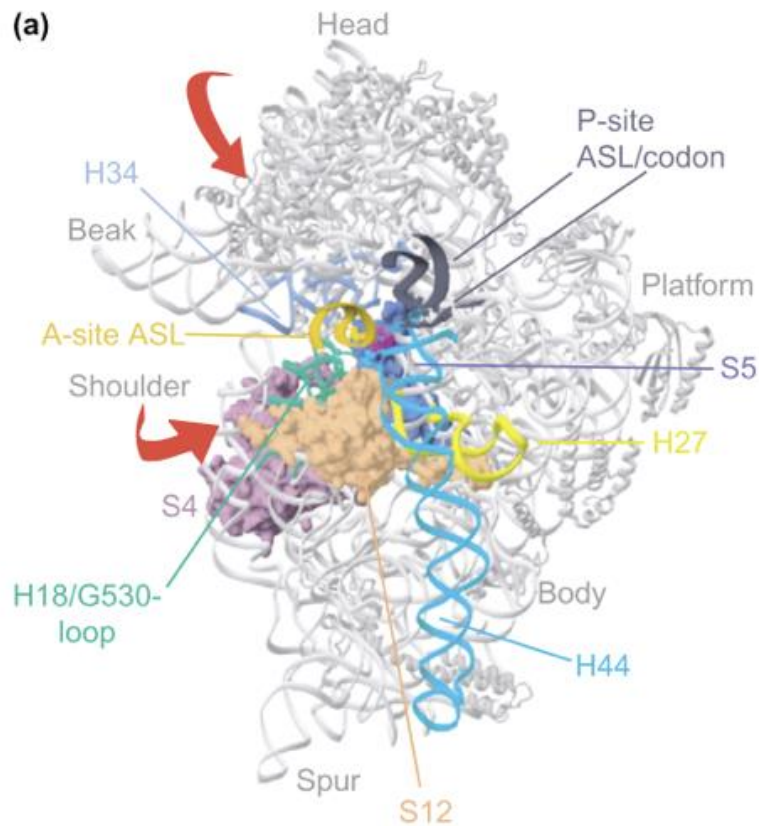


Figure I–13. A cognate tRNA binding causes domain closure.

30S subunit structure with the A-site tRNA anticodon stem–loop (ASL in gold). The decoding center is made up of four different domains: the head, shoulder, platform and helix 44. Red arrows represent the closure of 30S subunit. P site tRNA-ASL (dark gray), helices 44 (cyan) and helix 27 (yellow). In the shoulder domain, helix 18 with the G530-loop (turquoise), and proteins S12 (orange), S4 (violet), S5 (dark blue) and helix 34 (blue) (Ogle et al., 2002).

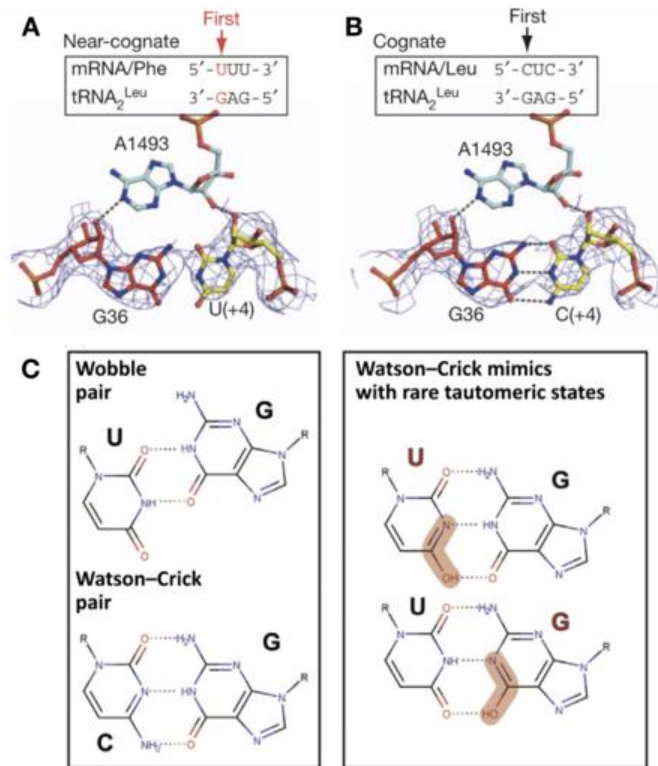


Figure I-14. Near-cognate codon-anticodon mimics Watson-crick base pairing and interacts with 16S rRNA.

(A) and (B) The first base pair of near-cognate UG mismatch and cognate mRNA-tRNA duplex and this duplex interacts with A1493 of 16S rRNA (Demeshkina et al., 2012). (C) Schematic geometry of non-canonical wobble pair and canonical pair (Left) and Watson-Crick-like base pairs formed by rare tautomeric states of U or G (in red) and structural changes (in pink) (Right) (Rozov et al., 2016)

chain from peptidyl-tRNA to the aa-tRNA and forming of a peptide bond between the two tRNAs. The PTC is located in the 50S subunit and surrounded by nucleotides of the central loop of 23S rRNA domain V, which is called the “peptidyl transferase loop” (Figure I-7 and Figure I-15) (Nissen, 2000). Peptidyl transferase activity only required certain components of the 50S subunit because removal of several ribosomal proteins of the large subunit did not affect activity (V. G. Moore, Atchison, Thomas, Moran, & Noller, 1975; Nierhaus & Montejó, 1973). Two studies showed that U2619 and U2620 (U2584 and U2585 in *E. coli* respectively) are adjacent to the CCA-end of the tRNA in the P site (Barta et al., 1984; Vester & Garrett, 1988). These nucleotides belong to a highly conserved internal loop in the center of domain V of 23S rRNA. Mutations in the loop confer cells resistant to peptidyl transferase inhibitors, further supporting the hypothesis that this internal loop of 23S rRNA participates in the peptidyl transferase activity (Noller, 1991). Other evidence supporting this theory has continued to mount (Barta et al., 1984; Vester & Garrett, 1988; Moazed & Noller, 1989; Noller et al., 1992). However, none of these results were strong enough to identify the active site of PTC. A crystal structure of 50S subunit derived from the *Haloarcula marismortui* provided the most solid evidence. This structure confirmed that peptidyl transferase activity happens in the active site of PTC, which is only surrounded by 23S rRNA. The 3'CCA end of tRNA substrate analogs is contacted exclusively by conserved rRNA nucleotides from domain V of 23S rRNA. During peptide bond formation, no protein side-chain is closer than ~18Å (Nissen et al., 2000)

B. Translation initiation

Eukaryotic translation initiation is a highly regulated process. There are different types of initiation pathways. One is the eukaryotic cap-dependent initiation pathway, which is the canonical scanning mechanism of initiation (Iizuka et al., 1994). The other is internal ribosome

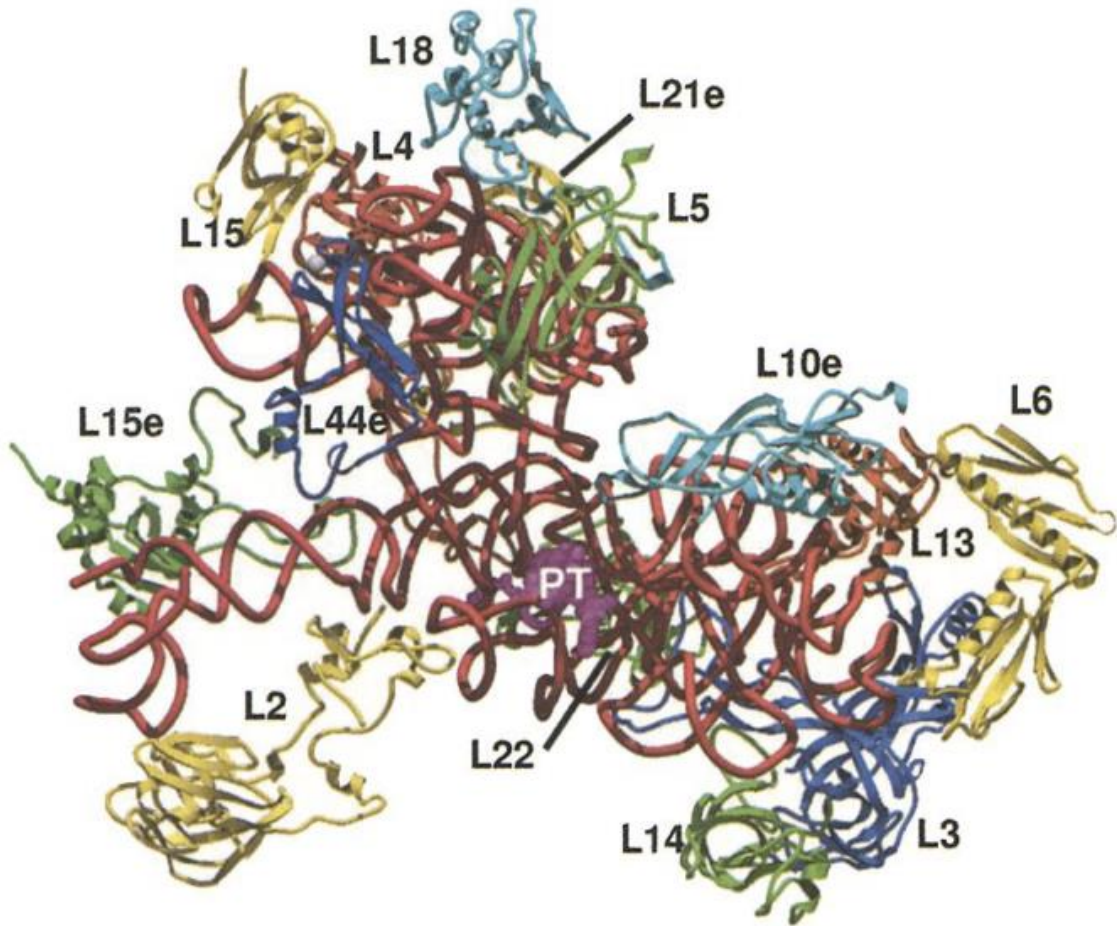


Figure I–15. The active site of peptidyl transferase center in the 50S subunit.

The active site of peptidyl transferase center (PTC) in the 50S subunit is surrounded by 23S rRNA (shown in red). An aa-tRNA analog is shown in pink and the 14 50S proteins that approach the PTC most closely in additional colors (Poul Nissen et al., 2000).

entry site (IRES)-mediated translation initiation, which is the nonscanning mechanism of initiation (Doudna & Sarnow, 2007; Jackson, 2013). Here I will mainly focus on the cap-dependent initiation pathway.

Cap-dependent initiation can be divided into several stages, and the process involves about 20 initiation proteins (Figure I-16 and Table I-2). Translation initiation starts from separated ribosomal subunits that derive from recycling of post-termination ribosomal complexes (post-TCs). These post-TCs are still bound to mRNA, P-site deacylated tRNA and eukaryotic release factor 1 (eRF1) (Frolova et al., 1996). Dissociation of post-TC into free 60S and 40S subunits require several proteins. Eukaryotic initiation factor 3 (eIF3), cooperating with its associated subunit eIF3j subunit, eIF1 and eIF1A, dissociate post-TCs into 60S large subunits, mRNA and tRNA-bound 40S subunits (Asano et al., 1997; Fletcher et al., 1999; Olsen et al., 2003; Kolupaeva et al., 2005). Then eIF1 and eIF3j mediates release of the tRNA and mRNA, respectively (Unbehaun et al., 2004). eIF3, in cooperation with eIF1 and eIF1A, remain binding with free 40S subunits to prevent the 40S subunits re-associate with 60S subunits (Jackson et al., 2010). Subsequently, the ternary complex eIF2-GTP-Met tRNA^{Met} (TC) attaches to recycled 40S subunits, which together form the 43S preinitiation complex (PIC) (Kimball, 1999).

In the second stage of eukaryotic initiation, 43S complexes attach to mRNA with the assistance of several other eukaryotic initiation factors. First, the 5' UTR of mRNA needs eIF4F, in cooperation with eIF4B or eIF4H, to unwind the 5' cap-proximal region for 43S complex binding (Merrick, 2004). eIF4F is composed of the cap-binding protein eIF4E, the DEAD-box RNA helicase eIF4A and eIF4G. eIF4G functions as a 'scaffold' that it has binding domains for mRNA, eIF4E, eIF4A, poly(A) binding protein (PABP) and eIF3 (Figure I-16) (Gross et al.,

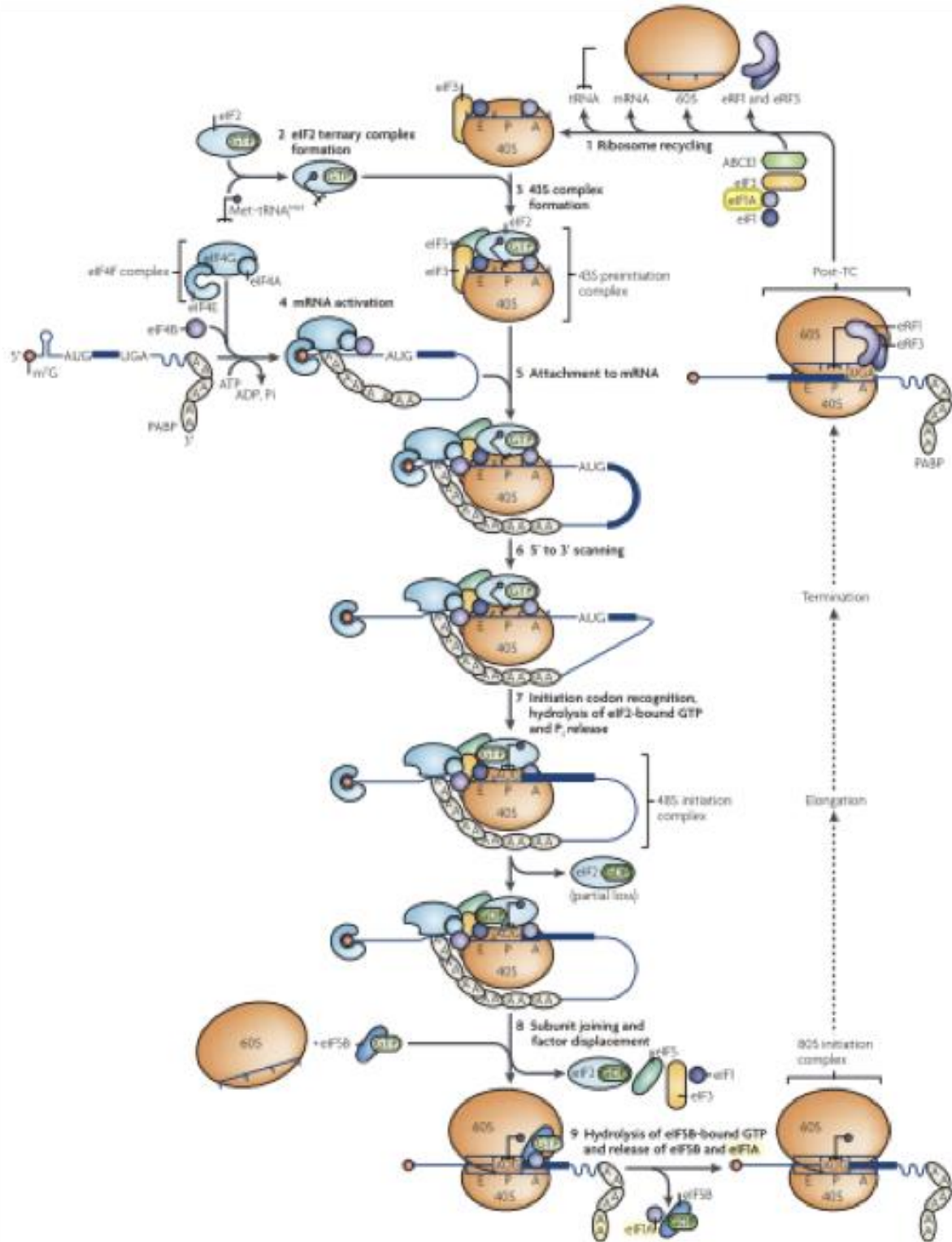


Figure I-16. Schematic of the eukaryotic translation initiation.

The initiation pathway starts with the formation of the ternary complex, eIF2.GTP.Met-tRNAⁱ. In the assistance of eIF1, IA, 3 and 5, the ternary complex is recruited to the 40S subunit to form the pre-initiation complex (PIC). Meanwhile, eIF4 and PABP bind to the mRNA to form an activated mRNP. The PIC starts scanning to locate the start codon AUG once it binds to the 5' end of the mRNA. Start codon recognition triggers eIF1 dissociating from the mRNA and hydrolysis of GTP. Therefore, eIF2 converts to its GDP-bound state. eIF2. GDP and eIF5 then dissociate from the mRNA, clearing the way for the joining of the 60S subunit. Once the 60S subunit joins, eIF5B hydrolyzes GTP and other factors dissociate from the complex to form the 80S initiation complex (Jackson et al., (2010).

Table I-2. Eukaryotic initiation factors and their function (Jackson et al., 2010)

Name	Function
Core initiation factors	
eIF2	Forms an eIF2–GTP–Met-tRNA _i ternary complex that binds to the 40S subunit, thus mediating ribosomal recruitment of Met-tRNA _i
eIF3	Binds 40S subunits, eIF1, eIF4G and eIF5; stimulates binding of eIF2–GTP–Met-tRNA _i to 40S subunits; promotes attachment of 43S complexes to mRNA and subsequent scanning; and possesses ribosome dissociation and anti-association activities, preventing joining of 40S and 60S subunits
eIF1	Ensures the fidelity of initiation codon selection; promotes ribosomal scanning; stimulates binding of eIF2–GTP–Met-tRNA _i to 40S subunits; and prevents premature eIF5-induced hydrolysis of eIF2-bound GTP and P _i release
eIF1A	Stimulates binding of eIF2–GTP–Met-tRNA _i to 40S subunits and cooperates with eIF1 in promoting ribosomal scanning and initiation codon selection
eIF4E	Binds to the m ⁷ GpppG 5' terminal 'cap' structure of mRNA
eIF4A*	DEAD-box ATPase and ATP-dependent RNA helicase
eIF4G [†]	Binds eIF4E, eIF4A, eIF3, PABP, SLIP1 and mRNA (see FIG. 3a) and enhances the helicase activity of eIF4A
eIF4F	A cap-binding complex, comprising eIF4E, eIF4A and eIF4G; unwinds the 5' proximal region of mRNA and mediates the attachment of 43S complexes to it; and assists ribosomal complexes during scanning
eIF4B	An RNA-binding protein that enhances the helicase activity of eIF4A
eIF4H	An RNA-binding protein that enhances the helicase activity of eIF4A and is homologous to a fragment of eIF4B
eIF5	A GTPase-activating protein, specific for GTP-bound eIF2, that induces hydrolysis of eIF2-bound GTP on recognition of the initiation codon
eIF5B	A ribosome-dependent GTPase that mediates ribosomal subunit joining
eIF2B	A guanosine nucleotide exchange factor that promotes GDP–GTP exchange on eIF2

2003). These binding domains of eIF4G for eIF4E, PABP, and mRNA allow assembly of a very stable circular mRNA-protein complex, which is termed a "closed loop" structure (Kozak, 1999; Hinnebusch, 2011; Aitken & Lorsch, 2012). eIF4B together with eIF4H enhance the activity of eIF4A. eIF4A eventually dissociates from mRNA with its 5' end being anchored by the eIF4E-cap interaction (Rogers et al., 2001). These complexes continue unwinding to keep the 5' proximal region constantly prepared for ribosomal binding (Lefebvre et al., 2006). Therefore, attachment of 43S complexes is ultimately finished by a series of interactions of the cap- eIF4E- eIF4G- eIF3- 40S subunit.

In the next stage, the attached 43S ribosomal complex scans mRNA downstream of the cap to the initiation codon. This scanning process consists of two steps—unwinding of the secondary structure of the mRNA 5'UTR and movement of the ribosome along it. The closed loop structure prevents multiple complexes from scanning simultaneously on a single 5' UTR of mRNA, allowing only one 43S complex to scan at a time. Both of the two steps in the scanning process requires energy that is provided by ATP hydrolyzed by eIF4A (Rogers, Lima, & Merrick, 2001). The scanning process also needs an open conformation of 43S complexes, which is stabilized by eIF1 and eIF1A with the assistance of eIF5, eIF2, and eIF3. The eIF2-GTP-Met tRNA^{Met} ternary complex (TC) is attached to the open PIC, which can sample triplets entering the P site for a start codon AUG.

In the initiation codon recognition step, the PIC discriminates against partial base pairing of triplets in the 5' UTR with the Met-tRNA^{Met} anticodon to promote PIC recognizing initiation codon AUG. The first AUG is usually in an optimum context-GCC(A/G)CCAUGG, which has a purine at the -3 position (relative to the A of the AUG codon) and a G at the +4 position (Kozak, 1991). eIF1 is essential in ensuring initiation fidelity in this step. It enables the 43S PIC to distinguish from non-

AUG codons and AUG codons that have very poor context, dissociating the ribosomal complexes that abnormally form at these triplets in its absence (Pestova et al., 1998; Pestova & Kolupaeva, 2002). Studies have also suggested that eIF1 is a determinant of initiation recognition (Hershey et al., 2012). However, to establish a stable codon-anticodon duplex, eIF1A must be tightly bound with the 40S and eIF1 has to be displaced from near the P-site (Unbehaun et al., 2004). This chain of reactions switches the PIC complex from an open to a closed conformation, which locks the PIC onto the mRNA at the initiation codon.

Once the PIC complexes recognize an initiation codon, ribosomes commit to initiation at that codon. This step is regulating by eIF5, an eIF2-specific GTPase-activating protein (GAP) (Kong & Lasko, 2012). One hypothesis states that eIF5 induces the GTPase activity of eIF2's β subunit in eIF2-GTP-Met-tRNA^{Met} complexes, which are bound to 40S subunits (Paulin et al., 2001). Alternatively, eIF5 has been suggested to derepress eIF2 γ 's GTPase activity (Marintchev & Wagner, 2004). On the other hand, eIF1 prevents premature hydrolysis of eIF2-bound GTP in 43S PIC and releasing of P_i (Unbehaun et al., 2004; Algire et al., 2005). Displacement of eIF1 by the establishment of codon-anticodon base pairing relieves repression of GTP hydrolysis and P_i release (Unbehaun et al., 2004; Algire et al., 2005; Maag et al., 2005). Therefore, eIF1 plays a pivotal role in maintaining initiation fidelity in addition to its role in initiation codon selection, as do eIF2 and eIF5, which also participated in the maintenance of the accuracy of initiation codon selection (Donahue, 2000).

The 60S large subunit then joins the complexes following the recognition of initiation. Subsequently, eIF1, eIF1A, eIF3 and eIF2-GDP dissociate from the complexes, which is mediated by eIF5B (Pestova et al., 2000; Unbehaun et al., 2004). Hydrolysis of eIF5B-bound GTP is

essential for it to dissociate from assembled 80S ribosomes but 60S joining is not required (Pestova et al., 2007). Complete dissociation of eIF2-GDP from 40S subunits requires 60S subunit joining because eIF5B alone can only partially displace eIF2-GDP (Majumdar et al., 2007). Eventually, eIF1A dissociates from assembled ribosome with eIF5B (Acker et al., 2006). The complete 80S ribosome then is competent for translation elongation.

C. Translation elongation

1. The Elongation Cycle

The mechanism of translation elongation is very well conserved between eukaryotes and bacteria (Rodnina & Wintermeyer, 2009). Therefore, it is assumed that the mechanisms underlying elongation are the same in eukaryotes owing to this conservation. Generally, studies on the mechanism of translation elongation have been focused on bacterial systems (Hopfield, 1974; Thompson & Stone, 1977; Pape et al., 1999; Ogle et al., 2001; Rodnina & Wintermeyer, 2001; Ogle et al., 2002; Ogle et al., 2003; Ogle & Ramakrishnan, 2005; Jenner et al., 2010; Demeshkina et al., 2012). The three major steps occur during each cycle, which is cognate aa-tRNA selection, peptide bond formation, and translocation of the tRNA-mRNA complexes (Figure I-17)(Rodnina et al., 1994; Green and, Noller, 1997; Ogle et al., 2002). In the bacterial system, three protein factors participate in the elongation cycle. They are elongation factor Tu (EF-Tu), elongation factor G (EF-G) and elongation factor Ts (EF-Ts) (Czworkowski et al., 1994; Rodnina et al., 1997; Schuette et al., 2009; Villa et al., 2009). In eukaryotes, eukaryotic

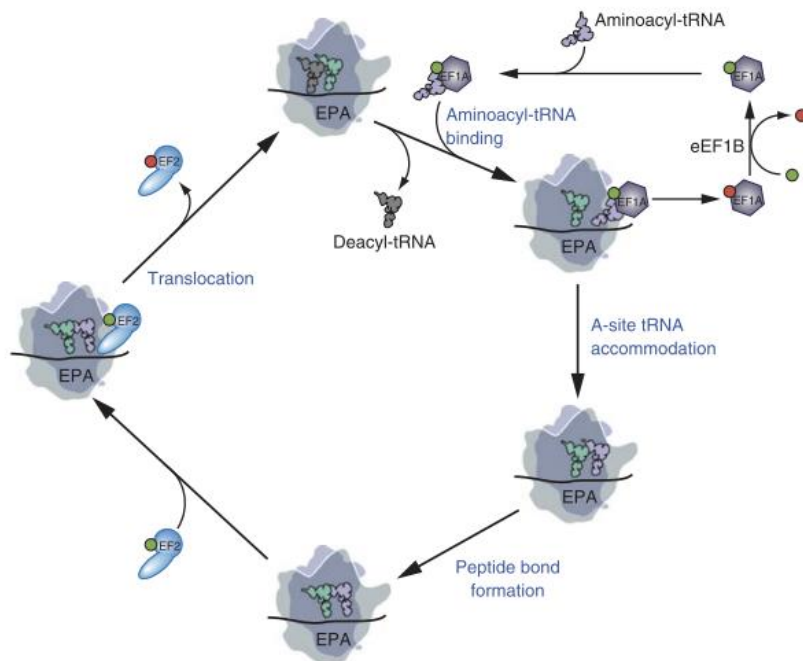


Figure I–17. Model of eukaryotic translation elongation pathway.

The process starts with eEF1A.GTP delivering an aminoacyl-tRNA (aa-tRNA) to the 80S ribosome A site. The anticodon loop of the tRNA interacts with the mRNA in the A site of the small subunit. The aa-tRNA is accommodated into the A site following dissociation of eEF1A.GDP. The eEF1A.GDP is recycled by the exchange factor eEF1B into its GTP form. Meanwhile, peptide bond formation is achieved by transition of the A- and P- site tRNAs into hybrid states along with the acceptor ends of the tRNAs moving to the P and E sites. This process is followed by release of eEF2.GDP. The ribosome is then ready for the next round of elongation with release of the deacylated tRNA from the E site and binding of another eEF1A.GTP.aa-tRNA ternary complex (Dever and Green, 2012)

elongation factor 1A (eEF1A), eukaryotic elongation factor 1B (eEF1B) and eukaryotic elongation factor 2 (eEF2) participate in eukaryotic elongation process (Carr-Schmid et al., 1999; Kaul et al., 2011).

a. Aminoacyl-tRNA (aa-tRNA) Selection

Following translation initiation, an 80S ribosome is located on a messenger RNA with the anticodon of Met-tRNA_i in the P site with its tRNA anticodon paired with the start codon. Then the elongation cycle starts. The next codon of the open reading frame is in the A site and waiting for binding of the cognate aa-tRNA. The eukaryotic elongation factor 1A (eEF1A), which is the homolog of bacterial elongation factor Tu (EF-Tu), binds aa-tRNA in a GTP dependent manner. EF-Tu delivers the tRNA in a codon independent manner (Pape et al., 1998) (Figure I-18). The initiation complex then undergoes a codon recognition step, in which the tRNA anticodon pairs with the mRNA codon in the A site of the 40S subunit. Cryo-EM structures have revealed that a distortion of the anticodon stem loop (ASL) or 'kink' in the aa-tRNA and at the junction between the acceptor and D loops enables the aa-tRNA to interact with both the decoding center and with EF-Tu (Schmeing et al., 2009; Schmeing et al., 2011). Binding of the ternary complex to the ribosome leads to a shift of the 50S GTPase-associated center between 'open' and 'half-closed' states. This conformational change makes the aa-tRNA D loop contact 23S rRNA helix 69 (H69), which causes a distortion of the aa-tRNA ASL for codon recognition in the 30S A site (Frank et al., 2005). A previous study suggested that the energetic penalty for this distortion is paid by the perfect matched codon-anticodon interaction. Consequently, stable interactions between the A site codon and cognate tRNA anticodon promotes high-fidelity decoding (Schmeing et al., 2009; Schmeing et al., 2011). These interactions between the aa-tRNA and ribosome might involve

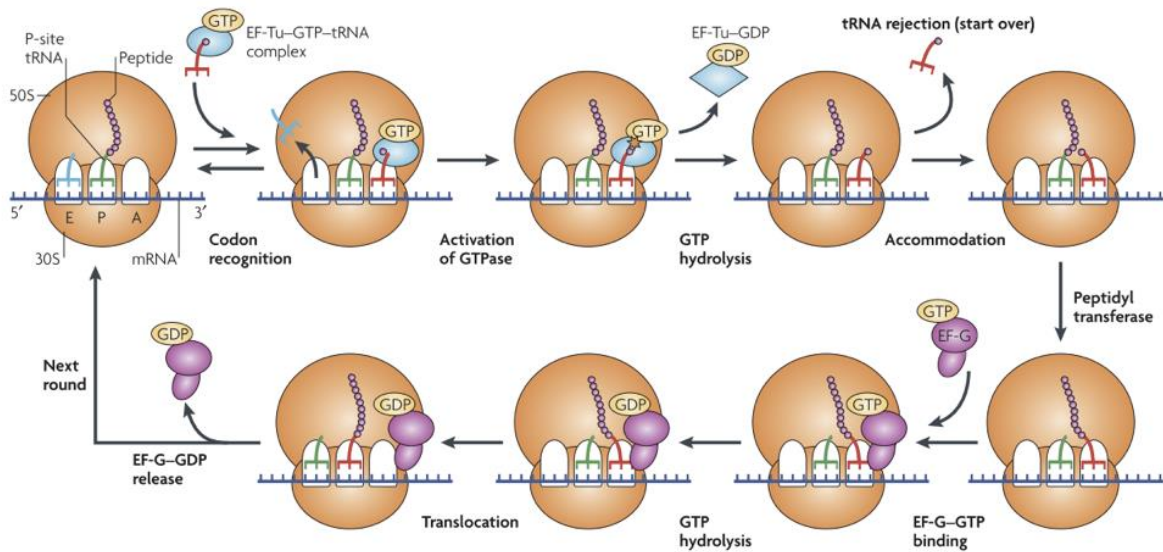


Figure I-18. An overview of ribosomal structure and mRNA translation.

mRNA translation is initiated with the binding of tRNA^{fmet} to the P site (not shown). An incoming tRNA is delivered to the A site in complex with elongation factor (EF)-Tu-GTP. Correct codon-anticodon pairing activates the GTPase centre of the ribosome, which causes hydrolysis of GTP and release of the aminoacyl end of the tRNA from EF-Tu. Binding of tRNA also induces conformational changes in ribosomal (r)RNA that optimally orientates the peptidyl-tRNA and aminoacyl-tRNA for the peptidyl-transferase reaction to occur, which involves the transfer of the peptide chain onto the A-site tRNA. The ribosome must then shift in the 3' mRNA direction so that it can decode the next mRNA codon. Translocation of the tRNAs and mRNA is facilitated by binding of the GTPase EF-G, which causes the deacylated tRNA at the P site to move to the E site and the peptidyl-tRNA at the A site to move to the P site upon GTP hydrolysis. The ribosome is then ready for the next round of elongation. The deacylated tRNA in the E site is released on binding of the next aminoacyl-tRNA to the A site. Elongation ends when a stop codon is reached, which initiates the termination reaction that releases the polypeptide (Steitz, 2008).

more than 16S rRNA bases, which are A1492, A1493, and G530, with the minor groove of the codon-anticodon duplex (discussed in the ribosome structure section) (Ogle et al., 2001). These interactions may include residues in ribosomal proteins and other regions of the tRNA (Jenner et al., 2010).

Codon recognition involving a correct codon-anticodon duplex in the small subunit A site triggers activation of GTP hydrolysis by eEF1A. The hydrolysis changes the conformation of the complex from GTP to GDP-bound form, which has low affinity to the ribosome. Dissociation of factors and GDP enables the 50S GTPase activation center to shift to an 'open' conformation. The conformation rearrangement leads to loss of contact with the aa-tRNA D loop, which had stabilized the tRNA (Frank et al., 2005). Now the aa-tRNA is no longer stabilized and moves into the 50S A site (A/A). Hence, the serial of reaction enables the aa-tRNA to be accommodated into the A site (Spirin, 2002). The acceptor stem of the aa-tRNA accommodates into the peptidyl transferase center in the 50S subunit. These mechanisms of initial aa-tRNA binding, codon recognition, and GTPase activation are expected to be shared between bacteria and eukaryotes (Kapp & Lorsch, 2004; Rodnina & Wintermeyer, 2009).

Both EF-Tu and eEF1A are released from the ribosome with GDP as a complex following GTP hydrolysis. A guanine nucleotide exchange factor then is required for recycling EF-Tu and eEF1A because the dissociation speed of GDP from these factors is slow. The recycling factor promotes recycling the inactive GDP-bound elongation factor to its active GTP-bound form. In bacteria, EF-Ts is responsible for nucleotide exchange. In eukaryotes, the eukaryotic factor eEF1B, which is the homolog of EF-Ts, catalyzes guanine nucleotide exchange on eEF1A (Dever & Green, 2012).

b. Peptide Bond Formation

The peptidyl transferase center (PTC) is mainly composed of conserved ribosomal RNA (rRNA) elements on the large subunit, in which the substrates are positioned for catalysis (Rodnina et al., 2007). Crystal structures of the *Saccharomyces cerevisiae* 80S ribosome and the *T. thermophila* 60S large subunit have demonstrated that the rRNA of the PTC is nearly the same between the eukaryotic and bacterial ribosomes, being consistent with the idea that the mechanism of peptide bond formation is highly conserved (Ben-Shem et al., 2010; Ben-Shem et al., 2011; Klinge et al., 2011).

The catalytic center for peptide bond formation is located on the large subunit (Figure I-19)(Moore & Steitz, 2003; Rodnina et al., 2007). In bacteria, the 50S large subunit is consisting of two RNA molecules, 23S rRNA and 5S rRNA, and more than 30 proteins. The high-resolution crystal structures of ribosomes have shown that the PTC is composed of RNA only, and there was no protein surrounded within 15 Å of the active site, supporting earlier evidence that rRNA is the key element in the catalysis of peptide bond formation (Ban et al., 2000; Nissen et al., 2000; Selmer et al., 2006). An earlier study has suggested that the 23S rRNA catalyzes peptidyl transferase (Noller et al., 1992). Nucleotide A2451 of the 23S rRNA has been suggested to act as a direct catalytic residue in peptidyl transfer (Poul Nissen et al., 2000). However, mutations in A2451 do not affect peptide bond formation (Youngman et al., 2004; Beringer et al., 2005). Rather, the A2451U mutation changes the structure of the PTC (Beringer et al., 2005). Therefore, A2451 seems to play a vital role in stabilizing the ordered structure of the active site rather than function directly in chemical catalysis (Beringer et al., 2005).

Peptide bond formation with the P-site peptidyl tRNA rapidly occurs following accommodation of the aa-tRNA into the A site. The peptidyl tRNA and the aa-tRNA are the only two tRNA

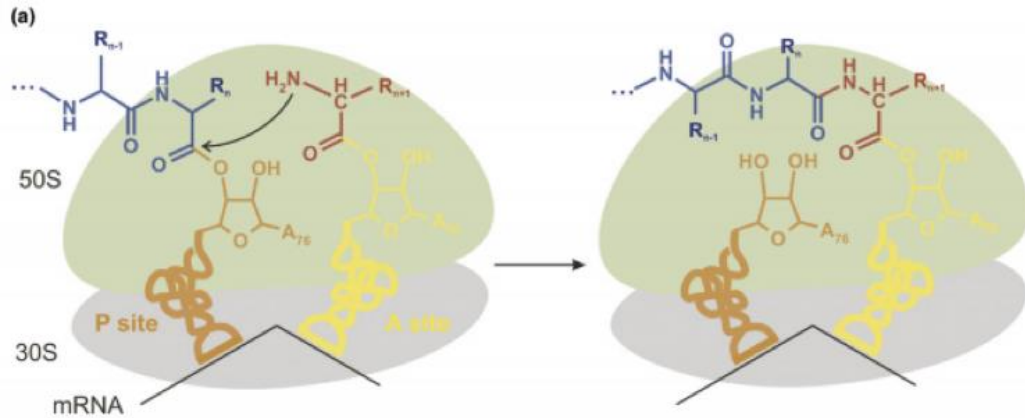


Figure I-19. Peptide-bond formation on the ribosome.

The α -amino group of aminoacyl-tRNA in the A site (yellow) attacks the carbonyl carbon of the peptidyl-tRNA in the P site (orange) to produce a new peptidyl-tRNA that is one amino acid longer in the A site and a deacylated tRNA in the P site. The peptidyl-transferase center is on the 50S subunit (green). On the 30S subunit (gray), aminoacyl-tRNA are recognized according to the match between their anticodons and the codon of mRNA in the A site (Rodnina et al., 2007).

substrates binding to the ribosome. The peptidyl tRNA in the P site is with the growing peptide chain attached by a high-energy ester linkage to its 3' hydroxyl, and the aa-tRNA is a single amino acid esterified to its 3' hydroxyl. During peptide bond formation, the nascent polypeptide chain is transferred from the peptidyl tRNA to the aa-tRNA (Figure 20)(Rodnina et al., 2007). The most favorable mechanism of catalysis involves intra-reactant proton shuttling through the P site tRNA's A₇₆ 2'-OH, which follows the attack of the α -amino group of the aa-tRNA (Figure I-19)(Weinger et al., 2004) (Schmeing et al., 2005). This catalysis forms a new peptidyl-tRNA, which is one amino acid longer in the A site. Subsequently, the tRNA in the P site is deacylated (Figure I-19 and Figure I-20).

c. Translocation

The final step of the elongation cycle is translocation. Ratcheting of the ribosomal subunits triggers movement of the tRNAs after peptide bond formation, resulting in the tRNAs in a status called hybrid P/E and A/P states. In these states, the acceptor ends of the tRNAs in the E and P sites and the anticodon loops stay in the P and A sites, respectively. This process is termed translocation (Figure I-21). Then the ribosome has an empty A site, peptidyl-tRNA in the P site, and deacylated tRNA in the E site post translocation. In eukaryotes, translocation of the tRNAs to the E and P sites needs the elongation factor (eEF2), which is the homolog of bacterial EF-G (Kaul et al., 2011). Binding of GTPase eEF2 or EF-G and attendant GTP hydrolysis catalyzes translocation.

The tRNA anticodon and acceptor end have been shown to happen in a two-step mechanism of translocation. Translocation of tRNAs was proposed to occur independently on the two ribosomal subunits during elongation (Bretscher, 1968; Spirin, 1968).

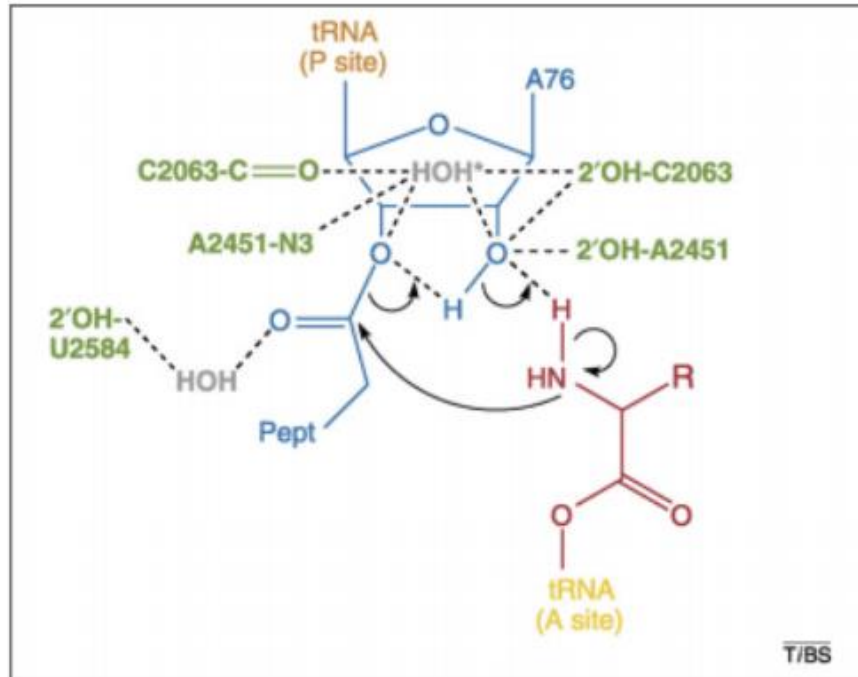


Figure I–20. Concerted proton-shuttle mechanism.

The P-site and A-site tRNA substrates are blue and red, respectively, ribosome residues are green, and ordered water molecules that stabilize the developing charges are gray. The attack of the α -NH₂ group on the ester carbon results in a six-membered transition state, in which the 2'-OH group of the A-site A76 ribose moiety donates its proton to the adjacent 3' oxygen while simultaneously receiving one of the amino protons. Alternatively, the water molecule (*) might be used for a proton shuttle (Rodnina et al., 2007).

Direct chemical footprinting monitored the location of tRNA through the ribosome and led to the hybrid state tRNA model (D Moazed & Noller, 1989). In the experiment, *N*-acetyl-Phe-tRNA bound to the ribosome P site, which was further confirmed by the full reactivity of *N*-acetyl-Phe-tRNA with puromycin. Hence, the nucleotides that were protected by the *N*-acetyl-Phe-tRNA in 16S and 23S rRNA could be assigned to the 30S and 50S P sites, respectively. The complex was footprinted again after it reacted with puromycin. The footprint of 16S rRNA remained the same, whereas the 23S rRNA footprint was entirely different. The 23S rRNA P site nucleotides were no longer protected by the *N*-acetyl-Phe-tRNA. Instead, a new set of E site bases became protected. Therefore, the data suggested a spontaneous movement of the acceptor end of the tRNA from the 50S P site to the E site, while the anticodon end of the tRNA was still bound to the 30S P site. Accordingly, this state was termed the P/E hybrid state (D Moazed & Noller, 1989). The tRNA from the classical 'P site' (P/P state) moves to the P/E hybrid state without the presence of EF-G or GTP.

The *N*-acetyl-Phe-tRNA bound in the P site and aa-tRNA in the A site showed a quite similar behavior. The 50S A site footprint disappeared, and an E-site footprint appeared following the peptidyl transfer, suggesting that the two tRNAs had moved from their A/A and P/P states to the A/P and P/E hybrid states, again, without the presence of EF-G or GTP. Another complex, in which *N*-acetyl-Phe-tRNA was bound in the A site, was also studied. *N*-acetyl-Phe-tRNA bound to ribosomes, following the binding of deacylated tRNA to ribosomes. The footprinting results showed A and P site footprints on 16S rRNA and P and E site footprints on 23S rRNA, indicating binding of tRNAs in the A/P and P/E hybrid states (D Moazed & Noller, 1989). Cryo-EM reconstruction revealed structures for a location of tRNA in the P/E hybrid state, further supporting the hybrid states model (Agrawal et al., 1998; Valle et al., 2003; Taylor et al., 2007).

The fact that incubation of these hybrid-state complexes with EF-G and GTP led to footprints indicated P/P and E binding indicated movement of the tRNAs with respect to the 30S subunit required EF-G and GTP with spontaneously concomitant moving with respect to the 50S large subunit.

Bretscher (1968) first proposed that translocation of tRNAs is accomplished in two steps (Bretscher, 1968). In the first step, EF-G binds to an unstable pretranslocation ribosome in a complex with GTP. The binding of the complex then induces a new conformation of the ribosome. According to the normal conformation, the small subunit is in a different orientation with respect to the large subunit by a counterclockwise rotation, which is called ratchet motion (Frank & Agrawal, 2000). Studies have shown that this ratchet motion occurs even without the presence of ribosomal factors and that it is coincident with tRNAs moving from the classic state to the hybrid states, which facilitate translocation (Ermolenko et al., 2007; Chen et al., 2013). Therefore, this binding of EF-G•GTP complex is thought to stabilize the hybrid-state tRNAs (Ermolenko et al., 2007; Spiegel et al., 2007). This happens due to the deacylation of the P site tRNA, which frees the tRNA CCA end. Therefore, the end can move to the E site on the 50S subunit and the small subunit is allowed to ratchet forward, whereas the mRNA-tRNA are still locked with the small subunit at its P site. Meanwhile, the empty P site on the large subunit develops the precondition for the formation of the A/P hybrid state (Munro et al., 2007). Once this state is accomplished and stabilized by EF-G•GTP complex, the second step of translocation then starts. In this step, EF-G•GTP hydrolyzes GTP with concurrent movement of the mRNA and the tRNAs with respect to the small subunit, also resulting in a conformational change of the EF-G factor to the GDP-bound form (Frank et al., 2007). GTP hydrolysis and P_i release along with conformational changes in EF-G were thought to unlock the ribosome, allowing the tRNA and mRNA to move and then lock the

ribosome in the posttranslocation (Taylor et al., 2007) Dissociation of EF-G•GDP complex from the ribosome allows the 30S subunit head to rotate back. Therefore, the whole 30S subunit undergoes a reverse ratchet motion, resulting in the hybrid P/E and A/P tRNAs moving into the classical E/E and P/P states, respectively (Figure I-21) (Frank et al., 2007). Eventually, the ribosome is in a posttranslocation state, in which a deacyl-tRNA is in the E site, the peptidyl-tRNA is in the P site and an empty A site is ready for the next tRNA substrate and to undergo next translation cycle.

2. Maintenance of Fidelity During aa-tRNA selection

Maintenance of fidelity is one of the most important aspects of protein translation, which largely depends on the selection of the correct aa-tRNA during decoding. During decoding, there can be three types of interaction between codon and anticodon: cognate, near-cognate and non-cognate (Figure I-22)(Ogle et al., 2003). There are 61 different mRNA sense codons, meaning any of these codons can be present in the A site waiting for 45 unique aa-tRNAs with different anticodons (Sprinzl et al., 1998). Discriminating a cognate tRNA against a near-cognate or a non-cognate tRNA could be very difficult for the ribosome, owing to so many different potential substrates (tRNAs). The ribosome has to accomplish the discrimination very fast so that this process will not affect the speed of generating proteins for the cell's demand. Consequently, the ribosome translates at a speed of up to 50 amino acids per second in *E. coli* (Lovmar & Ehrenberg, 2006) The protein accuracy is predicted to be around 4×10^{-4} on average, which is one mistake per 2500 amino acids incorporated (Parker, 1992)

The ribosome selects a correct aa-tRNA based on the complementary base pairing between the codon on mRNA and the anticodon on tRNA. A cognate aa-tRNA with the anticodon interacts

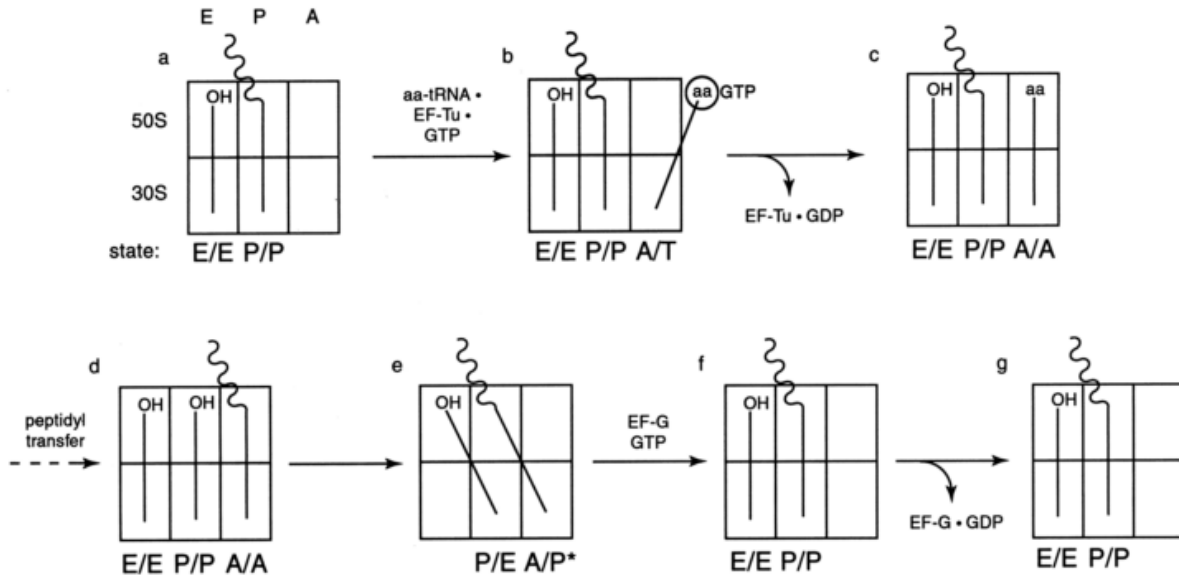


Figure I-21. Model of the main steps of tRNA hybrid-states translocation cycle.

The 70S ribosome is drawn as a rectangle, which is divided into 30S and 50S subunits. Each of them has an A, P and E site. The tRNAs are shown as vertical lines, and the mRNA is not shown in the figure (Noller et al., 2002).

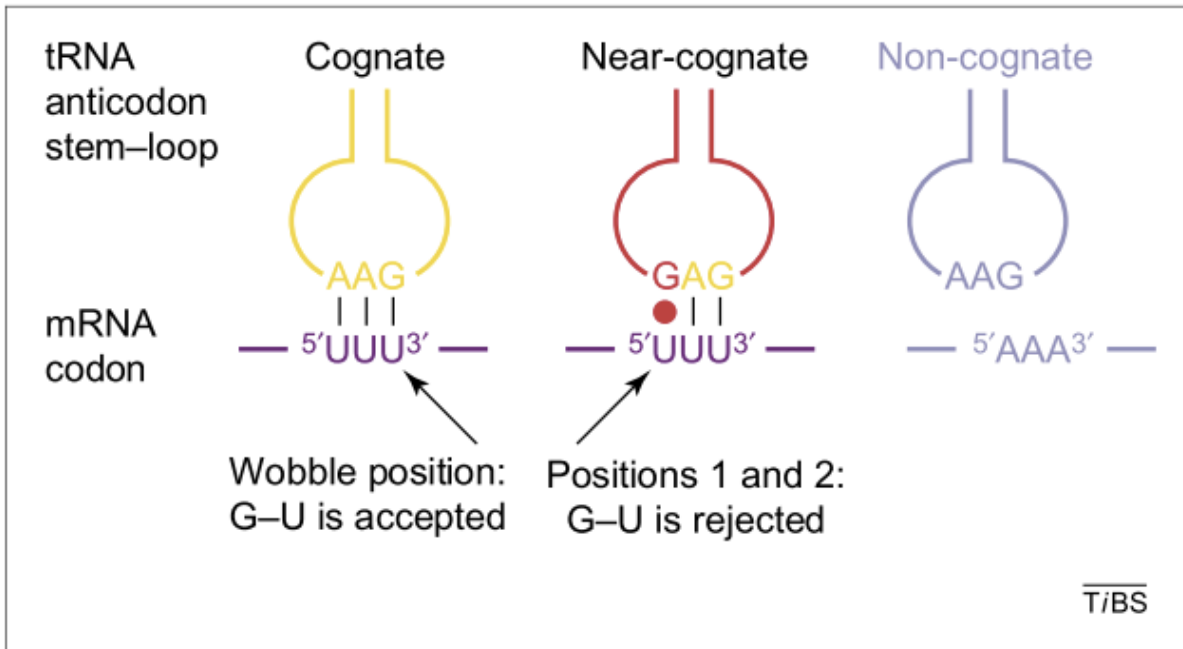


Figure I-22. Cognate, near-cognate and non-cognate codon-anticodon interaction.

The G.U pair is only allowed at the third position (wobble position) (Ogle et al., 2003).

with the codon in the first and second position following Watson crick base pairs (G•C or A•U), or certain non-canonical base pairs (wobble base pair) with the codon in the third position (Figure I-22). The wobble position 34 can pair with more or less nucleotide, which greatly depends on tRNA modification. For example, at the wobble position, G can pair with C or U, I can pair with U, C or A, U with different modifications can pair with A, U, or G (Agris et al., 2007). A near-cognate aa-tRNA has one base pair mismatch with the codon. A non-cognate aa-tRNA has two or more mismatches between the codon-anticodon base pair (Figure I-22). These two types of incorrect aa-tRNA are also potential substrates for the ribosome. A near-cognate tRNA may make less stable base pairing with the mRNA anticodon; however, the difference in base pairing stability is too weak to explain the observed low error frequency (Uhlenbeck et al., 1971; Grosjean et al., 1978). Therefore, the ribosome has sophisticated strategies to ensure that protein translation occurs fairly accurate. These strategies include kinetic proofreading, induced fit and structural arrangement (Pape et al., 1998, 1999; Rodnina & Wintermeyer, 2001a; Rodnina & Wintermeyer, 2001b; Ogle et al., 2003; Ogle & Ramakrishnan, 2005; Rodnina et al., 2005; Demeshkina et al., 2012; Rozov et al., 2015, 2016). Both biochemical and kinetic studies have demonstrated that the movement of aa-tRNA into the ribosomal A site undergoes a serial of intermediate states (Rodnina & Wintermeyer, 2001; Pape et al., 200; Rodnina et al., 2002). Crystal structures showed the interaction between the codon and anticodon in the decoding center (Ogle et al., 2001; Ogle et al., 2002; Ogle et al., 2003; Demeshkina et al., 2012; Rozov et al., 2015, 2016). Also, cryo-EM provided a lot of information about the conformational arrangements of aa-tRNA and EF-Tu on the ribosome as well as interactions and conformational rearrangements of aa-tRNA and EF-Tu during decoding process (Stark et al., 2002).

In the 1970s, Ninio and Hopfield proposed kinetic proofreading as a specific mechanism, which

ensures low error rate during DNA replication, aminoacylation, and translation (Hopfield, 1974; Ninio, 1975). GTP hydrolysis by elongation factor EF-Tu, which is an irreversible reaction, separates tRNA selection into two successive 100-fold steps, which are the initial selection and proofreading (Hopfield, 1974; Ninio, 1975; Thompson & Stone, 1977; Ruusala et al., 1984; Rodnina & Wintermeyer, 2001). These two discrimination steps explained the how proposed 10,1000-fold preference for cognate tRNA came out.

The kinetic mechanism of aa-tRNA selection starts from the EF-Tu•GTP complex delivering aa-tRNA to the ribosome A site on the small subunit of a ternary complex. This step, termed initial binding, is a codon-independent process (Figure I-23). In other words, all tRNAs (cognate, near-cognate and non-cognate tRNA) exhibit the same rate of binding the ribosome A site and dissociating from the ribosome (Rodnina et al., 1994). In this step, the ternary complex forms a very unstable complex with the ribosome (Figure I-23). The forward rate constant is defined as k_1 , and the backward rate constant is defined as k_{-1} . The next step is codon recognition, which is codon-dependent. Subsequently, codon recognition (k_2, k_{-2}) step triggers GTPase activation of EF-Tu (k_3), which is the rate determining step for GTP hydrolysis (k_{GTP}).

Then proofreading initiates from here. The release of Pi induces the conformational rearrangement of EF-Tu from GTP to the GDP-bound form (k_4). Consequently, the EF-Tu•GDP complex dissociates from the ribosome (k_6). This dissociation of the factor frees the end of aa-tRNA and accommodates it in the PTC in the large subunit A site (k_5) where peptide bond formation (k_{pep}) occurs. Alternatively, the aa-tRNA may be rejected from the ribosome (k_7) (Gromadski & Rodnina, 2004a) (Figure I-23). All of the rate constants were detected by using the ternary complex containing tRNA_{UUU}^{Phe}. The ribosomes either have cognate codon UUU or near-cognate codon CUC in the A site under conditions of high binding fidelity of aa-tRNA selection

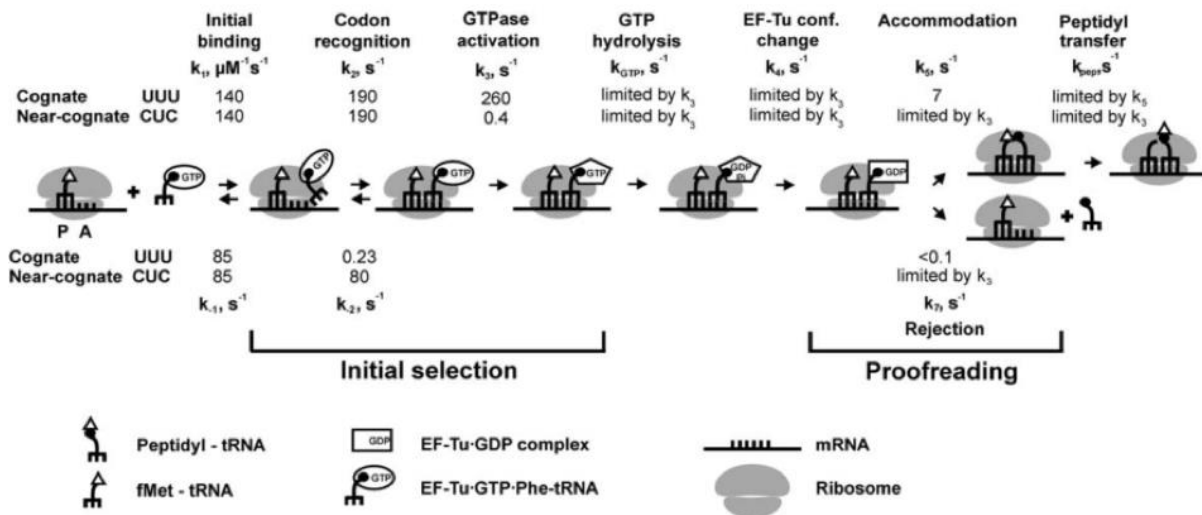


Figure I-23. Kinetic proofreading model

Kinetic proofreading undergoes two steps: initial selection and proofreading (Rodnina et al., 2002).

(Gromadski & Rodnina, 2004a) (Figure I-23).

The initial step in the interaction, initial binding, is a codon-independent process. The interactions between EF-Tu with the ribosome primarily determines the rate of binding (Rodnina et al., 1996; Blanchard et al., 2004). Therefore, it is reasonable that the value of k_1 is high and the same for cognate or near-cognate complex (Figure I-23).

Biochemical and single molecule fluorescence resonance energy transfer (smFRET) studies identified that the second step, codon recognition, undergoes a series of intermediates (Rodnina et al., 1994; Blanchard et al., 2004). The smFRET study observed that when the interaction between the tRNA anticodon and the mRNA codon is established in the decoding center, it forces a fixed orientation on the ternary complex EF-Tu•GTP•aa-tRNA with respect to the P-site tRNA (Blanchard et al., 2004a). An earlier study suggested that the establishment of the cognate codon-anticodon complex induces conformational changes of the conserved nucleotide bases A1492, 1493, and G530 of 16S rRNA (Ogle et al., 2001). These bases alter their positions and form A-minor interactions with the minor groove of the first two positions of interactions specifically following Watson-Crick base pair geometry. Such conformational rearrangements were thought to be induced or facilitated by cognate codon-anticodon interaction (as discussed in ribosome section). However, this conclusion has been challenged (Demeshkina et al., 2012). Kinetic study showed that the cognate and near-cognate ternary complex have very similar overall rate constants of codon recognition (k_2) (Figure I-23)(Pape et al., 1999; Gromadski & Rodnina, 2004). However, a mismatch between codon-anticodon substantially decreases the stability of aa-tRNA binding the ribosome (k_{-2}) (Figure I-23).

GTPase activation of EF-Tu can be considered as a rearrangement of the active site. This

conformational change is necessary to assemble all components for GTP hydrolysis. Formation of contact between cognate aa-tRNA and the ribosome increases the rate of GTPase activation (Rodnina et al., 1995), whereas the interaction of near-cognate or non-cognate aa-tRNA impairs the activation (Gromadski & Rodnina, 2004b) (Figure I-23). The rate of GTP activation (k_3) is ~650-fold higher when binding a cognate aa-tRNA than a near-cognate aa-tRNA. Earlier studies suggested that such local changes within the decoding center induce a global rearrangement, of which the 30S small subunit switches from an open to a closed conformation as I discussed in ribosome section (Ogle et al., 2002). In this study, the binding of a near-cognate aa-tRNA did not seem to affect the conformation of the 30S subunit, and therefore the small subunit could not form the closed conformation. During the process of GTPase activation, the conformational changes in the decoding center signal the GTPase center on the 50S subunit, which accelerates rearrangement step of proceeding and limiting the rate of GTP hydrolysis (Rodnina & Wintermeyer, 2001).

GTP hydrolysis by EF-Tu on the ribosome divides the whole process of aa-tRNA recognition and selection into two parts, initial selection and proofreading. Cryo-EM showed that there are extensive interactions between the switch regions of the G domain of EF-Tu with the sarcin-ricin loop (SRL) of 23S rRNA, suggesting that the SRL participates in stabilizing the transition state conformation of the switch regions of EF-Tu (Stark et al., 2002; Valle et al., 2003). Cleavage of the SRL hinders the GTPase activated state, leading to the abolishment of GTP hydrolysis by EF-Tu (Blanchard et al., 2004b). Besides, ribosomal protein L7/L12, L11 and the L11-binding region of 23S rRNA may also play a role in GTP hydrolysis (Stark et al., 2002; Valle et al., 2003). The interaction of EF-Tu with L7/L12 enhances a 2500-fold stimulation of GTP hydrolysis (Mohr et al., 2002). However, all these contacts are likely to happen far from the nucleotide binding pocket. Therefore, they must be involved indirectly by inducing or stabilizing conformational transitions

of EF-Tu.

GDP and inorganic phosphate, Pi are products of GTP hydrolysis by EF-Tu. The rate of Pi release limits the rate of the conformational change of EF-Tu•GTP to EF-Tu•GDP. The dissociation of aa-tRNA from EF-Tu is likely to occur during the conformational transition of EF-Tu (Knudsen et al., 2001). Aminoacyl-tRNA accommodation in the PTC limits the rate constants of peptide bond formation that is intrinsically very fast (Pape et al., 1998; Pape et al., 1999). Accommodation of cognate aa-tRNA occurs quickly and efficiently having no drop-off of aa-tRNA, whereas the ribosome rejects most of the near-cognate aa-tRNAs owing to a low stability of binding and a lower rate of accommodation.

Acceleration of GTPase activation of EF-Tu and aa-tRNA accommodation by the conformational change of the ribosome, which is induced by correct tRNA binding, is termed induced fit (Pape et al., 1999). This structural change is similar to an enzyme that undergoes a conformational change induced by its correct substrate binding to fit the shape of its substrate (Rodnina & Wintermeyer, 2001). Such conformation changes were thought to be unfavorable by incorrect tRNA binding, and therefore this may explain the slow rate of GTPase activation of EF-Tu by near-cognate tRNA binding (Pape et al., 1999). Hence, previous studies suggested that the communication between the decoding center of the 30S small subunit and 50S large subunit as well as induced fit are both important during proofreading and for maintaining translational accuracy.

However, very recently published work observed that the 30S subunit undergoes the same domain closure irrespective of the binding of a cognate tRNA or a near-cognate tRNA (Demeshkina et al., 2012). Six X-ray structures of the 70S ribosome showed that U•G and G•U mismatches at the first two positions in the A site were forced to form a Watson-Crick-like base pair, which led to domain

closure. A1492, A1493, and G530 interacted with the minor groove helix in a similar way when a near-cognate tRNA binds (Figure I-24). They argued that the three conserved bases A1492, A1493 and G530 are not capable of monitoring the geometry of the base pair of the codon-anticodon interaction minor groove. When a near-cognate tRNA is forced to form a canonical base pair in the A site, this would create repulsion or require energy for tautomerization, which may lead to the dissociation of a near-cognate tRNA (Figure I-25). Thus, tautomerism or repulsion might be a plausible source of discrimination between a cognate tRNA and a near-cognate tRNA (Demeshkina et al., 2012).

D. Translation Termination and Ribosome Recycling

1. Translation Termination

Translation termination occurs when a stop codon, UAA, UGA or UAG, enters the A site. The result of termination is the release of a nascent polypeptide (Kisselev, 2003).

Eukaryotic translation termination requires two protein factors, eukaryotic release factor 1 (eRF1) and eukaryotic release factor 3 (eRF3) (Stansfield et al., 1995; Zhouravleva et al., 1995; Alkalaeva et al., 2006). The class I factor, eRF1, recognizes the stop codon, and is responsible for peptidyl-tRNA hydrolysis, whereas the class II factor, eRF3, is a GTPase that is more related to EF-Tu than EF-G (Atkinson et al., 2008). Though in bacteria, there are also class I release factors 1 and 2, and class II factor 3 (RF1, RF2, and RF3), these release factors are very different from those in eukaryotes, indicating that the process of translation termination is distinct in prokaryotes and eukaryotes (Freistroffer et al., 1997)

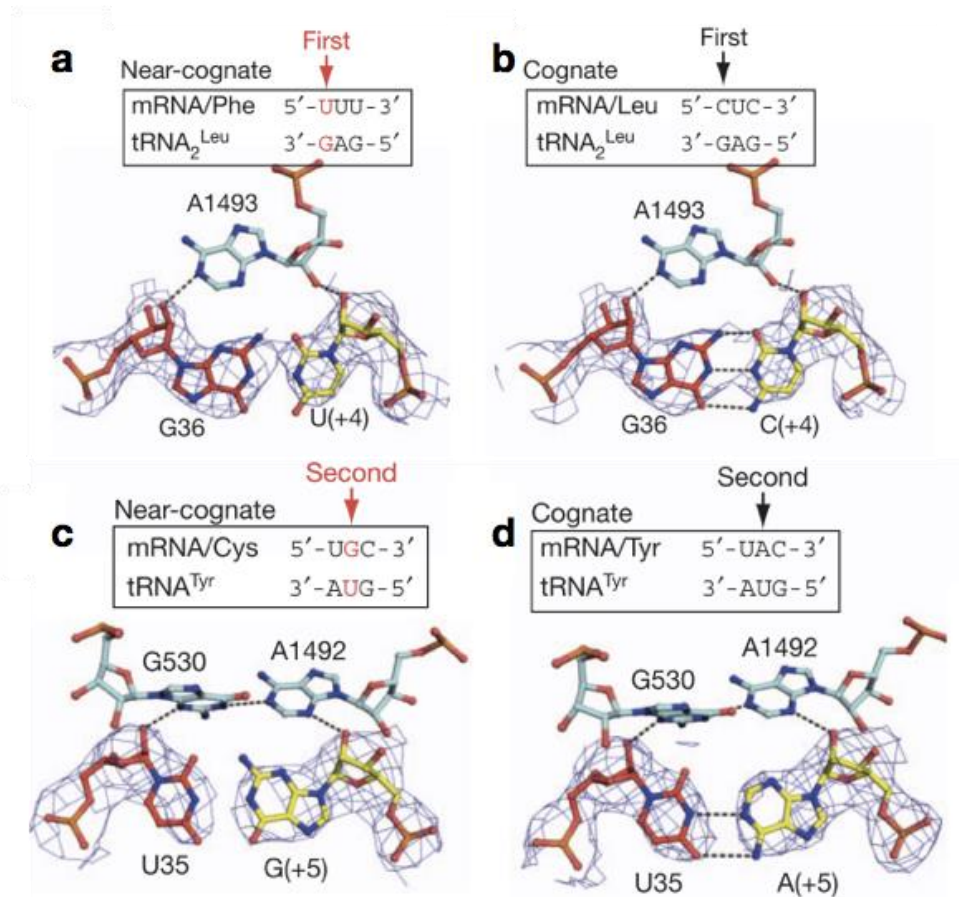


Figure I-24. Watson-Crick-like geometry at the first and second position of codon-anticodon complex.

Mismatches at the first and the second position of codon-anticodon interaction mimic Watson Crick base pair geometry (Demeshkina et al., 2012)

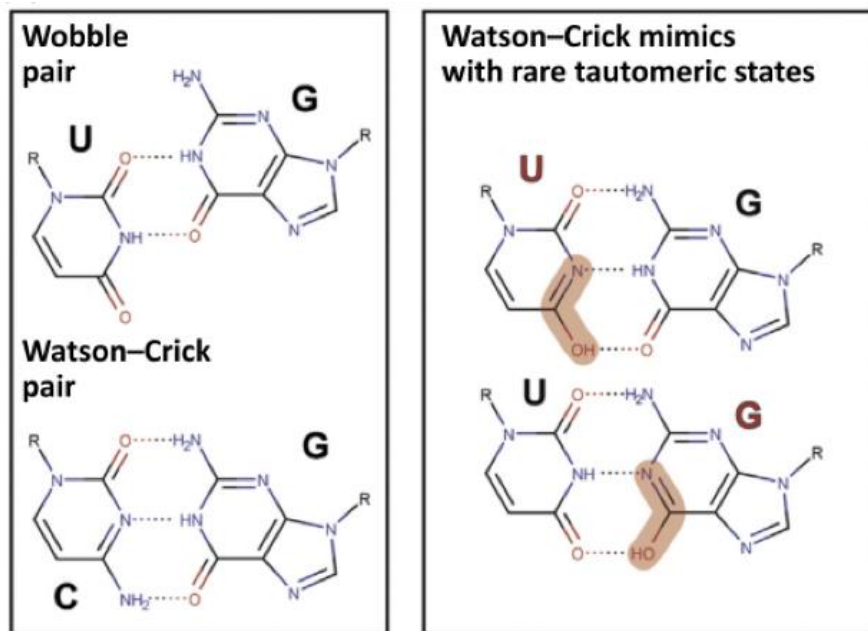


Figure I-25. Schematic geometry of rare tautomeric states

Schematic geometry of non-canonical wobble pair and canonical Watson-Crick pair (left) and Watson-Crick-like pairs formed by rare tautomeric states of uracil or guanosine (indicated with red letters, structural changes highlighted by pink) (right) (Rozov et al., 2016).

Distinct from the prokaryotic factors, eRF1 is the only class I factor present in eukaryotes. Accordingly, eRF1 is capable of decoding all the three stop codons as well as promote the hydrolysis of peptidyl-tRNA in response to any of the three termination codons (Konecki et al., 1977; Frolova et al., 1994). The other release factor, eRF3, plays a role in triggering the release of eRF1 from the ribosome following peptidyl-tRNA hydrolysis. The two translational factors, eRF1 and eRF3, bind to each other without the presence of ribosome. In *S. cerevisiae*, such interaction is required for optimal efficiency of termination (Ito et al., 1996; Le Goff et al., 1997; Pel et al., 1998).

eRF1 is composed of three domains (Song et al., 2000). The amino-terminal domain is responsible for recognizing stop codons, which has a distal loop with a highly conserved NIKS motif. This motif has been proposed to decode termination codons in a similar manner of codon-anticodon interactions. Chemical experiments suggest that this loop is very close to the stop codon nucleotides (Carlberg et al., 1990). Other regions of eRF1 also seem to facilitate recognition of stop codons, including the YxCxxxF motif (Kolosov et al., 2005; Fan-Minogue et al., 2008; Bulygin et al., 2010). The middle (M) domain of eRF1 exerts the function as the tRNA acceptor stem that it extends into the PTC to facilitate peptide release (Song et al. 2000). This domain has a highly conserved Gly-Gly-Gln (GGQ) motif, which seems to promote the chemistry of peptide hydrolysis (Frolova et al., 1999; Laurberg et al., 2008; Weixlbaumer et al., 2008). The carboxyl terminus of eRF1 cooperatively interacts with the class II release factor eRF3 (Merkulova et al., 1999; Kononenko et al., 2008; Cheng et al., 2009). This release factor has a variable amino terminus (Ter-Avanesyan et al., 1993) and a more conserved carboxyl terminus, which directly interacts with the M and C domains of eRF1. In yeast, the carboxyl-terminal fragment of eRF3

sufficiently complements the deletion of eRF3 despite the fact that eRF3 is an essential gene (Ter-Avanesyan et al., 1993; Kononenko et al., 2008; Cheng et al., 2009).

In vitro, eRF3 accelerates peptide release as well as promotes termination efficiency at stop codons in a GTP-hydrolysis dependent manner (Alkalaeva et al., 2006). The eRF1-eRF3-GTP ternary complex binds to the ribosome, triggering GTP hydrolysis (Frolova et al., 1996), which eventually leads to the M domain of eRF1 being deposited in the PTC. Here eRF3 exerts the function as EF-Tu that it delivers a tRNA-like molecule into the PTC. During this process, eRF1 discriminates a termination codon from a sense codon in the A site (Salas-Marco & Bedwell, 2005).

Overall, elongation termination process is achieved in multiple steps (Figure I-26). First, the entry of a stop codon into the A site triggers termination. In eukaryotes, eRF1 binds to the ribosome as a ternary complex (des Georges et al., 2014). eRF1 also participates in peptidyl-tRNA hydrolysis and peptide release from the PTC, following the hydrolysis of GTP by eRF3. Next, eRF1 undergoes a conformational change, which allows the Gly-Gly-Gln motif to enter the PTC in the large subunit and facilitate peptidyl-tRNA hydrolysis. The eRF3-GDP complex dissociates from the protein following GTP hydrolysis and peptide chain release, whereas eRF1 remains bound to the ribosome, which is called the post-termination complex (Nürenberg & Tampé, 2013). These changes initiate the ribosome for ribosomal recycling.

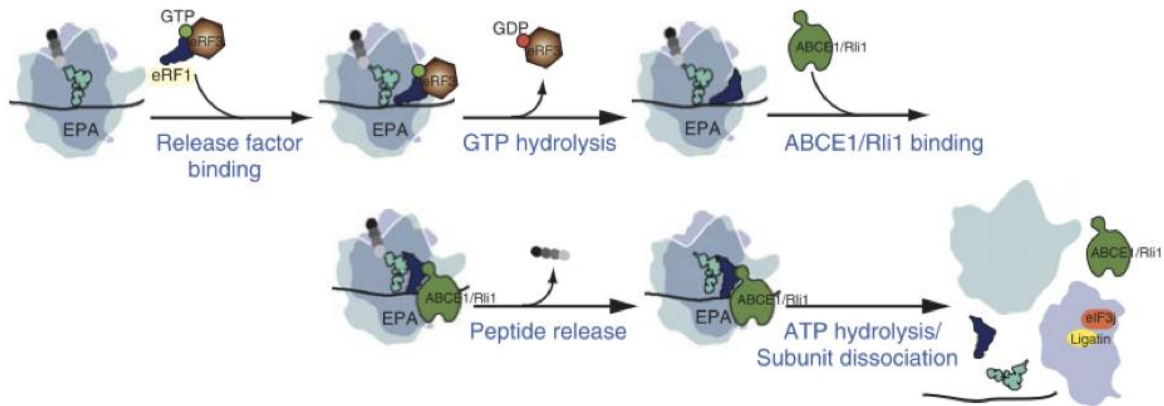


Figure I–26. Model of eukaryotic translation termination and recycling pathways.

On recognition of a termination codon, the eRF1.eRF3.GTP ternary complex binds to the A site of the ribosome in a pre-accommodated state. GTP hydrolysis takes place along with release of eRF3. ABCE1/Rli1 binds and promotes the accommodation of eRF1 into an optimally active structure (Dever & Green, 2012).

2. Ribosomal recycling

Ribosomal recycling is the final step in translation. It occurs once the newly synthesized polypeptide chain has been released from the ribosome. At this time, the 80S ribosome, the mRNA, the newly deacylated tRNA and the factor eRF1 are still bound. The ribosomal subunits, as well as the mRNA and deacylated tRNA, must be dissociated to regenerate the required molecules for the next round of translation.

Recycling is very well studied in bacterial systems and requires ribosomal recycling factor (RRF), which interacts with the post-termination complex following the dissociation of the RF1 or RF2 by RF3. The EF-G-GTP complex facilitates ribosomal subunit dissociation. Initiation factor 3 (IF3) binds to the dissociated small subunit to stabilize it and promote the release of the deacylated tRNA and the mRNA (Hirokawa et al., 2005; Peske et al., 2005). The split ribosomal subunits are then ready for the next round of initiation.

As discussed above, eRF1 and a deacylated tRNA remain bound with the ribosomal complex following termination. However, in eukaryotes, there is no homolog of RRF. Besides, the termination factors are structurally and mechanistically distinct in the bacterial system and eukaryotic system. eRF3 does not involve in dissociation of the class I release factor eRF1 as RF3 (Freistroffer et al., 1997), suggesting other proteins beyond translational factors may participate in the process of ribosomal recycling in eukaryotes.

Emerging studies demonstrate that ribosome splitting process requires the multifunctional ABC-family protein, ABCE1 (Rli1) in eukaryotes and archaea (Pisarev et al., 2010; Barthelme et al.,

2011; Young et al., 2015). Though the release factors seem to possess some intrinsic ribosome recycling activity, the presence of ABCE1 substantially increase the efficiency of the reaction (Pisarev et al., 2010; Shoemaker & Green, 2011), and this activity depends on ATP hydrolysis. Besides a role in recycling, Rli1 has also been suggested to directly increase the rate of peptide release by eRF1-eRF3 complex in an ATP hydrolysis-independent manner (Khoshnevis et al., 2010; Shoemaker & Green, 2011).

Overall, all possible functional factors can be put together into a ribosomal recycling model (Figure I-26). After dissociation of eRF3-GDP complex, peptide chain release activity is promoted by the binding of ABCE1/Rli1 in an ATP-independent manner. Finally, ATP hydrolyzed by ABCE1/Rli1 with concomitant dissociation of subunits. Separated subunits are then bound by various initiation factors or other proteins, which stabilize subunits and prepare them for the next cycle of initiation (Pisarev et al., 2010).

E. Translational errors

Despite mechanisms, such as kinetic proofreading, induced fit or tautomerization, to ensure the accuracy during decoding, errors do occasionally occur, which leads to the production of non-canonical protein products. Translational errors can be divided into three types: processivity errors, frameshift errors, and missense errors (D N Wilson & Nierhaus, 2006). Processivity errors happen due to spontaneous dissociation of a peptidyl tRNA from the ribosome, leading to premature termination (Jørgensen & Kurland, 1990). Changes in reading frame termed frameshift errors, result in loss of genetic information (Bebenek & Kunkel, 1990). Missense errors are caused by incorrect incorporation of an amino acid (Bouadloun, Donner, & Kurland, 1983; I Stansfield et al., 1998).

In most cases, processivity errors cause premature termination, in which the peptidyl-tRNAs spontaneously drop off (dissociate) from the ribosome (Menninger, 1976). The frequency was reported to be $\sim 4 \times 10^{-4}$ (Menninger, 1976). The released peptidyl-tRNA can be deleterious for cells. The ester bond between the peptidyl residue and the tRNA is more stable than the corresponding bond of an aa-tRNA. Therefore, the released peptidyl-tRNAs tend to accumulate in the cell, limiting the number of free tRNAs to participate the next cycle of translation. Consequently, this accumulation restricts protein synthesis. However, the existence of peptidyl-tRNA hydrolase prevents this. It cleaves the relevant ester bond of the released peptidyl-tRNA, thus recycling the free-tRNAs (Schmitt et al., 1997). Processivity errors, in rare cases, lead to a read through of a stop codon by a ternary complex aa-tRNA•EF-Tu•GTP, resulting in an extended protein product.

Translational frameshifting errors alter the reading frame of the mRNA, precluding completion of the nascent peptide chain in its standard reading frame. Consequently, the sequence of the peptide is no longer as the original one. Frameshifting errors are rare events that the estimated frequency is less than 10^{-5} (Kurland, 1992). A forward (3') frameshift by insertion of one nucleotide is called a +1 frameshift, which is the same as the deletion of one nucleotide directly after the last codon before the frameshift. A backward (5') frameshift by one nucleotide causes a -1 frameshift and is the same as an insertion of one nucleotide.

Missense errors can take place during aminoacylation of a tRNA, in which a tRNA is mischarged with an incorrect amino acid by an aminoacyl tRNA synthetase (aaRS) (misacylation) (Jakubowski, 1999). Therefore, the wrong amino acid is incorporated into the polypeptide chain. However, aaRSs have high specificity in recognizing their substrate (as discussed in aminoacylation section),

and some of them have editing mechanisms that can recognize and correct the mischarged tRNA (Fersht, 1977; Ahel et al., 2003; Beebe et al., 2003; Ling et al., 2009). Thus, those properties make the aminoacylation of tRNAs a highly accurate process, with error frequency lower than 10^{-5} (Zaher & Green, 2009).

Alternatively, missense errors can occur during the decoding process, in which the ribosome selects an incorrect aminoacyl-tRNA (misreading)(Luisa Cochella & Green, 2005). If a wrong aa-tRNA remains in the A site long enough and go through initial selection and proofreading process, involving in peptidyl transferase, then the incorrect aa-tRNA is added to the polypeptide chain. Obviously, the stage of aa-tRNA selection by the ribosome is the most error-prone process in translation. Earlier studies demonstrated that near-cognate aa-tRNAs could be selected by the ribosome and incorporated into the polypeptide chain (Lofffield & Vanderjagt, 1972; Singh et al., 1979; Bouadloun et al., 1983; Parker et al., 1983; Parker & Friesen, 1980; Parker & Holtz, 1984; Rice et al. 1984; Toth, Murgola, & Schimmel, 1988; Stansfield et al., 1998; Salas-Marco & Bedwell, 2005; Plant et al., 2007; Kramer & Farabaugh, 2007; Kramer et al., 2010; Manickam et al., 2014).

Some studies have measured various errors involving misreading at each position of the codon-anticodon complex. These studies utilized distinct methods and reporter systems to detect missense error frequency, which makes it hard to compare these results. This research reported that the missense error frequency is 10^{-3} to 10^{-4} per codon in bacteria (Parker, 1989). This wide range of error frequency was due to the use of different methods and reporter systems. For example, one of these methods takes advantage of some bacterial proteins that lack a particular amino acid. Thus, incorporation of the amino acid into a protein represents misreading and can be used to calculate

misreading error rate. For instance, the protein that makes up the bacterial flagellum filament, flagellin, normally contains no cysteine. Incorporation of ^{35}S -labeled cysteine into flagellin was used to measure a misreading frequency in flagellin of 10^{-4} errors per codon translated. This misincorporation of cysteine was due to the first position misreading of arginine codons CGU or CGC by $\text{tRNA}_{\text{GCA}}^{\text{Cys}}$, which usually decodes UGU/UGC (Edelmann & Gallant, 1977). Another method relies on changes in isoelectric charges caused by the substitution of a charged amino acid by an uncharged one or vice versa. Proteins with different charges of the correct and the incorrect incorporated amino acid in the protein can be separated using a two-dimensional gel electrophoresis (Parker et al., 1978). In addition, an enzyme-based reporter system was also used to estimate error frequency. Usually, an essential amino acid residue is mutated, which inactivates the enzyme. If this mutant codon is misread by a wild type tRNA, it will restore enzyme activity. Thus, the misreading frequency is the ratio of the mutant enzymatic activity to the wild type enzyme activity. Serine 68 (AGC) of β -lactamase is an essential amino acid because of its nucleophilic side chain. It was mutated to glycine (GGC and GGU), which inactivates β -lactamase activity. However, glycine 68 GGC can be misread as serine 68 AGC by $\text{tRNA}_{\text{GCU}}^{\text{Ser}}$ at a frequency of 10^{-3} per codon (Toth et al., 1988).

To better understand the error frequency of missense errors in vivo, Kramer and Farabaugh developed a dual-luciferase reporter system based on an enzymatic reaction that can test all possible near-cognate missense errors at a single position in the firefly *luciferase* gene by $\text{tRNA}_{\text{UUU}}^{\text{Lys}}$ in both *E. coli* and the yeast *Saccharomyces cerevisiae* (Kramer & Farabaugh, 2007; Kramer et al., 2010). The codon for an essential amino acid residue, lysine 529 (K529), was mutated to all possible near-cognate codons that have one nucleotide difference from the wild type, and synonymous non-cognate codons that have more than two different nucleotides from the wild

type lysine (AAA/AAG) of firefly *luciferase* (luc). The firefly (F-luc) and *Renilla* luciferase genes (R-luc) were fused together to express as a single polypeptide. Thus, their relative concentration should be identical, and any difference of F-luc activity relative to R-luc activity should reflect a change in the enzymatic activity of firefly luciferase. Based on this method, they estimated error frequencies by $\text{tRNA}_{\text{UUU}}^{\text{Lys}}$ in both *E. coli* and *S. cerevisiae* ranging from 4×10^{-3} to 3×10^{-4} per codon and 6.9×10^{-4} to 4×10^{-5} per codon, respectively.

Two models may explain why some mutant codons showed higher activities: the functional replacement model and the misreading model. Synonymous near-cognate and non-cognate codons are very useful to distinguish these two models from each other. Synonymous codons encode the same amino acid residue such as arginine codons AGA, AGG, CGU, CGC, CGA, and CGG. AGA and AGG are near-cognate codons since there is only one nucleotide difference between these two codons and wild type codons; therefore, CGU, CGC, CGA, and CGG are termed synonymous non-cognate codons because they have two nucleotides different from the wild type codons. The functional replacement model states that any luciferase activity in the mutant proteins is due to the mutant amino acid, suggesting all codons that generate the same amino acid should show the same amount of activity. Thus, this model predicts that all synonymous non-cognate mutations should produce proteins with the same activity. In contrast, the misreading model states that mutant codons, for example, those that encode arginine, are misread by lysyl-tRNA as lysine, resulting in the production of the small amount of wild type activity. Other synonymous non-cognate arginine codons are unlikely to be misread by lysine tRNA because these codons have two or more mismatches with the anticodon $\text{tRNA}_{\text{UUU}}^{\text{Lys}}$. Consequently, $\text{tRNA}_{\text{UUU}}^{\text{Lys}}$ will not recognize arginine codons CGU, CGC, CGA, and CGG as lysine. Therefore, these codons should result in proteins that have much lower activity. Besides, a significant variation of protein activity between different

synonymous near-cognate codons also implies that these protein activities are due to misreading but not functional replacement, because use of synonymous near-cognate codons should produce the same amount of activity according to the functional replacement model.

Kramer and Farabaugh's data showed that the higher activities of some mutant codons were due to misreading but not functional replacement (Kramer and Farabaugh, 2007; Kramer et al., 2010). Two frequently misread arginine codons, AGG and AGA, which showed higher activities of mutant luciferase, are decoded by one of the least abundant tRNAs in *E. coli* (Dong et al., 1996). Thus, the frequent misreading of AGG and AGA by tRNA_{UUU}^{Lys} could be due to a low abundance of the correct tRNA_{UCU}^{Arg}. If so, excess tRNA_{UCU}^{Arg} should reduce the misreading frequencies of AGA and AGG. To address this question, Kramer and Farabaugh overexpressed the cognate tRNA_{UCU}^{Arg}, and they found that the missense error frequencies of misreading AGA and AGG as lysine were significantly decreased, strongly suggesting that competition between a correct tRNA and a near-cognate tRNA could affect translational accuracy (Kramer and Farabaugh, 2007). Restrictive *rpsL* mutations that occur in residues of rpS12 have contact with 16S ribosomal RNA helix 44 and helix 27 upon small subunit 30S closure. Such interaction caused a weak form of closed 30S subunit by these mutations, which results in hyperaccuracy during decoding. Therefore, these *rpsL* mutations will decrease misreading errors (Ogle et al., 2002). Kramer and Farabaugh (2007) reported that a mutation in *rpsL* reduced misreading of all error-prone codons to near background level activity. This result supports the misreading model as well.

Translational accuracy and efficiency have been widely and intensively studied in both prokaryotes and eukaryotes (Edelmann & Gallant, 1977; Parker et al., 1978; Toth et al., 1988; Parker, 1989; Salas-Marco & Bedwell, 2005; Kramer & Farabaugh, 2007; Kramer et al., 2010;

Manickam et al., 2014; Manickam et al., 2016). Surprisingly, only a few experiments have focused on translational fidelity in mammalian cells. Estimation of error frequencies range between 10^{-1} to 10^{-5} errors per codon mainly depending on the type of measurement, the tRNA that performs misreading, and the position of codon that was studied (Kurtz, 1975; Parker et al., 1978; Luce & Bunn, 1989; Mori, Funatsu, Hiruta, & Goto, 1985). One of the methods to measure misreading frequency in mammalian cells relied on testing the amount of incorporation of a new amino acid that is known not to exist in some proteins *in vitro* (Kurtz, 1975; Luce & Bunn, 1989; Mori et al., 1985). For example, polyuridylic acid (poly (U)) was used as misreading template that was translated using microsomes prepared from the livers of mice of various ages. Both L-[^{14}C] Phenylalanyl-tRNA and L-[^{14}C] leucyl-tRNA were used. The misreading assay measured the amount of leucine incorporation due to translational error relative to phenylalanine incorporation on a poly (U) template, which results from correct translation. The error frequency was reported to be as high as 10^{-1} per codon in young mouse liver and 10^{-2} per codon in old mouse liver (Kurtz, 1975). The coat protein of the cowpea variant of tobacco mosaic virus (CcTMV) contains no cysteine or methionine. Thus, incorporation of cysteine into this coat protein represents a translational error event. A study was performed in extracts from human diploid fibroblasts of different ages. The translational error frequency was calculated as cysteine incorporation/total amino acids in CcTMV, which assumed that all codons sites had equal chance to be misread as cysteine. The study reported that the error frequency was a range from 4.2×10^{-5} cysteine/amino acid to 2.9×10^{-4} cysteine/amino acid (Luce and Bunn, 1989).

Despite that the error frequency from 4.2×10^{-5} to 2.9×10^{-4} is in a reasonable range, the error frequencies reported by the poly(U) experiment were very likely overestimated because the process of protein translation is more complicated *in vivo*, and these studies cannot mimic it

completely in vitro. For example, essential components for proofreading may not exist in vitro so that the sophisticated mechanism of proofreading cannot be replicated, thus that more errors would be detected in vitro studies.

This wide range was due to estimating errors on a limited number of codons and positions in different organisms using different approaches. For example, histidine (CAU/CAC) is substituted for asparagine (AAU/AAC), and the missense error frequency only reflects the misreading on the first position (Parker et al.,1978). None of these approaches can test all possible missense errors of a codon and give a comprehensive insight of missense error frequencies in human cells. Besides, most earlier studies measured error frequencies in stressed cells, in which errors were stimulated by either antibiotic or amino acid starvation. Therefore, the error frequencies may be abnormally higher than that under normal conditions (Parker, 1989). Thus, it is hard to compare results from different studies and conclude a particular range of missense error frequency in human cells.

In this study, I developed two novel assay systems that were used to quantify the frequency of translational misreading and to investigate the effect of ribosomal protein S23 and aminoglycoside antibiotics on the error frequencies in various mammalian cell lines and yeast, respectively.

CHAPTER II

MATERIALS AND METHODS

Chapter II. MATERIAL AND METHODS

A. Strains, Growth Conditions and Storage

1. Bacterial strains

DH5 α is the *Escherichia coli* strain used in this study.

A single colony was selected and grew in 2 ml of liquid Luria-Bertani (LB) medium (10 g NaCl, 10 g tryptone, and 5 g yeast extract per liter of dH₂O) at c with required antibiotic. Each ml of overnight culture was added to 1 ml of stock solution (65% glycerol, 0.1 M MgSO₄, 0.025 M Tris·Cl at pH 8). Bacterial strain was stored at -80°C (Ausubel et al., 1995).

2. Yeast strains

The *Saccharomyces cerevisiae* strains used in this study were:

1. BY4728 (*MAT a; his3 Δ 200; trp1 Δ 63; ura3 Δ 0*),
2. PF896 (*MAT α ; ura3 Δ 0; leu2 Δ 0; his3 Δ 1; MET15; lys2 Δ 0; YFL001w::kanMX4*),
3. PF897 (*MAT α ; his3 Δ 1; leu2 Δ 0; lys2 Δ 0; ura3 Δ 0; Elp3::KanMx*),
4. PF908 (*MAT a; ura3 Δ 0; his3 Δ 1; leu2 Δ 0; Ncs6::KanMx*).
5. PF398 (*MAT α ; his3 Δ 1; leu2 Δ 0; lys2 Δ 0; ura3 Δ 0; rps23 Δ*)

A single yeast colony was selected and grew with YPD medium at 30°C for overnight. This overnight culture was added to 60% glycerol to have a final concentration of 30% glycerol. Yeast strain was stored at -80°C.

3. Mammalian cell lines

3.1 Cell lines, growth condition

HeLa, HEK293T and HEK293 cell lines were gifted by Dr. Wilson's lab; NIH 3T3 cell line was gifted by Dr. Sue Rosenberg's lab; 22RV1 cell was gifted by Dr. Bieberich's lab.

The base medium for *HeLa*, HEK293T, HEK293 and NIH 3T3 cells is Dulbecco's Modified Eagle's Medium (DMEM, CORNING 10-013-CV). A final concentration of 10% fetal bovine serum (FBS, CORNING 35-015-CV) was added to DMEM to make the complete growth medium. The base medium for 22RV1 cells is RPMI-1640 medium (CORNING 10-040) with 10% of FBS.

3.2 Sub-culturing and storage

To thaw a frozen stock, stock tube was incubated in 37°C water bath until frozen cells were completely thawed. 1 ml stock cells were diluted with 9 ml of growth medium (DMEM or RPMI-1640 with 10% FBS). After centrifuging at 100 to 120 RPM for 2-3 minutes, culture medium was generally removed. Cell pellet was suspended with 10 ml of growth medium and transferred to a 100 cm tissue culture dish and incubated in 37 °C cell culture incubator.

To subculture, culture medium was removed and discarded. The cell layer was briefly rinsed with 1XPBS (10XPBS: 25.6 g Na₂HPO₄·7H₂O, 80 g NaCl, 2 g KCl, 2 g KH₂PO₄, Bring to 1 liter with H₂O and autoclave for 40 minutes at 121°C) twice. 3 ml of Trypsin-EDTA 1X solution (CORNING 25-051-cl) was added to culture dish. The culture dish was then placed at 37 °C for 5 minutes to detach cells. Then 3 ml of complete growth medium was added and cells were aspirated by gently pipetting. After centrifuge, medium was removed. Cell pellet was suspended by using 10 ml of fresh growth medium. Appropriate aliquots of the cell suspension were added to a new

culture dish with fresh growth medium to make a proper subculture ratio as instructed. Cells were incubated at 37 °C. Medium was renewed for every 2 to 3 days.

To make a frozen stock, the protocol was as same as above except cell pellet was suspended with 3 ml of frozen medium (5% DMSO with complete growth medium) after centrifuge. Each ml of cell suspension was stocked into a 1ml tissue stock tube. Cell stock was placed at 4 °C decreased to -80°C.

B. Transformation and transfection

1. Bacterial transformation

1.1 Preparation of chemical treated competent cells

Preparation of competent cells is a two-day procedure. A stock of DH5 α was streaked onto a LB plate. The plate was incubated overnight at 37°C. A single colony was selected and inoculated into 5mL of LB medium and placed in a rotator wheel for overnight at 37°C. In the second day, 500 μ L of the overnight culture was re-inoculated with 50 mL of LB medium and placed at 37°C on a rotator wheel till desired density (absorbance OD₆₀₀, 0.3 to 0.4). Placed the cell culture on ice for 10 minutes to stop cell growth. Cells were harvest at 1600xg at 4°C for 7 minutes without a break. Medium was carefully removed. Ice-cold 60 mM CaCl₂ (15% glycerol, 10 mM PIPES [piperazine-N, N' -bis (2-hydroxypropanesulfonic acid)] pH7) was used to wash cell pellet. Cells were harvested again at 1100xg at 4°C for 5 minutes a without break. Medium was discarded. Cells were suspended in 2 mL of ice-cold 60 mM CaCl₂. Aliquots of 100 μ L of cell suspension were dispensed into ice-cold micro-centrifuge tubes and frozen immediately by placing in an ethanol/dry ice bath. Individual competent cells were stored at -80°C.

1.2 Bacterial transformation

Competent cells were first completely thawed on ice. An appropriate amount of DNA was added to 100 μ L of competent cells. DNA and competent cells were gently mixed by pipetting up and down and by tapping the tube. The mixture was incubated on ice for 5 minutes. Heat shocked the mixture at 42°C for 45 seconds and returned on ice for 2 minutes. Added 900 μ L of LB medium to each mixture and placed at 37°C for 1 hour. Cells were harvested at 2000xg for 3 minutes. Nine hundred μ L of medium was removed. Cells were suspended and plated onto a LB plate with appropriate selection drug. Plates were incubated at 37°C overnight.

2. Yeast transformation

This high efficiency yeast transformation protocol was adapted and adjusted based on LiAc/ss-DNA/PEG protocol (Gietz & Woods, 2002).

Yeast frozen stock was patched on an YPD plate and incubated at 30°C for a few days to obtain single colonies. A single colony was selected and inoculated with 5 mL of liquid YPD medium with shaking overnight at 30°C. One mL of the overnight cell culture was added to 9 mL of YPD to perform a 1:10 dilution. Cell culture was inoculated at 30°C with roller until OD600 was 0.7 to 0.8. Cells were harvested at 3000xg for 5 minutes. Medium was removed. Cells were washed by 5 mL of ddH₂O and harvested at 3000xg for 5 minutes. Water was removed. Cell pellet was suspended in 200 μ L of 100 nM lithium acetate (LiAc) (1.0 M LiAc: 10.2g LiAc, 100 mL ddH₂O, sterile filter) and transferred into a micro-centrifuge tube. Cells were pelleted at top speed for 15 seconds. Liquid was removed and cell pellet was re-suspended in 100 μ L of 100nM LiAc. Cell suspension can be stored at 4°C or used immediately.

Fifty μL sample of single strand DNA (ssDNA) was boiled at 100°C for 5 minutes and chilled on ice. Cell suspension was harvested for 5 second at low speed. The LiAc was removed. The following components were added in order to make the basic transformation mix: 240 μL PEG (50% w/v, 50g PEG3350, 50 mL water, autoclave or sterile filter), 36 μL of 1.0 M LiAc, 5 μL of ssDNA, 15 μL of DNA, 36 μL of ddH₂O. Each tube was vortexed thoroughly to completely mix the cell pellet. Then the cell suspension was incubated at 30°C with roller for 30 minutes. The cell suspension was transferred to 42°C and incubated for 25 minutes to heat shock cells. Cells were harvested at 6000- 8000 rpm for 15 seconds. Liquids were removed and 0.2 mL of ddH₂O was added to suspend cell pellet. Cell suspension was plated onto an appropriate dropout plate and placed at 30°C .

3. Mammalian cell transfection

Mammalian cell transfection was performed using LipoD293 in vitro DNA transfection reagent (SignaGen SL100668). LipoD293 transfection reagent uses liposomes to deliver DNA.

3.1 Seeding cells

Cells were collected and plated into a 6-well plate at least 18 hours prior to transfection to get optimal cell density for transfection. Number of cells to seed for 6-well plate is 6×10^5 as guided by the company's instruction. Medium in each well was replaced by fresh complete culture medium with serum 60 minutes before transfection

3.2 Preparation of LipoD293-DNA complex and transfection

In a 6-well plate for each well, 6 μL of LipoD293 transfection reagent was added to 100 μL complete culture medium without serum as LipoD293 mixture, while 2 μg of DNA was mixed with

100 μ L of complete culture medium without serum as DNA mixture. LipoD293 transfection reagent was added to DNA mixture immediately and gently mixed well. The solution mixture was then incubated at room temperature for 15 minutes. Then the LipoD293-DNA complex mixture was added to each well.

3.3 Post transfection

LipoD293-DNA complex mixture was removed 12-hour post-transfection. Fresh complete medium with serum was added to each well. The plate was incubated at 37°C for 48 hours.

C. DNA Oligonucleotides

Table II-1, II-2, II-3 and II-4 show all the DNA oligonucleotides used in this study. All the oligonucleotides were generated by Integrated DNA Technologies (IDT). Oligonucleotides were used at a concentration of 0.2 to 1 pmol in PCR, site-directed mutagenesis and DNA sequencing reaction.

D. Plasmids

1. Yeast Plasmids and Plasmid Constructions

The yeast plasmid pYP was constructed using pANU7 (Sundararajan et al., 1999) as the backbone. All *LacZ* mutants at position 624 and 625 were constructed using Quikchange Site-directed mutagenesis (QuikChange II XL Site-directed mutagenesis, Agilent Technologies) (Table II-5). PCR with appropriate oligonucleotides was performed to introduce the mutation from wild type CAA/CAG using the following reaction mixture and amplification cycles in Table II-6.

The PCR product was then digested with restriction endonuclease DpnI at 37°C for 1 hour and transformed into XL10-Gold Ultracompetent cells. One to three transformants were selected and sequenced to confirm the presence of the desired mutation.

Table II-1. Site-directed mutagenesis oligonucleotides

Lysine 60 (AAA) Mutagenesis

Number	Target gene	Codon	Sequence
5581	RPS23	<u>AGA</u>	GTAGGAGTTGAAGCCAGACAGCCAAATTCTGC
5582			GCAGAATTTGGCTGTCTGGCTTCAACTCCTAC
5583		<u>ACA</u>	GTAGGAGTTGAAGCCACACAGCCAAATTCTGCC
5584			GGCAGAATTTGGCTGTGTGGCTTCAACTCCTAC

Table II-1. Site-directed mutagenesis oligonucleotides:

Glutamine 624(CAG) Mutagenesis

Number	Target gene	Codon	Sequence
5814	<i>LacZ</i>	<u>CGG</u>	AAAACACCAGCGGCAGTTTTTCCAGTTCGGTTTATCCG
5815			CTGGAAAACTGCCGCTGGTGTTTTGCTTCCGTCAGCGCT
5810		<u>CAU</u>	AAAACACCAGCATCAGTTTTTCCAGTTCGGTTTATCCG
5811			GGAAAACTGATGCTGGTGTTTTGCTTCCGTCAGCG
5812		<u>CAC</u>	AAAACACCAGCACCAGTTTTTCCAGTTCGGTTTATCCG
5813			GGAAAACTGGTGCTGGTGTTTTGCTTCCGTCAGCG
5714		<u>CGA</u>	ACGGAAGCAAAACACCAGCGACAGTTTTTCCAGTTCGGTT
5715			AACGGAACTGGAAAACTGTCGCTGGTGTTTTGCTTCCGT
5716		<u>AGA</u>	GCTGACGGAAGCAAAACACCAG <u>AGAC</u> AGTTTTTCCAGTTCGGTTTAT
5717			ATAAACGGAACTGGAAAACTGTCTCTGGTGTTTTGCTTCCGTCAGC
5741		<u>CUG</u>	GGAAGTGGAAAACTGCAGCTGGTGTTTTGCTTCC
5742			TGGAAGCAAAACACCAGCTGCAGTTTTTCCAGTTC
5743		<u>CUA</u>	AACGGAACTGGAAAACTGTAGCTGGTGTTTTGCTTCCGT
5744			ACGGAAGCAAAACACCAGCTACAGTTTTTCCAGTTCGGTT
5751		<u>CCA</u>	AACGGAACTGGAAAACTGTGGCTGGTGTTTTGCTTCCGT
5752			ACGGAAGCAAAACACCAGCCACAGTTTTTCCAGTTCGGTT

5753	<u>CCG</u>	GGA	ACTGGAAAACTGCGGCTGGTGT	TTTGCTTCC	
5754		GGAAGCAAAACACCAGCCGCAGT	TTTTCCAGTTC		
5755	<u>AAA</u>	AACGGA	ACTGGAAAACTGTTTCTGGTGT	TTTGCTTCCGTC	
5756		GACGGAAGCAAAACACCAGAACAGT	TTTTCCAGTTCGGT		
5757	<u>AAG</u>	GAACTGGAAAACTGCTTCTGGTGT	TTTGCTTCCG		
5758		CGGAAGCAAAACACCAGAAGCAGT	TTTTCCAGTTC		
5759	<u>GAA</u>	AACGGA	ACTGGAAAACTGTTCTGGTGT	TTTGCTTCCGTC	
5760		GACGGAAGCAAAACACCAGGAACAGT	TTTTCCAGTTCGGT		
5761	<u>GAG</u>	CGGAAGCAAAACACCAGGAGCAGT	TTTTCCAGTTC		
5762		GAACTGGAAAACTGCTCCTGGTGT	TTTGCTTCCG		
5763	<u>UAA</u>	AACGGA	ACTGGAAAACTGTTACTGGTGT	TTTGCTTCCGTC	
5764		GACGGAAGCAAAACACCAGTAACAGT	TTTTCCAGTTCGGT		
5765	<u>UAG</u>	GAACTGGAAAACTGCTACTGGTGT	TTTGCTTCCG		
5766		CGGAAGCAAAACACCAGTAGCAGT	TTTTCCAGTTC		
5937	<u>UUA</u>	ATAAACGGA	ACTGGAAAACTGTA	ACTGGTGT	TTTGCTTCCGTCAGC
5938		GCTGACGGAAGCAAAACACCAGTTACAGT	TTTTCCAGTTCGGTTAT		
5939	<u>CCU</u>	AACGGA	ACTGGAAAACTGAGGCTGGTGT	TTTGCTTCCGT	
5940		ACGGAAGCAAAACACCAGCCTCAGT	TTTTCCAGTTCGGT		
5941	<u>UGA</u>	ATAAACGGA	ACTGGAAAACTGTC	ACTGGTGT	TTTGCTTCCGTCAGC
5942		GCTGACGGAAGCAAAACACCAGTGACAGT	TTTTCCAGTTCGGTTAT		

Glutamine 625(CAG) Mutagenesis

Number	Target Gene	Codon	Sequence
5591	<i>LacZ</i>	<u>CAU</u>	AAAACACCAGCATCAGTTTTTCCAGTTCGGTTTATCCG
5592			GGAAAACTGATGCTGGTGTTTTGCTTCGGTCAGCG
5593		<u>CAC</u>	AAAACACCAGCACCAGTTTTTCCAGTTCGGTTTATCCG
5594			GGAAAACTGGTGTGCTGGTGTTTTGCTTCGGTCAGCG
5849		<u>CGA</u>	GATAAACGGAAGCTGGAAAAATCGCTGCTGGTGTTTTGCTTCC
5850			GGAAGCAAAACACCAGCAGCGATTTTTCCAGTTCGGTTTATC
5589		<u>CGG</u>	AAAACACCAGCGGCAGTTTTTCCAGTTCGGTTTATCCG
5590			CTGGAAAACTGCCGCTGGTGTTTTGCTTCGGTCAGCGCT
5851		<u>AGA</u>	CGGATAAACGGAAGCTGGAAAAATCTCTGCTGGTGTTTTGCTTCCGTC
5852			GACGGAAGCAAAACACCAGCAGAGATTTTTCCAGTTCGGTTTATCCG
5865		<u>CUA</u>	GATAAACGGAAGCTGGAAAAATAGCTGCTGGTGTTTTGCTTCC
5866			GGAAGCAAAACACCAGCAGCTATTTTTCCAGTTCGGTTTATC
5867		<u>CUG</u>	AACGGAAGCTGGAAAAACAGCTGCTGGTGTTTTGCT
5868			AGCAAAACACCAGCAGCTGTTTTTCCAGTTCGGTT
5869		<u>CCA</u>	GATAAACGGAAGCTGGAAAAATGGCTGCTGGTGTTTTGCTTCC
5870			GGAAGCAAAACACCAGCAGCCATTTTTCCAGTTCGGTTTATC
5871		<u>CCG</u>	AACGGAAGCTGGAAAAACGGCTGCTGGTGTTTTGCT
5872			AGCAAAACACCAGCAGCCGTTTTTCCAGTTCGGTT

5873	<u>UAA</u>	GATAAACGGAAGCTGGAAAAATTACTGCTGGTGTGTTTGCTTCCG
5874		CGGAAGCAAAACACCAGCAGTAATTTTCCAGTCCGTTTATC
5875	<u>UAG</u>	AACGGAACTGGAAAACTACTGCTGGTGTGTTTGCTTC
5876		GAAGCAAAACACCAGCAGTAGTTTTTCCAGTCCGTT
5877	<u>AAA</u>	GATAAACGGAAGCTGGAAAAATTTCTGCTGGTGTGTTTGCTTCCG
5878		CGGAAGCAAAACACCAGCAGAAATTTTCCAGTCCGTTTATC
5879	<u>AAG</u>	AACGGAACTGGAAAACTTCTGCTGGTGTGTTTGCTTC
5880		GAAGCAAAACACCAGCAGAAGTTTTTCCAGTCCGTT
5881	<u>GAA</u>	GATAAACGGAAGCTGGAAAAATTCCTGCTGGTGTGTTTGCTTCCG
5882		CGGAAGCAAAACACCAGCAGGAATTTTCCAGTCCGTTTATC
5883	<u>GAG</u>	ACGGAACTGGAAAACTCCTGCTGGTGTGTTTGCTT
5884		AAGCAAAACACCAGCAGGAGTTTTTCCAGTCCGTT

Glutamine 623(CAG) Mutagenesis

Number	Target gene	Codon	Sequences
5718	<i>LacZ</i>	<u>AGA</u>	CGCTGACGGAAGCAAAACAC <u>AGAC</u> AGCAGTTTTTCCAGTCCG
5719			CGGAACTGGAAAACTGCTGTCTGTGTTTGCTTCCGTCAGCG

Table II-2. RT-qPCR Oligonucleotides

Number	Target Gene	Sequence
5745	eRF1	TGC ATC TAA CAT TAA GTC ACG AGT
5746		TCCACAGTATAACAACCAGACCATT
5747	eRF3	CGCCAGGTGCTCCTAAGAAAG
5748		CAAATACATTATTTGTCCTCCAATGGT

Table II-3. Northern Dot-blot biotin labeled Oligonucleotides

Number	Target tRNA	Codon	Sequence
5737	Lysine	CTT	GCTCGAGCCCACGACCCTGAGATTAAGAGTCT
5738		TTT	TTGAACCTGGACCCTCAGATTA AAAAGTCT
5791	Asparagine	ATT	TCTTGA ACTACTCACC GTTCGGTTAATAGCCGAACGCT
5792		GTT	TGGGCTCGAACCACCAACCTTTCGGTTAACAGCCGAATC
5793	Arginine	TCT	TTTGAATGACCACACTAGGCTCAGCTAGAAGTCCAAT
5794		CCT	ACTCGAACCCACAATCCCTGGCTTAGGAGGCCAGTGCCT

Table II-4. DNA Sequencing Oligonucleotides

Number	Target Gene	Sequence
5599	<i>LacZ</i>	tgaaaacggcaaccctggctcgg
5637	rps23	ACTTTCCAAAATGTCGTAATAACC

Table II-5. Yeast Plasmids

Plasmid Name	Mutation from wild Type		Plasmid Source
Wild Type Plasmid			
pANU7			Sundararajan et al. 1999
Glutamine 624 on <i>LacZ</i>			
pYP4	Arg	CGA	This Study
pYP19		CGG	
pYP5		AGA	
pYP6	Leu	CUA	
pYP8		CUG	
pYP9	Pro	CCA	
pYP10		CCG	
pYP11	Lys	AAA	
pYP12		AAG	
pYP13	Glu	GAA	
pYP14		GAG	
pYP15	Stop	UAA	
pYP16		UAG	
pYP17	His	CAC	
pYP18		CAU	

Plasmid Name	Mutation from wild Type	Plasmid Source	
Wild Type Plasmid			
pANU7		Sundararajan et al. 1999	
Glutamine 625 on <i>LacZ</i>			
pYP1	His	CAC	This Study
pYP2		CAU	
pYP3	Arg	CGG	
pYP20		CGA	
pYP21		AGA	
pYP22	Leu	CUA	
pYP23		CUG	
pYP24	Pro	CCA	
pYP25		CCG	
pYP26	Stop	UAA	
pYP27		UAG	
pYP28	Lys	AAA	
pYP29		AAG	
pYP30	Glu	GAA	
pYP31		GAG	

Table II-6. Site-directed mutagenesis PCR reaction mixture and amplification cycle

PCR Reaction Mixture Components	Amount
Template DNA	50-200 ng
Forward Primer	1.25 μ L (10 μ Molar stock concentration)
Reverse Primer	1.25 μ L (10 μ Molar stock concentration)
dNTP mixture	1 μ L
10x Reaction Buffer	5 μ L
Quikchange Solution	3 μ L
DMSO	1.5 μ L (3% of the total volume)
<i>PfuUltra</i> HF DNA polymerase (2.5U/μL)	1.25 μ L
ddH₂O	Made up to a total volume of 50 μ L reaction

Table II-6. Site-directed mutagenesis PCR reaction mixture and amplification cycle

Step 1= 95°C for 1 minute
Step 2= 95°C for 50 seconds
Step 3= 78°C for 50 seconds
Step 4= 68°C for 12 minutes
Step 5= go to step 2, 18 cycles
Step 6= 68°C for 7 minutes

Table II-7. Mammalian Plasmids

Plasmid Name	Mutation from wild type		Plasmid Source
pNM1			Manickam
<i>Fluc Codon 529 Plasmids</i>			
pNM3	Stop	<u>UAA</u>	Manickam
pNM4		<u>UAG</u>	
pNM5	Gln	<u>CAA</u>	
pNM6		<u>CAG</u>	
pNM7	Glu	<u>GAA</u>	
pNM8	Ile	<u>AUA</u>	
pNM9	Met	<u>AUG</u>	
pNM10	Thr	<u>ACA</u>	
pNM11		<u>ACG</u>	
pNM12	Arg	<u>AGA</u>	
pNM13		<u>AGG</u>	
pNM14	Asn	<u>AAU</u>	
pNM15		<u>AAC</u>	
pNM16	Stop	<u>UGA</u>	
pNM17	Glu	<u>GAG</u>	
pNM19	Arg	<u>CGU</u>	
pNM20		<u>CGC</u>	
pNM21		<u>CGA</u>	
pNM22		<u>CGG</u>	
pNM23	Ile	<u>AUU</u>	
pNM24		<u>AUC</u>	
pNM25	Thr	<u>ACU</u>	
pNM26		<u>ACC</u>	

2. Mammalian Plasmids and Plasmids Constructions

The mammalian plasmid pNM was constructed using pcDNA 3.1 (-) as the backbone (Table II-7). The Fluc gene with different point mutations was sub-cloned from the yeast plasmids pEK (Kramer et al., 2010). Both pEK and pcDNA3.1 (-) plasmid was digested at 37°C with restriction endonucleases Bsu36I and EcoI for 1 hour. Desired products were purified by gel extraction (QIAquick gel extraction kit, QIAGEN). After purification, digested Fluc gene and pcDNA 3.1(-) products were ligated at 16°C overnight. The ligation reaction was transformed into DH5 α as described. The transformants were screened for the presence of the mutated Fluc gene by restriction endonuclease digestion Bsu36I and EcoI as well as PCR.

The neomycin gene was knocked out from pNM plasmid by doing a digestion with restriction endonucleases StuI and MscI. Both restriction endonucleases produce blunt end products. The digested pNM plasmid was then self-ligated at 16°C overnight. The ligation product was transformed into DH5 α . The transformants were screened by PCR to confirm the absence of the neomycin gene. The neomycin gene knockout plasmids are listed in Table II-8.

3. Plasmid DNA preparation and storage

Plasmid pYP DNA preparation was performed using a GeneJET Plasmid Miniprep kit (Thermo Fisher) following the company's protocol. Plasmid DNA preps were stored at -80°C for long-term use.

Plasmid pNM for mammalian cells transfection was prepared using a Midiprep kit (Thermo Scientific) following the company's protocol. Plasmid DNA preps were also stored at -80°C for long-term use.

Table II-8. Mammalian neomycin gene knockout plasmids

Wild type: pNM30			This Study
<i>Fluc</i> Codon 529 Plasmids			
pNM31	Stop	<u>UAA</u>	This Study
pNM32		<u>UAG</u>	
pNM33	Gln	<u>CAA</u>	
pNM34		<u>CAG</u>	
pNM35	Glu	<u>GAA</u>	
pNM36	Ile	<u>AUA</u>	
pNM37	Met	<u>AUG</u>	
pNM38	Thr	<u>ACA</u>	
pNM39		<u>ACG</u>	
pNM40	Arg	<u>AGA</u>	
pNM41		<u>AGG</u>	
pNM42	Asn	<u>AAU</u>	
pNM43		<u>AAC</u>	
pNM44	Stop	<u>UGA</u>	
pNM45	Glu	<u>GAG</u>	
pNM46	Arg	<u>CGU</u>	
pNM47		<u>CGC</u>	
pNM48		<u>CGA</u>	
pNM49		<u>CGG</u>	
pNM50	Ile	<u>AUU</u>	
pNM51		<u>AUC</u>	
pNM52	Thr	<u>ACU</u>	
pNM53		<u>ACC</u>	

E. Dual luciferase assay

1. Preparation of mammalian cell lysate

Cells were collected 48 hours post transfection. Medium was removed, and 1X PBS buffer was used to wash cells twice each well. Cells were then scraped in the presence of 1.5 ml 1X PBS buffer by using a culture cell scraper. Using 75% ethanol and ddH₂O, tissue scraper between was thoroughly washed after each usage. Cell suspension was collected and harvested. A sufficient amount of 1X PBS buffer was applied to cell pellet to wash again. Cells were harvested and PBS buffer was removed following by adding 300 μ L 1X Passive Lysis Buffer (PLB, Promega, 4 volume of ddH₂O added to 5X PLB). The cell mixture was placed at room temperature for at least 15 minutes and then stored at -80°C for further usage.

2. Dual luciferase assays

2.1 Preparation of Luciferase Assay Reagent II

Luciferase Assay Reagent II (LARII, Promega) was prepared freshly each time prior to dual luciferase assay. A 15 or 50mL conical tube was covered with foil paper. Preparation must be processed in dark. LARII was prepared by adding lyophilized Luciferase Assay Substrate in 10mL of the supplied Luciferase Assay Buffer II. Once the substrate and buffer have been mixed, it is stable for one month at -20°C or for one year at -70°C. The rest of LARII reagent was aliquot into 100 μ L and stored at -70°C.

2.2 Preparation of Stop and Glo Reagent

An adequate volume of Stop and Glo reagent (S&G) was prepared freshly each time prior to use. S&G reagent was prepared by adding 1 volume of 50X S&G Substrate to 50 volume of S&G Buffer in a foil paper covered conical tube. Reagent should be prepared in dark.

2.3 Dual luciferase assay

Cell samples, LARII reagent and S&G reagent were warmed up to room temperature. Luminometer was activated and primed by both LARII and Stop and Glo reagent prior to assay. About 900 μ L of both reagents were used for priming the machine. Each assay requires injection of 100 μ L of both LARII and Stop & Glo reagent. Twenty μ L of cell lysate from three individual transfections were assayed in triplicate by using a Microfluor 96-well microtiter plates. Twenty- μ L cell lysate was carefully dispensed into 96-well plates by having one well after each one. The luminometer was programmed to perform a 2 second pre-measurement delay followed by a 10 second measurement period for each assay. Both firefly luciferase activity (Fluc) and *Renilla* luciferase activity (Rluc) were detected by the luminometer and measured as Relative Light Units (RLU). Mutant type protein activities (misreading frequency) were calculated as the ratio of mutant (mt) Fluc to Rluc to the ratio of wild type (wt) Fluc to Rluc. The calculation formula is shown as below:

$$\text{Error frequency} = \frac{FLUC_{mt}/RLUC_{mt}}{FLUC_{wt}/RLUC_{wt}}$$

F. Beta-Glo Assay

Individual transformants were selected and inoculated in 2mL of YPD medium for two days. Cultures were inoculated to a dilution of 1:1000 in 5mL of YPD. Cultures were grown at 30°C to reach an OD600 of 0.8 to 1.0. Cells were washed with 5mL of ddH₂O two times. Washed cells can be stored at 4°C for 1 day or used directly for further assays.

Wild type transformant cells were suspended with 5mL of ddH₂O. A serial dilution of ten-fold was

performed to obtain a 100-fold dilution. One hundred microliters of diluted wild type cells were used for each assay. Mutant transformant cells were suspended with 500 μ L of ddH₂O, of which 100 μ L of cells were used for further beta glo assay.

100 μ L of cell culture of three individual colonies was assayed in triplicate for the Beta-Glo assay. Microfluor 96-well microtiter plates (ThermoFisher Scientific), Turner Biosystems MicroPlate II luminometer (Promega) and the Beta-Glo assay reagent (Promega) were used in the assay. 100 μ L of cell culture was added into consecutive columns of the 96-well microtiter plates. When dispensed, an empty well was intentionally left in between two samples to avoid any interference. An empty row was left as well: such as, row A, C, E, and G were used while rows B, D, F, and H were left empty. Equal amounts of Beta-Glo reagent were dispensed into each well containing cell cultures. The plate was shaken using the Beta-Glo shake program of the Turner Biosystems Luminometer. The plate was then protected from the light and inoculated in the dark at room temperature for one hour, then were measured by the Luminometer for Relative Light Units (RLU). The beta-glo assay uses reagent that consist of two components, forming a luciferin-galactoside substrate (6-O- β -galactopyranosylluciferin) (Promega). This substrate is cleaved by the product of *lacZ*, β -galactosidase, releasing luciferin and galactose. The luciferin is further utilized in the firefly luciferase reaction to emit light, which is measured as RLU. Therefore, the RLU is in correspondence with the activity of β -galactosidase. By using different mutant forms of *lacZ* gene, misreading error frequency was calculated as a ratio:

$$Error\ frequency = \frac{\beta - \text{galactosidase activity of the mutants}}{\beta - \text{galactosidase activity of the wild type}}$$

G. Western Blotting

1. Protein extraction

1.1 Protein extraction from mammalian cells

Cells were detached by trypsin (Trypsin EDTA 1x, Corning Life Sciences) and washed with 1xPBS buffer (pH7.4). Cell pellet was collected, and then frozen on dry ice immediately. Cells were lysed with 800 μ L to 1 ml lysis buffer (8M Urea, 250mM imidazole, 100 mM of NaH₂PO₄, pH7.6), and then centrifuged for 5 min. The supernatant was gently transferred and further used for Bradford protein quantification assay (Bio-Rad protein assay reagent). Equivalent amount of purified protein was aliquoted. An equal volume of 2x Laemmli buffer (4% SDS, 10% 2-mercaptoethanol, 20% glycerol, 0.004% bromophenol blue, 0.125M Tris HCl, pH6.8) was added to purified protein. Samples were stored at -20 °C for further use.

1.2 Protein extraction from yeast cells

Yeast protein extraction was performed by using Y-PER yeast protein extraction reagent (Thermo scientific 78991). A single colony was selected and cultured in a dropout medium overnight at 30°C. Cell pellet was obtained by centrifuge at 3000xg for 5 minutes at 4°C. Cell pellet was weighted and resuspended in an appropriate amount of Y-PER reagent. Vortexing was performed to thoroughly mix the mixture. The mixture was then agitated at room temperature for 20 minutes. The cell debris was pelleted by centrifuging at 14000 x g for 10 minutes. The supernatant was then reserved for future usage.

2. Protein blotting

Samples were separated by 12% SDS PAGE gel (TEMED, 10% SDS, 10% Ammonium Persulfate, 30% Acrylamide, 1.5M Tris pH8.8, ddH₂O) using a mini Protean-3 gel system (BioRad). 4%

stacking gel is composed of TEMED, 30% Acrylamide, 0.5M Tris pH6.8, 10% SDS, 10% APS and ddH₂O. SDS PAGE gel was run under 100 voltage for 1 to 2 hours depending on protein size. Once samples were successfully separated, the protein was transferred from gel to the PVDF membrane. PVDF membrane was first activated with methanol for 1 minute and rinsed with 1x transfer buffer (10x Tris/Glycine buffer from Biorad, 20% methanol and ddH₂O). Filter papers and sponge were soaked with 1x transfer buffer before preparing the stack. The stack was prepared following the general western blot protocol (Abcam general western blot protocol). The protein was transferred at 4°C under 100v for 1 to 2 hours. After transfer, membrane was blocked in 10 to 25 ml of blocking buffer (1XTBST buffer, 5% non-fat milk powder) for 1 hour at room temperature. Then the membrane was washed three times for 5 minutes each with 10 ml of TBST and processed to primary antibody incubation. Eukaryotic release factor 1 primary antibody (Abcam 31799) was added to blocking buffer with 1:1000 dilution. Membrane was incubated with primary antibody at 4°C overnight. The membrane was washed three times for 5 minutes each with 10 ml of TBST and processed to secondary antibody incubation (1: 10000 dilution with blocking buffer). The membrane was incubated for 1 hour at room temperature. Then the membrane was washed three times for 5 minutes each with 10 ml of TBST and processed to image developing procedure. Visualization of western blots was performed using the ECL western blotting substrate kit (GE RPN5785) according to the instruction. The membrane was placed on plastic wrap and covered by a sufficient amount of ECL substrate and incubated at room temperature in dark for five minutes. Excess substrate was carefully removed and the membrane was placed in a C-DiGit blot scanner with protein side down.

H. Northern dot blot analysis

1. Total RNA extraction and RNA storage

Sample cells were collected and extract RNA from each sample by standard methods provided by the company (QIAGEN RNeasy mini kit 74104). RNA samples were confirmed by running a 2% electrophoresis agarose gel at 4°C. RNA concentration was tested by a Nanodrop and aliquoted into 5µg RNA for each tube. Samples were stored at -80°C until needed.

2. Sample preparation

One, two and four micrograms of total RNA were resuspended in 1mM EDTA to a final volume of 50 µL (0.5M EDTA, pH8: 186.12 grams EDTA.Na₂.2H₂O with Milli-Q water up to 1L, adjust pH to 8 using 10N NaOH). Then 30µL of 20X SSC (175.3g of NaCl, 88.2g of sodium citrate, add distilled water up to 1L, using 1M HCl to adjust pH to 7.0), 20µL of 37% formaldehyde (Science Company NC-1930) were added to RNA mixture. Samples were transferred on ice after they were incubated at 60°C for 30 minutes.

3. Apparatus preparation and slot blotting

Pour through apparatus slots with vacuum on with 100mL hot water to clean the apparatus. Allow the apparatus to air dry.

Nylon membrane (Positively charged nylon transfer membrane, GE RPN303B) and 3 pieces of Whatman paper were prepared to the size of gasket support plate. Membrane was first soaked in water and then transferred to 10X SSC. Membrane was placed on one piece of bio-dot SF filter paper 60. The SF apparatus was set up as directed by manufacture. Membrane was rehydrated with 200µL 10X SSC per well followed by vacuum applied. Rehydration step was repeated. Five

micrograms of each RNA sample were applied with the vacuum on. The membrane was washed by 200 μ L 10X SSC per well followed by vacuum. The membrane was removed to air dry. UV crosslink was applied for 3 minutes to immobilize samples.

4. Hybridization

The membrane was pre-hybridized for 3 hours at 42°C soaked in pre-hybridization buffer (10% SDS, 100mM Na₂HPO₄ (pH 7.0), 5 μ g/ml salmon sperm DNA). The pre-hybridization buffer was replaced with hybridization buffer with 50 pmol/ml biotin labeled probe. The membrane was then incubated at 42°C overnight. The membrane was washed using washing buffer (1x SSC, 0.1% SDS) for 2 times at room temperature for 15 minutes each and 2 times at 48°C for 20 minutes each (Huang et al., 2014).

5. Detection

The biotin-labeled probes were detected using biotin chromogenic detection kit (ThermoFisher, K0661). After washing, the membrane was incubated with Blocking/Washing buffer for 5 minutes at room temperature with gentle shaking. Then the membrane was blocked with blocking solution for 1 hour at room temperature with moderate shaking. The membrane was then incubated with freshly prepared diluted streptavidin-AF conjugate for 30 minutes at room temperature with moderate shaking. After washing 2 times 15 minutes each using washing buffer, the membrane was incubated with detection buffer for 10 minutes at room temperature with moderate shaking. Finally, the membrane was incubated with freshly prepared substrate solution at room temperature in the dark, allowing the color to develop overnight. Solution was discarded and the membrane was washed with Milli-Q water and air-dry. The result was then documented after one day of air

drying.

I. Reverse Transcriptase Quantitative PCR

DNA removal treatment was applied to total RNA samples (Ambion, AM1906). Treated RNA was collected. RNA concentration was determined by Nanodrop. One microgram of total RNA was used in the following cDNA synthesis reaction (RevertAid First Strand cDNA synthesis kit, ThermoFisher). Synthesized cDNA was used as template in the following RT-qPCR (SYBR Green PCR Master Mix, ThermoFisher). A 1:10 dilution was performed to dilute the synthesized cDNA template. The following PCR reaction mixture and amplification cycle program was used:

PCR Reaction Mixture Components	Amount
SYBR	6.5 μL
cDNA template	3 μL
Forward Primer	0.3 μL
Reverse Primer	0.3 μL
ddH ₂ O	4.9 μL

Step 1= 95°C for 5 minutes

Step 2= 95°C for 12 seconds

Step 3= 54°C for 15 seconds

Step 4= 72°C for 12 seconds

Step 5= go to step 2, 36 cycles

Step 6= 95°C for 10 seconds

Step 7= 65°C for 5 seconds

Step 8= 95°C for 50 seconds

CHAPTER III

AN INVESTIGATION OF THE MISREADING FREQUENCY IN DIFFERENT MAMMALIAN CELL LINES

Chapter III. AN INVESTIGATION OF THE MISREADING FREQUENCY IN DIFFERENT MAMMALIAN CELL LINES

A. Introduction

Translational errors can be divided into three types: processivity errors, frameshift errors and missense errors (Wilson & Nierhaus, 2006). Processivity errors happen due to premature dissociation of a peptidyl tRNA from the ribosome. Changes in reading frame termed frameshift errors lead to a loss of genetic information. Missense errors are caused by incorrect incorporation of an amino acid (Rodnina & Wintermeyer, 2001; Wilson & Nierhaus, 2006). Missense errors can occur during aminoacylation of a tRNA, in which a tRNA is mischarged with an incorrect amino acid by an aminoacyl tRNA synthetase (aaRS). However, most aaRSs have extreme specificity in recognizing their substrate, and some of them have editing mechanisms that can recognize and correct any mischarged tRNA (A. Fersht, 1977). Thus, those properties make the aminoacylation of tRNAs process highly accurate, with error frequency lower than 10^{-5} (Zaher & Green, 2009). Alternatively, missense errors can take place due to incorrect selection of a tRNA by the ribosome during the decoding process leading to the incorporation of a non-encoded amino acid into the newly synthesized protein.

A number of studies have measured various errors involving misreading at each position of the codon-anticodon complex. This research reported missense error frequencies between 10^{-3} and 10^{-4} per codon in bacteria (Parker, 1989). This wide range of error frequency was due to the use of different methods and reporter systems. For example, one of these methods takes advantage of some bacterial proteins that lack a particular amino acid. Thus, incorporation of the amino acid

into a protein represents misreading and can be used to calculate a misreading error rate. For instance, the protein that makes up the bacterial flagellum filament, flagellin, normally contains no cysteine. Incorporation of ^{35}S -labeled cysteine into flagellin was used to measure a misreading frequency for flagellin of 10^{-4} errors per codon translated. This misincorporation of cysteine was due to the first position misreading of arginine codons CGU or CGC by $\text{tRNA}_{\text{GCA}}^{\text{Cys}}$, which normally decodes UGU/UGC (Edelmann & Gallant, 1977). Another method relies on changes in isoelectric point caused by the substitution of a charged amino acid by an uncharged one or vice versa. Errors were quantified by separating variant proteins by isoelectric point using two-dimensional gel electrophoresis (Parker et al., 1978). In an alternative approach, enzyme-based reporter systems were used to estimate error frequency. If a mutation alters an essential amino acid, then it would inactivate the enzyme. If the mutant codon is misread by a tRNA inserting the wild type amino acid, it would restore enzyme activity. Thus, the misreading frequency is calculated as the ratio of the mutant enzymatic activity to the wild type activity. Serine 68 (AGC) of β -lactamase is an essential amino acid because of its nucleophilic side chain. It was mutated to glycine (GGC and GGU), which inactivates β -lactamase activity. Glycine 68 GGC can be misread as serine by $\text{tRNA}_{\text{GCU}}^{\text{Ser}}$ at a frequency of 10^{-3} per codon (Toth et al., 1988).

These experiments have limitations, however. For example, each of them only investigates a few codons misread by a particular tRNA, so that the average of missense error frequencies can only reflect part of all possible errors. Additionally, the fact that error frequency in different experiments was estimated by different methods might make comparisons difficult, as I will discuss below.

To better understand the error frequency of missense errors in vivo, Kramer and Farabaugh developed a dual-luciferase error reporter system that can test all possible near-cognate missense errors at a single position in the firefly luciferase gene by tRNA_{UUU}^{Lys} in both *E. coli* and the yeast *Saccharomyces cerevisiae* (Kramer & Farabaugh, 2007; Kramer et al., 2010). An essential amino acid residue, lysine 529 (K529), was mutated to all possible near-cognate codons that have one nucleotide difference from the wild type Lys codon, and synonymous non-cognate codons that have two or more different nucleotides from the wild type lysine (AAA/AAG) of the firefly luciferase gene (*luc*). The firefly and *Renilla* luciferase genes (*Fluc* and *Rluc*) were fused together to express as a single polypeptide. Thus, the relative concentration of the two enzymes should be identical and any difference of *Fluc* activity relative to *Rluc* activity should reflect a change in the enzymatic activity of firefly luciferase. Based on this method, they estimated error frequencies by tRNA_{UUU}^{Lys} in both *E. coli* and *S. cerevisiae* ranging from 4×10^{-3} to 3×10^{-4} per codon and 6.9×10^{-4} to 4×10^{-5} per codon, respectively.

Two models may explain why some mutant showed higher activities: the functional replacement model and the misreading model. The validity of these two models was tested using synonymous near-cognate and non-cognate codons. Synonymous codons encode the same amino acid as near-cognate codons, for example in the K529 system, the near-cognate arginine codons AGA, AGG are synonymous with the non-cognate codons CGU, CGC, CGA, and CGG. AGA and AGG are near-cognate codons because they are only one nucleotide different from the wild type Lys codons AAA and AAG. The arginine codons CGU, CGC, CGA, and CGG are non-cognate codons because they differ by two or more nucleotides. The functional replacement model states that any luciferase activity in the mutant proteins is due to the mutant amino acid, suggesting all codons that encode the same amino acid should produce the same activity. Thus, this model predicts that

all synonymous non-cognate mutations should produce proteins with the same activity as each other and as the synonymous near-cognates. In contrast, the misreading model states that mutant codons, for example those that encode arginine, are misread by lysyl-tRNA as lysine, resulting in the production of small amount of wild type activity. The synonymous non-cognate arginine codons are unlikely to be misread by lysine tRNA because these codons have two or more mismatches with the anticodon tRNA_{UUU}^{Lys}. Consequently, tRNA_{UUU}^{Lys} will recognize arginine codons CGU, CGC, CGA, and CGG as lysine much less efficiently than it does AGA and AGG. Therefore, these non-cognate codons should result in much lower enzymatic activity. In addition, a significant variation of protein activity between synonymous near-cognate codons also implies that these protein activities are due to misreading but not functional replacement because synonymous near-cognate codons should produce the same amount of activity according to functional replacement model.

Crystal structures of the 30S small subunits with codon and near-cognate tRNA anticodon stem loops showed that binding of a cognate tRNA induces a global conformational change in the 30S subunit. These movements include rotations of the head toward the shoulder and the subunit interface, and rotations of the shoulder (S4, G530 loop with surrounding regions of 16S rRNA and S12) toward to the intersubunit space and the helix 44/27/platform region (Ogle et al., 2002). These alterations led to a transition to a closed form of the 30S subunit (domain closure). However, this domain closure induced by a cognate tRNA binding was found to be unfavorable for near-cognate tRNAs unless in the presence of antibiotic paromomycin. In conclusion, the study suggested that tRNA selection during decoding requires stabilization of a closed 30S conformation.

It is known that ribosomal proteins S12, S4 and S5, which are encoded by *rpsL*, *rpsD*, and *rpsE*,

respectively, can profoundly influence the accuracy of translation in *E. coli* (Ozaki et al., 1969; Rosset & Gorini, 1969; Biswas & Gorini, 1972; Olsson & Isaksson, 1980). The structural model of tRNA selection supports the idea that mutant forms of S12, S4 and S5 affect translational fidelity. Ogle et al. (2002) suggested that the closed form induced by tRNA binding leads to a breakage of the protein-protein interface between S4 and S5, which is located on the back of the subunit body/shoulder area. Mutations in S4 and S5 that disrupt the interface would favor the transition to the closed form by eliminating the energetic cost of separating these contacts. On the other hand, the closed form brings elements of S12, helix 44, and helix 27 closer, leading to the formation of contacts between S12 and the ribosomal RNA. Mutations in S12 would destabilize these interactions with ribosomal RNA. Hence, these mutations lead to antibiotic resistance or dependence and a hyperaccurate phenotype by destabilizing the closed form (James M Ogle et al., 2002). These conformational changes brought by mutant forms of ribosomal proteins explains the effects of S12, S4 and S5 on translational accuracy.

Since mutant forms of ribosomal proteins S12, S4 and S5 disrupt the decoding process, any enzyme activity caused by misreading should also be affected by error modulating mutations. Therefore, these *rpsL* mutations will decrease misreading errors, whereas *rpsD* mutations should increase misreading errors. Kramer and Farabaugh (2007) reported that a mutation in *rpsL* reduced misreading of all potential error-prone codons to near background level activity. Meanwhile, mutations in *rpsD* increased the frequency of misreading of error-prone codons. These data further support the misreading model that high residual activities of those error-prone codons result from misreading events by tRNA_{UUU}^{Lys}.

Kramer and Farabaugh's data showed that the higher activities of some mutant codons were due

to misreading but not functional replacement (Kramer & Farabaugh, 2007; Kramer et al., 2010). In *E. coli*, two arginine codons, AGG and AGA, are frequently misread as shown by the higher Fluc activities for these mutants. AGA and AGG are decoded by one of the least abundant tRNAs in *E. coli* (Dong et al., 1996). Thus, frequent misreading of AGG and AGA by tRNA_{UUU}^{Lys} could be due to a low abundance of the correct tRNA_{UCU}^{Arg}. If so, excess tRNA_{UCU}^{Arg} should reduce the misreading frequencies of AGA and AGG. To address this question, Kramer and Farabaugh overexpressed the cognate tRNA_{UCU}^{Arg}, and found that the missense error frequencies were significantly decreased, strongly suggesting that a competition between a correct (cognate) tRNA and incorrect (near-cognate) tRNA modulates misreading error frequency (Kramer & Farabaugh, 2007).

Translational accuracy has been widely and intensively studied in both prokaryotes and eukaryotes (Edelmann & Gallant, 1977; Parker et al., 1978; Toth et al., 1988; Parker, 1989; Salas-Marco & Bedwell, 2005; Kramer & Farabaugh, 2007; Kramer et al., 2010; Manickam et al., 2014; Manickam et al., 2016). Surprisingly, only a few experiments have focused on translational fidelity in mammalian cells. Estimation of error frequencies in mammalian cells range from 10⁻¹ to 10⁻⁵ errors per codon largely depending on the type of measurement, the tRNA that performs misreading, and the position of codon that was studied (Kurtz, 1975; Parker et al., 1978; Mori et al., 1985; Luce & Bunn, 1989;).

One of the methods to measure misreading frequency in mammalian cells relied on testing the amount of incorporation of a new amino acid that is known not to exist in some proteins *in vitro* (Kurtz, 1975; Mori et al., 1985; Luce & Bunn, 1989). For example, polyuridylic acid (poly (U)), which encodes polyphenylalanine, was used as misreading template that was translated using

microsomes prepared from the livers of mice of various ages. The incorporation of L-[¹⁴C] Phenylalanyl-tRNA and L-[¹⁴C] leucyl-tRNA were compared to measure misreading frequency. The misreading assay measured the amount of leucine incorporation due to translational error relative to phenylalanine incorporation due to correct translation of the poly (U) template. The error frequency was reported to be as high as one in ten per codon in young mouse liver and one in 100 per codon in old mouse liver (Kurtz, 1975).

Another experiment exploited the fact that the coat protein of the cowpea variant of tobacco mosaic virus (CcTMV) contains no cysteine or methionine. Thus, incorporation of cysteine into this coat protein would represent a translational error event. A study was performed in extracts from human diploid fibroblasts of different ages. The translational error frequency was calculated as cysteine incorporation/total amino acids in CcTMV, which assumed that all codons sites had equal chance to be misread as cysteine. The study reported that the error frequency was a range from 4.2×10^{-5} cysteine/amino acid to 2.9×10^{-4} cysteine/amino acid (Luce & Bunn, 1989). This error frequency is calculated as misreading activity divided by all codons, whereas other studies divided the misreading activity by a small subset of codons, which results in a larger error frequency. Given this fact, we are unable to compare misreading error frequencies.

The error frequency from 4.2×10^{-5} to 2.9×10^{-4} is in a reasonable range, but the error frequencies reported from the poly(U) experiment were very likely overestimated because the process of protein translation is more complicated *in vivo* than can be mimicked *in vitro*. For example, essential components for proofreading may not exist *in vitro*, so the sophisticated mechanism of proofreading cannot be replicated and more errors would be detected in these studies.

The wide range of estimated errors resulted from estimating errors based on a limited number of

codons and codon positions in different organisms using different methods. None of these experiments tested all possible missense errors of a codon to give a comprehensive insight into missense error frequencies in human cells. In addition, most earlier studies measured error frequencies in stressed cells, in which errors were stimulated by either antibiotic or amino acid starvation environment. Therefore, the error frequencies would be abnormally higher than those under normal conditions (Parker, 1989). Thus, it is difficult to compare results from different studies and conclude a specific range of missense error frequency in human cells.

To better study translational misreading errors in human cells, I introduced a dual luciferase measuring system into a mammalian plasmid that can be used in mammalian cells. Thus, I was able to measure misreading error frequency by a single tRNA in several mammalian cell lines including HEK293, *HeLa*, 22RV1 and 3T3. My results showed that translation is more accurate in mammalian cells than in *E. coli* and yeast. The variation in misreading error frequency between different codons is smaller than in yeast and or *E. coli*, although a similar subset of error-prone codons in all four cell lines were observed, and most of these had been identified as error-prone in bacteria and yeast. There were differences in error frequency between each cell line yet each one displayed its unique character. This the first study that comprehensively investigates misreading error frequency in mammalian cells at the same codon position by a single tRNA.

B. Results

I. General investigation of misreading error frequencies in several mammalian cell lines

The dual luciferase reporter system depends on two enzymes: *Photinus pyralis* (firefly) luciferase (Fluc), and *Renilla reniformis* (sea pansy) luciferase (Rluc). Both of these enzymes catalyze

reactions that emit light (Figure III-1). Firefly luciferase catalyzes a reaction converting its substrates D-luciferin and ATP to D-luciferyl adenylate, which reacts with oxygen to generate an

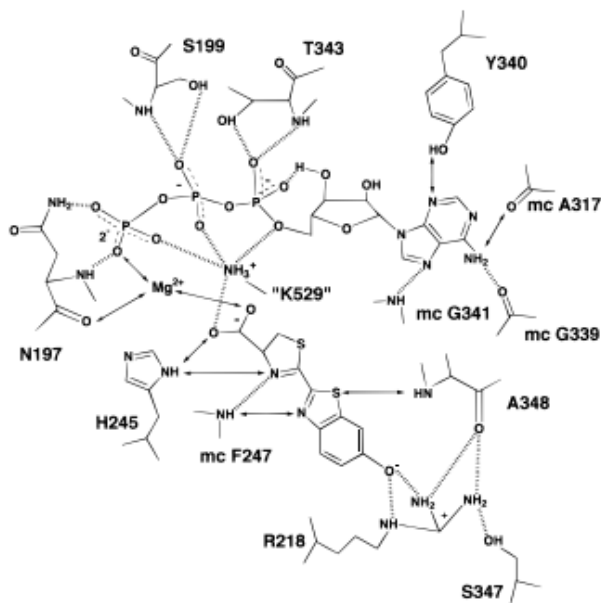


Figure III-1. Model of the firefly luciferase active site

The NH₃ of a lysine residue at position 529 is proposed to orient the substrates luciferin and ATP and is essential for enzymatic activity. The histidine at position 245 is also important for activity (Branchini et al., 2000).

unstable product that then spontaneously breaks down further with release of a photon of light (Branchini et al., 2000). *Renilla* luciferase is an anthozoan coelenterate capable of emitting bioluminescence. *Renilla* luciferase catalyzes the bioluminescent oxidation of *Renilla* luciferin producing light (Matthews et al., 1977; Lorenz et al., 1991). Both Firefly *Photinus pyralis* and *Renilla reniformis* have activity that can be quantified in relative light units (RLUs), which are measured using a luminometer. Biochemistry and mutagenesis studies showed that lysine 529 (K529) is a highly conserved amino acid residue in the adenylate-forming enzyme family and plays an essential role in the firefly luciferase reaction (Branchini et al., 1999). Mutations that were introduced at this residue (K529A and K529Q) caused up to 1,600-fold decrease of the enzymatic activities because of the loss of positive charge; even when researchers introduced arginine at lysine 529, which does not change the charge, the enzymatic activity was reduced up to 625-fold. The lysine side chain of firefly luciferase has multiple contacts with its substrates luciferin and ATP, assisting in the orientation of them and suggesting that no other amino acid residue could replace lysine 529, which further explains the severe loss of activity of the K529 mutants (Branchini et al., 2000)(Figure III-1).

The codons for the wild type lysine (AAA or AAG) were mutated to all possible near-cognate and synonymous non-cognate codons (Kramer & Farabaugh, 2007; Kramer et al., 2010). Our approach is to measure the firefly luciferase activity of K529 mutants. Due to the importance of this amino acid residue, the Fluc activity of K529 mutants should only be minimal because any mutation would produce a protein that fails to make the contacts with the substrate made by Lys. Higher activities of K529 mutants could reflect misreading by $\text{tRNA}_{\text{UUU}}^{\text{Lys}}$.

In an earlier study, Kramer generated all possible near-cognate codons and synonymous non-cognate codons of K529 by replacing one or two or three nucleotides of the codon to test

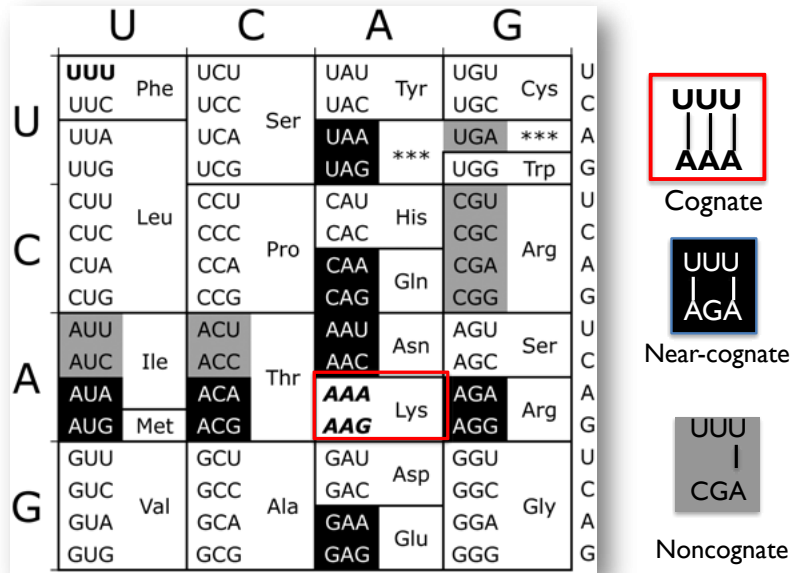


Figure III–2. Near-cognate and synonymous non-cognate mutations for Lysine 529

The two Lysine codons AAA and AAG are shown in italics. Near-cognate codons, which are one position different from Lysine codons, are shown in reverse on black. Non-cognate codons, which are two or more positions different from Lysine codons, are shown in black on grey (Kramer & Farabaugh, 2007).

misreading errors in *E. coli* and the yeast *S. cerevisiae* (Figure III-2) (Kramer & Farabaugh, 2007; Kramer et al., 2010). In the dual luciferase reporter system, Firefly luciferase serves as the experimental protein while Renilla luciferase serves as an internal control. Fluc and Rluc were fused together so they would be expressed as a single polypeptide and their relative concentration should always be identical; any changes in the activity of firefly luciferase relative to *Renilla* luciferase must reflect a change of the activity of Firefly luciferase (Kramer & Farabaugh, 2007; Kramer et al., 2010). Recently, Dr. Nandini Manickam and I introduced all of these mutants to a human expressing vector pcDNA3.1 and termed this human dual luciferase vector pNM. The misreading error frequency is calculated as a ratio of the mutant enzyme activity to the wild type enzyme activity:

$$\text{Error frequency} = \frac{\text{Flucmut/Rlucmut}}{\text{Flucwt/Rlucwt}}$$

Four mammalian cell lines were studied including human embryonic kidney cell HEK293 (Russell et al., 1977), mouse fibroblast cell NIH 3T3 (Jainchill, Aaronson, & Todaro, 1969), human cervical cancer cell line *HeLa* (Harding et al., 1956), and human prostate cancer cell line 22RV1 (Sramkoski et al., 1999). Activities of all possible near-cognate codons of K529 were measured and calculated (Figure III-3).

II. Several codons induce increased misreading frequencies in the human cell line HEK 293

In HEK293 cells, the relative protein activities of near-cognate codons varied by a factor of seventeen in a range of 2×10^{-5} (AAU) to 3.5×10^{-4} (GAA) (Table III-1). A two tailed Student's

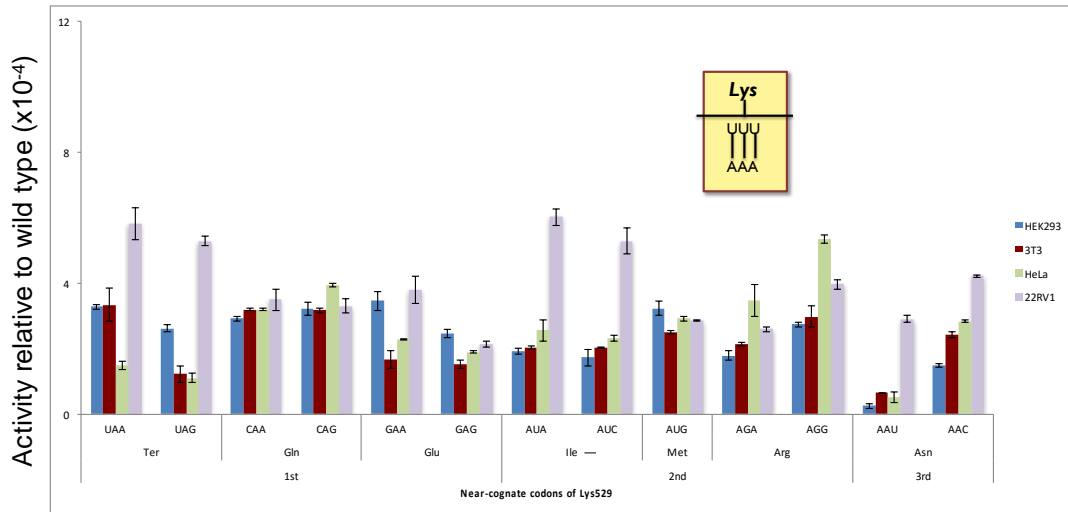


Figure III-3. Mutant Fluc activities of near-cognate codons of K529 in different mammalian cell lines

Blue bar represents activity in HEK293 (n=5); red bar represents activity in 3T3 cell line (n=3); green bar represents activity in *HeLa* (n=3); light purple bar represents activity in 22RV1 cell line (n=4). Mutant bases are underlined. Error bars represent SEM.

Table III-1. Misreading frequency by tRNA^{Lys}_{UUU} at near-cognate codons UUU

Mismatch position	Amino acid	Codon ^a	Mutant activity relative to wild type ($\times 10^{-4}$) ^b (Fold change from HEK293)			
			HEK293	3T3	<i>HeLa</i>	22RV1
1st	Ter	<u>UAA</u>	3.3	<u>3.3(1.0)</u>	1.5(0.5)	5.8(1.8)
		<u>UAG</u>	2.6	1.2(0.5)	1.1(0.4)	5.3(2.0)
	Gln	<u>CAA</u>	2.9	3.2(1.1)	3.2(1.1)	3.5(1.2)
		<u>CAG</u>	3.2	3.2(1.0)	3.9(1.2)	3.3(1.0)
	Glu	<u>GAA</u>	<u>3.5</u>	1.7(0.5)	2.3(0.7)	3.8(1.1)
		<u>GAG</u>	2.5	1.5(0.6)	1.9(0.8)	2.1(0.8)
2nd	Ile	<u>AUA</u>	1.9	2.0(1.1)	2.6(1.4)	<u>6.0(3.2)</u>
		<u>AUC</u>	1.7	2.0(1.2)	2.3(1.4)	5.3(3.1)
	Met	<u>AUG</u>	3.2(1.0)	2.5(0.8)	2.9(0.9)	2.9(0.9)
	Arg	<u>AGA</u>	1.8(1.0)	2.1(1.2)	3.5(1.9)	<u>2.6(1.4)</u>
		<u>AGG</u>	2.7(1.0)	3.0(1.1)	<u>5.3(2.0)</u>	4.0(1.5)
3rd	Asn	<u>AAU</u>	<u>0.2(1.0)</u>	<u>0.6(3.0)</u>	<u>0.5(2.5)</u>	2.9(14.5)
		<u>AAC</u>	1.5(1.0)	2.4(1.6)	2.8(1.9)	4.2(2.8)

^a mutation from a lysine codon (AAA or AAG) is underlined

^b highest and lowest misreading error frequency are in bold and underlined

t-test was used to determine the significance of differences in activity between each set of synonymous codons. The Fluc activity of three of the mutants, GAA (3.5×10^{-4}), AGG (2.7×10^{-4}), and AAC (1.5×10^{-4}), was significantly higher than their synonymous codons GAG (2.5×10^{-4}), AGA (1.8×10^{-4}) and AAU (2×10^{-5}) ($P < 0.05$) (Figure III-4). These differences in activity were not consistent with the functional replacement model but suggested that the activities of these mutants resulted from misreading. I further tested this possibility by comparing activity between synonymous near-cognate and/or non-cognate codons. Another two potential error-prone codons would be termination codons UAA and UAG. The high residual activity of the two termination codons UAA and UAG result from misreading because premature termination should produce a truncated protein that should be inactive. The higher activities of some mutant codons were due to misreading but not functional replacement in *E. coli* and *S. cerevisiae* (Kramer & Farabaugh, 2007; Kramer et al., 2010). Kramer tested these two models via comparing Fluc activity of synonymous mutant codons (Figure III-6). To test these two models, I used the same strategy by comparing the activities of synonymous mutant codons with UAA, UAG, AGA, AGG, and AAC (Figure III-5). Additional synonymous codons are non-cognate codons for $\text{tRNA}_{\text{UUU}}^{\text{Lys}}$ including one termination codon (UGA), four arginine codons (CGU, CGC, CGA and CGG), and one asparagine codon (AAU) (Figure III-6). The activities of the potential error prone codons (UAA, UAG, GAA, AGG and AAC) were all significantly higher than their synonymous codons ($P < 0.05$). This result was inconsistent with the functional replacement model but supports the misreading model, suggesting that the higher Fluc activities of UAA, UAG, GAA, AGG and AAC resulted from misreading by $\text{tRNA}_{\text{UUU}}^{\text{Lys}}$. The estimated misreading error frequencies at these error-prone codons are in a range of 2.4×10^{-5} (AAU) to 3.5×10^{-4} (GAA) (Figure III-5 and table III-1). Synonymous near-

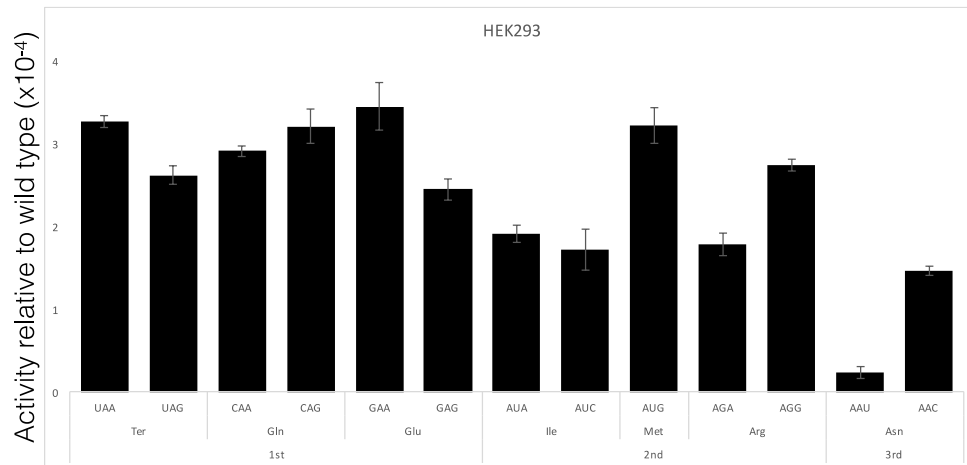


Figure III-4. Variation in Fluc activity of K529 mutants in HEK293 cells

The graph shows the Fluc expression of mutants relative to the expression of wild-type Fluc. The mutants are replacing the AAA K529 codon with the indicated codon. Indicated below each codon is the amino acid it encodes. Error bars are standard errors of the mean.

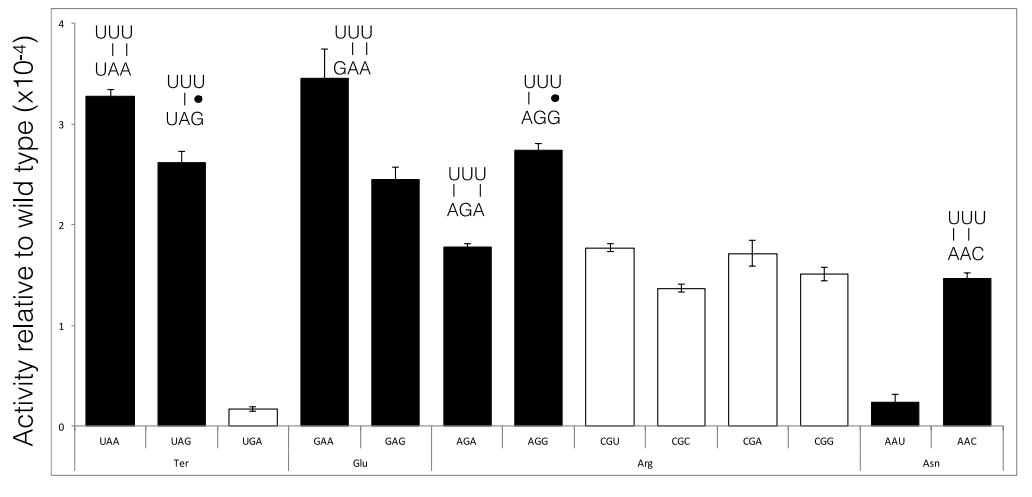


Figure III-5. Comparison of Fluc activity relative to wild type of synonymous near-cognate and non-cognate codons in HEK293 cells

Error bars represent SEM. Codon-anticodon complexes shows misreading events for each mutant that their misreading frequencies differ significantly. The upper line represents anticodon while the lower line represents codon. Vertical lines represent Watson-Crick pairs, filled circle represents wobble pairs and blank represents a mismatch. The error bars represent the standard error of the mean.

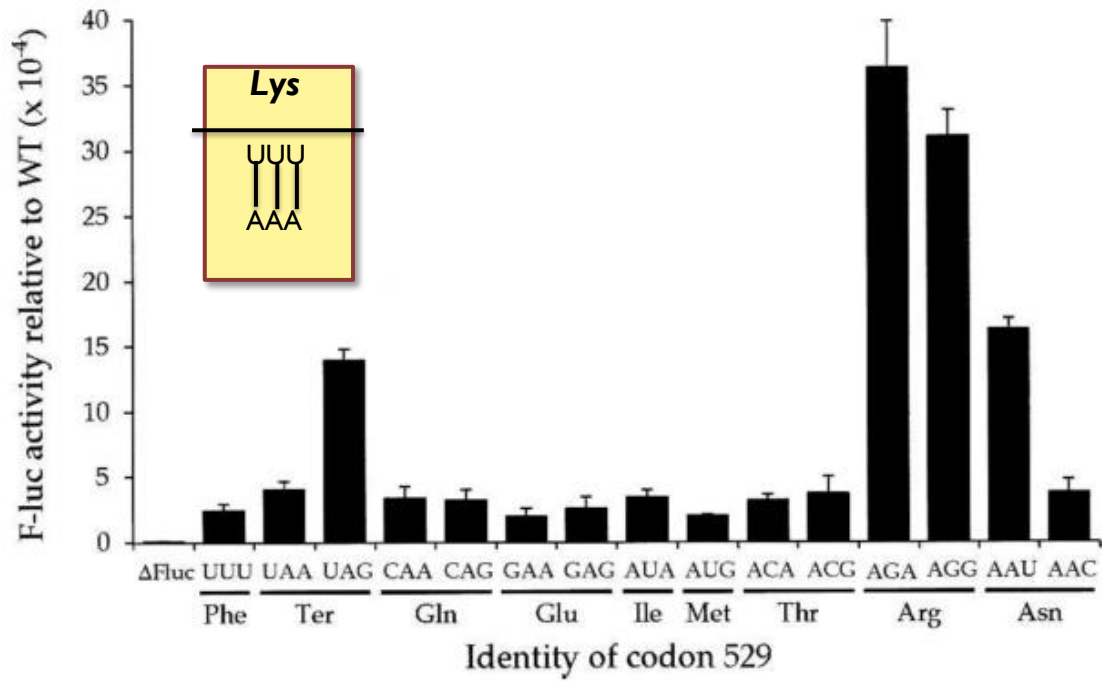


Figure III–6. Mutant Fluc activity of K529 in *E. coli*

Some near-cognate codons showed higher activities than their synonymous codons. This result is consistent with misreading model (Kramer and Farabaugh, 2007).

cognate codons CAA and CAG had similar activities, 2.9×10^{-4} and 3.2×10^{-4} respectively. This result failed to invalidate either the functional replacement model or the misreading model. The similar level of protein activity is consistent with the functional replacement model, however, under the misreading model the two synonymous near-cognate codons also could have the same activity. The only method to further investigate the reason is to measure misreading errors in the presence of factors known to disrupt translational accuracy (e.g. an antibiotic or a mutant ribosomal protein, details will be discussed later) because CAA and CAG do not have synonymous non-cognate codons. The activity of the mutant introducing the isoleucine codon AUA was also not statistically different from its synonymous non-cognate codon AUC; their relative protein activities were 1.9×10^{-4} and 1.7×10^{-4} respectively. Apparently, these activities were caused by functional replacement. Though these data cannot completely rule out the possibility that these increased activities result from errors during tRNA aminoacylation or mRNA transcription, additional data will be presented in a later section.

III. Misreading error frequency shows different features in HEK293 cell line as compared with *E. coli* and yeast

The result obtained with HEK293 cells is qualitatively different from those in yeast and bacteria. The missense error frequency in HEK293 ranged from 2×10^{-5} (AAU) to 3.5×10^{-4} (GAA). The estimated missense error frequencies in *E. coli* ranged from 1.4×10^{-3} (UAG) to 3.6×10^{-3} (AGA) while the missense error frequencies in yeast ranged from 8×10^{-5} (GAA and AAU) to 6.9×10^{-4} (AGG). In general, protein translational errors exhibited smaller variation among near-cognate codons in HEK293 cells compared to *E. coli* and yeast, suggesting that translational fidelity is highest in HEK293, lower in yeast and lowest in *E. coli* (Figure III-6 and Figure III-7).

IV. The distribution of misreading frequencies in *HeLa* is similar to HEK 293 but shows a novel error-prone codon, CAG

No study has been done to measure missense error frequency in multiple mammalian cell lines or organisms. All previous studies used cells or translation extracts from one cell line or animal model. To comprehensively study missense error frequency in mammalian cells, I decided to test multiple cell lines and compare missense error frequency among them. Will error-prone codons be the same in different cell lines? Will the error frequencies be similar or significantly different from each other? The accuracy of protein synthesis is higher in HEK293 compared to *E. coli* and yeast. Will this also be true in other cell lines? Comparing missense error frequency between different cell lines provides a novel and more complete insight into translational fidelity in mammalian cells.

The features of translational fidelity in the immortal *HeLa* cell line were similar to those of HEK293, but a new potential error-prone codon, glutamine codon CAG, was observed. Thus, potential error-prone codons in *HeLa* were UAA, UAG, CAG, AGA, AGG and AAC. Termination codons UAA and UAG again showed protein activity owing to misreading, however their activities were much lower than that in HEK293 and 3T3 cells (Table III-1). Arginine AGG showed the highest protein activity, 5.3×10^{-4} per codon, while AAU showed the lowest, 5×10^{-5} (Table III-1 and Figure III-8).

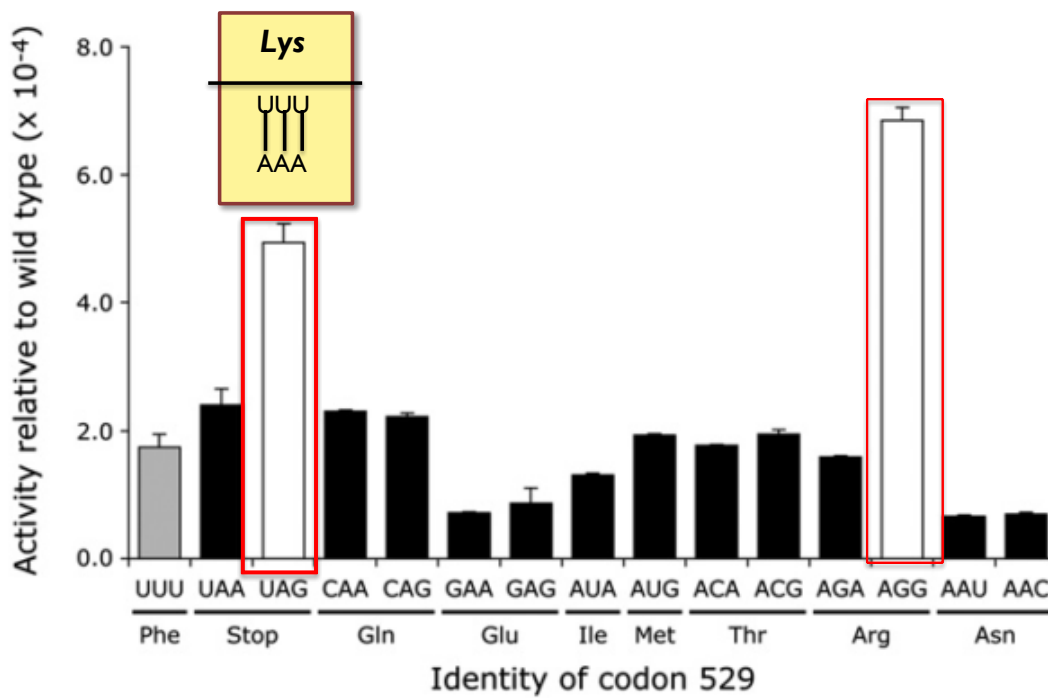


Figure III-7. Variation in mutant Fluc activity of K529 in yeast

Near-cognate codons UAG and AGG showed significantly higher activities than their synonymous codons. Again, this phenotype supports misreading model but not functional replacement (Kramer et al., 2010).

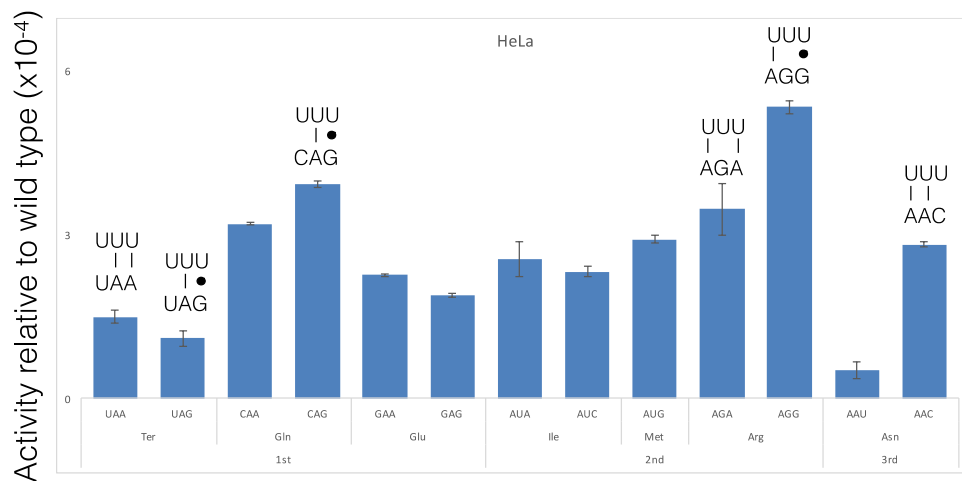


Figure III–8. Comparison of Fluc activity relative to wild type of synonymous near-cognate and non-cognate codons in *HeLa* cells

Error bars represent SEM. Codon-anticodon complexes shows misreading events for each mutant that their misreading frequencies differ significantly. The upper line represents anticodon while the lower line represents codon. Vertical lines represent Watson-Crick pairs, filled circle represents wobble pairs and blank represents a mismatch. The error bars represent the standard error of the mean.

V. Prostate cancer cell line 22RV1 has the highest error frequency among all the cell lines

Analysis of the cell line 22RV1, a prostate cancer cell line, showed the highest error frequencies among all the cell lines tested (Figure III-3 and Table III-1). Stop codon UAA and UAG, glutamic acid codon GAA, arginine codon AGG and asparagine codon AAC were potential error-prone codons (Figure III-9). The estimated error frequency ranged from 2.6×10^{-4} (AGA) to 6.0×10^{-4} (AUA) (Table III-1). Termination codons UAA and UAG showed higher error frequencies than in the other cell lines. Interestingly, isoleucine codon AUA also showed very high activity, however, the data indicated this high activity was due to functional replacement because its synonymous non-cognate codon AUC had the similar level of Fluc activity. Among the four cell lines, wobble errors at the codon AAU and AAC are the highest in 22RV1. (Figure III-3 and Figure III-9).

VI. The distribution of misreading frequencies in NIH 3T3 cell line is the same as in HEK 293 but did not show errors at codon GAA and CAG

I was also interested in measuring missense errors in a related mammalian species using mouse cell line NIH 3T3. In 3T3 cells, activity of mutant forms of K529 showed a pattern similar to the three human cell lines, however, misreading at GAA and CAG was not observed. Error-prone codons include UAA (3.3×10^{-4}), UAG (1.2×10^{-4}), AGG (3.0×10^{-4}) and AAC (2.4×10^{-4}) (Table III-1 and Figure III-10). For these codons, the activities of synonymous codons were statistically different ($P < 0.05$). For others, synonymous codon mutants did not have different activities. The glutamine CAA and CAG had

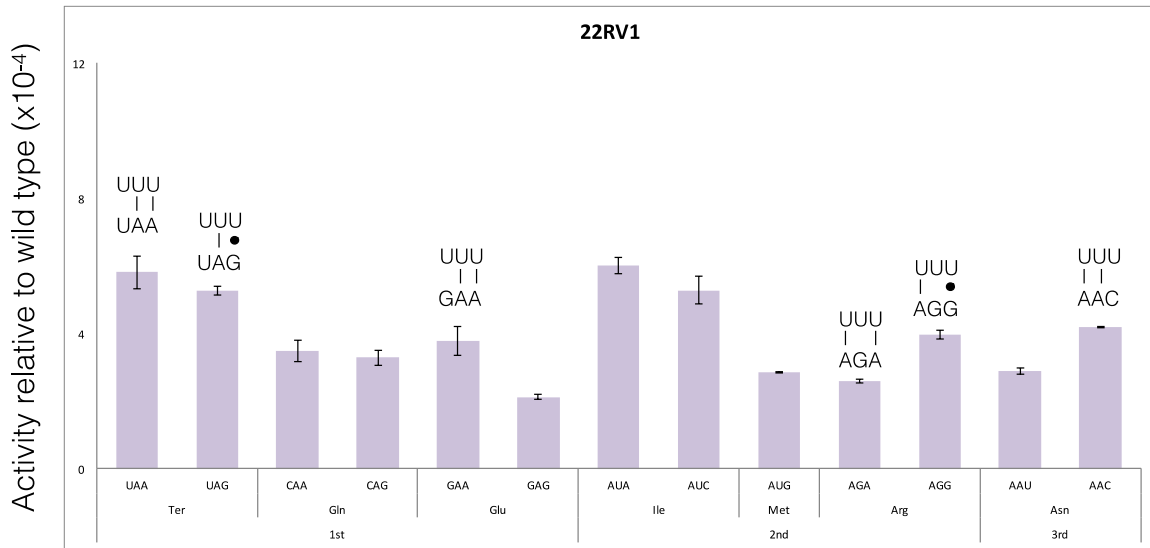


Figure III–9. Comparison of Fluc activity relative to wild type of synonymous near-cognate and non-cognate codons in 22RV1 cells

Error bars represent SEM. Codon-anticodon complexes shows misreading events for each mutant that their misreading frequencies differ significantly. The upper line represents anticodon while the lower line represents codon. Vertical lines represent Watson-Crick pairs, filled circle represents wobble pairs and blank represents a mismatch. The error bars represent the standard error of the mean.

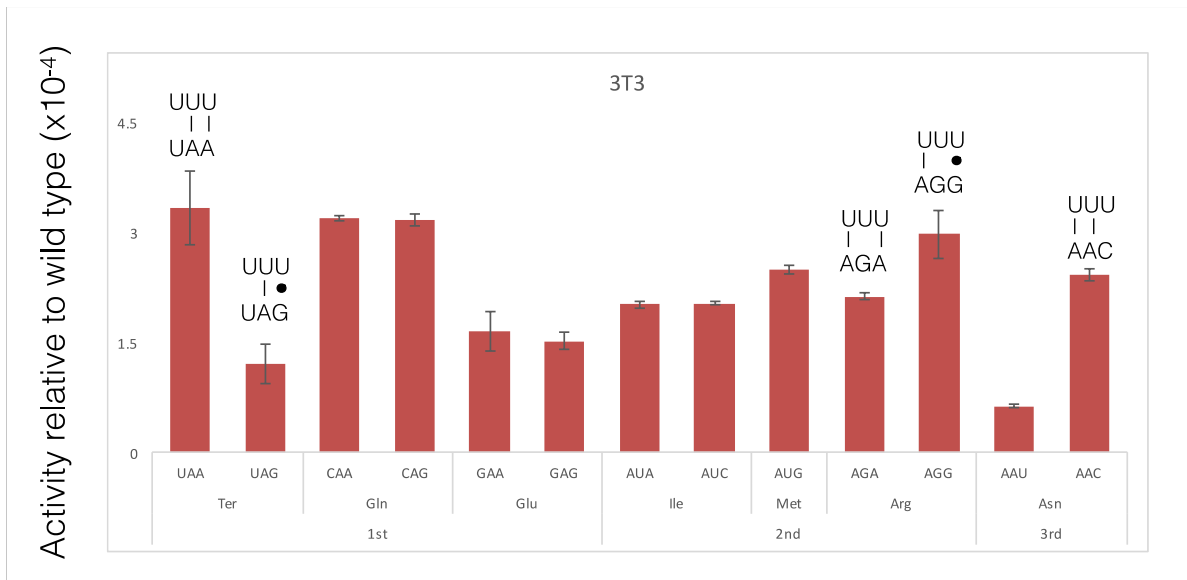


Figure III–10. Comparison of Fluc activity relative to wild type of synonymous near-cognate and non-cognate codons in mouse 3T3 cells

Error bars represent SEM. Codon-anticodon complexes shows misreading events for each mutant that their misreading frequencies differ significantly. The upper line represents anticodon while the lower line represents codon. Vertical lines represent Watson-Crick pairs, filled circle represents wobble pairs and blank represents a mismatch. The error bars represent the standard error of the mean.

an activity of 3.2×10^{-4} ; glutamic acid GAA and GAG showed activity of 1.7×10^{-4} and 1.5×10^{-4} respectively; isoleucine AUA and its synonymous non-cognate codon AUC had the same level of activity, which was 2.0×10^{-4} . Thus, these codons are apparently not error-prone codons because synonymous codons produce the similar amount of activity. The misreading frequency in 3T3 varied from the lowest asparagine codon (AAU) 6×10^{-5} to the highest frequency termination codon (UAA) 3.3×10^{-4} (Table III-1 and Figure III-10).

VII. Comparison of error frequency codon by codon in all the four mammalian cell lines

The frequency of misreading of some error-prone codons ranged differently in various cell lines. Fold change was calculated by dividing the error frequency in 3T3, *HeLa*, or 22RV1 by the frequency in HEK293 (Table III-1). The frequency of misreading of UAA ranged from 1.5×10^{-4} to 3.3×10^{-4} in the four cell lines (Table III-1). There is no difference of error frequency of UAA between HEK293 and 3T3 cell line. But the frequency of errors at UAA in *HeLa* is only half of that in HEK293. In the meantime, the error frequency in 22RV1 was nearly 2-fold higher than that in HEK293. The frequency of UAG distributed differently when compared to UAA. The error frequencies of UAA in 3T3 and *HeLa* were only half of that in HEK293, while 22RV1 again had 2-fold higher error frequency than that in HEK293. The frequency of stop codons showed that 22RV1 had the most frequent misreading events of UAA and UAG by tRNA_{UUU}^{Lys}, whereas *HeLa* showed the least error frequency of the two stop codons. The fact that the two cancer cell lines possess opposite levels of misreading frequencies of UAA and UAG is very interesting (detailed discussion below).

Other sense codons also display distinct error frequencies in the four cell lines. The activities of GAA and GAG in 3T3, *HeLa*, and 22RV1 were all lower than that in HEK293. Isoleucine codons

AUA and AUC are not error-prone codons but they had very high activities in 22RV1 as compared to the other three cell lines. The error frequencies occurring at AGA and AGG were quite similar in HEK293, 3T3 and 22RV1 but the frequency in *HeLa* is about two-fold higher than that in HEK293. The frequencies of AAU and AUG spread widely that both of them showed the lowest frequency in HEK293. The activity of AAU in 3T3 was 3-fold higher than that in HEK293 meanwhile the activity was almost 15 times higher in 22RV1 than that in HEK293. The differences of the activity of AAU between HEK293 and 22RV1 seem enormous, however one must pay attention that the activities of AAU in HEK293, 3T3 and *HeLa* were only comparable to the background. The frequencies of AAC in the four cell lines showed the similar pattern as AAU. The frequency was the lowest in HEK293, and 3T3 and *HeLa* had the median error frequency compared to HEK293. The frequency of AAC was about 3-fold higher than that in HEK293. There was no obvious difference of the activity of CAA, CAG, AUG in the four cell lines.

Overall, the five codons: the termination codons UAA and UAG, arginine codon AGA, AGG, and asparagine codon AAC are potential error-prone codons in all four cell lines despite the fact that they had different activities in various cell lines. Moreover, there are two novel putative error-prone codons. Glutamine codon CAG is an error-prone codon in *HeLa*, while the glutamic acid codon GAA is error-prone in HEK293 and 22RV1. In addition, the ranges of mutant Fluc activities were different in each cell line (Table III-1 and Table III-2).

VIII. Does variation in misreading of termination codons reflect differences in the abundance of peptide release factors?

Translation termination occurs when a stop codon (UAA, UAG or UGA) enters the A site. Two enzymes catalyze translation termination in eukaryotes, eukaryotic release factor 1 (eRF1) and 3 (eRF3). eRF1 recognizes stop codons and hydrolyzes peptidyl-tRNA. eRF3 accelerates peptide release and boosts termination efficiency at stop codons (Dever & Green, 2012).

The variation of protein activities at stop codon UAA and UAG prompted me to speculate that the abundance of eRF1 and eRF3 may play a critical role in this process. To address this question, I performed both western blotting and reverse transcriptase quantitative PCR (qPCR) (Figure III-11 and Figure III-12) to test the abundance of eRF1 and eRF3 at both translational and transcriptional levels in different cell lines. Ten micrograms of total protein of each was loaded and detected using eRF1 antibody and eRF3 antibody. β -actin was also detected as a loading control to normalize blot intensity. As shown in Figure III-11 A and B, the difference of eRF1 protein expression between HEK293, 22RV1 and 3T3 was not significant, however, *HeLa* had slightly lower expression than the other three cell lines ($P < 0.05$). Results from qPCR showed that *HeLa* also expressed less of the eRF1 transcript than the other three ($P < 0.05$). I calculated

Table III-2. Comparison of potential error-prone codons in different cell lines

Cell line	Potential error-prone codons
HEK293	UAA,UAG, <u>GAA</u> ,AGA,AGG,AAC
3T3	UAA,UAG,AGA,AGG,AAC
<i>HeLa</i>	UAA,UAG, <u>CAG</u> ,AGA,AGG,AAC
22RV1	UAA,UAG, <u>GAA</u> ,AGA,AGG,AAC

All potential error-prone codons in different cell lines are summarized in this table. New observed error-prone codons that only present in one or two cell lines are in bold with underlined.

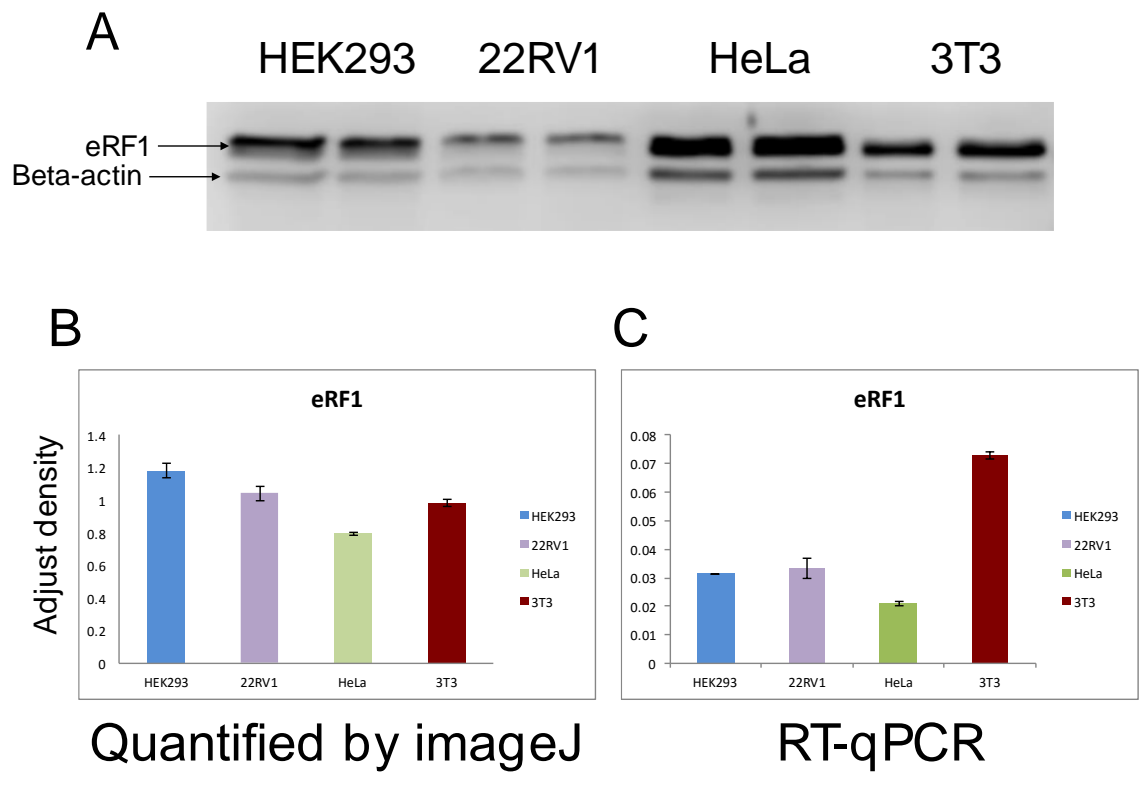


Figure III–11. eRF1 expression level in different cell lines

A) Western blot assay of eRF1 in different cell lines. Protein extraction was performed from each mammalian cell line. 10 μ g of total protein for each sample was loaded and detected using eRF1 antibody and β -actin (loading control). B) Graph showing sample blot intensity of Western blot of eRF1. Each bar represents the ratio of sample intensity of blot of eRF1 to the sample intensity of blot of β -actin. C) qPCR of eRF1. Each color bar represents one cell line, which was indicated under each bar.

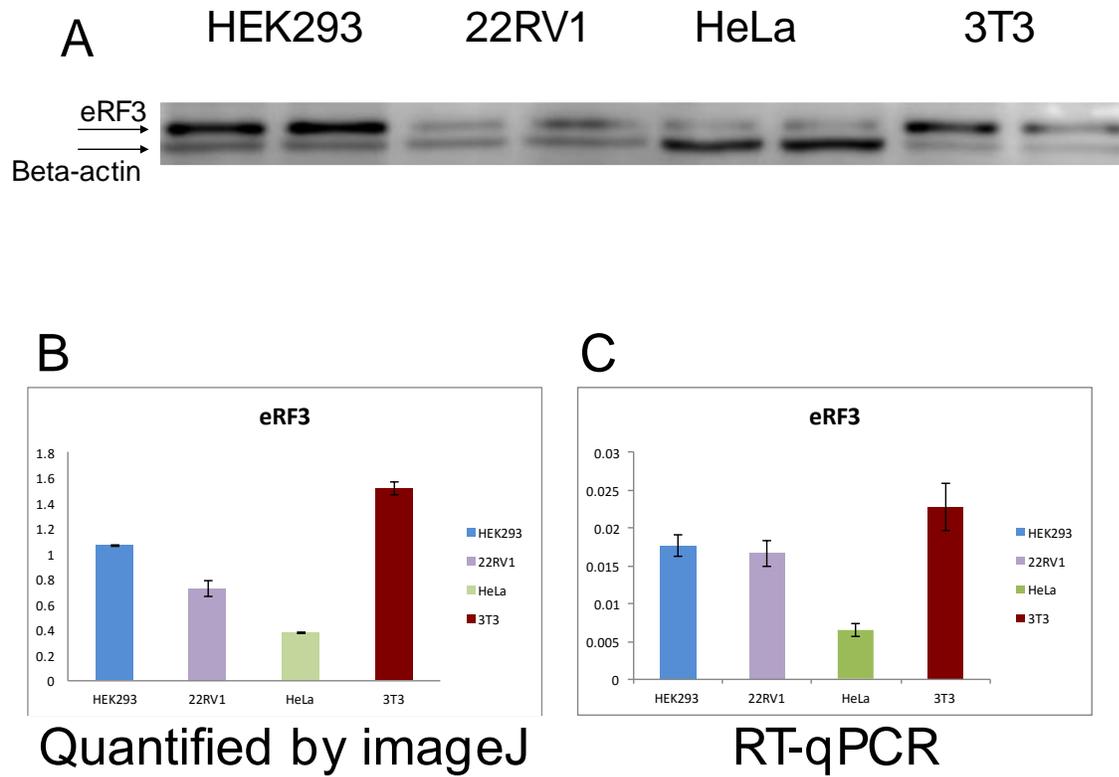


Figure III–12. eRF3 expression level in different cell lines

A) Western blot assay of eRF1 in different cell lines. Protein extraction was performed from each mammalian cell line. 10 μ g of total protein for each sample was loaded and detected using eRF3 antibody and β -actin (loading control). B) Graph showing sample blot intensity of Western blot of eRF1. Each bar represents the ratio of sample intensity of blot of eRF3 to the sample intensity of blot of β -actin. C) qPCR of eRF3. Each color bar represents one cell line, which was indicated under each bar.

normalized protein expression to qPCR (Table III-3) finding that NIH3T3 and 22RV1 had the highest number for eRF1 and eRF3 respectively, suggesting there was more translation per mRNA of eRF1 and eRF3 in NIH3T3 and 22RV1 respectively. In addition, the western blotting result of eRF3 agreed with the result of qPCR in all the four cell lines (Figure III-12). Combining the western blotting data and qPCR data, I can conclude that *HeLa* had the lowest eRF3 expression at both transcriptional and translational level whereas 3T3 had the highest eRF3 expression at both transcriptional and translational level (Figure III-12). 22RV1 had the highest missense error frequency at both UAA and UAG while *HeLa* had the lowest error frequency at both UAA and UAG. If the variation in misreading error was due to the abundance of two termination factors, then I would expect that *HeLa* would have the highest level of termination factors because effective termination process would lead to lower misreading at the termination codons. In contrast, 22RV1 should have the lowest expression of termination factors since 22RV1 had the highest missense error frequencies at both UAA and UAG. However, the western blot and qPCR data were not consistent with the hypothesis. Measurement of eRF1 and eRF3 expression quantitatively did not explain the variation of missense errors at two termination codons UAA and UAG between each cell line.

IX. Aminoglycoside antibiotic G418 increased misreading of some near-cognate mutants in all four cell lines

Aminoglycoside antibiotics are able to disrupt translational accuracy in *E. coli* (Kramer and Farabaugh, 2007). In *E. coli*, the antibiotics paromomycin and streptomycin increased translational error frequencies of the stop codons UAA and UAG, isoleucine

Table III-3. Normalized protein to qPCR expression ratio

Cell line	Normalized protein to qPCR expression ratio	
	eRF1	eRF3
HEK293	1.0	1.1
22RV1	1.2	1.5
HeLa	1.0	1.1
3T3	2.8	1.0

AUA, arginine codons AGA and AGG, and asparagine codons AAU and AAC (Kramer and Farabaugh, 2007). However, in yeast, paromomycin only increased inaccuracy of UAA, UAG, and marginally increased error frequency of AAU (Kramer et al., 2010).

In mammalian cells, G418 has been shown to increase readthrough frequency for both termination codons UAA and UAG (Phillips-Jones et al., 1995). In fact, many studies have used G418 to drive premature termination codon readthrough, suggesting that it might be utilized as a molecular treatment for nonsense mutation disease (Azimov et al., 2008; Cogan et al., 2014). However, so far G418 has not been shown to induce misreading errors at sense codons in mammalian cells. Thus, I measured the activity of the K529 near-cognate and non-cognate codons of Fluc in the presence and absence of G418. G418 is commonly used as a selective drug from stable transfection in mammalian cells. Different tolerance to G418 exists. To ensure the viability of cells, different cell lines were cultured on various concentrations of G418: 50 $\mu\text{g/ml}$ in HEK293, 100 $\mu\text{g/ml}$ in *HeLa*, 50 $\mu\text{g/ml}$ and 200 $\mu\text{g/ml}$ in 3T3. I observed that, in addition to affecting the two termination codons UAA and UAG, G418 also increased translational error frequencies of a subset of K529 mutant codons (Figure III-13 to Figure 15). In the presence of G418, error frequencies of UAA, UAG, AGA and AAC were increased in HEK293; error frequencies of UAA, UAG, CAA, AGA and AAC were increased in *HeLa*; and error frequencies of only UAG and AUG were increased in 3T3.

Of all cell lines tested, misreading in HEK293 cells was the most sensitive to G418 (Figure III-13). The error frequency on the stop codons UAA and UAG was dramatically increased with 8 and ~18-fold change when cells were exposed to G418 (student's *t* test,

P<0.001). Error frequencies on the arginine codon AGA, and the asparagine codon AAC were also increased but to a lesser extent, showing a fold change of 2.3 and 4.3 respectively (Figure III-13).

G418 induced misreading of the error-prone codons UAA, UAG, AGA and AAC in *HeLa* cells and induced misreading of one codon, CAA, that was not error-prone in its absence. The error frequency on the stop codon UAA increased 3.4-fold, and on the UAG it increased 6-fold. The error frequency at CAA slightly increased, about 1.5-fold. Misreading was induced by G418 less on the other codons, on AGA 1.8-fold and on AAC 2-fold (Figure III-14). The effect of G418 in *HeLa* was generally much smaller than on HEK293 despite the fact that HeLa was treated with twice the level of G418 received by HEK293. For example, the nonsense codons UAA and UAG were much more affected in HEK293 cells (8-fold and 18.3-fold respectively) than in HeLa (3.4- and 6-fold).

Among all the three cell lines, the NIH 3T3 cell line was the least sensitive to G418, and displayed the lowest increase of misreading errors in the presence of G418 (Figure III-15). Originally, 3T3 cells were exposed to a final concentration of 50 µg/ml G418. However, there was no effect on any codons being misread except UAG increased 3.25-fold, and AAU increased 6-fold. In an earlier study, 400 µg/ml of G418 had been used for stable selection in 3T3 cells suggesting 400 µg/ml of G418 has the ability of kill most of the cells. Accordingly, I increased the concentration of G418 from 50 µg/ml to 200 µg/ml, to test its effect on translational errors without affecting the viability of cells. Nevertheless, the influence of G418 was not greatly increased. Misreading errors on

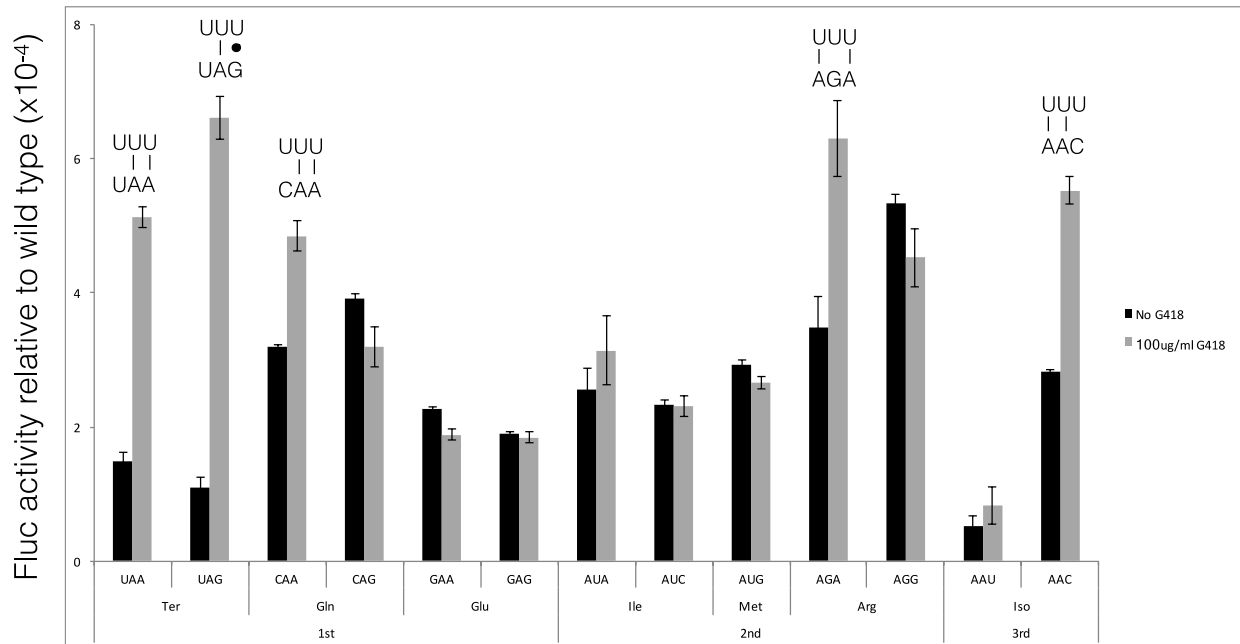


Figure III–14. Effect of G418 on translational fidelity in *HeLa* cells

Black bar represents non-treatment group; grey bar represents 24-hour G418 treatment with 100 µg/ml final concentration (n=2). Error bars represent SEM.

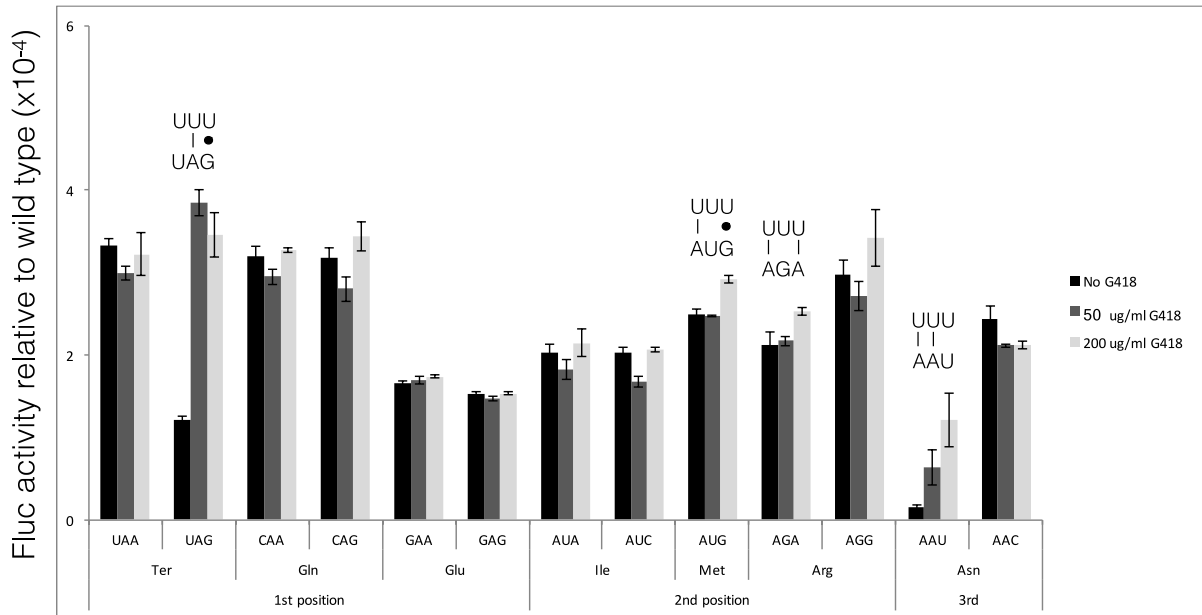


Figure III-15. Effect of G418 on translational fidelity in 3T3 cells

Black bar represents non-treatment group; dark grey bar represents 24-hour G418 treatment with 50 µg/ml final concentration; grey bar represents 24-hour G418 treatment with 200µg/ml final concentration (n=2). Error bars represent SEM.

AAU, AUG and AGA were each 1.2-fold; stop codon UAG had the same level of increase even with 200 µg/ml of G418 (Figure III-15 and table III-3). 3T3 is the only cell line that had a significant difference of misreading error frequency at AAU induced by G418.

Misreading errors in HEK293 showed the highest effect of G418 compared with the other two cell lines on the codons UAA (8-fold), UAG (18-fold), AGA (2.3-fold) and AAC (4.3-fold) (Table III-4). In general, HEK293 and 3T3 had the similar level of misreading error frequency except GAA had higher activity in HEK293 than in 3T3 cells (Table III-4). The probable reason why HEK293 is affected most by G418 will be discussed in the discussion section.

X. Mutant forms of human ribosomal protein S23 did not affect translational accuracy in HEK293 cells

Some small subunit ribosomal proteins play a crucial role in translational fidelity. Ribosomal proteins S4, S5 and S12 (encoded by the *rpsD*, *rpsE* and *rpsL* genes, respectively) can greatly affect translational accuracy in *E. coli*. Mutations in S4 and S5 reduce translational accuracy, and make a strain hypoaccurate; while mutations in S12 reduce translational errors, and make a strain hyperaccurate (Bouadloun et al., 1983; Davies, 1964).

Mutations in *rpsL* were first found to confer streptomycin resistance and dependence phenotype in bacteria *E. coli* (Newcombe & Nyholm, 1950). Other scientists explored the mechanism of streptomycin altering phenotypes in bacteria *E. coli* (Spotts & Stanier,

Table III-4. Mutant activity relative to wild type in HEK293, HeLa, and 3T3 with and without the presence of G418

Mismatch position	Amino acid	Codon ^a	Mutant activity relative to wild type (x10 ⁻⁴)										
			HEK293			HeLa			3T3				
			NO 418	50ug/ml G418	Fold change	No G418	100ug/ml G418	Fold change	No G418	50 ug/ml G418	Fold change	200 ug/ml G418	Fold change
1st	Ter	<u>U</u> AA	3.3	26.6	8.0^b	1.5	5.1	3.4	3.3	3.0	0.9	3.2	1.0
		<u>A</u> AG	2.6	47.6	18.3	1.1	6.6	6	1.2	3.9	3.3	3.5	3.0
		<u>G</u> GA	0.2	0.2	1.0	n.d ^a							
	Gln	<u>C</u> AA	2.9	3.0	1.0	3.2	4.8	1.5	3.2	2.9	0.9	3.3	1.0
		<u>A</u> AG	3.2	3.3	1.0	3.9	3.2	0.8	3.2	2.8	0.9	3.4	1.1
		<u>G</u> GA	3.5	3.0	0.9	2.3	1.9	0.8	1.7	1.7	1.0	1.7	1.0
2nd	Glu	<u>G</u> AG	2.5	1.9	0.8	1.9	1.8	0.9	1.5	1.5	1.0	1.5	1.0
		<u>A</u> U <u>U</u>	1.2	1.0	0.8	n.d ^a							
		<u>A</u> U <u>C</u>	1.7	1.7	1.0	2.3	3.1	1.3	2.0	1.8	0.9	2.1	1.1
	Met	<u>A</u> U <u>A</u>	1.9	2.0	1.0	2.6	2.3	0.8	2.0	1.7	0.9	2.1	1.1
		<u>A</u> U <u>G</u>	3.2	2.9	0.9	2.9	2.7	0.9	2.5	2.5	1.0	2.9	1.2
		Arg	<u>A</u> G <u>A</u>	1.8	4.1	2.3	3.5	6.3	1.8	2.1	2.2	1.0	2.5
<u>A</u> G <u>G</u>	2.7		2.5	0.9	5.3	4.5	0.8	3.0	2.7	0.9	3.4	1.1	
<u>C</u> G <u>U</u>	1.8		1.8	1.0	n.d ^a	n.d ^a	n.d ^a	n.d ^a	n.d ^a	n.d ^a	n.d ^a	n.d ^a	
3rd	Asn	<u>A</u> A <u>U</u>	0.2	0.4	2	0.5	0.8	1.6	0.1	0.6	6	1.2	12
		<u>A</u> A <u>C</u>	1.5	6.5	4.3	2.8	5.5	2.0	2.4	2.1	0.9	2.1	0.9

^aNot determined

^bFold change of mutants have significant difference of error frequency in the absence and presence of G418

1961; Cox et al., 1964; Davies, 1964). Spotts and Stanier hypothesized that streptomycin dependent mutations targeted ribosomes, causing slight modifications in the structure of ribosomes (Spotts & Stanier, 1961). Later, studies showed that the streptomycin resistance phenotype is associated with mutations affecting the 30S ribosomal subunit (Cox et al., 1964; Davies, 1964). Davies showed that streptomycin induced mistranslation *in vitro* and that mutations to streptomycin resistance (*rpsL*) block streptomycin-induced errors during translation (Davies, 1964), while wild type ribosomes were vulnerable to streptomycin-induced mistranslation (Gorini & Kataja, 1964). Further study showed that streptomycin resistant ribosomes have lower translational error rates than wild type ribosomes (Anderson et al., 1965).

Mutations of S12 increase accuracy, whereas “ribosomal ambiguity mutations” (*ram*) in S4 or S5 decrease accuracy and increase sensitivity to antibiotics (Strigini & Brickman, 1973; Parker & Friesen, 1980; Bouadloun et al., 1983; Parker & Holtz, 1984; Precup & Parker, 1987; Toth et al., 1988). Our lab has found that a mutation in *rpsL* (K42N) significantly decreased translational error frequency of error-prone codons in *E. coli* (Kramer & Farabaugh, 2007). Moreover, a deletion of nucleotides C528-A532 in *rpsD* results in a truncated S4 protein, significantly increased misreading of a subset of the codon 529 mutations (Kramer & Farabaugh, 2007). These results further provide evidence that mutant forms of S4 and S12 can affect translational fidelity in *E. coli*.

In the yeast *Saccharomyces cerevisiae*, *SUP44* and *SUP46* encode ribosomal protein S4 and S13, which are homologs of the *E. coli* S5 and S4. Mutations in *SUP46* and *SUP44*, leading to “omnipotent suppressor” that can suppress all three nonsense mutations and increase sensitivity to the aminoglycoside antibiotic paromomycin, cause similar phenotypes to the *ram* mutations in *E. coli* (Wakem & Sherman, 1990; Ishiguro et al., 1981).

RPS23, encoded by the *RPS23A* and *RPS23B* genes, is the homologue of prokaryotic S12 (encoded by the *rpsL* gene). By using site-directed mutagenesis, Alksne et al. (1993) introduced a set of mutations into the ribosomal protein S23, which substitute Lys 62 with arginine, threonine, glutamine and asparagine. They then substituted the mutant gene for one of the wild type genes in the wild type strain and in *SUP44*- and *SUP46*- containing strains, which suppress both the amber (UAG) *met8-1* allele and the ochre (UAA) *leu2-1* allele, to enable a phenotypic screening. The data showed that amino acid substitution (K62N, Q, T and R) altered translation fidelity in yeast. Mutation K62N, Q and T increased translational accuracy and decreased antibiotic sensitivity as was observed in *E. coli*, whereas K62R substitution caused more translational errors and increased sensitivity to the drug. Together, this study suggested that this conserved ribosomal protein (rpS12 in *E. coli* and rpS23 in yeast) has the same function in regulating translational fidelity in bacteria and yeast (Alksne et al., 1993)

Human ribosomal protein S23 (RPS23) gene is homologous to yeast RPS23. Human ribosomes and yeast ribosomes are very alike except that human ribosomes are larger because of more eukaryotic extensions of both rRNA and ribosomal proteins. However, the functions of most ribosomal proteins are highly conserved in all eukaryotes (Anger et al., 2013). A blast comparison of the human and yeast RPS23 shows that the two proteins are 78% identical and 90% similar (Table III-5). Based on the alignment of the two genes, the same amino acid substitution K62R and T were introduced in human RPS23 (K60R and T) to address the question that if mutant forms of human RPS23 can affect translational accuracy.

Table III-5. Alignment of the yeast and human ribosomal protein S23

40S ribosomal protein S23 [Homo sapiens]

Sequence ID: [gi|4506701|NP_001016.1](#) Length: 143 Number of Matches: 1

[▶ See 11 more title\(s\)](#)

Range 1: 2 to 143 [GenPept](#) [Graphics](#) ▼ Next Match ▲ Previous Match

Score	Expect	Identities	Positives	Gaps
231 bits(590)	1e-78	111/142(78%)	128/142(90%)	0/142(0%)
Query 4	GKPRGLNSARKLRVHRRNNRWAENNYKKRL	LGTA	K++PFGG+SHAKGIVLEKLGIES	KC 63
Sbjct 2	GK RGL +ARKLR HRR+ +W + YKK	LGTA	K++PFGG+SHAKGIVLEK+G+E	KC 61
Query 64	PNSAIRKCVRVQLIKNGKKVTAFVPNDGCLNFVDENDEVLLAGFGRKGKAKGDIPGVRFK			123
Sbjct 62	PNSAIRKCVRVQLIKNGKK+TAFVPNDGCLNF++ENDEVL+AGFGRKG A GDIPGVRFK			121
Query 124	VVKVSGVSLALWKEKKEKPRS	145		
Sbjct 122	VVKV+ VSLLAL+K KKE+PRS	143		

I first cloned wild type human RPS23 gene to pcDNA3.1. Using site directed mutagenesis, I mutated RPS23 at K62 to arginine (R) and threonine (T) respectively. Co-transfection was performed to express both exogenous RPS23 and the dual luciferase reporter system in HEK293 cells. Then I measured the Fluc activity of several of the K529 near-cognate mutants in HEK293 cells carrying mutations. Neither mutant form of RPS23, the hypoaccurate mutant nor the hyperaccurate mutant, significantly affected translational accuracy in HEK293 cells (Figure III-16 and Table III-6). In the hypoaccurate background, *rpS23* K60R mutant only slightly increased misreading frequency of arginine codon AGA from 2.1×10^{-4} to 2.3×10^{-4} while no other mutants were affected. In the hyperaccurate background, *rpS23* K60T mutant only reduced misreading error frequency of asparagine codon AAC from 2.5×10^{-4} to 2.4×10^{-4} (Figure III-16 and Table III-6). Anthony and Liebman hypothesized that the mutants they found are likely applicable to other eukaryotic ribosomes because eukaryotic ribosomal proteins are highly conserved (Anthony & Liebman, 1995). However, my data is not consistent with their hypothesis. One possibility is the endogenous activity of wild type RPS23 rescues any defects despite that the mutations are dominant. Alternatively, transiently expressed mutant form of RPS23 led to insufficiently populated ribosomes (more details will be discussed in the discussion section).

C. Discussion

Using mutant versions of the firefly luciferase gene with all possible single point mutants at essential amino acid residual lysine 529, I was able to measure misreading errors by tRNA_{UUU}^{Lys} in HEK293, 3T3, *HeLa*, and 22RV1 cell lines. Seven of thirteen mutant codons

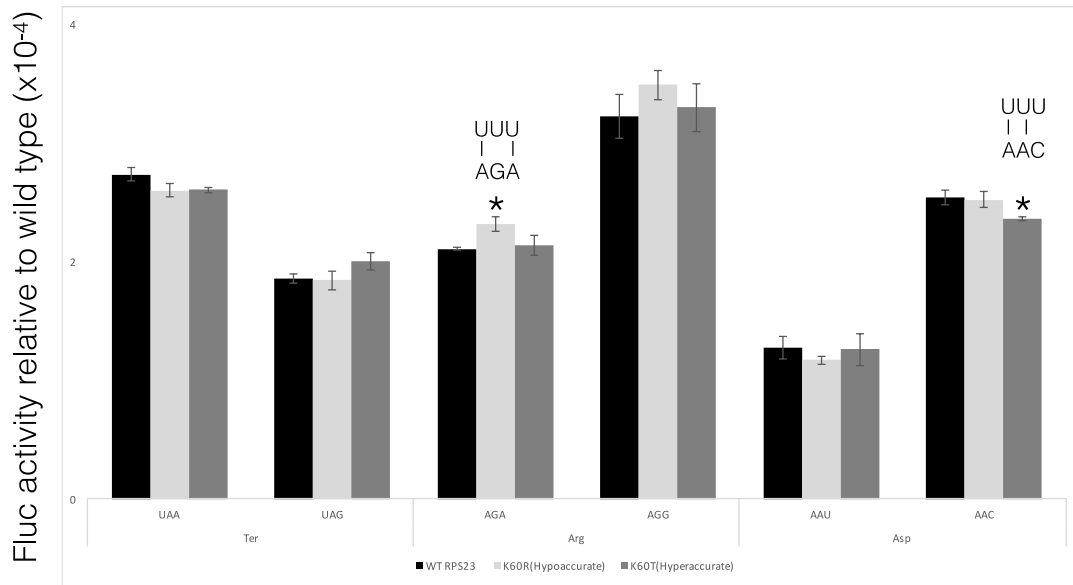


Figure III–16. Mutations in RPS23 only affected two near-cognate codons

The Fluc activities relative to wild type of the indicated K529 codon replacements are shown from a wild-type strain (black bars) and a strain carrying the *RPS23* K60R mutation (light gray bars) and a strain carrying the *RPS23* K60T mutation (dark gray bars). Error bars represents SEM.

Table III-6. Mutant enzyme activity relative to wild type in HEK293 cells transfected with wild type and mutant forms of RPS23

Amino acid	Codon	Misreading error frequency (x10 ⁻⁴)		
		WT RPS23	K60R(Hypoaccurate)	K60T(Hyperaccurate)
Ter	UAA	2.7	2.6	2.6
	UAG	1.9	1.8	2.0
Arg	AGA	2.1	2.3	2.1
	AGG	3.2	3.5	3.3
Asp	AAU	1.3	1.2	1.3
	AAC	2.5	2.5	2.4

are putative error-prone codons. They are two stop codons UAA and UAG, one glutamine codon CAG, one glutamic acid codon GAA, two arginine codons AGA and AGG, and one asparagine codon AAC. UAA, UAG, AGA, AGG and AAC are the five error-prone codons present in all the four cell lines. In *E. coli*, our lab observed several frequent error-prone codons. Increased errors by tRNA^{Lys}_{UUU} occur at UAG, AGA, AGG and AAU, by tRNA^{Glu}_{UCC} at GGA, GGG, GAU, and GAC, by tRNA^{Asp}_{QUC} at GGC, and GAA, and by tRNA^{Tyr}_{QUA} at UGU, UGC, UAA, and UAG (Kramer & Farabaugh, 2007; Manickam et al., 2014). These errors involve several mismatches. The most frequent errors by these four tRNAs involved U1•U36, U2•U35, G2•U35, U3•U34, C3•U34, A3•Q34, G3•Q3. These mismatch conditions are summarized in Figure III-17. In another study, Kramer (2010) tested the frequency of misreading by tRNA^{Lys}_{UUU} in yeast. The misreading errors only involved UAG and AGG. These mismatches involved U1•U36 and G2•U35 but there were no apparent wobble errors. In addition, our lab has investigated misreading events by tRNA^{Glu}_{UUC} in yeast, and found that misreading errors involved G2•U35 (to GGA and GGG), U3•U34 (to GAU) and U•3C34 (to GAC) mismatches (unpublished data by Kartik Joshi). Among these error-prone codons, the most frequent one was GGA misread by tRNA^{Glu}_{UUC} (G2•U35), then GAU and GAC with wobble errors, and the least frequent one was GGG. Overall, misreading events appear to be less frequent in yeast than that in *E. coli*. Though several other studies measured misreading errors in *E. coli* and yeast, there is no available comprehensive study of all the possible misreading errors by one single tRNA.

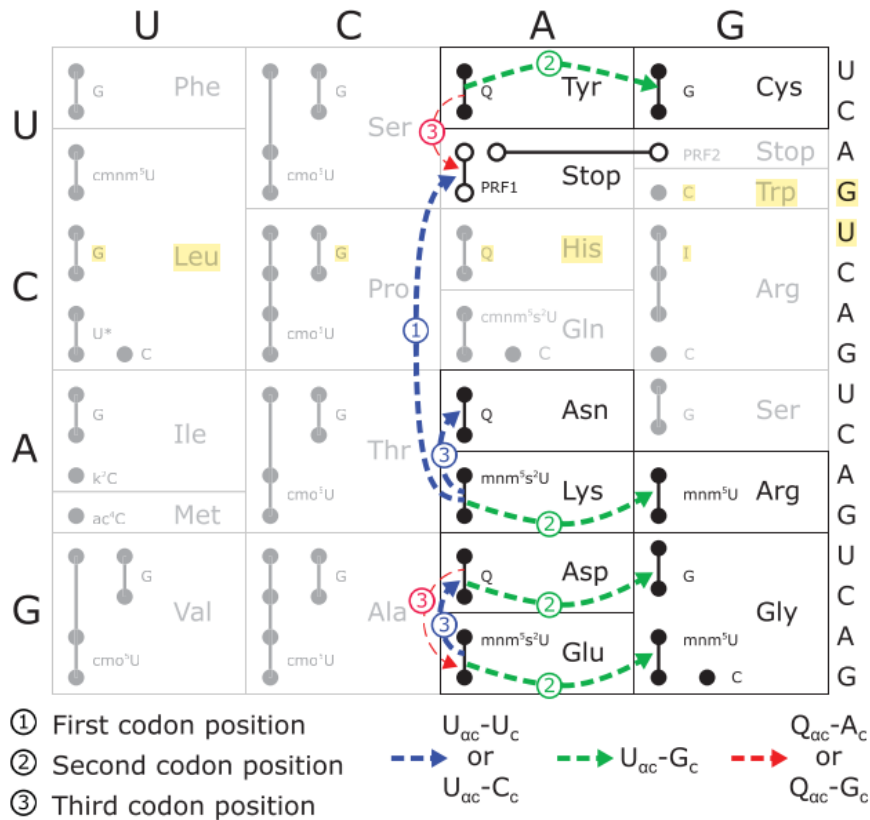


Figure III–17. The pattern of tRNA misreading involves two types of base mismatches

A filled circle represents each codon. A single tRNA recognizes filled circles that are connected by lines, with the anticodon wobble nucleotide of each tRNA identified immediately to the right using the standard convention. Unfilled circles represent the stop codons and lines connect those recognized by each of the prokaryotic release factors (PRF1 or PRF2). **Each arrow represents a misreading event.** The thickness of the arrow indicates relative frequency of the misreading event, the thicker the arrow, the higher the frequency. Each arrow is labeled by a number to represent the position of mismatch and is color coded for the nature of the mismatched base pair (Manickam et al., 2014).

We were interested in determining if the same set of base mismatches are responsible for the errors in mammalian system. I found similar but distinguishable features of error-prone codons. Stop codons UAA, UAG (U1•U36 mismatch), arginine codons AGA, AGG (G2•U35 mismatch), and asparagine codon AAU, AAC (U3•U34 or C3•U34 mismatch) were common error-prone codons in all the four cell lines. I also observed two novel potential error-prone codons in this study including glutamic acid GAA (G1•U36 in HEK293 and 22RV1) and glutamine CAG (C1•U36 in *HeLa*). There were no significant errors involving second position U2•U34 mismatch although in *E. coli* in the presence of error inducing antibiotics we found errors by tRNA_{UUU}^{Lys} at AUA, which requires that mismatch (Kramer & Farabaugh, 2007). I also found the misreading frequency in different cell lines varied despite these four cell lines sharing error-prone codons. In general, 22RV1 showed more errors than the other three mammalian cells (Figure III-3 and Table III-1). The misreading frequency of UAA is almost 2-fold higher in 22RV1 than in HEK293 and 3T3 cell lines, and about 4-fold higher than in *HeLa* (Table III-1). The misreading frequency of UAG in 22RV1 is ~2-fold higher than that in HEK293, and ~4-fold higher than in 3T3 and *HeLa*. The misreading frequency of AGA is quite similar in the four cell lines with ~1.5-fold to 2-fold difference between the four cell lines. The error frequency for AGG is highest in *HeLa*, ~2-fold, 1.7-fold and ~1.3-fold higher than HEK293, 3T3 and 22RV1 respectively. Again, 22RV1 has the highest error frequency of AAC, which is nearly 3-fold higher than 22RV1 and 2-fold higher than 3T3 and *HeLa*.

In all cell lines, tRNA_{UUU}^{Lys} made first position errors at stop codons UAA and UAG (U1•U36 mismatch). This result is expected since these were error-prone codons in both *E. coli* and yeast. Activities at termination codons were obviously due to misreading because a premature stop codon would lead to a truncated protein with very low activity (Kramer & Farabaugh, 2007; Kramer et

al., 2010; Manickam et al., 2014). In both *E. coli* and yeast the UAG mutant had significantly higher activity than UAA. In fact, the near-cognate codon UAA had very low residual Fluc activity with an estimated misreading frequency 4.1×10^{-4} in *E. coli* (Kramer & Farabaugh, 2007) and a much lower misreading frequency 8×10^{-5} in yeast (Kramer et al., 2010). Apparently, the very low activity of UAG in yeast was due to a prematurely terminated protein product. Lysine tRNA was expected to misread UAA somewhat more than UAG in mammalian cells, but there was no significant difference of Fluc activity between UAA and UAG except in the mouse cell line 3T3 (3.3×10^{-4} at UAA and 1.2×10^{-4} at UAG). The other three human cell lines had very similar activity of UAA and UAG: 3.3×10^{-4} versus 2.6×10^{-4} in HEK293, 1.5×10^{-4} versus 1.1×10^{-4} in *HeLa*, 5.8×10^{-4} versus 5.3×10^{-4} in 22RV1. The fact that stop codon UAA had somewhat higher activity than UAG in mammalian cell lines is very different from the results in *E. coli* and yeast. This comparison is not surprising when considering the difference of termination codon usage in the three organisms (Brown et al., 1990a, 1990b; Bonetti et al., 1995). UAA is the preferred stop codon in both *E. coli* and yeast while UAG is the least preferred termination codon (Sun et al., 2005). Release factors recognize and interact with the most preferred stop codon more efficiently. In this scenario, in *E. coli* and yeast release factor recognizes UAA more efficiently than UAG. Therefore, UAG is more easily misread by a near-cognate tRNA such as tRNA_{UUU}^{Lys}. However, the codon frequency of UAA and UAG is almost the same in *Homo sapiens*, which explains why the misreading error frequency of two termination codons is at similar levels in mammalian cell lines.

I hypothesized that the observed variation of misreading frequency at stop codons UAA and UAG among mammalian cell lines was due to differences in the abundance of two termination factors. In eukaryotes, translation termination is governed by two proteins, eukaryotic release factor 1 (eRF1) and eukaryotic release factor 3 (eRF3). During termination, eRF1 directly recognizes and

interacts with stop codons (Bertram et al., 2000). Meanwhile, eukaryotic release factor 3 (eRF3) stimulates eRF1 in the presence of GTP (Zhouravleva et al., 1995; Dever & Green, 2012). To determine if this might explain the result, I used qPCR and Western blotting to quantify the amount of eukaryotic termination factor 1 and 3 (eRF1 and eRF3) at both transcriptional and translational levels. Accordingly, 22RV1 should have the lowest abundance of eRF1 and/or eRF3 since it had the highest misreading error frequency at the stop codons while *HeLa* should have the highest abundance of eRF1 and eRF3. However, both qPCR and western blot assay indicated that 3T3 possessed the highest expression of both eRF1 and eRF3 while *HeLa* showed the lowest expression level of eRF1 and eRF3. These data are inconsistent with my hypothesis, suggesting the misreading error frequency at stop codons is not associated with the abundance of termination factors.

The fact that the two cancer cell lines *HeLa* and 22RV1 exhibited different misreading patterns at stop codons led me to ask whether the tissue or cell type of the cell lines could be responsible for the differences in accuracy? A distinguishing feature of the four cell lines is that they all originate from different tissues although some are the same cell type. I therefore suspected that the variation in errors might be either cell type-specific or tissue-specific. Table III-7 shows the tissue and cell type of each of the cell line. HEK293 and NIH/3T3 both originate from embryo. *HeLa* cells originate from adult cervix, and 22RV1 originate from adult prostate. Though these cell lines originate from different tissues, HEK293, *HeLa*, and 22RV1 are all epithelial while NIH/3T3 is fibroblastic (Table III-7). HEK293, *HeLa*, and 22RV1 showed distinct patterns of misreading errors at UAA and UAG despite the fact that they are all epithelial, indicating the variation of error frequency is not related to cell type (Figure III-3 and Table III-7). Nevertheless, two embryonic cell lines, HEK293 and NIH/3T3, showed similar frequencies of misreading stop codons (Figure

Table III-7. Tissue and cell type of each cell line

Cell line	Tissue	Cell type
HEK293	Embryo kidney	Epithelial
<i>HeLa</i>	Cervix	Epithelial
22RV1	Prostate	Epithelial
NIH/3T3	Embryo	Fibroblast

III-3). The prostate cancer cell line, 22RV1, showed the highest misreading errors of stop codons while the cervix cancer cell line, *HeLa*, had the lowest errors, suggesting the variation of error frequency of stop codons might be tissue specific. However, concluding that tissue type is responsible for the variation among cell lines would require testing misreading frequency of stop codons in more cell lines. For example, I could investigate misreading frequency in another prostate cancer cell line, PC3, or in Ect1/E6E7, a cervix cell line.

In addition to structural research, *in vivo* studies have demonstrated that the G2•U35 base mismatch is the most frequent mismatch in *E. coli* and yeast (Kramer & Farabaugh, 2007; Kramer et al., 2010; Zhang et al., 2013; Manickam et al., 2014; Demeshkina et al., 2012; Demeshkina et al., 2012). Not surprisingly, in this study arginine AGA and AGG again were error prone codons as observed in both *E. coli* and yeast; these errors require second position U2•G35 mismatches. For tRNA^{Lys}_{UUU}, AGA and AGG were misread most frequently because they are among the rarest codons and are decoded by the minor tRNA (Ikemura, 1981). Such codon usage bias causes slow codon recognition by the correct tRNA, which may be the reason for their dramatically high misreading frequency at AGA and AGG in *E. coli* (Kramer & Farabaugh, 2007). AGG also had the highest misreading error frequency in yeast where its codon usage is also low (Zhang, 1991). Therefore, the previous work on translational errors concluded the competition between near-cognate tRNAs (incorrect tRNAs) and cognate tRNAs (correct tRNAs) was a major factor contributing to the high misreading errors of AGA and AGG (Kramer & Farabaugh, 2007; Kramer et al., 2010).

However, tRNA competition alone cannot explain my data in this study. The concentration of cognate tRNAs of AGA and AGG is above the median in human cells (gtrnadb.ucsc.edu/).

Additionally, AGA and AGG are not rare codons neither in human nor in mouse cells (www.kazusa.or.jp/). Though an abundance of nuclear tRNA was characterized as tissue-specific, there was no large difference between *HeLa* and HEK293 (Dittmar et al., 2006). Missense errors at AGA and AGG occurred despite the existence of abundant arginine tRNAs and equally preferred codon usage. Thus, tRNA abundance and codon usage are not the causes of misreading errors at AGA and AGG. My conclusion is consistent with our lab's previous work, stating that there is no association of high error frequency with low abundance of the cognate tRNA. Therefore, competition between cognate and near-cognate tRNAs are not responsible for missense errors (Manickam et al., 2014).

Misreading errors at the wobble position were expected (Friedman & Weinstein, 1964) since the wobble position is less monitored by contacts from the ribosome compared with the first and second codon positions, leading to a more flexible base-pair geometry in the wobble position (Ogle & Ramakrishnan, 2005). Our lab has observed high wobble errors in *E. coli* but no or low wobble errors in yeast and mammalian system.

In *E. coli*, wobble errors occurred at the asparagine codon AAU showing that the activity at AAU was higher than at AAC. This result is consistent with the previous finding that tRNA_{UUU}^{Lys} misread AAU about eight times more frequently than AAC in *E. coli* (Parker et al., 1983). Besides, the high wobble errors for tRNA_{UUU}^{Lys} on AAU and tRNA_{UUC}^{Glu} on GAU both involved a U•U mismatch (Kramer & Farabaugh, 2007; Manickam et al., 2014). All the evidence above showed that in *E. coli* U•U is a more frequent mismatch at the wobble position than U•C. However, wobble errors in yeast were not as frequent as in *E. coli*.

Initially, Kramer et al. (2010) did not see any evidence of wobble errors in yeast (Kramer et al., 2010). Recently, Kartikeya Joshi in our laboratory has observed wobble errors in yeast by tRNA^{Glu}_{UUC} but with lower frequency than in *E. coli* (unpublished data). I have also observed wobble errors at lower frequencies than in *E. coli* at AAC. Indeed, Fluc activity of the AAU mutant was the lowest in HEK293, 3T3 and *HeLa* cell line. I had expected a lower error frequency at AAC than at AAU by tRNA^{Lys}_{UUU} based on previous results in *E. coli* (Kramer et al., 2010). However, AAC wobble misreading (C3•U34 mismatch) was more frequent than AAU (U3•U34 mismatch) in all the tested mammalian cell lines. This result is consistent with many other earlier studies. The previous study reported frequent misreading of the serine codon AGC by tRNA^{Arg}_{UCU}, which would require a wobble position U•C mismatch (Rakwalska & Rospert, 2004; Plant et al., 2007). Additionally, tRNA^{Glu}_{UUC} misread GAC at the wobble position involved C3•U34 (Manickam et al., 2014). Moreover, a mass spectrometry-based method was used to detect amino acid misincorporation and reported that C3•U34 mismatch was one of the principal causes of amino acid misincorporations (Zhang et al., 2013). Altogether these data along with mine strengthen the possibility of a non-canonical geometry of U•C base pairing in the wobble position. No structural study investigating this mismatch has yet been published.

Two more uncommon mismatch base-pairs are the G1•U36 mismatch tRNA^{Lys}_{UUU} used to misread GAA in HEK293 and 22RV1, and the C1•U36 mismatch to misread CAA in *HeLa*. My study is the first one that reported the C1•U36 mismatch, but Zhang et al. using mass spectrometry found that the G•U mismatch is the most frequent mismatch during codon recognition (Zhang et al., 2013). G•U mismatches were predicted to occur frequently during codon-anticodon recognition owing to its binding energy being similar to a canonical base pair (Freier et al., 1986; Ogle &

Ramakrishnan, 2005). This mismatch was also predicted to be frequent at the wobble position during protein translation (Agris et al., 2007) and G•U mismatches in the first and second base during decoding process were hypothesized as early as 1972 (Loftfield & Vanderjagt, 1972). Although G•U mismatches in the first position during codon recognition were predicted to have a very similar binding affinity to the cognate U•A match (Uhlenbeck et al., 1970), the G•U is observed less often in the first position than in the wobble position.

In summary, here I report the most frequent errors by the tRNA^{Lys}_{UUU} involved U1•U36 (to stop codon) or C1•U36 (to glutamine codon) or G1•U36 (to glutamic acid codon) or G2•U35 (to arginine codon) or C3•U34 (to asparagine codon) mismatches. There were no significant errors involving second position U•U and third position U•U mismatches. These results are distinct from our lab's previous work in bacteria. In bacteria, we observe both U2•U35 (tRNA^{Lys}_{UUU} misreads Ile AUA), U3•U34 (tRNA^{Lys}_{UUU} misreads Asn AAU) at the wobble position. Studies of missense error frequencies *in vivo* ranked G•U, U•U or C•U mismatches as the most frequent pairs while A•A and C•A mismatches as the least possible errors during protein translation (Blanchet et al., 2014; Manickam et al., 2014). In addition, a mass spectrometry method based study reported U•G, U•C, U•U mismatches were the most frequent misreading pairs among all the detected amino acid (Zhang et al., 2013). Different misreading errors, therefore, appear to occur in mammalian systems than in *E. coli* or yeast.

Variation of missense errors between different cell lines could result from differences in tRNA modification. It is well known that tRNA modifications play a pivotal role in the decoding process (Johansson et al., 2008). The presence of tRNA modification can either expand or restrict codon-anticodon pairing. For example, inosine (I), a modified A, expands wobble position base-pairing.

A₃₄ can only base pair with U while a tRNA with I₃₄ can recognize A, U and C. On the other hand, 5-methoxycarbonylmethyluridine (mcm⁵U) and 5-methoxycarbonylmethyl-2-thiouridine (mcm⁵s²U) modifications restrict a tRNA to recognize only A instead of A and G (Lim, 1994; Agris et al., 2007; Björk et al., 2007; Lyko & Tuorto, 2016; Rozov et al., 2016). A previous study reported that tRNA modifications greatly affected translational fidelity in *E. coli* (Manickam et al., 2016). tRNA modification has also been shown to play other roles during protein translation. Vendeix et al. presented a model of the bacterial 30S subunit with the ASL of human tRNA_{UUU}^{Lys}, which has identical anticodon loop sequence to *E. coli* lysine tRNA but carries three modifications in the anticodon loop: 5-methoxycarbonylmethyl-2-thiouridine (mcm⁵s²U34), 2-methylthio-N⁶-threonylcarbamoyladenine (ms²t⁶A37), and pseudouridine (ψ39) (Vendeix et al., 2012). With these three modifications, lysine tRNA recognized and bound to AAA and AAG codons while unmodified lysine tRNA was barely found binding lysine codons. These data suggested that these three modifications play an essential role in stabilizing the codon-anticodon interaction and therefore tRNA modifications are essential for efficiency and accuracy of decoding process. Indeed, Vendeix et al. showed that ψ39 enhanced the stability of the ASL while ms²t⁶A37 restrained the anticodon to adopt an open loop conformation, which is required for ribosomal binding. They concluded that mcm⁵s²U34 together with ms²t⁶A37 contribute to the stability of the codon-anticodon complex interaction (Vendeix et al., 2012). This study suggests that the variation of error frequencies between each cell line might be owing to the variation of lysine tRNA modifications in different cell lines. For example, loss of one or even all of the three modifications might lead to a more flexible codon-anticodon complex, which would decrease the efficiency and accuracy of tRNA_{UUU}^{Lys} recognizing the cognate codon and would allow it to misread other near-

cognate codons. One method to test this hypothesis would be to isolate tRNA_{UUU}^{Lys} from each cell line and then analyze tRNA modifications by mass spectrometry.

Though some studies investigated missense errors in mammalian cells, they have had some limitations. The studies reported a wide range of error frequencies, from 10^{-1} to 10^{-5} per codon. The primary reason for this range of values is that different methods were used to detect errors at different positions of the codon-anticodon complex. This diversity of methods makes it difficult to estimate an average missense error frequency in mammalian cells (Kurtz, 1975; Luce & Bunn, 1989; Mori et al., 1985). In addition, missense error frequency was likely overestimated in some studies. For example, Kurtz claimed that the error frequency was as high as 10^{-1} in young mice and 10^{-2} in old mice. These results were determined *in vitro* using mouse extracts, which might be much more error prone than *in vivo*. For all these reasons, the frequency of missense errors reported might be exaggerated. Moreover, *in vitro* assays did not distinguish between misreading (wrong decoding), mischarging (misacylation), either of which could be greatly increased *in vitro*.

To comprehensively characterize the misreading error frequency in mammalian cells, I also exposed cells to the aminoglycoside antibiotic G418, a neomycin derivative. Resistance to G418 is conferred by the Neomycin resistance gene (*neo*). This gene was isolated from the transposon Tn5. *Neo* codes for the aminoglycoside 3'-phosphotransferase enzyme, which inactivates a range of aminoglycoside antibiotics including G418 by phosphorylation (Kochupurakkal & Iglehart, 2013). In my experiment, the *neo* is carried by the pcDNA 3.1 human vector as a marker so I knockout this gene completely from the plasmid. Hence, any cell line transfected with this plasmid is no longer resistant to G418.

G418 had different levels of influence on misreading in the three tested cell lines. HEK293 is the most sensitive cell line to the drug so that a relatively low concentration of G418 will disrupt cell viability. In addition, G418 had the largest impact on misreading in HEK293 cells. Therefore, the increased antibiotic sensitivity observed in HEK293 may result from the additive effect of translational errors induced by the antibiotic.

It is well known that aminoglycoside antibiotic G418 can affect translation in mammalian cells. Primarily, G418 has been used to promote nonsense codon readthrough and has been recognized as a potential molecular treatment for nonsense mutation diseases (Burke & Mogg, 1985; Martin et al., 1989; Phillips-Jones et al., 1995; Manuvakhova et al., 2000; Azimov et al., 2008; Heier & DiDonato, 2009; Floquet et al., 2011; Floquet et al., 2011; Tobe et al., 2013). The very first study using G418 as an amber mutation (UAG) suppressor found that G418-induced readthrough can restore the activity of the mutant to about 20% of wild type activity in COS-7 monkey cells (Burke & Mogg, 1985). The effect of this case was due to the decreased efficiency of protein termination in the presence of the drug. Thus, an amino acid is added at the stop codon position, allowing a production of a full-length protein sequence. Additionally, previous studies have shown context effects on G418-dependent suppression of nonsense mutations in mammalian cells (Manuvakhova et al., 2000; Martin et al., 1989; Phillips-Jones et al., 1995). Many studies have demonstrated that the sequence context, surrounding a stop codon, especially the 3' base, can affect aminoglycoside antibiotic mediated suppression of nonsense codons (Martin et al., 1989; Phillips-Jones et al., 1995; Manuvakhova et al., 2000). For example, Phillips-Jones et al., tested context effects on misreading and suppression at the stop codon UAG in HEK293, MRC5V1 and COS-7 mammalian cell lines (Phillips-Jones et al., 1995). The base 3' to UAG was either A, C, G or U in the *lacZ* gene. They observed a pattern of 3' context effects on the tRNA^{Ser} UAG suppressor and reported the relative

effect of the base 3' to UAG was $A > U = G > C$. Moreover this effect is the same in different mammalian cell lines (Phillips-Jones et al., 1995). Manuvakhova et al. (2000) investigated G418 induced readthrough in a more comprehensive way by studying UGA(N), UAG(N), and UAA(N). They found readthrough levels for UAG(N) ranked in an order of suppression of $U > C, G > A$ (Manuvakhova et al., 2000). These previous studies bring the possibility that part of the mutant activity of Fluc at the stop codon UAA and UAG may include readingthrough activity by tRNAs other than $\text{tRNA}_{\text{UUU}}^{\text{Lys}}$.

Because of its effect on nonsense suppression, G418 has been used to study premature termination diseases (Azimov et al., 2008; Heier & DiDonato, 2009; Floquet et al., 2011; Tobe et al., 2013). All these studies utilized a proper concentration of G418 as a treatment to rescue phenotypes caused by premature termination codons *in vivo*. Promising results suggested that G418 could be used as a treatment to reduce the degree of premature termination and to restore the active conformation of essential proteins affected by genetic diseases (Azimov et al., 2008; Heier & DiDonato, 2009; Floquet et al., 2011; Tobe et al., 2013). My study showed that G418 increased missense error frequencies at AGA and AAC (HEK293), CAA, AGA and AAC (*HeLa*), AUG and AGA (3T3) in addition to UAA and UAG. Accordingly, G418 may also be used as a treatment for a disease that is caused by these mutations in any essential genes.

Ribosomal proteins play a pivotal role in translational fidelity. Prior studies have demonstrated that mutant forms of ribosomal proteins can significantly affect translational fidelity and deficiency of some is associated with human disease (Rice et al., 1984; Kramer & Farabaugh, 2007; Angelini et al., 2007; Flygare et al., 2007; Horos et al., 2012; Manickam et al., 2014). For example, Diamond-blackfan anemia (DBA) is caused by aberrant ribosomal biogenesis due to

ribosomal protein mutants such as ribosomal protein S19 (RPS19) or ribosomal protein L11 (RPL11).

No study, however, has associated any ribosomal protein's affect on translational fidelity to any role in human disease. This is also a motivation for my study to investigate how mutant ribosomal proteins could affect translational accuracy in human cells. Unfortunately, I did not see any significant impact of the RPS23 mutation on translational accuracy in HEK293 cells. One possible reason is that RPS23 is not important to translational accuracy in humans, despite its known effect in yeast (Anthony & Liebman, 1995). Second, the amino acid residue mutated in my study might not be essential to accuracy as the corresponding residue is in yeast. Third, an excess of endogenous wild type RPS23 may have overwhelmed the expression of mutant RPS23, even though equivalent RPS23 mutations in bacteria and yeast are dominant. A feasible approach to overcome the disruption from wild type RPS23 is to use CRISPR to delete one of the RPS23 genes from the genome.

My work is the first to report all possible missense errors by a single tRNA in four different mammalian cell lines. The results show that protein translation is more accurate in mammalian cells than in *E. coli* or yeast. This may suggest a more sophisticated decoding exists in mammalian cell lines or, given that the abundance of tRNAs across the various isoacceptors in humans is nearly equivalent, the lack of tRNA limitation may reduce the chance of near-cognate decoding. My data together with prior studies on missense errors in mammalian systems increase our knowledge on protein translation, which may also shed light on potential human diseases associated with infidelity in protein translation.

CHAPTER IV

INVESTIGATION OF MISREADING ERROR FREQUENCY BY A GLUTAMINE TRANSFER RNA REPORTER SYSTEM IN THE YEAST

Saccharomyces cerevisiae

Chapter IV. INVESTIGATION OF MISREADING ERROR FREQUENCY BY GLUTAMINE TRANSFER RNA REPORTER SYSTEM IN YEAST *Saccharomyces cerevisiae*

A. Introduction

Accurate and sufficient protein translation is crucial for all organisms. Cellular mechanisms exist to maintain the translational error rate at a low level from DNA to protein. The transcriptional error rate is no higher than $\sim 1 \times 10^{-5}$ per nucleotide (Erie et al., 1992). In comparison with transcriptional errors, translational errors are more frequent. Three types of errors can occur during protein translation: missense errors resulting from incorrect aminoacylation or incorrect tRNA selection that causes insertion of a wrong amino acid (misreading), frameshift errors resulting from changing the normal reading frame, and processivity errors arising from a spontaneous release of the peptidyl-tRNA (Kurland et al., 1996). Previous studies have suggested that misreading errors are the most common type of translational errors (Kramer & Farabaugh, 2007; Kramer, Vallabhaneni, Mayer, & Farabaugh, 2010; Manickam et al., 2014).

The ribosome discriminates between a correct aa-tRNA (cognate tRNA) and an incorrect tRNA (near-cognate or non-cognate tRNA) based on complementary base pairing between the codon in mRNA and the anticodon in tRNA. The discriminating process depends on many mechanisms including kinetic proofreading, induced fit and structural rearrangement of the ribosome. A comprehensive understanding of tRNA selection has emerged by both kinetic and structural studies.

Kinetic proofreading was first proposed by Ninio and Hopfield (Hopfield, 1974; Ninio, 1975). They proposed that tRNA selection is separated into two distinct steps by an irreversible reaction,

which is GTP hydrolysis. At the beginning of tRNA selection, the aa-tRNA is delivered to the ribosome A site on the small subunit as a part of a ternary complex with elongation factor Tu (EF-Tu) and GTP. This step, termed initial selection, is codon-independent, meaning all tRNAs (cognate, near-cognate and non-cognate tRNA) exhibit the same rate of binding the ribosome A site and dissociating from the ribosome (Rodnina et al., 1994). The following step, codon recognition, is codon-dependent. Though the overall rate of this step is almost indistinguishable between a cognate tRNA and a near-cognate tRNA, the dissociation rate constants from the ribosome are strikingly different. A near-cognate tRNA dissociates from the ribosome approximately 1,000-fold faster than a cognate tRNA. The ribosome rejects non-cognate tRNAs efficiently during codon recognition step because non-cognate tRNAs are not able to form a stable codon-anticodon complex in the A site. tRNAs that are rejected by the ribosome during this step leave the ribosome without GTP hydrolysis. Although the rate constant of GTPase activation of the near-cognate tRNAs is much smaller than that of the cognate tRNAs, rapid and irreversible GTP hydrolysis precludes the chance of completely rejecting the near-cognate tRNAs, and thus the near-cognate tRNAs can enter a second proofreading stage (Rodnina & Wintermeyer, 2001). GTP hydrolysis causes a conformational change of EF-Tu to its GDP bound state. Consequent dissociation of the EF-Tu with GDP from the aa-tRNA allows the aminoacyl acceptor end of the tRNA to enter the A site on the large subunit (accommodation), followed by the formation of a peptide bond with the amino acid in the P site. Alternatively, incorrect aa-tRNAs would tend to be rejected during this period. As well as GTPase activation being more rapid, a cognate tRNA accomplishes the accommodation step faster than a near-cognate tRNA does; meanwhile, a near-cognate tRNA dissociates from the ribosome much more rapidly than a cognate tRNA. Under this kinetic model, a preference for selecting a correct tRNA gives 100-fold discrimination between a

cognate and a near-cognate tRNA at each step and hence provides 10,000-fold discrimination between a cognate tRNA and a near cognate tRNA (Rodnina et al., 2005).

In addition to discrimination of the ribosome based on different stabilities of a correct and an incorrect tRNA, it is proposed that the ribosome uses another strategy to discriminate between a correct and an incorrect tRNA, which is termed induced fit (Pape et al., 1999). Studies showed that the correct codon-anticodon interaction not only decreases the rate of dissociation but also significantly accelerates GTPase activation of EF-Tu and accommodation. This acceleration is due to a conformational change of the ribosome that is induced by a correct tRNA binding. This structural change is similar to one induced by a correct substrate binding to an enzyme so as to fit the shape of its substrate (Rodnina & Wintermeyer, 2001). However, the failure of incorrect tRNAs to induce this conformational change may explain the slow rate of GTPase activation of EF-Tu by a near-cognate tRNA binding (Pape et al., 1999). Thus, the ribosome uses an induced fit mechanism to distinguish between a cognate and a near-cognate tRNA during each stage. A correct codon-anticodon interaction, which involves Watson-Crick base pairing geometry, can induce a conformational change of the decoding center in 30S subunit (domain closure). In contrast, the conformational change was not observed for incorrect codon-anticodon interactions (Ogle et al., 2002).

Structural studies provide an insight into the mechanism of decoding, showing that 16S rRNA plays an essential role during the tRNA selection and the domain closure of the 30S subunit. X-ray crystallographic studies revealed that the decoding site includes the A site in the 30S subunit, encompassing helix 34, helix 44 and helix 18 of 16S rRNA. When a cognate tRNA binds to the A site, two universally conserved bases, A1492 and A1493, flip out from a position stacked within

an internal loop of helix 44. These conformational changes position the nucleotides to monitor the interactions between the codon and the anticodon at the first two positions. Simultaneously, base G530 of helix 18 converts its conformation from *syn* to *anti* to monitor the second and third position (Ogle et al., 2001). At the same time, cognate-tRNA binding induces an overall ribosome conformational change (domain closure), which involves a rotation of the head toward the shoulder and the subunit surface, and of the shoulder toward the intersubunit space and the helix44/helix27/platform region (Figure IV-1). In contrast, for a near-cognate tRNA the same movement of the ribosome was not observed, suggesting that the closure of the ribosome is initiated by the interaction between the ribosome and a cognate tRNA (Ogle et al., 2002).

However, the role of this universal ribosome structural change for the tRNA selection has been questioned. Ogle et al. (2001, 2002) studied the decoding process by soaking 30S small subunit with U₆ RNA (a mimic of mRNA) and cognate or near-cognate anticodon stem-loops (ASLs) (mimics of tRNA) (Ogle et al., 2001; Ogle et al., 2002). However, later studies used structures of 70S ribosomes and intact mRNA and tRNAs and revealed another of the decoding mechanisms (Demeshkina et al., 2012). Analysis of the 70S ribosome complex with mRNA, P-site tRNA, and E-site tRNA showed a distinct conformation of the vacant A-site (Jenner et al., 2010). The mRNA path has a kink between the A- and P-site codon, called P/A kink. This is a special universal feature of mRNA that enables simultaneous binding of tRNAs to the A- and P-site. The 16S rRNA, the P-site tRNA and a metal ion stabilize the structure of this kink, which constrains movement of the A-site codon and the wobble geometry. It is a striking fact that in the vacant decoding center, A1493 nucleotide flips out, while A1492 nucleotide is held and in a 'in conformation' by stacking with A1913 of H69 of the 23S rRNA from the 50S subunit (Jenner et al., 2010). This structural model differs from what was proposed in the earlier studies. Moreover, Demeshkina et al. (2012)

reported that the 30S subunit undergoes the same domain closure upon binding of

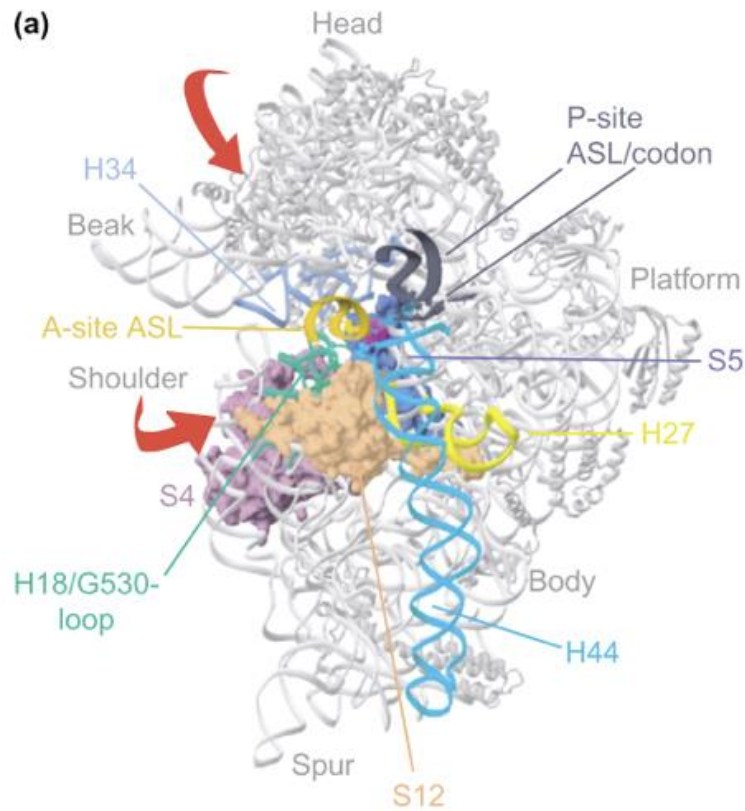


Figure IV–1. A cognate tRNA binding causes domain closure

30S subunit structure with the A-site tRNA anticodon stem–loop (ASL in gold). The decoding center is made up of four different domains: the head, shoulder, platform and helix 44. Red arrows represent the closure of 30S subunit. P site tRNA-ASL (dark gray), helices 44 (cyan) and helix 27 (yellow). In the shoulder domain, helix 18 with the G530-loop (turquoise), and proteins S12 (orange), S4 (violet), S5 (dark blue) and helix 34 (blue) (Ogle et al., 2002).

either a cognate tRNA or a near-cognate tRNA (Demeshkina et al., 2012). Based on six X-ray structures of the 70S ribosome, it was observed that U•G and G•U mismatches at the first two positions in the A site were forced to form a Watson-Crick-like base pair, resulting in domain closure. A1492, A1493, and G530 interacted with the minor groove helix in a similar way when either a cognate or certain near-cognate tRNAs bound. Demeshkina et al. argued that the three conserved bases A1492, A1493 and G530 do not discriminate between cognate and near-cognate tRNAs based merely on monitoring the geometry of a base pair of the codon-anticodon by interacting in the minor groove. When a near-cognate tRNA is forced to form a canonical base pair in the A site, this would create repulsion or require energy for tautomerization, which may lead to the dissociation of a near-cognate tRNA. Thus, they proposed that tautomerism or repulsion might be a plausible source of discrimination between a cognate tRNA and a near-cognate tRNA (Demeshkina et al., 2012).

Translational error frequency has been widely studied in yeast. Studies on misreading error frequency in the yeast *Saccharomyces cerevisiae* have largely depended on enzymatic assays of firefly luciferase and chloramphenicol acetyltransferase (CAT) (Stansfield et al., 1998; Salas-Marco & Bedwell, 2005; Plant et al., 2007; Kramer et al., 2010). However, a broad range of missense error frequencies have been reported from 10^{-3} to 10^{-5} errors per decoding event. Most of these studies tested error frequencies as the amount of incorporation of certain amino acids not encoded in the mRNA. Error frequencies from those studies vary from one to another, which may be due to estimating errors at different positions of different codons. Additionally, these estimates measured the error frequency of one or a few codons but not all possible codons as well, making it difficult to compare those results to have a general conclusion.

In our lab, we have exploited two enzyme-based reporter systems to study translational misreading errors: the dual luciferase and the β -galactosidase reporter systems. We can use both the systems to analyze the frequency of missense errors by individual tRNAs (Kramer & Farabaugh, 2007; Kramer et al., 2010; Manickam et al., 2014). The dual luciferase reporter system depends on an essential active site amino acid residue in firefly luciferase, lysine 529 (K529). Lysine 529 is responsible for orienting the substrates ATP and luciferin in the active site. Enzymatic activity is severely reduced by changes to K529, leading to up to 1600-fold reduced activity (Branchini et al., 2000). All possible near-cognate codons (those that have one nucleotide difference from wild type), and synonymous non-cognate codons (that have two or more different nucleotides from wild type lysine AAA/AAG), have been introduced to K529. Since near-cognate codons and their synonymous non-cognate codons encode the same amino acid, all near-cognate codons and their synonymous non-cognate codons should have a similar level of protein activity if the activity is due to functional replacement. Alternatively, near-cognate codons are more likely to be misread than their synonymous non-cognate codons. For example, in the Lys 529 reporter system $\text{tRNA}_{\text{UUU}}^{\text{Lys}}$ should prefer to misread arginine codon AGA, and AGG (one base mismatch with the anticodon of $\text{tRNA}_{\text{UUU}}^{\text{Lys}}$) over synonymous non-cognate codons CGA, CGG, CGU, and CGC (two base mismatches with the anticodon of $\text{tRNA}_{\text{UUU}}^{\text{Lys}}$). Hence, protein activity of AGA or AGG mutants should be higher than the other four synonymous non-cognate codons (Figure IV-2). In this way, we take advantage of near-cognate and synonymous non-cognate codons to demonstrate activity is due to error. Our lab has used this system to successfully estimate error frequencies by $\text{tRNA}_{\text{UUU}}^{\text{Lys}}$ in both *E. coli* and the yeast *Saccharomyces cerevisiae* (Kramer & Farabaugh, 2007; Kramer et al., 2010; Manickam et al., 2014).

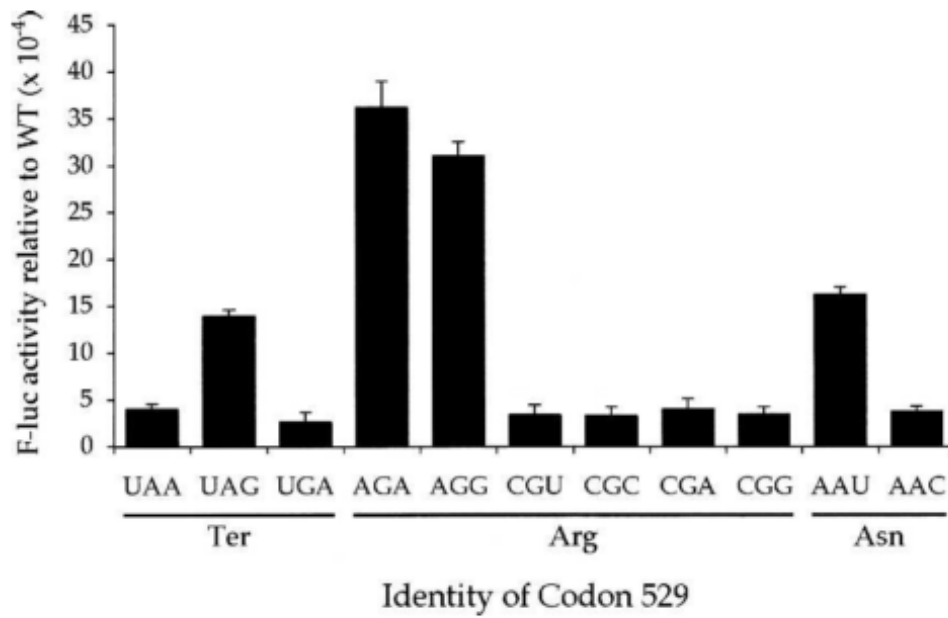


Figure IV–2. High residual F-luc activity of some K529 codons results from near-cognate decoding

Near-cognate codons UAG, AGA, AGG and AAU had significantly higher activities than their synonymous non-cognate codon mutants (Kramer & Farabaugh, 2007).

Our laboratory has demonstrated that luciferase has a limited number of essential amino acids (Kramer et al., 2010). However, many critical active site amino acid residues have been shown to affect the activity of β -galactosidase, such as glutamic acid 537 (E537), aspartate 201 (D201), and tyrosine 503 (Y503) (Manickam et al., 2014). The active site of β -galactosidase is very complicated so many essential residues make important interactions with the substrate (Xu et al., 2004; Juers et al., 2012). Glutamic acid 537 (E537) is one pivotal amino acid in the active site. Substitutions for E537 of β -galactosidase resulted in considerable decreases in catalytic activity, varying between 100-fold to 300,000-fold reduction, suggesting that E537 is a critical catalytic residue of β -galactosidase (Yuan et al., 1994). We suspected that activity of some of the E537 mutants might be due to the misreading rather than the activity of the mutant protein. Manickam et al. (2014) introduced a full set of near-cognate and synonymous non-cognate codons of E537 and found evidence for misreading at three codons. By using the same method, our laboratory identified three essential amino acid residues and was able to analyze missense errors by $\text{tRNA}_{\text{UUC}}^{\text{Glu}}$, $\text{tRNA}_{\text{QUC}}^{\text{Asp}}$, and $\text{tRNA}_{\text{QUA}}^{\text{Tyr}}$ (Manickam et al., 2014).

In previous work, Tsai and Curran reported that glutamine 625 (Gln625/Q625) is an essential amino acid residue in β -galactosidase. Changing the CAG codon encoding Q625 to its near-cognate codon (codon that differs from the Gln CAG or CAA codons by a single substitution) the arginine CGA codon resulted in a very low level activity, $\sim 1 \times 10^{-3}$ relative to wild type β -galactosidase. Tsai and Curran only substituted Gln CAG with the arginine codon CGA and studied the misreading frequency of CGA. However, the limitation of their study was that they did not have a

Gln	Ser	Leu	Ile	Lys	Tyr	Asp	Glu	Asn	Gly	Asn	Pro	Trp	Ser	Ala	Tyr	Gly	Gly	Asp	Phe				
											580												590
																Glutamine (625)							
Phe	Ala	Asp	Arg	Thr	Pro	His	Pro	Ala	Leu	Thr	Glu	Ala	Lys	His	Gln	Gln	Gln	Phe	Phe				
		610													620					p625			

Figure IV-3. Partial amino acid sequence of β -galactosidase

proper control to show the activity of CGA was due to misreading rather than functional replacement.

In my project, I introduced all possible near-cognate codons and synonymous non-cognate codons of CAG to Q625 in order to analyze the full range of misreading errors by tRNA^{Gln}_{UUG} in yeast. I noticed that Q625 is one of three glutamine codons in a row: 623, 624 and 625 (Figure IV-3). Because three glutamine codons are in a row, I also introduced the non-cognate arginine codon AGA to both Q623 and Q624 to explore the possibility that these might be important for enzyme activity and suitable for measuring misreading errors. My result indicated that Q623 is not an essential amino acid residue for β -galactosidase, but Q624 and Q625 may play a major role in the protein activity. Therefore, I investigated whether glutamine 624 and 625 could be used as a reporter system for testing misreading frequency by tRNA^{Gln}_{UUG}.

My data showed that Q624 was more important than Q625 and more of the mutations at Q624 were useful for measuring errors.

In this study, I demonstrated that Q624, but not Q625 as earlier reported, is a useful site for misreading error measurement. Moreover, I analyzed errors by tRNA^{Gln}_{UUG}, showing that errors involved a small subset of all possible non-canonical base pairs. These mismatches included U1•G36 and G2•U35. There was no significant error of C2•U35. These results are consistent with previous studies stating that G•U is one of the most frequent mismatches (Zhang et al., 2013; Manickam et al., 2014; Rozov et al., 2016). Additionally, I also showed that aminoglycoside antibiotic paromomycin and mutations of ribosomal protein S23 can affect misreading errors of a small subset of near-cognate codons, further confirming that activity of these putative error-prone codons was due to misreading but not functional replacement.

B. Results

I. Glutamine 624 (Q624) is an essential amino acid residue of β -galactosidase activity

Though Tsai and Curran reported that tRNA^{Gln}_{UUG} misread the arginine codon CGA as CAG at 625 in β -galactosidase, they failed to show the activity of the CGA mutant was due to misreading. Their work showed that the mutant protein activity relative to wild type is 1×10^{-3} . However, only one near-cognate codon CGA was studied. Lack of a proper negative control makes their result less convincing that this high relative activity ratio resulted from misreading. Therefore, I intended to investigate all potential misreading events at Q625 by Gln tRNA. According to the *lacZ* sequence, residues 623, 624 and 625 each encode glutamine. There is a possibility that the other two adjacent glutamines may also play a critical role in β -galactosidase activity. Hence, this became another motivation that drew me into investigating the importance of each of these residues. To achieve this goal, I mutated CAG to its non-cognate arginine codon AGA at all of the three sites, meaning there could be no base pairing between the cognate tRNA^{Gln}_{UUG} and the non-cognate arginine codon. With such a mutant, I expect that the β -galactosidase activity would be as little as background activity if this amino acid residue were essential. By contrast, if the glutamine were not vital to enzyme activity there would be a slight impact on protein activity when CAG is substituted with AGA. The β -galactosidase activity of AGA mutant at Q624 was 2×10^{-5} relative to wild type. However, the β -galactosidase activity of AGA at Q623 and Q625 had activity as high as 2×10^{-3} relative to wild type, which was 200-fold greater than that at Q624. These data indicated that Q624 might be significantly more important for β -galactosidase activity than is Q625. Therefore, all possible near-cognate codons and some synonymous mutants were introduced to Q624 and Q625 by doing site-directed mutagenesis (Table IV-1).

II. Higher activities of mutants at Q625 were due to functional replacement but not misreading

To attempt to measure errors by tRNA^{Gln}_{UUG} I constructed a reporter system based on a yeast β -galactosidase reporter plasmid, pANU7 (Sundararajan et al.,1999). As I stated above, Q625 does not seem essential unlike what was reported by Tsai and Curran. To further confirm this conclusion, I made all possible near-cognate mutants of CAG or CAA at Q625 (Table IV-1). Then I tested the β -galactosidase activity of some near-cognate codons of Q625, including CAU and CAC (histidine), CGA, CGG, and AGA (arginine), UAA and UAG (termination), and lysine (AAG) (Figure IV-4). I had three reasons to start with testing these near-cognate codons: 1) histidine codons CAU and CAC had wobble position mismatch with CAG, and 2) the arginine codon CGA was reported to be misread by tRNA^{Gln}_{UUG} (Tsai & Curran, 1998) and CGG and AGA are synonymous near-cognate and non-cognate codons of CGA, and 3) termination codons UAA and UAG were commonly misread by their near-cognate tRNAs in other studies. Therefore, all these codons except AGA should have a greater chance to be misread by tRNA^{Gln}_{UUG}

Table IV-1. All possible near-cognate mutations for *lacZ* Glutamine 624 and 625

	U	C	A	G
U	UUU Phe	UCU Ser	UAU Tyr	UGU Cys
	UUC	UCC	UAC	UGC
C	UUA	UCA	UAA ***	UGA ***
	UUG	UCG	UAG	UGG Trp
	CUU Leu	CCU	CAU His	CGU Arg
	CUC	CCC	CAC	CGC
A	CJA	CCA Pro	CAA <i>Gln</i>	CGA
	CUG	CCG	CAG	CGG
A	AUU Ile	ACU Thr	AAU Asn	AGU Ser
	AUC	ACC	AAC	AGC
	AUA	ACA	AAA Lys	AGA Arg
G	AUG Met	ACG	AAG	AGG
	GUU Val	GCU Ala	GAU Asp	GGU Gly
	GUC	GCC	GAC	GGC
	GUA	GCA	GAA Glu	GGA
	GUG	GCG	GAG	GGG

U	
C	
A	GUU
G	
U	CAG
C	
A	Cognate
G	
U	GUU
C	
A	CGA
G	
U	Near-cognate
A	
G	GUU
U	
C	AGA
A	
G	Non-cognate

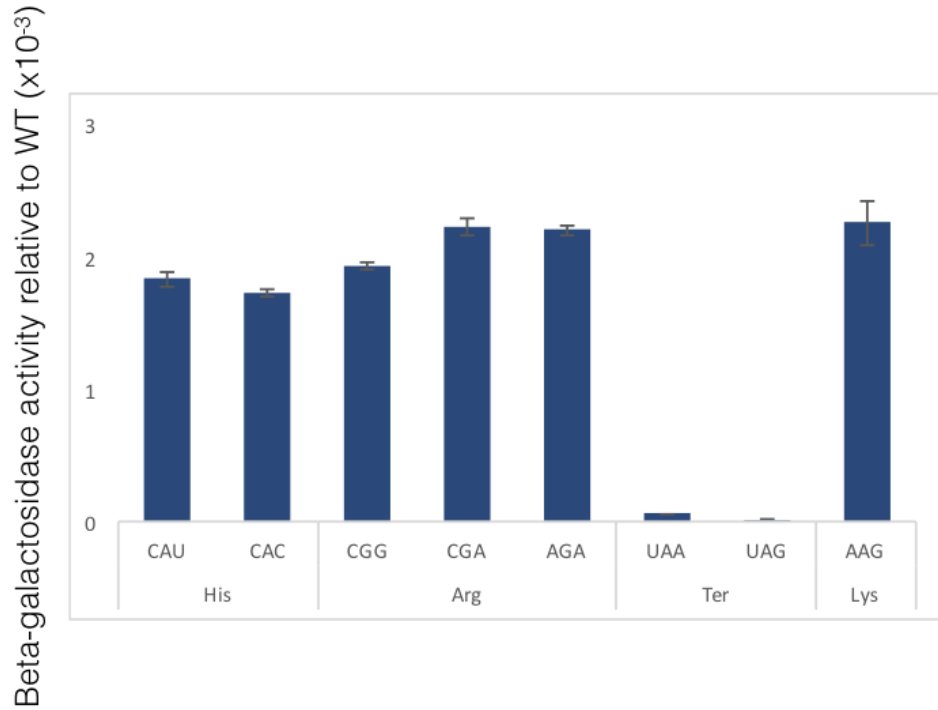


Figure IV-4. The high residual activity of some Q625 codons does not result from near-cognate decoding

A comparison of β -galactosidase activity relative to wild type synonymous near-cognate codon mutants. Codon identity is shown as in table IV-2. The error bars represent the standard error of the mean.

if they were potential error-prone codons. The residual activity of each mutant codon was calculated as a ratio, which was the mutant β -galactosidase activity divided by wild type activity:

$$\text{Misreading frequency} = \frac{\text{Mutant activity}}{\text{Wild type activity}}$$

This calculation would allow me to determine the misreading error frequency of each mutant.

As shown in Figure IV-4 and Table IV-2, except for the two termination codons, these mutants had an activity that was not different from the AGA control from 170×10^{-5} (CAC) to 220×10^{-5} (CGG and AGA). Histidine codons CAU and CAC resulted in very similar protein activity of 180×10^{-5} and 170×10^{-5} respectively. Arginine codons CGA and CGG and their synonymous non-cognate codon AGA also showed a similar level of protein activity of 190×10^{-5} , 220×10^{-5} and 220×10^{-5} , respectively. The two termination codons UAA and UAG, however, had much lower activity than the other tested codons of 6×10^{-5} and 16×10^{-5} , respectively.

Two models may explain the high activity of some near-cognate codon mutants. These two models are the functional replacement model and the misreading model (Kramer and Farabaugh, 2006). The functional replacement model states that any protein activity in the mutant proteins is due to the mutant amino acid, suggesting all codons that generate the same amino acid should show the same amount of activity. The misreading model states that mutant codons, for example, those that encode arginine CGA and CGG, are misread by tRNA^{Gln}_{UUG} as glutamine, resulting in the production of the small amount of protein with wild type activity. My data showed that though mutants with near-cognate codons histidine CAU and CAC, arginine codons CGA and CGG, and lysine codon AAG had very high activity, their activities were quite similar with the non-cognate codon mutant, AGA. These data were consistent with functional replacement model but not the misreading model,

Table IV-2. Misreading frequency by tRNA^{Gln}_{UUG} at Q625 near-cognate codons

<i>Identity of Codon 625</i>		<i>β-galactosidase relative to WT (x10⁵)</i>
<i>His</i>	CAU	180
	CAC	170
<i>Arg</i>	CGA	190
	CGG	220
	AGA	220
<i>Termination</i>	UAA	5.9
	UAG	1.3
<i>Lysine</i>	AAG	170

suggesting that these high activities were not due to errors since under the functional replacement model synonymous codons should have almost identical activity. The high level of activity of these mutants inhibits measuring an error frequency so I cannot conclude what that frequency of misreading might be.

The β -galactosidase activities of the UAA mutant were significantly higher than for UAG with the activities of 6×10^{-5} and 1×10^{-5} respectively ($P < 0.05$). These results suggest that the activities of the UAA and UAG mutants are due to misreading (Figure IV-4 and Table IV-2).

In conclusion, the high residual activities of mutants altering glutamine at position 625 were not due to near-cognate decoding but functional replacement so the Q625 mutants cannot be used as a misreading reporter system.

III. High activity of mutations at Glutamine 624 are misreading events by tRNA^{Gln}_{UUG}

After finding that Q625 is not a useful target for a misreading reporter system, I tested mutations at glutamine 624 (Q624) to determine if they might be more useful. The same method was utilized. All possible near-cognate mutants were introduced to the Q624 position (Table IV-1). The near-cognate codons included two termination codons UAA and UAG, two lysine codons AAA and AAG, two glutamic acid codons GAA and GAG, two leucine codons CUA and CUG, two proline codons CCA and CCG, two arginine codons CGA and CGG, and two histidine codons CAU and CAC. These codons all involved one nucleotide mismatch with the tRNA^{Gln}_{UUG} in either the first, second or wobble position. I also substituted CAA or CAG with non-cognate mutants synonymous with these near-cognate codons, including the termination codon UGA, leucine codon UUA, proline codon CCU, and arginine codon AGA (Figure IV-5 and Table IV-3). The relative β -

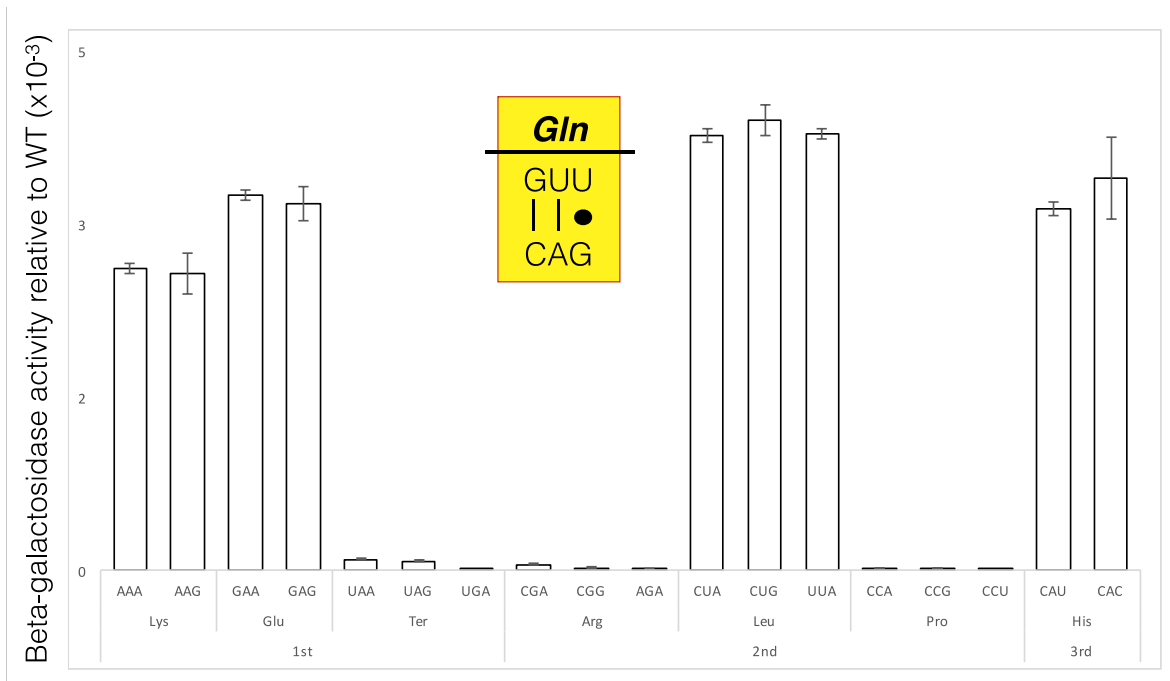


Figure IV–5. β -galactosidase activity of Q624 near-cognate codons

High protein activity of some near-cognate codons is due to functional replacement. The error bars represent the standard error of the mean.

galactosidase activity varied by a factor of ~2000-fold from 390×10^{-5} (CUG) to 8×10^{-6} (UGA) (Table IV-3 and Table IV-4). Eight of these mutants showed dramatically higher activity, which ranged from about 37 to more than 200-fold higher than the other near-cognate mutants. These mutants include two lysine codons AAA and AAG, two glutamic acid codons GAA and GAG, two leucine codons CUA and CUG, and two histidine codons CAU and CAC. Each of these pairs of mutants produced very similar activities (Figure IV-5 and Table IV-3). These data are consistent with the functional replacement model but not the misreading model. Again, the high level of activity of the mutant protein precludes measuring misreading errors occurred at the wobble position of the codons CAU and CAC.

A subset of mutant codons had much lower enzymatic activities including termination codons UAA, UAG, and UGA, arginine codons CGA, CGG and AGA, and proline codons CCA, CCG and CCU (Figure IV-6 and Table IV-4). Each set of codons has near-cognate codons and one synonymous non-cognate codon. Stop codons UAA and UAG had a relative activity of 10×10^{-5} and 8×10^{-5} , which was significantly higher than their synonymous non-cognate codon UGA (8×10^{-6}) ($P < 0.01$) (Figure IV-6 and Table IV-4). The activity of the nonsense mutants presumably occurs by misreading since a premature stop codon leads to a non-functional, truncated protein. This hypothesis is supported by the fact that UAA and UAG had significantly higher activity than UGA. Arginine codons CGA and CGG had an activity of 5×10^{-5} and 3×10^{-5} , which was also higher than their synonymous non-cognate codon AGA (1×10^{-5}) ($P < 0.05$) suggesting that their activity was also due to misreading. Proline codons CCA and CCG had the same relative activity of 2×10^{-5} . Their activity was different from the synonymous non-cognate codon CCU (9×10^{-6}), but this difference was not statistically significant. Their similarity suggests that activities of the CCA, CCG, and CCU mutants were probably not due to misreading. The fact that

Table IV-3. Misreading frequency by tRNA^{Gln}_{UUG} at Q624 near-cognate and synonymous non-cognate codons

Mismatch position	Amino acid	Codon	β -galactosidase activity relative to WT ($\times 10^{-5}$)
1st	Lys	<u>A</u> AA ^a	260
		A <u>A</u> G	260
	Glu	<u>G</u> AA	320
		<u>G</u> AG	320
	Ter	<u>U</u> AA	10
		<u>U</u> AG	8
		<u>U</u> GA	0.8
2nd	Arg	CG <u>A</u>	5
		C <u>G</u> G	3
		<u>A</u> GA	1
	Leu	CU <u>A</u>	380
		CU <u>G</u>	390
		<u>U</u> UA	380
	Pro	<u>C</u> CA	2
		<u>C</u> CG	2
		<u>C</u> CU	1
3rd	His	CA <u>U</u>	310
		CAC	340

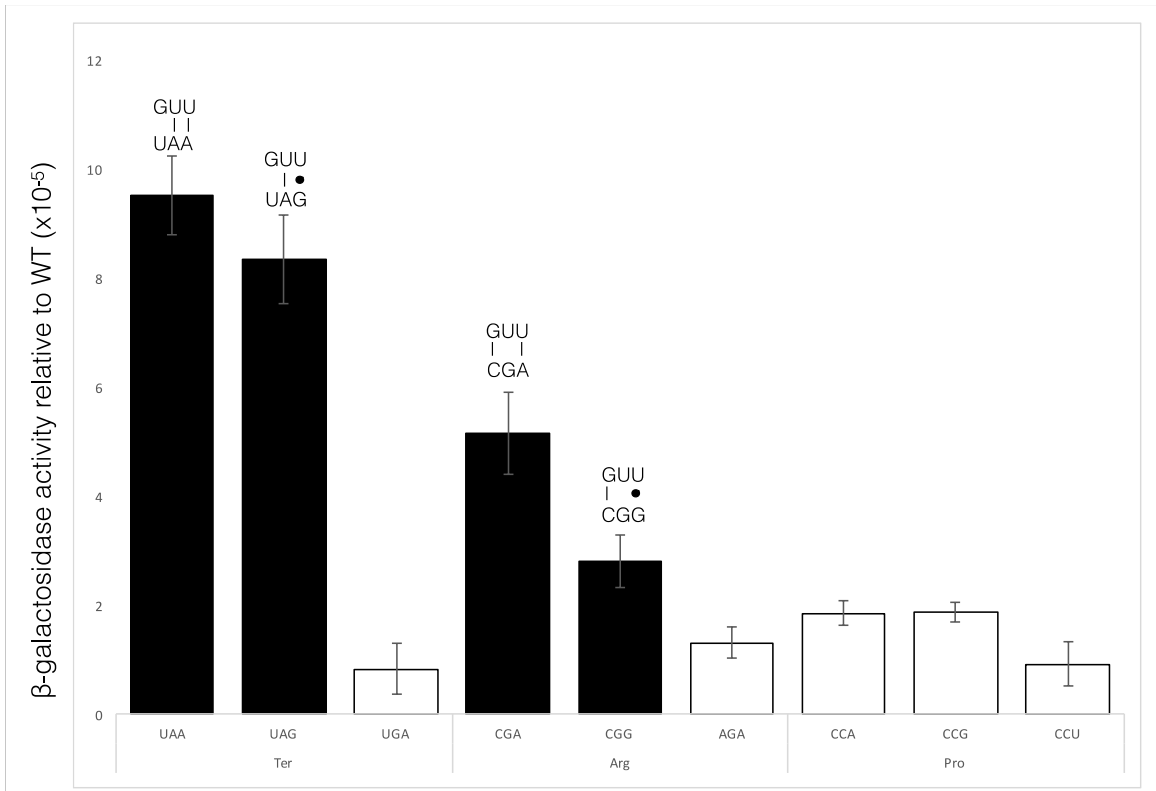


Figure IV–6. High residual β -galactosidase activities of some Q624 codons result from near-cognate decoding

A comparison of β -galactosidase activity relative to the wild type of synonymous near-cognate and non-cognate codon mutants. The error bars represent the standard error of the mean.

Table IV-4. Mutant β -galactosidase activity relative to wild type by tRNA^{Gln}_{UUG} at Q624 near-cognate and synonymous non-cognate codons

Mismatch position	Amino acid	Codon	β -galactosidase activity relative to WT ($\times 10^{-5}$)
1st	Ter	<u>UAA</u> ^a	10
		<u>UAG</u>	8
		<u>UGA</u>	1
2nd	Arg	<u>CGA</u>	5
		<u>CGG</u>	3
		<u>AGA</u>	1
	Pro	<u>CCA</u>	2
		<u>CCG</u>	2
		<u>CCU</u>	1

^aMismatch nucleotide is underlined.

^bThe highest and lowest activity are in bold in a grey box.

the activity of termination and arginine near-cognate mutants was influenced by error-modulating mutants of RPS23 (in the later section) and deficient tRNA modifications (chapter 5) further supports this possibility.

In conclusion, some near-cognate codons at Q624 including termination codons UAA and UAG, and arginine codons CGA and CGG appear to be error-prone codons. Therefore, glutamine 624 (the second Q in the row) is a validated amino acid residue to be utilized to measure misreading events by the tRNA^{Gln}_{UUG} in yeast.

IV. The aminoglycoside antibiotic paromomycin only affects misreading of termination codon UAG

Aminoglycoside antibiotics are known to induce translational misreading via stabilizing and promoting the binding of incorrect tRNAs to the ribosome (Newcombe & Nyholm, 1950; Pape et al., 2000; Ogle et al., 2003). Paromomycin is thought to increase misreading by inducing a conformational change in the decoding center which mimics the binding of a cognate tRNA (Ogle et al., 2003). This binding alters the kinetics of decoding that increases the possibility of accepting a near-cognate tRNAs in the A site (Pape et al., 2000). This antibiotic stimulates mistranslation of poly(U) in yeast extracts and induces phenotypic suppression of both nonsense and missense mutations in yeast cells (Palmer et al., 1979; Singh et al., 1979). Previous studies in yeast showed paromomycin dramatically increased Fluc activity of one near-cognate codon in the tRNA^{Lys}_{UUU} reporter system, AAU (Kramer & Farabaugh, 2010), and of four near-cognate codon mutants in a tRNA^{His}_{GUG} reporter system, GAC, CGC, CUC, and CAG (Salas-Marco & Bedwell, 2005). Previously, our lab used aminoglycoside antibiotics to confirm that the high activity of some near-

cognate codons was due to misreading in both *E. coli* and yeast (Kramer & Farabaugh, 2007; Kramer et al., 2010).

To confirm that higher activity of β -galactosidase resulted from misreading, I used paromomycin to stimulate misreading errors. As expected, errors of the stop codon UAG increased from 8×10^{-5} to 17×10^{-5} , more than 2-fold, when I exposed cells to 200 $\mu\text{g/ml}$ of paromomycin (Figure IV-7 and Table IV-5). The activity of the UAA mutant was also altered slightly by paromomycin from 10×10^{-5} to 12×10^{-5} . However, this difference was not statistically significant. Paromomycin did not affect the other mutants that appear to be error-prone including CGA and CGG. The result indicated that paromomycin only influences a subset of misreading events (Figure IV-7 and Table IV-5). This result is quite similar to the observations of Kramer et al. (2010) in yeast. They found paromomycin significantly increased errors of stop codons UAA and UAG and marginally affected one asparagine codon AAU (Kramer et al., 2010). In *E. coli*, the antibiotic increased misreading errors of all error-prone codons (Kramer and Farabaugh, 2006). The mechanism behind this more limited effect of paromomycin in eukaryotes is unclear.

V. A mutation in ribosomal protein S23 affected misreading error frequency of several near-cognate codons

As an essential component of ribosomes, ribosomal proteins also play an important role in tuning translational accuracy. For example, the accuracy of translation in *E. coli* is significantly affected by ribosomal protein S12 (encoded by the *rpsL* gene), S4, and S5 (encoded by the *rpsD* and *rpsE* genes respectively). Mutations of S12 increase accuracy and are hyperaccurate. On the other hand, "ribosomal ambiguity mutations" (*ram*) in S4 or S5 decrease accuracy and are hypoaccurate (Bouadloun et al., 1983; Parker & Friesen, 1980; Parker & Holtz, 1984; Precup & Parker, 1987; Strigini & Brickman, 1973; Toth et al., 1988).

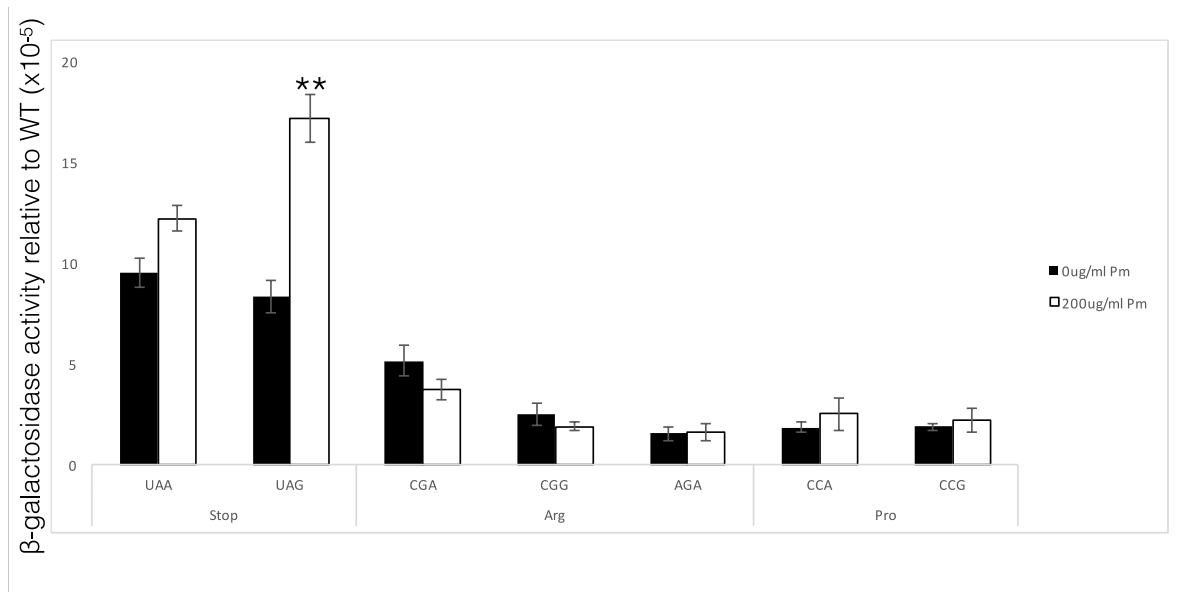


Figure IV-7. Aminoglycoside antibiotics increase misreading of a subset of near-cognate 624 codons

The β -galactosidase activities relative to wild type are shown for mutants carrying the indicated Q624 codon replacements in the presence of no antibiotic (black bars), 200 $\mu\text{g}/\text{mL}$ paromomycin (white bars). The error bars represent the standard error of the mean.

Table IV-5. The mutant β -galactosidase activity relative to wild type in the presence and absence of paromomycin

Amino acid	Codon	β -galactosidase activity relative to WT ($\times 10^{-5}$)		
		0 $\mu\text{g/ml}$ Pm	200 $\mu\text{g/ml}$ Pm	Fold Change
Stop	UAA	10	12	1.2
	UAG	8	17	2
Arg	CGA	5	4	1
	CGG	3	2	1
	AGA	1	1	1
Pro	CCA	2	2	1
	CCG	2	2	1

Significantly changed mutant protein activities are in bold.

In the yeast *Saccharomyces cerevisiae*, mutations in *SUP46* and *SUP44*, encoding the proteins homologous to S4 and S5 in *E. coli*, also cause less accurate translation. By using site-directed mutagenesis, Alksne et al. (1993) were able to substitute Lys62 with arginine, threonine, glutamine, and asparagine. A substitution of the mutant gene was introduced to one of the wild type genes in the wild type strain and *SUP44*- and *SUP46*-containing strains to enable a phenotypic screen. The data showed that amino acid substitution (K62N, Q, T, and R) altered translation fidelity in yeast. Mutation K62N, Q, or T, as it was observed in *E. coli*, decreased paromomycin sensitivity and therefore increased translational accuracy; K62R substitution, however, caused more translational errors and increased sensitivity to a drug. Together, this study suggested that this conserved ribosomal protein (rpS12 in *E. coli* and its homologue rpS23 in yeast) has the same function in regulating translational fidelity in bacteria and yeast (Alksne et al., 1993).

To further confirm those putative error-prone codons, I measured the β -galactosidase activity of several of the Q624 near-cognate codons in yeast carrying the mutant form of *RPS23*. An A113V mutation in rpS23 confers a hyperaccurate phenotype while a K63R mutation in rpS23 confers a hypoaccurate phenotype in yeast (Alksne et al., 1993; Anthony & Liebman, 1995). I tested potential error-prone codons including termination codons UAA and UAG, arginine codons CGA, CGG and AGA, and proline codons CCA and CCG (Figure IV-8). The A113V mutation significantly reduced misreading error frequency of the three error-prone near-cognate codons UAA, UAG, and CGG an average of 1.8-fold ($P < 0.05$) but had little or no influence on the remaining codons (Figure IV-8 and Table IV-6). Misreading errors of stop codons UAA and UAG were reduced from 14×10^{-5} and 11×10^{-5} to 6×10^{-5} and 6×10^{-5} respectively, which were ~2.5 and 1.7-fold decreases. The misreading frequency of CGG was reduced from 4×10^{-5} to 3×10^{-5} ,

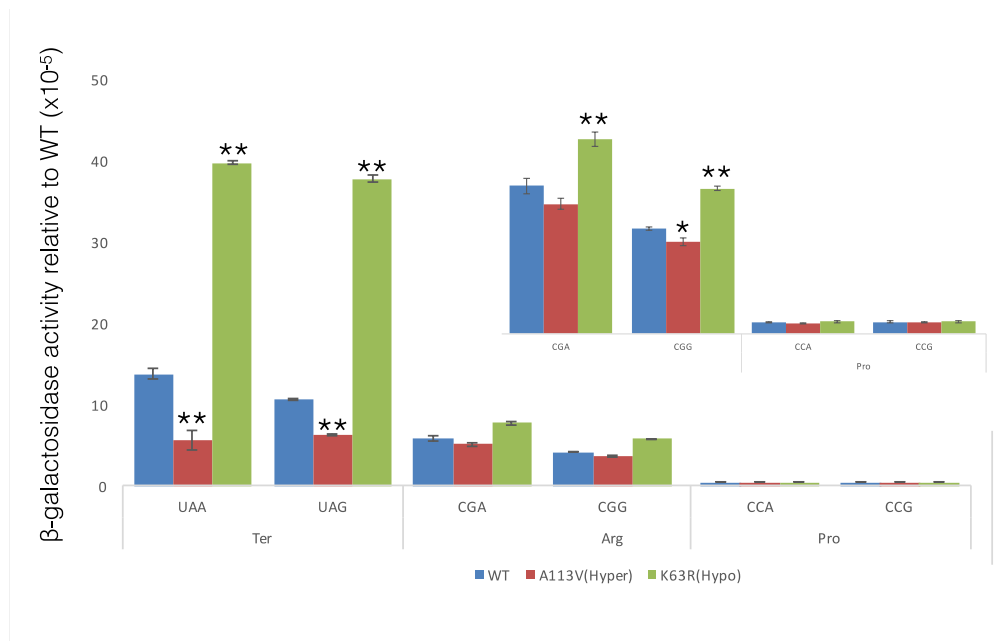


Figure IV–8. Mutations in *rps23* only affect β -galactosidase activities of Q624 termination codon mutants

The β -galactosidase activities relative to wild type of the indicated Q245 codon replacements are shown from a wild-type strain (blue bars), a strain carrying the hyperaccurate (A113V) *rps23* mutation (red bars) and a strain carrying the hypoaccurate (K63R) *rps23* mutation (green bars). The error bars represent the standard error of the mean.

Table IV-6. Mutant β -galactosidase activity relative to wild type of Q624 by tRNA^{Gln}_{UUG}

Amino acid	Codon	β -galactosidase activity relative to WT ($\times 10^{-5}$)				
		WT	A113V(Hyper)	A113V fold change	K63R(Hypo)	K63R fold change
Ter	<u>U</u> AA	14	6	2.5	40	2.9
	<u>U</u> AG	11	6	1.7	38	3.6
Arg	<u>C</u> GA	6	5	1.1	8	1.3
	<u>C</u> GG	4	3	1.2	6	1.4
Pro	<u>C</u> CA	0.4	0.4	1.0	0.5	1.3
	<u>C</u> CG	0.5	0.5	1.0	0.5	1.0

a ~1.2-fold change ($p < 0.05$). In the A113V mutant background, no codon had a relative activity higher than 6×10^{-5} . The potential error-prone arginine codon CGA had errors reduced from 6×10^{-5} to 5×10^{-5} , which was about a 1.1-fold decrease; this change was not statistically significant. There was no significant change for the other three non-error-prone codons, the arginine AGA and the proline codons CCA and CCG (Figure IV-8 and Table IV-6). These data suggested that the A113V mutation only reduces misreading frequency of error-prone near-cognate codons but does not affect the frequency of misreading of non-error-prone codons.

I also tested the β -galactosidase activity of the above codons in yeast carrying the hypoaccurate K63R mutation. In this background, there were statistically significant increases in the misreading of UAA, UAG, CGA, CGG (Figure IV-8 and Table IV-6) ($p < 0.05$). The stop codon UAG had the largest increase from 11×10^{-5} to 38×10^{-5} , or a ~3.5-fold change, and the stop codon UAA increased from 14×10^{-5} to 40×10^{-5} and had a 2.9-fold change (Table IV-6). The other affected codons, CGA and CGG, had misreading frequency increased from 6×10^{-5} to 8×10^{-5} , and 4×10^{-5} to 6×10^{-5} , respectively, or 1.3 and 1.5-fold respectively. Likewise, *rpS23* with mutation K63R affected misreading frequency of the error-prone codons (UAA, UAG, CGA and CGG) but this effect was larger than the effects of the hyperaccurate mutation or treatment with the aminoglycoside antibiotic paromomycin.

The fact that hyperaccurate and hypoaccurate mutations in RPS23 altered the frequency of misreading of potential error-prone codons UAA, UAG, CGA and CGG further confirmed that these codons are error-prone codons.

VI. Western analysis of mutant proteins

To further confirm that the difference in activity of Q624 error-prone codons was not due to varying amounts of protein expression in the cell, I performed a western blot assay of wild-type and mutant β -galactosidase (Figure IV-9). These mutants included five near-cognate mutants, which were UAA, UAG, CGA, CGG and CCG, and one non-cognate mutant, which was AGA. PGK1 was used as a loading control. Western blotting with an antibody against anti- β -galactosidase showed that the expression of β -galactosidase in all mutants was virtually identical to that of wild type except two nonsense mutants. There are 1027 amino acids in β -galactosidase. The nonsense mutation is located at position 625, which is about half of the full length. Consequently, the presence of nonsense mutation leads to a truncated protein product. I was unable to visualize this truncated product suggesting that the protein is probably degraded in vivo. Expression of the loading control PGK1 was roughly equivalent in all strains. Thus, this assay confirms that the differences in β -galactosidase activity of Q624 mutants are from a cause other than differences in protein expression level.



Figure IV-9. Western blot of β -galactosidase of wild type and some mutants of Q624

Extracts from yeast transformants were made. 10 micrograms of total protein for each sample was loaded and detected using β -galactosidase and PGK1 antibody. PGK1 was used as a loading control.

C. Discussion

In this chapter, I have tested the possibility of two codons in the *lacZ* gene, which encodes β -galactosidase, being useful sites to measure misreading events by the tRNA^{Gln}_{UUG}. One residue tested is Q625, and the other is Q624.

The conclusion claimed by Tsai and Curran that misreading caused the activity of a CGA mutant at Q625 was incorrect. They had limited their study only to the near-cognate mutant CGA but did not have any proper control such as AGA or other synonymous non-cognate codons of arginine. A proper negative control is necessary otherwise a study may be misleading. For example, Salas-Marco and Bedwell studied misreading events at H245 of Firefly luciferase by tRNA^{His}_{GUG}. They had mutated CAC at H245 to eight near-cognate codons of CAC. However, there was no synonymous non-cognate mutant. Therefore, they did not have a negative control to test the functional replacement model or the misreading model (Salas-Marco & Bedwell, 2005). Our lab has developed a more comprehensive system and included synonymous non-cognate codons (Kramer et al., 2010). The results showed that the high activity of many near-cognate codons at H245 was due to functional replacement but not misreading (Kramer et al., 2010). In Tsai and Curran's study, they also reported that tRNA^{Gln}_{UUG} misread CGA at a frequency of 1×10^{-3} (Tsai & Curran, 1998). I found the β -galactosidase activity of CGA mutant relative to wild type is 2.2×10^{-3} . To test if this high protein activity was due to misreading errors, I measured the activity of three synonymous arginine codons, CGA, CGG, and AGA. AGA is a non-cognate codon of the wild type CAG. AGA was used as a negative control because it is very unlikely to be misread by tRNA^{Gln}_{UUG} because fewer than two base pairs can form between the codon and anticodon. My data showed the three synonymous arginine mutants had nearly the same relative activity (Figure IV-4 and

Table IV-2). Therefore, my data demonstrated that the activity of CGA was not due to misreading but functional replacement, meaning that the activity measured results from the glutamine being functionally replaced by arginine. Thus, this result invalidated the conclusion that tRNA^{Gln}_{UUG} misread CGA as CAG (Tsai & Curran, 1998). To further study if Q625 is an essential amino acid residue for β -galactosidase, I also measured the activity of near-cognate codon lysine AAG, and two histidine codons CAU and CAC. I found that all of the three near-cognate codons had similar activity relative to wild type at a frequency of 10^{-3} , which was quite similar to the negative control AGA (Figure IV-4 and Table IV-2). The high residual activity of lysine codon AAG may also be due to functional replacement, but in that case, there is no synonymous non-cognate codon, so theoretically it is possible that this mutant is misread by tRNA^{Gln}_{UUG}. If the activity of AAG were due to misreading, then this misreading event would involve an A1•G36 mismatch. Based on previous work, the first position A1•G36 mismatch is not expected to be frequent (Manickam et al., 2014). That work reported there were no significant errors for eight first position mismatches and A1•G36 was one of them (Manickam et al., 2014). Therefore, it is unlikely that tRNA^{Gln}_{UUG} misreads AAG. The other two near-cognate codons histidine CAU and CAC would make wobble errors at the third position. The wobble errors would involve U3•U34 and C3•U34 mismatches. The high residual activities of CAU and CAC also seems unlikely to have resulted from misreading events by tRNA^{Gln}_{UUG}. Again, they both had activity as high as the negative control AGA (Figure IV-4 and Table IV-2). It may be that misreading at CAU and CAC does occur, but the activity caused by misreading errors is too low to be detected given the high activity resulting from functional replacement. Therefore, I was unable to detect wobble errors of CAU and CAC by tRNA^{Gln}_{UUG}.

The termination codons UAA and UAG had much lower activities than the other codons. UAA had at least ~28-fold less activity than other codons, and UAG had at least ~130-fold lower activity (Table IV-2). In addition, the activity of UAG was about 4.5-fold higher than UAG, indicating that the activity of these two codons was probably caused by misreading.

In summary, my data show that Q625 is not essential as reported by the previous work (Tsai & Curran, 1998) and the activity they detected did not result from a misreading event but was due to functional replacement. Overall, Q625 is not a suitable site for measuring misreading events by tRNA^{Gln}_{UUG}.

The other glutamine site, Q624, however, was a better reporter site for studying misreading errors by tRNA^{Gln}_{UUG}. In this yeast project, I generated a full set of mutations to near-cognate codons of Q624 CAG as well as some synonymous non-cognate codons (Table IV-1). I found that yeast tRNA^{Gln}_{UUG} misreads a subset of the near-cognate codons of Q624 including UAA, UAG, CGA, and CGG. The frequencies vary 3.3-fold from as high as 10×10^{-5} (UAA) to no greater than 3×10^{-5} (CGG) (Figure IV-6 and Table IV-4). These misreading events involved U1•G36 (to stop codons UAA and UAG), and G2•U35 (to arginine codons CAG and CGG) mismatches. I have not found misreading occurring at CCA or CCG proline codons, which would require a second position C2•U35 mismatch. Therefore, there were only purine-pyrimidine mismatches but no purine-purine mismatch. Previously, our lab has demonstrated the most frequent errors in bacteria by tRNA^{Glu}_{UUC}, tRNA^{Tyr}_{QUA}, tRNA^{Asp}_{QUC}, and tRNA^{Lys}_{UUU} involve U3•U34, C3•U34, G2•U35, and U1•U36 (Manickam et al., 2014). However, Manickam et al. (2014) did not see significant errors involving U1•G36. Zhang et al. reported that G•U mismatch at any of the three codon positions along with C3•U34 is the primary cause of misincorporation (Zhang et al., 2013). A structural study revealed two

misreading events (Demeshkina et al., 2012). They are near-cognate codon UUC misread by tRNA^{Leu}_{GAG} involving a G36•U1 mismatch and near-cognate codon UGC misread by Tyr tRNA^{Tyr}_{QUA} involving a G2•U35 mismatch (Demeshkina et al., 2012). They had found that when these two mismatch events occurred at the first and second position, the decoding center constrained mismatched nucleotides to adopt Watson-Crick geometry. Meanwhile, these events induced a conformational change of the decoding center (Demeshkina et al., 2012). My results are in high agreement with previous work and also have broadened our lab's previous study, showing that U1•G36 and G2•U35 are the most frequent errors by tRNA^{Gln}_{UUG}. In conclusion, Q624 is a more useful amino acid site to study misreading errors by tRNA^{Gln}_{UUG} as compared with Q625.

The frequency of misreading at Q624 was surprisingly low compared with our lab's previous work in yeast. Kramer et al. estimated that misreading frequencies at error-prone codons by tRNA^{Lys}_{UUU} ranged from 5×10^{-4} to 7×10^{-4} (UAG and AGG) (Kramer et al., 2010). The near-cognate mutant UAA at Q624 had the highest misreading frequency by tRNA^{Gln}_{UUG} yet was only 1.0×10^{-4} , which was about 10-fold lower. Misreading at CGA and CGG involving G•U mismatch only had 5×10^{-5} and 3×10^{-5} respectively. These frequencies were much lower than the misreading frequency of AGG, which also involved G•U at the second position.

Another intriguing result is that the activity of UAA and UAG at Q624 was much higher than that at Q625. The activity of UAA is about 2-fold higher at Q624 than Q625. Meanwhile the activity of UAG is about 6-fold higher at Q624 than Q625 (Table IV-2 and Table IV-3). One explanation is that readthrough of nonsense codons may reflect the rate of termination. The sequence surrounding nonsense codons, especially the fourth base of stop codons, can significantly affect the efficiency of nonsense codon suppression. This is termed context effect. Previous studies have

demonstrated the context effects on suppression at UAA and UAG in the mammalian system (Phillips-Jones et al., 1995; Manuvakhova et al., 2000). Both studies ranked the order of the context effect on nonsense readthrough as C > U. The sequence was UAAC and UAAU respectively when introducing the stop codon UAA to Q624 and Q625. The sequence was UAGC and UAGU respectively when introducing the stop codon UAG to Q624 and Q625. These sequences are consistent with more rapid readthrough at 624 than at 625.

The aminoglycoside antibiotic paromomycin presumably induces translational misreading by altering conformation rearrangements in the ribosome that interfere with the ribosome discriminating between near-cognate and cognate tRNAs in the A site (Benveniste & Davies, 1973; Fourmy, Recht, Blanchard, & Puglisi, 1996; Carter et al., 2000; Pape et al., 2000). Kramer et al. showed that, in yeast, paromomycin only stimulates misreading of three near-cognate mutants by tRNA_{UUU}^{Lys} including UAA, UAG, and AAU in yeast. Among the three mutants, paromomycin had a small effect on AAU but it increased misreading UAA and UAG much more strongly (Kramer et al., 2010). Using the same concentration, I found paromomycin increased the frequency of misreading of UAG only ~2-fold, but it had no effect on other error-prone codons UAA, CGA, and CGG. Kramer et al. found that paromomycin simulated the frequency of misreading events involving U•U mismatch in all the three cases (Kramer et al., 2010). I found the drug only affected a misreading event involving a U•G mismatch at the first position. Altogether, paromomycin seems to have a more limited effect on misreading events by tRNA_{UUG}^{Gln} in yeast. Paromomycin significantly increased readthrough frequency at all three stop codons UAA, UAG, and UGA but only induced misreading errors on a small subset of near-cognate mutants (Salas-Marco & Bedwell, 2005), suggesting paromomycin may have much more restricted and specific effects on sense decoding than on termination. My observation is similar but has a difference with previous work

in that paromomycin only increased misreading errors at UAG by tRNA^{Gln}_{UUG}.

Ribosomal proteins are critical components involved in translational accuracy. Ribosomal protein mutations confer antibiotic resistance (such as paromomycin) and cause hyperaccurate translation. Meanwhile, ribosomal mutations suppress nonsense mutations, increase drug sensitivity, and decrease translational fidelity (Gorini & Kataja, 1964; Alksne et al., 1993; Anthony & Liebman, 1995; Kramer & Farabaugh, 2007; Kramer et al., 2010). Ribosomal protein S23 (RPS23), encoded by *RPS23A* and *RPS23B*, is comparable to bacterial S12. Alksne et al. (1993) screened several mutations in ribosomal protein S23 and found one of the mutations, K62R, reduced translational accuracy by increasing suppression of nonsense mutations and sensitivity to the aminoglycoside antibiotic paromomycin (Alksne et al., 1993). By using the same method, Anthony and Liebman discovered that substitution of Alanine (GCT) to Valine (GTT) (A113V) significantly reduced sensitivity to paromomycin, leading to an increased fidelity phenotype (Anthony & Liebman, 1995). However, these two studies only phenotypically investigated the effects of *RPS23* mutants on translational fidelity. Neither of them quantitatively measured the changes that resulted from *RPS23* mutations.

To further correlate translational fidelity with selected ribosomal mutants, I measured misreading error frequency of potential near-cognate mutants in either a hyperaccurate background (*rps23*-A113V) or a hypoaccurate background (*rps23*-K62R). My data are consistent with earlier studies that both mutations affected misreading frequency of error-prone codons as hypothesized (Alksne et al., 1993; Anthony & Liebman, 1995). In the A113V hyperaccurate background, the frequency of misreading of UAA, UAG, and CGG decreased. However, there was no measurable effect on CCA and CCG. Alteration on misreading frequency of CGA was not statistically significant

despite the fact that CGA is a putative error-prone codon. The effect on CGG was subtle but was greater on the stop codons. This result is consistent with the phenotype alteration that the presence of A113V substitution reversed nonsense mutations. Moreover, an earlier study showed that the A113V substitution significantly decreased the antibiotic sensitivity, suggesting the A113V mutation increased translational fidelity (Anthony & Liebman, 1995). In the K62R hypoaccurate background, misreading errors of UAA, UAG, CGA and CGG all significantly increased. The increase in the frequency of misreading of the stop codons UAA and UAG was much higher than the other error-prone codons. The previous study showed that the K62R mutation in the S23 acts as an omnipotent suppressor, which suppresses both amber and ochre codons (Alksne et al., 1993). My data is consistent with this previously observed phenotype that the K62R mutation and the A113V mutation in S23 can significantly affect misreading frequency of UAA and UAG. My results in combination with previous studies may signal a particular effect of RPS23 on the error prone codons: *RPS23* mutations are more likely to affect the translational fidelity of stop codons but have a very subtle influence on the other error-prone codons. As I stated above, RPS23 is encoded by duplicate genes, *RPS23A* and *RPS23B* (Alksne et al., 1993). A complete deletion of RPS23 is lethal. The yeast strain that I used in my study harbors a deletion in *RPS23B*. Therefore, the presence of a copy of wild type RPS23A in the background may attenuate the effect of RPS23 mutations despite that the mutations are dominant.

CHAPTER V

LACK OF SOME tRNA MODIFICATIONS LEADS TO MORE ACCURATE PROTEIN TRANSLATION IN THE YEAST *Saccharomyces cerevisiae*

Chapter V. LACK OF SOME tRNA MODIFICATIONS LEADS TO MORE ACCURATE PROTEIN TRANSLATION IN THE YEAST *Saccharomyces cerevisiae*

A. Introduction

The universal genetic code has 61 codons for 20 amino acids, and three stop codons, meaning that most amino acids are encoded by more than one codon (Agris, 2004). This phenomenon is called degeneracy (El Yacoubi et al., 2012a). The 61 codons plus three stop codons can be represented in degenerate codon family boxes. In these boxes, synonymous codons code for the same amino acid. There are eight unsplit boxes (all codons code for the same amino acid), five two-split boxes (the two purine-ending codons code for one amino acid and the two pyrimidine-ending codons encode for another, such as Gln/His), and three special codon boxes (Ile/Met, Tyr/Stop, and Cys/Stop Trp) (El Yacoubi et al., 2012a) (Table V-1). In the yeast *Saccharomyces cerevisiae*, there are only 42 tRNAs to decode 61 codons (Phizicky & Hopper, 2010).

Posttranscriptional modifications occur in transfer RNAs from all organisms (Björk et al., 2007). As many as 80 modifications have been reported (El Yacoubi et al., 2012). tRNA modifications can play many roles. Many modifications within the core of the tRNA play an essential role in tRNA structural stabilization; loss of these modifications can cause rapid degradation of hypomodified tRNAs (Phizicky & Alfonzo, 2010). The most diverse and complicated chemical structures are found in the anticodon stem loop or the vicinity. The two most frequently modified positions in tRNA are position 34, which is the wobble position, and position 37, which is the

Table V-1. The genetic code and distribution of cytoplasmic *S. cerevisiae* tRNAs

U			C			A			G			
codon	anticodon	amino acid	codon	anticodon	amino acid	codon	anticodon	amino acid	codon	anticodon	amino acid	
U	UUU	-	UCU	IGA	Ser	UAU	-	Tyr	UGU	-	Cys	
	UUC	GmAA	UCC	-		UAC	GψA		UGC	GCA		
	UUA	ncm⁵UmAA	UCA	ncm⁵UGA		UAA	-		UGA	-		n.a.
	UUG	m ⁵ CAA	UCG	CGA		UAG	-		UGG	CmCA		Trp
C	CUU	-	CCU	AGG	Pro	CAU	-	His	CGU	ICG	Arg	
	CUC	GAG	CCC	-		CAC	GUG		CGC	-		
	CUA	UAG	CCA	ncm⁵UGG		CAA	mcm⁵s²UUG		CGA	-		Gln
	CUG	-	CCG	-		CAG	CUG		CGG	CCG		
A	AUU	IAU	ACU	IGU	Thr	AAU	-	Asn	AGU	-	Ser	
	AUC	-	ACC	-		AAC	GUU		AGC	GCU		
	AUA	ψAψ	ACA	ncm⁵UGU		AAA	mcm⁵s²UUU		AGA	mcm⁵UCU		Arg
	AUG	CAU	ACG	CGU		AAG	CUU		Lys	AGG		CCU
G	GUU	IAC	GCU	IGC	Ala	GAU	-	Asp	GGU	-	Gly	
	GUC	-	GCC	-		GAC	GUC		GGC	GCC		
	GUA	ncm⁵UAC	GCA	ncm⁵UGC		GAA	mcm⁵s²UUC		GGA	mcm⁵UCC		
	GUG	CAC	GCG	-		GAG	CUC		Glu	GGG		CCC

The anticodon sequences of the 42 different tRNA species (1 initiator and 41 elongator tRNAs) are indicated. For anticodons with an uncharacterized RNA sequence, the primary sequence is shown. The initiator and elongator tRNA^{Met} species have identical anticodon sequences. The wobble rules suggest that an inosine (I₃₄) residue allows pairing with U, C, and sometimes A. A tRNA with a G or its 2'-O-methyl derivative (Gm) at the wobble position should read U- and C-ending codons. Presence of a C34 residue or its 5- methyl (m⁵C) or 2'-O-methyl (Cm) variant should only allow pairing with G. The pseudouridine (C)-containing tRNA^{Ile} is presumably unable to pair with the methionine AUG codon. The anticodons containing mcm⁵U, mcm⁵s²U, ncm⁵U and ncm⁵U_m derivatives are shown in bold (Johansson et al., 2008).

nucleotide next to and 3' of the anticodon (El Yacoubi et al., 2012) (Figure V-1).

Post-transcriptional modifications at the wobble positions play a pivotal role in the codon-anticodon decoding process (Agris et al., 2007). In a correct decoding process, the first and second base of the codon and the third and second base of the anticodon interact following the Watson-Crick rules (A:U, U:A, G:C, C:G). Crick proposed in his wobble hypothesis that interaction between the third base of the codon and the first base of the anticodon (wobble position) is relatively less constrained (F. H. C. Crick, 1966). The variation of hypermodified nucleotides occurring at the wobble position and position 37 of the anticodon enables the flexibility of base pairing during decoding (Gustilo et al., 2008; El Yacoubi et al., 2012). For example, some post-transcriptional modifications at the wobble position expand the capability of base pairing while some restrict the wobble position base-pairing (Persson, 1993). For example, inosine (I), a modified A, expands wobble position base-pairing. Adenosine should only base pair with U while inosine can recognize A, U and C (F. H. C. Crick, 1966). Another example would be carboxymethoxyuridine (cmo^5U), which expands the ability of tRNA decoding. Carboxymethoxyuridine can base pair with A, G and U while unmodified uridine only pairs with A and G (Björk, 1995). By contrast, 5-methoxycarbonylmethyl-uridine (mcm^5U) and 5-methoxycarbonylmethyl-2-thiouridine ($\text{mcm}^5\text{s}^2\text{U}$) modification was thought to restrict a tRNA to only recognize A instead of A and G when the U is unmodified (Agris et al., 2007). In addition, modifications at position 37 can indirectly affect decoding by stabilizing adjacent codon-anticodon pairing. For example, a tRNA with a 2-methylthio-N⁶-isopentenyladenosine ($\text{ms}^2\text{i}^6\text{A}_{37}$) modification at position 37 recognizes codons beginning with A; this modification is thought to stabilize the weak A1•U36 pairing. Loss of this modification reduces the efficiency of decoding (Björk & Hagervall). Emerging evidence demonstrates that lack of some tRNA modifications can

affect protein production or translational accuracy (Lyko & Tuorto, 2016; Manickam et al., 2016). Studies of the effect of modification on mispairing have given more information on how tRNA modifications affect translational accuracy. Loss of modifications mnm⁵s²U or the hypermodified base queuosine at wobble position 34 and ms²i⁶A at position 37 modulates translational accuracy in *E. coli* (Manickam et al., 2015). Manickam *et al.* (2015) developed four misreading error reporter systems to quantify misreading errors by four tRNAs: tRNA^{Lys}_{UUU}, tRNA^{Glu}_{UUC}, tRNA^{Asp}_{QUC} and tyrosine tRNA^{Tyr}_{QUA}. Their data showed that misreading errors increased when there is no modification of tRNA^{Glu}_{UUC} and tRNA^{Asp}_{QUC}, and misreading errors decreased when there is no modification of tRNA^{Lys}_{UUU} and tRNA^{Tyr}_{QUA}. This is striking that the same modifications showed opposite effects on misreading errors in different tRNAs. They have suggested that the effect of the anticodon loop modifications on decoding depends on the tRNA's structural context. Most tRNA modifications in the anticodon loop seem to modulate the anticodon loop structure, improving the efficiency that tRNAs read cognate codons. Some tRNA's anticodon loops are intrinsically unstable. These tRNAs strongly require modifications in the anticodon loop for either cognate or near-cognate decoding. Hence, the absence of these tRNA modifications would reduce misreading errors during decoding (Manickam et al., 2015).

The importance of the cellular function of tRNA modifications has been extensively characterized, however, less information has been provided on how tRNA modifications affect translational error frequency. Therefore, I tested the effects of loss of three modifications—mcm⁵ and s² at the wobble position, and pseudouridine at position 38—on the frequency of misreading errors using the Gln tRNA reporter system that I developed in chapter 4.

The Elongator complex is a 6-subunit protein complex that is highly conserved in eukaryotes. The role of this complex has been controversial. However, recent results suggest that the primary and probably the only role of Elongator complex is in the formation of the 5-methoxycarbonylmethyl (mcm^5) and 5-carbamoylmethyl (ncm^5) side chains on uridines at the wobble positions in tRNA (Huang et al., 2005; Björk et al., 2007; Karlsborn et al., 2014). In *Saccharomyces cerevisiae*, loss of any of the six Elongator protein subunit (Elp1-Elp6) genes disrupts an early step in the synthesis of the mcm^5 and ncm^5 groups present on uridine at the wobble position in tRNAs. It is known that in *S. cerevisiae* five tRNA species contain a wobble mcm^5 side chain, including arginine tRNA $_{mcm^5UCU}$, glycine tRNA $_{mcm^5UCC}$, lysine tRNA $_{mcm^5s^2UUU}$, glutamine tRNA $_{mcm^5s^2UUG}$, and glutamic acid tRNA $_{mcm^5s^2UUC}$ (Smith et al., 1973; Kobayashi et al., 1974; Kuntzel et al., 1975; Björk et al., 2007; Johansson et al., 2008). These modifications are missing in the *elp3Δ* mutant strain but not the wild type strain. However, the presence of a plasmid carrying the wild type *ELP3* gene rescued the formation of these nucleosides. Interestingly, in the *elp3Δ* mutant a novel modification detected in tRNA^{Glu} was characterized as 2-thiouridine (s^2U) (Huang et al., 2005). All these data demonstrated that loss of *ELP3* abolished the formation of the mcm^5 or ncm^5 side chains on the uridine, but *elp3Δ* did not block the synthesis of 2-thiolation in tRNA^{Glu} (Huang et al., 2005).

Wobble uridine modifications play an essential role in protein translation owing to their influence on codon-anticodon decoding. The wobble uridine nucleosides mcm^5U and ncm^5U were suggested to restrict pairing only with A-ending codon (Agris, 2004). However, emerging evidence contradicts this hypothesis, showing that the presence of mcm^5 side chain in yeast Gln, Lys, and Glu tRNAs promotes reading of codons ending with G (Björk et al., 2007). Indeed, the existence of both mcm^5 and s^2 groups improve reading of both A- and G-ending codons (Johansson et al.,

2008). In the yeast *S. cerevisiae*, 11 of 42 different cytoplasmic tRNA species have modified uridines at the wobble position including mcm⁵U and mcm⁵s²U (Figure V-2). Johansson et al. (2008) studied the role of tRNA modifications, including mcm⁵, s² and mcm⁵s² in decoding (Johansson et al., 2008). The fact that yeast tRNA species possess U34 and C34 containing isoacceptors suggests A- and G- ending codons are decoded by distinct tRNAs (Percudani, 2001). For example, both tRNA^{Arg}_{mcm5UCU} and tRNA^{Gly}_{mcm5UCC} decode in split codon boxes (Table V-1). In the two-split codon box, a C34 containing tRNA complementary to the G-ending codon exists, suggesting that tRNA^{Arg}_{mcm5UCU} does not have to read the G-ending codons. Based on this assumption, Johansson et al. (2008) deleted the genes coding for tRNA^{Arg}_{CCU}, and found that these deletions did not affect the viability of yeast cells, suggesting tRNA^{Arg}_{mcm5UCU} is capable of reading its corresponding G-ending codon AGG. Then they further explored the function of mcm⁵ in a *elp3Δ* background lacking tRNA^{Arg}_{CCU}. They observed synergistic growth defects in the mutant strain, indicating the existence of an mcm⁵ side chain improves reading ability of G-ending codons of tRNA^{Arg}_{mcm5UCU} (Johansson et al., 2008). By using the same strategy, they also studied the role of mcm⁵s². tRNA^{Gln}_{mcm5s2UUG} also decodes in a split codon box where tRNA^{Gln}_{CUG} is present (Table V-1). A yeast strain deleted for tRNA^{Gln}_{CUG} was inviable, suggesting tRNA^{Gln}_{mcm5s2UUG} is not able to read G-ending codons. However, overexpression of tRNA^{Gln}_{mcm5s2UUG} counteracted inviability caused by lack of tRNA^{Gln}_{CUG} in a wild type but not an *elp3Δ* or *pus3Δ* background, suggesting the ability of tRNA^{Gln}_{mcm5s2UUG} to read G-ending codons requires both the mcm⁵ and s² groups. Their study demonstrated that the mcm⁵ and s² groups cooperatively enhance reading of G-ending codons. Therefore, the presence of mcm⁵ or mcm⁵s² indeed extends the decoding ability of tRNA^{Gln}_{mcm5s2UUG} (Johansson et al., 2008).

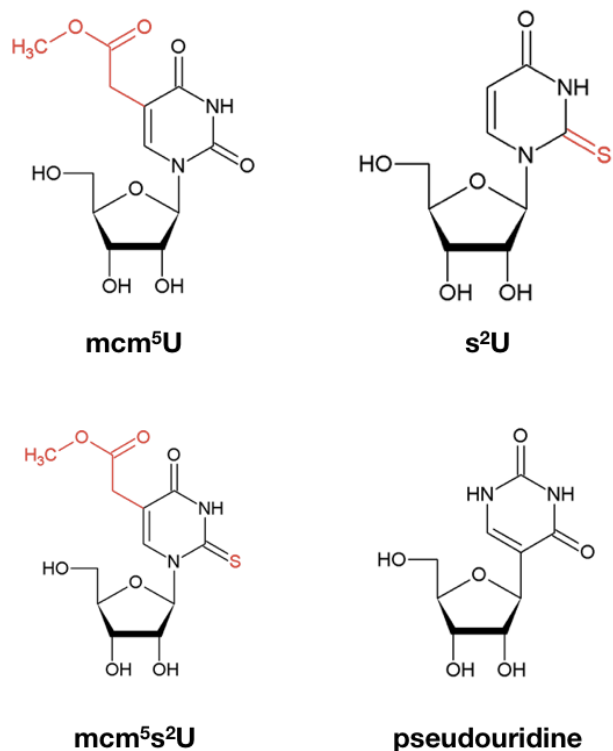


Figure V–2. Structure of some tRNA modifications

Structure of 5-methoxycarbonylmethyluridine (mcm⁵U) and methoxycarbonylmethyl-2-thiouridine (mcm⁵s²U), 2-thiouridine (s²U) and pseudouridine (Ψ). Highlighted in red are uridine side groups (modomics.genesilico.pl/).

Another tRNA modification that I have studied in this chapter is pseudouridine 38 (Ψ 38). The *DEG1* gene (also named *PUS3*) catalyzes the formation of pseudouridines Ψ 38 and Ψ 39. Deletion of *DEG1* in yeast strains only eliminated Ψ 38 and Ψ 39, whereas Ψ at other positions in tRNAs (13, 27, 28, 32, 34, 35, 36, and 55) were unaffected (Lecointe et al., 1998). Lack of pseudouridine Ψ 38 and Ψ 39 is not lethal but leads to slow growth rate at an elevated temperature (37 °C) (Lecointe et al., 1998; Han et al., 2015a). A study by Han et al. (2015) revealed another functional importance of pseudouridine Ψ 38 and Ψ 39. They investigated the reason of the temperature sensitivity of *pus3* Δ mutants in the yeast *S. cerevisiae*. Although Ψ 38 and Ψ 39 exist in at least 19 characterized cytoplasmic tRNA species, only expression of tRNA^{Gln}_{mcm5s2UUG} substantially enhanced cell growth at 37 °C, whereas overexpression of other tRNA species showed no significant influence on cell growth. Moreover, *pus3* Δ cells grew nearly as well as the *PUS3* strain when tRNA^{Gln}_{UUG} was overproduced in the *pus3* Δ strain. All these data suggested that Pus3 primarily targeted tRNA^{Gln}_{UUG} at high temperature (Han et al., 2015).

I have developed a novel misreading error reporter system to quantify misreading error frequency by tRNA^{Gln}_{UUG}. The advantage of this enzyme based reporter system is that it can give highly quantitative measurements of misreading events at all possible codons by a single tRNA. In chapter 4, I have stated that misreading events by tRNA^{Gln}_{UUG} involved two types of mismatches, which are U1•G36, G2•U35. Four near-cognate codons are putative error-prone codons, and they are stop codons UAA and UAG, arginine codons CGA and CGG. Stop codons UAA and UAG were the most frequent misread mutants by tRNA^{Gln}_{UUG}. In this chapter, I will focus on the experiments concerning the influence on misreading of the lack of three post-transcriptional tRNA

modifications: 5-methoxycarbonyl-methyl (mcm^5) and 2-thio (s^2) at the wobble position, and pseudouridine (Ψ) at position 38.

Most of the previous work focused on the consequences caused by lacking a combination of mcm^5s^2U and Ψ 38/39 on cognate decoding. However, there has been no study of the function of each individual modification in near-cognate decoding in yeast cells. Therefore, I intended to explore the role of each modification in translational errors in $tRNA_{UUG}^{Gln}$ since this tRNA carries both mcm^5s^2U and Ψ 38 modifications.

B. Results

In chapter 4, I have found that Gln625 is not essential for the activity of β -galactosidase as suggested by Tsai and Curran (Tsai & Curran, 1998). They did not have a proper control to show that the high activity of near-cognate codon CGA at Q625 was due to misreading. I have introduced all possible near-cognate codons and their synonymous non-cognate codons to both Q624 and Q625. Based on my results, I showed that the high activity of near-cognate codon CGA at Q625 was not because of misreading by $tRNA_{UUG}^{Gln}$ but due to functional replacement. Q625 indeed is not a useful residue to study misreading events. Instead, Q624 is a more important residue of β -galactosidase. Second, I showed that in a wild-type yeast strain, there was no obvious evidence for wobble errors despite the high activity of near-cognate codons CAU and CAC, at which $tRNA_{UUG}^{Gln}$ could make wobble errors. However, we found misreading errors by $tRNA_{UUG}^{Gln}$ on only four near-cognate codons: the stop codons UAA and UAG, and the arginine codons CGA and CGG.

Posttranslational modifications of tRNAs, especially modifications occurring in and around the anticodon loop, exert great effects through restricting or expanding tRNA decoding (Yarian et al.,

2002; Agris, 2004; Gustilo et al., 2008). Our lab has demonstrated that loss of some tRNA modifications indeed can directly affect translational accuracy *in vivo* (Manickam et al., 2016). Hence, I studied the role of three tRNA modifications in translational fidelity. Moreover, these studies allowed me to further confirm that the higher activity of the four putative error-prone codons was due to misreading.

Many studies have identified that tRNA^{Gln}_{UUG} has both mcm⁵s²U34 and Ψ38 modifications (Huang et al., 2005; Lu et al., 2005; Esberg et al., 2006; Glenn R Björk et al., 2007; Johansson et al., 2008; Han et al., 2015a; Klassen et al., 2016a; Klassen & Schaffrath, 2017). Analysis of these modifications of tRNA^{Gln}_{UUG} depends on high-performance liquid chromatography (HPLC) as described before (Gehrke & Kuo, 1989). tRNA^{Gln}_{UUG} was first purified and degraded to nucleosides by nuclease PI. Their composition was further analyzed by high-performance liquid chromatography (HPLC). Based on their relative retention time and UV absorption spectra, tRNA^{Gln}_{UUG} was characterized to carry both mcm⁵s²U and Ψ38 modifications (Esberg et al., 2006; Johansson et al., 2008; Han, Kon, & Phizicky, 2015a; Klassen et al., 2016).

Other emerging evidence further supports the notion that tRNA^{Gln}_{UUG} has both mcm⁵s²U and Ψ38 modifications. For example, γ-toxin secreted by killer strains *Kluyveromyces lactis* specially targets three tRNA species tRNA^{Gln}_{mcm5s2UUG}, tRNA^{Lys}_{mcm5s2UUU}, tRNA^{Glu}_{mcm5s2UUC} by cleaving these tRNAs at the 3' side of the modified wobble nucleoside mcm⁵s²U. This cleavage inhibits cell growth. However, γ-toxin cannot efficiently cleave tRNAs lacking the mcm⁵ group, explaining the γ-toxin resistance of the *elp3Δ* strain (Lu et al., 2005). One study (Han et al., 2015a) demonstrated that of the 25 tRNA species carrying a Ψ or uncharacterized uridine at position 38/39, only overexpressing

tRNA^{Gln}_{UUU} improved cell growth of the *pus3Δ* at high temperature, whereas overproduction of the other tRNA species did not significantly improve cell growth. Wild type cells grew nearly as well as the *pus3Δ* overexpressing tRNA^{Gln}_{UUU}. These data strongly suggested that tRNA^{Gln}_{UUU} is the major target of Pus3 at high temperature (Han et al., 2015a). Moreover, this study also showed that loss of both *mcm*⁵s²U and Ψ38 is detrimental to the cell. Remarkably, this phenotype was only suppressed by overexpression of tRNA^{Gln}_{UUU} (Han et al., 2015a). tRNA^{Lys}_{UUU} has the same *mcm*⁵s²U modification as tRNA^{Gln}_{UUU} and tRNA^{Pro}_{UGG} bears Ψ38. However, overproduction of neither of them counteracted the lethality caused by the double mutants. The lethality appears to result from the simultaneous loss of both modifications on tRNA^{Gln}_{UUU} (Han et al., 2015a).

I. Lack of modification of *mcm*⁵ side chain decreases misreading errors of error prone codons

Using this error reporter system for Gln codons, I have measured the effect of *mcm*⁵ on the frequency of misreading of some near-cognate mutants by tRNA^{Gln}_{UUU}. In yeast, the formation of *mcm*⁵ side chain requires the Elongator complex, Elp1-6. Deletion of any of these proteins eliminates the formation of *mcm*⁵. The absence of either *mcm*⁵ or s² or the entire modification *mcm*⁵s²U induces pleiotropic phenotypes, such as growth defects and temperature sensitivity (Esberg et al., 2006). I compared the misreading error frequency in both a wild type and an *elp3Δ* mutant strain. As shown in Figure V-3 and Table V-2, the β-galactosidase activity of the four error-prone mutants is reduced significantly in the absence of *mcm*⁵s²U₃₄ modification in the

Table V-2. Mutant form β -galactosidase activity relative to wild-type in the presence and absence of tRNA modifications

Amino Acid	Codon	β -galactosidase activity relative to WT ($\times 10^{-5}$)				Fold Reduction		
		WT	ELP3 Deletion	NCS6 Deletion	PUS3 Deletion	ELP3 Deletion	NCS6 Deletion	PUS3 Deletion
Stop	<u>U</u> A A	9.5	0.6	1.2	5.4	16	8.0	1.8
	<u>U</u> A G	8.3	4.2	6.2	7.4	2.0	1.3	1.0
Arg	<u>C</u> G A	5.2	1.9	2.2	2.1	3.0	2.4	2.5
	<u>C</u> G G	2.8	2.3	3.1	1.8	1.0	1.0	1.5
	<u>A</u> G A	1.3	2.1	2.1	1.4	1.0	1.0	1.0
Pro	<u>C</u> C A	1.9	2.0	2.1	1.2	1.0	1.0	1.5
	<u>C</u> C G	1.9	2.1	2.3	1.5	1.0	1.0	1.3

Fold reduction responding to each codon is highlighted in gray.

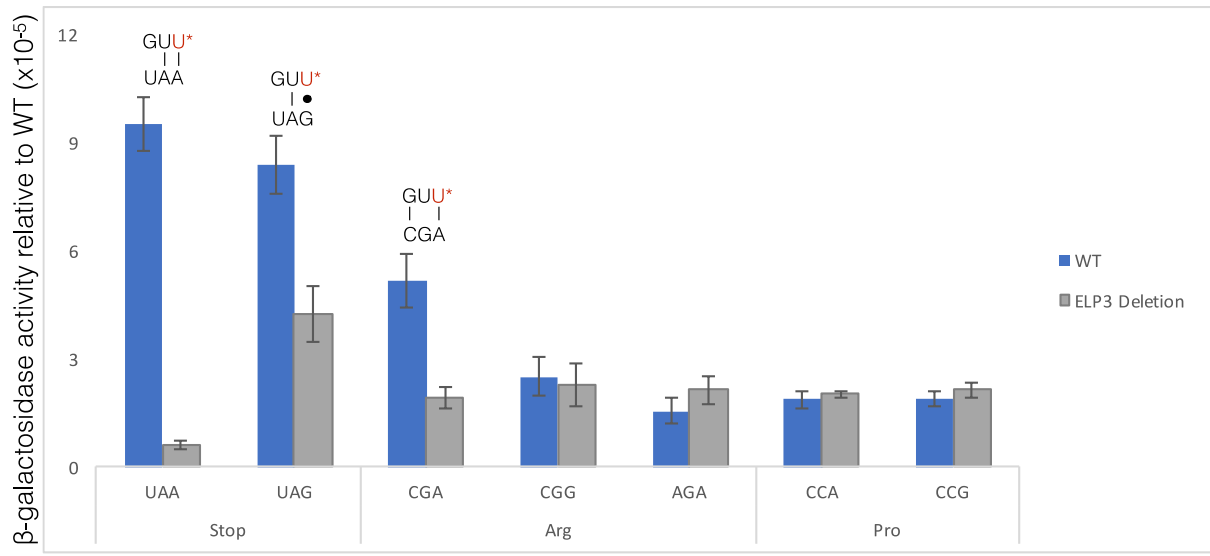


Figure V–3. Misreading frequency by tRNA^{Gln}_{UUG} at near-cognate codons in the presence and absence of the formation of mcm⁵

The relative β -galactosidase activity of Gln624 near-cognate mutants expressing in wild type strain and ELP3 deletion strain shown as blue and gray bars respectively. The error bars represent the standard error of the mean.

elp3Δ strain. The extent of this influence varies between the three codons. The termination codon UAA had the highest reduction, about 16-fold, decreasing from 9.5×10^{-5} to 6×10^{-6} , which is almost the background activity, suggesting that lack of the mcm^5 side chain may eliminate misreading errors. Misreading of UAG decreased from 8.3×10^{-5} to 4.2×10^{-5} , a ~2-fold reduction and misreading of CGA decreased from 5.2×10^{-5} to 1.9×10^{-5} , a ~3-fold reduction. None of the other codons displayed significant changes. $tRNA_{UUU}^{Gln}$ misreading of UAA and UAG requires a U1•G36 mismatch at the first position and of CGA involved G2•U35 mismatch at the second position. An earlier study has demonstrated and suggested that the presence of mcm^5s^2U improved $tRNA_{UUU}^{Gln}$ reading both A- and G-ending codons but primarily improved reading of the G-ending codons (Johansson et al., 2008). In this scenario, $tRNA_{UUU}^{Gln}$ with mcm^5s^2 side chain at the wobble position should improve reading of cognate glutamine codon CAG. Meanwhile, the same effect occurs on near-cognate codons and the tRNA modification increased misreading errors by $tRNA_{mcm^5s^2UUU}^{Gln}$. Hence, loss of the mcm^5 side chain reduced translational errors. In other words, the existence of this tRNA modification stabilizes the interaction between mismatched codon-anticodon pairs. I intended to study the generality of this effect on translational accuracy further. Therefore, I tested the effect of loss of another two tRNA modifications: 2-thiouridine (s^2) and pseudouridine Ψ38.

II. Lack of 2-thiouridine (s^2) also decreases misreading events by $tRNA_{UUU}^{Gln}$

Noma et al. (2009) identified five genes that are required for 2-thiouridine (s^2) formation of mcm^5s^2U in yeast *S. cerevisiae*. NCS6 is one of these genes (Noma et al., 2009). A yeast strain with a *ncs6* null allele lacks the s^2 group in mcm^5s^2U containing tRNAs, indicating the formation of mcm^5 side group is unaffected (Esberg et al., 2006; Noma et al., 2009;

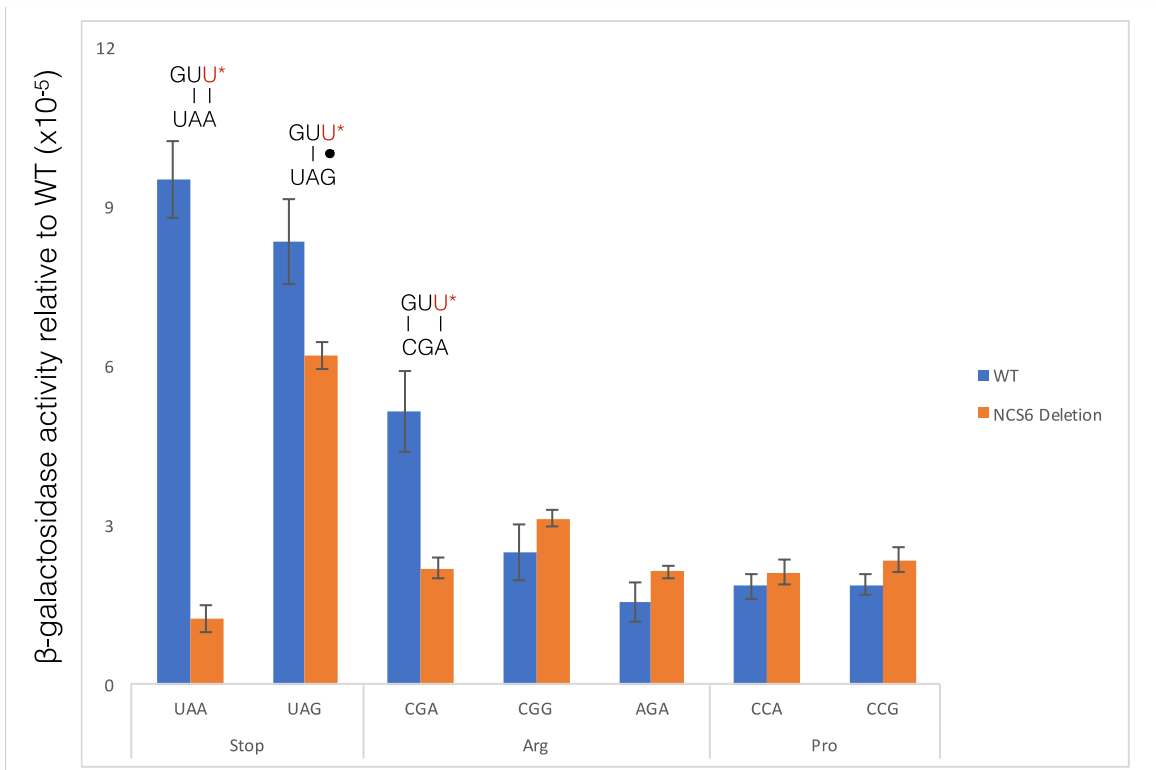


Figure V–4. Misreading frequency by tRNA^{Gln}_{UUG} at near-cognate codons in the presence and absence of s²U34 modification

The relative β -galactosidase activity of Gln624 near-cognate mutants expressing in wild type strain and NCS6 deletion strain shown as blue and orange bars respectively. Codon-anticodon complexes shows misreading events for each mutant that their misreading frequencies differ significantly between wild type background or NCS6 deletion background. The upper line represents anticodon while the lower line represents codon. Vertical lines represent Watson-Crick pairs, filled circle represents wobble pairs and open circle represents a mismatch. The error bars represent the standard error of the mean.

Karlsborn et al., 2014). The same Gln reporter system provided a test of misreading in a wild-type background and the *ncs6* mutant background. As shown in Figure V-4 and Table V-2, loss of the s^2 group affected the same three near-cognate mutants UAA, UAG, and CGA. The effect of loss of s^2 on misreading of UAA was the greatest, decreasing from 9.5×10^{-5} to 1.2×10^{-5} , an 8-fold change. The frequency of UAG decreased from 8.3×10^{-5} to 6.2×10^{-5} , a ~ 1.3 -fold change. Meanwhile, the frequency of CGA reduced from 5.2×10^{-5} to 2.2×10^{-5} , a ~ 2.4 -fold change. Loss of the mcm^5 side change and s^2 group exhibited much the same influence on three of the four putative error-prone codons. No other codons showed any change. My data suggested that these two modifications stabilize the interaction between tRNA anticodon and near-cognate codon.

III. Lack of pseudouridine ($\Psi 38$) decreased misreading errors by tRNA^{Gln}_{UUG}

Both of the mcm^5 and s^2 modifications occur at the wobble position of Gln tRNA. To expand the analysis, I tested the effect on misreading errors of modification at another frequently modified nucleotide, position 38. Modifications at positions other than the wobble nucleotide of the anticodon stem loop of tRNAs also affect tRNA function. Pseudouridine, for example, is the most common modifications in tRNAs (Charette & Gray, 2000). In *S. cerevisiae*, synthesis of $\Psi 38$ and $\Psi 39$ requires Pus3 (Lecointe et al., 1998). Loss of Pus3 is not lethal but causes temperature sensitivity and slow growth (Han et al., 2015a). Biochemical and structural studies showed that a water molecule is coordinated between the N1H group of Ψ and the adjacent 5' phosphates to stabilize both duplex and single-stranded RNA. Moreover, Ψ favors a 3' endo

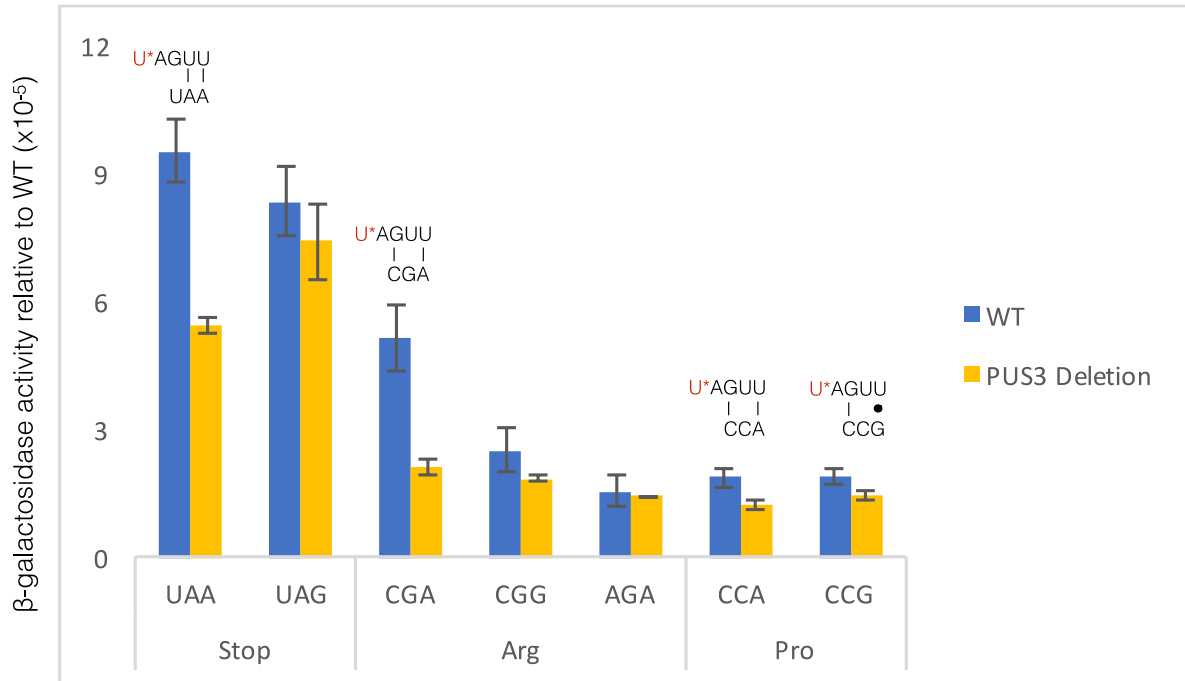


Figure V–5. Misreading frequency by tRNA^{Gln}_{UUG} at near-cognate codons in the presence and absence of pseudouridine 38 modification

The relative β -galactosidase activity of Gln624 near-cognate mutants expressing in wild type strain and PUS3 deletion strain shown as blue and orange bars respectively. The error bars represent the standard error of the mean.

conformation, enhancing stacking in both single-stranded and duplex helices (Davis, 1995; Charette & Gray, 2000). Hence, despite indirectly contacting the codon, Ψ38 and 39 plays an essential role in stabilizing tRNA structure and decoding interaction, which may attribute to translational accuracy.

In my study, I found that lack of pseudouridine Ψ38 (*pus3Δ*) had a similar effect on misreading error frequency as disruption of other modifications. However, the extent of the effect was the smallest one among the three tRNA modifications but it affected more codons than did the other two tRNA modifications. In the *pus3Δ* mutant background, misreading frequency was altered for the stop codon UAA, the arginine codon CGA, and the proline codons CCA and CCG. The frequency of misreading of the termination codon UAA decreased from 9.5×10^{-5} to 5.4×10^{-5} , only a 1.8-fold change. The frequency of misreading of CGA was altered the most, decreasing from 5.2×10^{-5} to 2.1×10^{-5} , a 2.5-fold change. Only in the mutant *pus3Δ* background the misreading frequency of CCA and CCG were altered from 1.9×10^{-5} to 1.2×10^{-5} and 1.5×10^{-5} respectively, about a 1.5-fold change (Figure V-5 and Table V-1). Lack of Ψ38 modification seems to have the least impact on misreading error frequency presumably because the nucleotide at position 38 does not directly participate in decoding process but is more involved in stabilizing the interaction between codon and anticodon.

I found it is intriguing that lack of these three tRNA modifications, in fact, decreases the chance of misreading events occurring, since most previous work implied that tRNA modifications benefit the process of protein translation. My data apparently goes against this idea. Our lab's previous work has shown that blocking of some tRNA modifications decreased translational accuracy

(Manickam et al., 2016). My data is consistent with some of this work's conclusions as will be discussed further below.

C. Discussion

Many post-transcriptional modifications within the core of tRNAs increase structural stabilization (Phizicky & Hopper, 2015; Lyko & Tuorto, 2016). Hypomodified tRNAs can be rapidly degraded (Guy et al., 2014). The primary effect of tRNA modifications in the anticodon loop is on the capability of tRNAs to recognize mRNA codons (Lyko & Tuorto, 2016). Abundant information is available concerning this effect on cognate decoding. Many fewer studies have focused on the effect of tRNA modifications on the near-cognate decoding process. In this chapter, I intended to analyze the role of some tRNA modifications in misreading errors by Gln tRNA_{UUG} and provide more knowledge about tRNA modification function in protein translation. Many previous studies focusing on tRNA modifications assumed that the existence of tRNA modifications in the anticodon domain benefit tRNAs and protein translation (Krüger et al., 1998; Yarian et al., 2000, 2002; Urbonavičius et al., 2001; Agris et al., 2007). The benefits of tRNA modifications have been extensively analyzed for tRNA_{UUU}^{Lys}. An NMR solution structural study demonstrated that three tRNA modifications together constrain the interaction between codon-anticodon, which may promote the decoding accuracy (Sundaram et al., 2000). This study of a fully modified 17-nucleotide *E. coli* Lys tRNA anticodon stem loop domain (ASL) revealed the functional importance of three tRNA modifications, 5-methylcarboxymethyl,2-thiouridine (mcm⁵s²U₃₄) at the wobble position, N6-threonylcarbamoyl-adenosine (t⁶A₃₇), and pseudouridine (ψ₃₉) (Sundaram et al., 2000). They presented several NMR structures of partially modified ASLs to transform the tRNA_{UUU}^{Lys} from a disordered unmodified tRNA ASL to highly ordered native tRNA

structure. Sundaram et al. (2000) showed the tRNA modifications structurally constrain the 17-nucleotide Lys tRNA ASL compared to unmodified, which may prevent non-native interactions between the hypermodified nucleotides. The three tRNA modifications are required to stabilize a canonical U-turn structure, leading to high-affinity codon recognition for tRNA_{UUU}^{Lys} (Sundaram et al., 2000). Likewise, Yarian et al. (2000) reported an unmodified tRNA_{UUU}^{Lys} did not bind to poly-A programmed ribosomes (Yarian et al., 2000). However, incorporation of tRNA modifications mnm⁵U34 and t⁶A37 along with Ψ39 restored the binding ability of tRNA_{UUU}^{Lys}, suggesting the importance of these tRNA modifications is critical for Lys tRNA anticodon recognition (Yarian et al., 2000). The previous work on Lys tRNA modification agrees with Murphy et al. (2004), which showed that tRNA_{UUU}^{Lys} can only recognize AAA and AAG when the tRNA is doubly modified with t⁶A37 and either mnm⁵U34 or s²U34 (Murphy et al., 2004).

Besides enhancing the capacity to bind and recognize tRNAs, several tRNA modifications were also reported to play an essential role in correct protein translation, such as maintaining the correct reading frame or translational accuracy (Urbonavičius et al., 2001; Nilsson et al., 2017). Alterations in a tRNA structure caused by defective modified nucleotides have an influence on reading frame maintenance (Urbonavičius et al., 2001). For example, in bacteria the modified 5-methylamino-methyl-2-thiouridine (mnm⁵s²U34) occurs in the wobble position in Gln, Lys and Glu tRNAs (Urbonavičius et al., 2001). Lack of either mnm⁵ or s² increased frameshifting frequency compared with wild-type, suggesting the importance of these two modifications in codon decoding in the A-site (Urbonavičius et al., 2001). Additionally, deficiency of mnm⁵s²U34 causes P-site frameshifting owing to a slow recruitment of the hypomodified tRNA to the A-site codon and thereby inducing a pause in the A-site (Urbonavičius et al., 2001). A recently published

study focused on $\text{mnm}^5\text{s}^2\text{U34}$ defective tRNAs in the bacterium *Salmonella enterica* Serovar Typhimurium LT2 reported inviability of double null mutants lacking the mnm^5 and s^2 modifications (Nilsson et al., 2017). They suggested the primary influence of deficiency of the tRNA modifications is increasing translational errors such as missense errors (Nilsson et al., 2017). However, other research showed contradictory results. Our lab has directly tested the impact of lack of some tRNA modifications on missense error frequency (Manickam et al., 2016). Our data showed that lack of some tRNA modifications indeed decreased misreading errors by some tRNAs (Manickam et al., 2016).

Manickam et al. (2016) studied the effect of lack of some tRNA modifications in *E. coli* including methylaminomethyl-modification (mnm^5s^2) at the wobble position, queuosine modification (Q) at the wobble position, and 2-methylthio-N6-isopentenyl modification ($\text{ms}^2\text{i}^6\text{A}$) in the 37 position (Manickam et al., 2016). Strikingly, their results showed that lack of the same tRNA modification influenced misreading frequency differently even for two tRNAs carrying the same modification. For example, both $\text{tRNA}_{\text{UUU}}^{\text{Lys}}$ and $\text{tRNA}_{\text{UUC}}^{\text{Glu}}$ have mnm^5 -modification at the wobble position. However, the absence of mnm^5 -modification increased errors by $\text{tRNA}_{\text{UUC}}^{\text{Glu}}$ but decreased errors by $\text{tRNA}_{\text{UUU}}^{\text{Lys}}$. They suggested that lacking mnm^5 -modification destabilized $\text{tRNA}_{\text{UUU}}^{\text{Lys}}$ since this tRNA has a very flexible anticodon loop (Durant et al., 2005; Manickam et al., 2016). A $\text{tRNA}_{\text{UUU}}^{\text{Lys}}$ lacking mnm^5 -modification is unable to bind to either cognate codon AAA or AAG in the A site (Yarian et al., 2000). Presumably, the decreased binding activity of $\text{tRNA}_{\text{UUU}}^{\text{Lys}}$ also results in reduced misreading errors. A previous study reported a similar effect that lack of $\text{mnm}^5\text{s}^2\text{U34}$ in the wobble position of $\text{tRNA}_{\text{UUU}}^{\text{Lys}}$ decreased misreading of asparagine codons (AAU and AAC) (Hagervall et al., 1998). Generally, tRNA modifications are assumed to restrict the capacity of

decoding at the wobble position and make the translation more accurate. Therefore, the existence of tRNA modifications should prevent misreading especially at the wobble position. However, the result of tRNA_{UUU}^{Lys} is opposite with general prediction of functions of tRNA modifications (Manickam et al., 2016). It is therefore surprising that a tRNA modification would have the contradictory effect of increasing misreading events. My results are consistent with the effect of deficient tRNA modification on missense errors by tRNA_{UUU}^{Lys}, showing that the existence of some tRNA modifications increase misreading errors.

Instead of increasing the frequency of misreading of some near-cognate tRNAs as suggested by Nilsson et al. (2017), lack of an mcm⁵ side chain or s² group or Ψ38 modifications actually reduced misreading errors, suggesting that the presence of mcm⁵ side chain or s² group or Ψ38 modifications is to stabilize the interaction between a mismatched pair and therefore reduce accuracy. Previous studies have suggested that deficient tRNA modification reduces binding of tRNA to the ribosomal A-site and in turn leads to reading frame slippage (Urbonavičius et al., 2001; Rezgui et al., 2013). Likewise, this suggestion might also be one possible explanation of my data that hypomodified tRNA_{UUU}^{Gln} has decreased and slower binding to the ribosomal A-site. Therefore, Gln tRNAs are less efficient at misreading their near-cognate codons. Previous work has shown the primary function of mcm⁵s²U34 in yeast is to increase the efficiency of Gln tRNA reading cognate codons rather than preventing missense errors (Esberg et al., 2006; Björk et al., 2007). Deletion of *ELP3* and *NCS6 (TUC1)* abolished the formation of both mcm⁵ and s² modifications, leaving an unmodified wobble position and reducing the viability of yeast cells. Overexpression of hypomodified tRNAs rescued the phenotype induced by deficiency of either mcm⁵, s², or mcm⁵s², suggesting that these two modifications in yeast improve cognate codon-

anticodon interaction (Björk et al., 2007). This function is different from (c)mnm⁵s²U34 modification in *E. coli*. Lack of the s² or (c)mnm⁵ group of (c)mnm⁵s²U34 caused a severe growth reduction, which could not be restored by an excess of hypomodified Gln tRNAs. Instead, overexpression of hypomodified tRNAs exaggerates this growth reduction but does not counteract the reduced cell growth, suggesting the primary role of (c)mnm⁵s²U34 is to prevent translational errors such as missense errors but not to improve cognate codon decoding (Nilsson et al., 2017). In the *ELP3*, or *NCS6*, or *PUS3* deletion mutant strain, I observed that misreading frequency of putative error-prone codons decreased; I stated one possible explanation that deficiency of tRNA modification may cause reduced availability of Gln tRNA. Alternatively, the presence of these three modifications may stabilize codon-anticodon interaction. Consequently, defective tRNA modifications may result in reduced affinity between near-cognate codon and tRNAs.

Though deficiency of all the three tRNA modifications decreased misreading frequency, they showed different extents of influence (Table V-2). Previous studies revealed that tRNA^{Gln}_{UU_G} carries both mcm⁵s²U and pseudouridine 38/39 (Lecointe et al., 1998; Han et al., 2015a; Klassen et al., 2016). In the *ELP3* and *NCS6* mutant strains, misreading of the stop codons UAA, UAG and the arginine codon CGA was reduced. In the *PUS3* mutant strain, lack of tRNA modification influenced errors on stop codon UAG, arginine codon CGA, and proline codons CCA and CCG. Stop codon UAA and arginine codon CGA are the two putative error-prone codons that had reduced misreading frequency in all the three mutant strains. UAA had 16-fold, 8-fold, and 1.8-fold changes in *ELP3*, *NCS6*, and *PUS3* deletion strains respectively. The other putative error-prone codons had quite similar fold changes in the three modification defective strains. Defective formation of mcm⁵ side chain had the highest impact on the frequency of misreading of UAA, UAG, and CGA. Lack of s² had less of an effect and loss of pseudouridine in the 38 position had

the least effect. Synthesis of mcm^5 and s^2 group is independent so that deletion of *ELP3* eliminates the mcm^5 group but has no effect on the formation of the s^2 group (Björk et al., 2007; Johansson et al., 2008). Therefore, the wobble position nucleotide is s^2U in the *ELP3* deletion strain and mcm^5U in the *NCS6* deletion strain. Comparison of the effect on misreading errors of the three tRNA modifications indicated two facts. First, lack of mcm^5 at the wobble position has the greatest influence on missense errors and absence pseudouridine the lowest influence (Table V-1). Second, all the three tRNA modifications seem to have a greater effect on codons ending with A than ending with G. For example, in the *elp3Δ* and *ncs6Δ* strains the frequency of misreading of UAA dramatically decreased while UAG only reduced for 2- and 1.3-fold. In the *pus3Δ* strain, misreading error of UAA had declined but UAG had no change. Moreover, all three tRNA modifications only had altered the frequency of misreading of CGA but had no effect on CGG (Table V-2).

Previous work has suggested that the xm^5s^2U modification preferentially promotes pairing with purines. The wobble uridine nucleoside mcm^5U was believed to restrict interaction with A-ending codon (Yokoyama et al., 1985). However, a more recent study has demonstrated that the presence of mcm^5 side chain at the wobble uridine improves decoding of G-ending codons. This conclusion challenges the earlier notion that tRNAs with mcm^5U34 only reads A-ending codons. Moreover, concurrent mcm^5 and s^2 groups enhance decoding of both A- and G-ending codons (Johansson et al., 2008). Hence, lack of mcm^5 should destabilize base-pairing with A- and G- ending codons. My data showed that misreading of UAA, UAG and CGA all decreased, which is consistent with the statement (Table V-1). An NMR study has predicted that the thio moiety in s^2U34 structurally stabilizes anticodon base pairing with A (Kumar & Davis, 1997; Testa et al., 1999). In the *ncs6Δ* strain lacking s^2U34 , therefore, decreased misreading of UAA and CGA may result from

hypomodified tRNAs binding less with near-cognate codons especially with A-ending codons. The isomer of uridine, pseudouridine (Ψ), seems to affect tRNA function subtly but does not influence the viability of cells, despite that it is ubiquitously present in tRNA (Giaever et al., 2002). Deletion of *PUS3* eliminates the pseudouridine modification in the position of 38 and 39. Indeed, recently published work study suggested that $\Psi_{38/39}$ indirectly stabilizes codon-anticodon base pairing by protecting the anticodon loop configuration from disruption by a lack of other modifications (Klassen & Schaffrath, 2017). Lack of Ψ_{38} only decreased misreading of UAA by 1.8-fold, which is almost 8-fold smaller than the effect of loss of an mcm^5 side chain on misreading frequency (Table V-1). This modification is not present in the anticodon loop, so it is reasonable that loss of Ψ_{38} has the least effect on reducing the frequency of misreading by $tRNA_{UUG}^{Gln}$.

Two mismatches were involved in all three tRNA modification null mutant backgrounds including U1•G36 ($tRNA_{UUG}^{Gln}$ misreads UAA or UAG) and G2•U35 ($tRNA_{UUG}^{Gln}$ misreads CGA). In the last chapter, my results have shown that UAA, UAG, CGA, and CGG are error-prone codons. Many previous studies demonstrated that tRNA modifications exert an important function on the decoding process in protein translation (Agris, 2004; Agris et al., 2007; Johansson et al., 2008; Lyko & Tuorto, 2016; Rozov, Demeshkina, Khusainov, et al., 2016). Consequently, the reduction of misreading frequencies of UAA, UAG, and CGA further supports my hypothesis that activities from proteins containing these mutant codons are due to misreading. My data in combination with previous work enlarges our knowledge about how tRNA modifications modulate the decoding process and directly affect protein translation fidelity.

CHAPTER VI

DISCUSSION

Chapter VI. DISCUSSION

A. Discussion

1. A summary of translational error frequency in yeast cells and mammalian system

In this study, I developed two reporter assays to quantify the frequency of all possible misreading error by tRNA_{UUU}^{Lys} in multiple mammalian cell lines, and by tRNA_{UUU}^{Gln} in *Saccharomyces cerevisiae*.

Development of a reporter system by tRNA_{UUU}^{Gln} verifies that Gln 624 but not Gln 625 is the essential amino acid for β -galactosidase to measure misreading events. Tsai and Curran (1998) reported that Gln 625 is a critical amino acid residue of β -galactosidase and that introducing a mutation at this site greatly affected protein activity. They reported that high activity of the CGA mutation (near-cognate codon) resulted from tRNA_{UUU}^{Gln} misreading the CGA Arginine codon as Glutamine with a frequency of 1×10^{-3} (Tsai & Curran, 1998). However, in the absence of an appropriate negative control it is not possible to determine that the cause was misreading of CGA by tRNA_{UUU}^{Gln}. By performing appropriate controls, I demonstrated that high residual activity at Gln 625 was due to functional replacement and not misreading because the relative protein activities of mutants with near-cognate codons CGA, CGG, and non-cognate codon AGA were nearly the same. This result also suggests that Gln 625 is not a suitable residual site for measuring misreading errors.

In the Gln 624 reporter system, I found four error-prone codons. These codons are stop codons UAA and UAG, and arginine codons CGA and CGG. Comparison of relative protein activity

between these near-cognate codons and synonymous non-cognate codons supported the hypothesis that misreading by tRNA^{Gln}_{UUG} occurred at some Gln 624 mutant codons.

The difference of misreading error frequency by tRNA^{Lys}_{UUU} in mammalian cell lines did not vary as much as it did in *E. coli* and yeast. In mammalian cell lines, misreading occurred within a range of 3.3×10^{-4} to 1.5×10^{-4} in HEK293 cells, 5.3×10^{-4} to 1.1×10^{-4} in *HeLa* cells, 5.8×10^{-4} to 2.1×10^{-4} in 22RV1 cells, and 3.3×10^{-4} to 1.2×10^{-4} in NIH 3T3 cells (Table VI-1). The highest error frequency was only two-fold higher than the lowest error frequency in HEK293, 22RV1, and 3T3 cells, and the difference was 5-fold in *HeLa* cells. I suspect that roughly equivalent isoacceptor tRNA concentrations led to this small variation in misreading frequency in mammalian cells. Several near-cognate codons are error-prone, which has been summarized in Table VI-1. As shown in this table, I observed novel mismatches in mammalian systems besides those "expected error-prone codons." Misreading of UAA, UAG, AGA, AGG and AAC by tRNA^{Lys}_{UUU} occurred in all four mammalian cell lines. tRNA^{Lys}_{UUU} misread CAG only in *HeLa* cells, while tRNA^{Lys}_{UUU} misread GAG in both HEK293 and 22RV1 cells. The involved mismatches will be discussed below.

2. A summary of possible mismatches in *E. coli*, yeast and mammalian cells

Previously, our lab has used various reporters to investigate the misreading frequency in *E. coli* and yeast (Kramer & Farabaugh, 2007; Kramer et al., 2010; Manickam et al., 2014). These reporters include using tRNA^{Glu}_{UUC}, tRNA^{Tyr}_{QUA}, tRNA^{Asp}_{QUC}, tRNA^{Lys}_{UUU}. Based on these data, our lab has summarized the pattern of tRNA misreading table (Figure VI-1). This table includes all types of mismatches that our lab has observed so far in both *E. coli* and yeast. As shown in Figure VI-1,

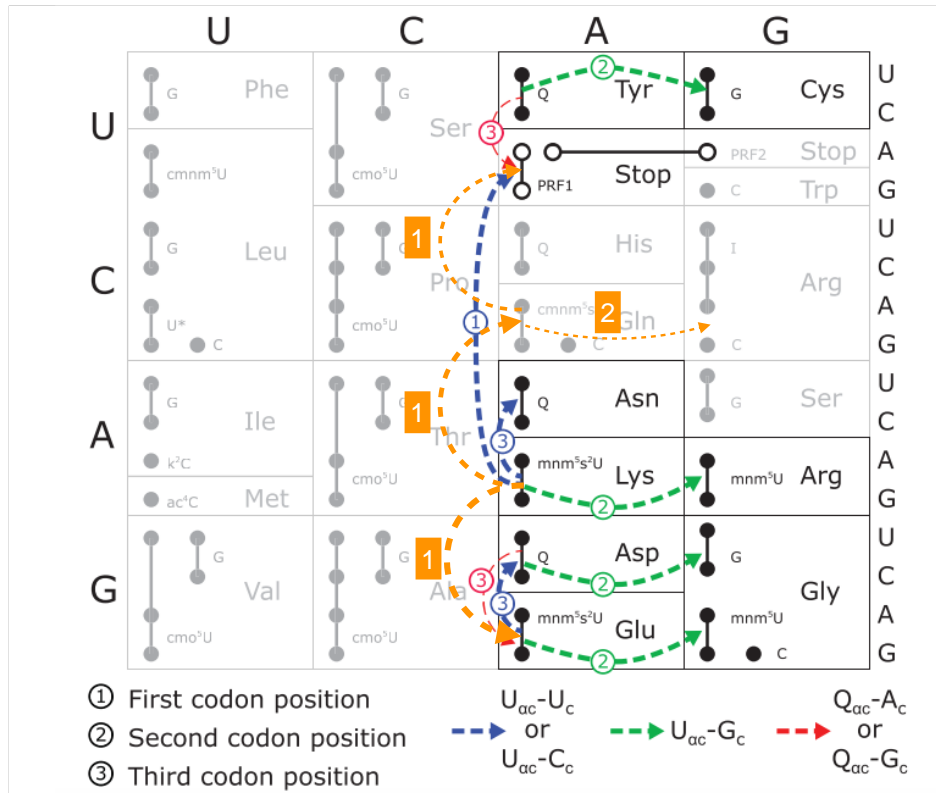


Figure VI-1. The pattern of tRNA misreading in *E. coli*, yeast and mammalian cells

The filled circles represent codons. These circles connected by lines are all recognized by a single tRNA. The right side of the filled circles represent the anticodon wobble nucleotide of each tRNA. Unfilled circles represent the stop codons and lines connect those circles recognized by each of the release factors in *E. coli* (PRF1 or PRF2). Misreading events in the wild-type background identified here (orange arrows) or by previous work (blue, green and red arrows) (Kramer & Farabaugh, 2007; Manickam et al., 2014) are shown as dashed arrows. The thickness of the arrow represents relative frequency of the events, the thicker the arrow the higher the error frequency. The arrows are labeled to indicate the position of the mismatch and color coded for the nature of the mismatched base pair as shown in the figure.

the most frequent errors by these four tRNAs involved U3•U34, C3•U34 (e.g., to Asn codons), G2•U35 (e.g., to Arg codons) or U1•U36 (to stop codons). In my study, the most frequent errors by tRNA^{Lys}_{UUU} and tRNA^{Gln}_{UUG} again involved U1•U36 (to stop codons), G2•U35 (to Arg codons), C3•U34 (to Asn codons). In addition, I observed another three types of mismatches, which have not been seen before. These novel mismatches include G1•U36 (to Glu codon), C1•U36 (to Gln codon), and U1•G36 (to stop codons) (Table IV-4 and Table VI-1). These mismatches involve purine-pyrimidine mismatches (G•U, U•G), and pyrimidine-pyrimidine mismatches (C•U, U•U) but there are no purine-purine mismatches. These data are summarized in Figure VI-1 highlighted in orange. My data in combination with our lab's previous work generate a more comprehensive insight about misreading errors in prokaryotes and eukaryotes.

3. Domain closure vs. tautomerism, which is the more compatible hypothesis with my data?

Decoding is the fundamental process of maintaining and studying translational fidelity. Over years, many structural studies have been devoting effort to understanding the mechanism of tRNA discrimination by the ribosome. Besides kinetic proofreading (discussed in chapter 1), there are two major hypotheses proposed by two individual groups. One is the domain closure (Ogle et al., 2002), and the other is tautomerism (Demeshkina et al., 2012).

Cognate anticodon stem loop (ASL) binding to the A site forms A-minor groove interactions between A1492/A1493 and G530 and the first two codon-anticodon base pairs (Ogle et al., 2002). A1492 and A1493 are located in an internal loop of helix 44 of 16S RNA. A crystal structure of the 30S complex with the antibiotic paromomycin showed that the antibiotic was bound in the internal loop of helix 44, inducing a flip out of A1492 and A1493 from helix 44 so that these nucleotides would interact directly with the minor groove of the codon-anticodon helix in the A

site (Carter et al., 2000). Using the 30S subunit crystals soaked with U6 RNA (a mimic of mRNA) and cognate or near-cognate ASLs (mimics of tRNA), it was reported that binding of cognate tRNA led to a same flipping of A1492 and A1493 as well as a flip out of G530 from a *syn* to an *anti*-conformation. These conformational changes in the 30S subunit result in ‘domain closure’ (Ogle et al., 2002). These bases interact directly with the minor groove of the first two positions of the codon-anticodon complex. These interactions require Watson-Crick geometry. However, the interactions between the ribosome and near-cognate tRNAs deviate from the canonical geometry, leading to uncompensated desolvation of the hydrogen-bonding at the wobble position minor groove. It was proposed that because of this desolvation a near-cognate tRNA binding to the A site makes the transition from an open to a closed form of 30S subunit unfavorable, resulting in the dissociation of near-cognate tRNAs. In this way, the ribosome would be able to closely monitor the first two position base pairing and discriminate between correct tRNA and incorrect tRNA (Ogle et al., 2002).

However, recent studies using structures of 70S ribosomes with covalently intact mRNA and naturally modified tRNAs challenge the domain closure hypothesis and provided new structural explanations of missense errors (Demeshkina et al., 2012; Rozov et al., 2015; Rozov et al., 2016). These studies demonstrated the same conformational changes with either a cognate or a near-cognate tRNA binding (Demeshkina et al., 2012). Though G530, A1492 and A1493 form part of the grip of the decoding center on the binding of either cognate or near-cognate tRNAs, the number of hydrogen bonds between the decoding center nucleotides and the minor groove of the cognate or near-cognate codon-anticodon helix are the same, indicating the ribosome is unable to distinguish cognate or near-cognate tRNA binding by the minor groove geometry of codon-anticodon base pairs (Westhof et al., 2014). Indeed, binding of either cognate or near-cognate

tRNAs in the decoding center of the 70S ribosome complex induces the same but rather smaller conformational changes than ‘domain closure’ - the ‘shoulder’ moves towards the neck of the 30S subunit but the other part of the 30S subunit stays still (Demeshkina et al., 2012; L. B. Jenner et al., 2010). These studies hypothesized that discrimination between tRNAs by the ribosome primarily relies on steric complementarity and shape acceptance but not the number of hydrogen bonds between the codon-anticodon duplex and the decoding center. Near-cognate codon-anticodon interactions can mimic Watson-Crick geometry via normally rare tautomeric shifts and therefore form Watson-Crick-like geometry (Demeshkina et al., 2012; Westhof et al., 2014; Rozov et al., 2016) (Figure VI-2 and Figure VI-3). Formation of tautomers may require energy and such energy expenditure could be a plausible mechanism for the ribosome rejecting near-cognate tRNAs (Demeshkina et al., 2012). Alternatively, the tautomeric shifts might be energy neutral but this condition is very rare (Westhof et al., 2014). Nevertheless, base tautomerism or ionization could cause near-cognate codon-anticodon interaction that mimics Watson-Crick base pairing, leading to protein translational infidelity (Rozov et al., 2016) (Figure VI-2). In addition, the kink between A and P sites (P/A kink) coordinate with magnesium ion, the decoding center (h18, h44 and ribosomal protein S12 and H69) constrains the allowed geometry of the first two nucleotides of the codon, but there is not such restrains on the third position (Figure VI-3). My data are much more consistent with the "tautomerism" model.

The previous studies reported that U1•G36 or G2•U35 forms Watson-Crick-like geometry through tautomerization, but they did not find the same interactions between the decoding center and A•A, C•A, G•U and U•U mismatched base pairs, or the interaction was unstable. Hence,

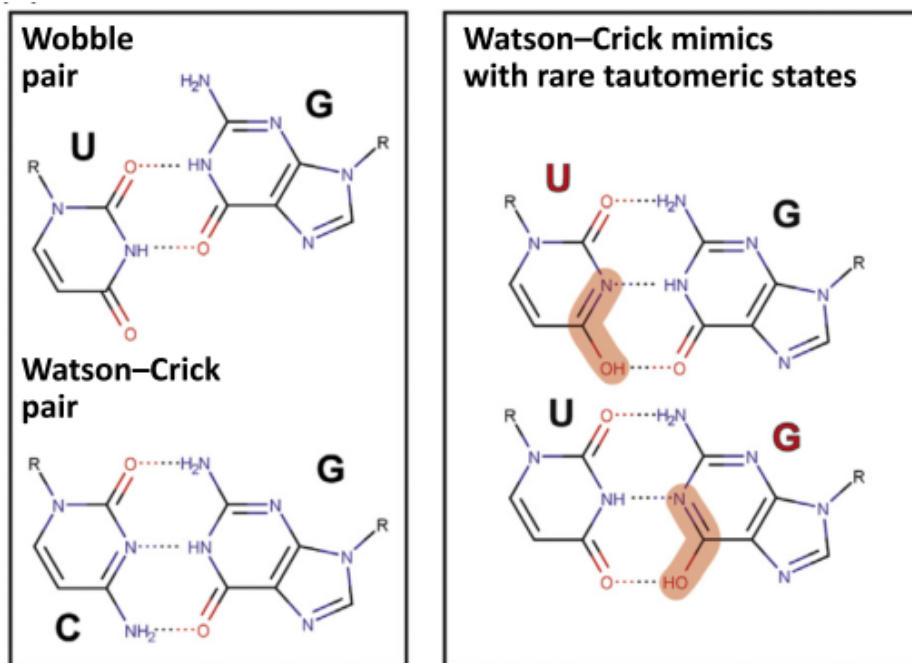


Figure VI-2. Geometry of canonical and rare tautomeric states

Geometry of canonical Watson-Crick pair and non-canonical wobble base pair (left) and Watson-Crick-like geometry formed by rare tautomeric states of uracil or guanosine, which are indicated with red letters. Structural changes are highlighted by pink (right) (Rozov et al., 2015)

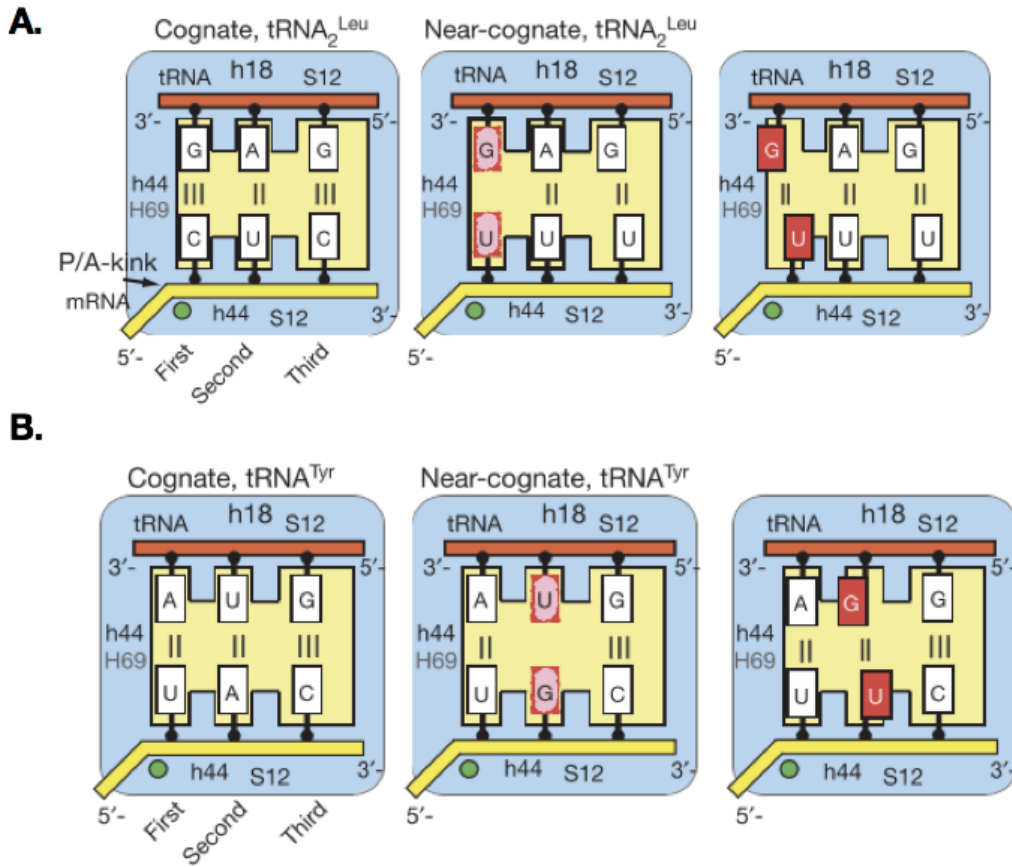


Figure VI–3. Illustration of the decoding principle

Illustration of the decoding principle: together with the constraints imposed on the A codon by the P/A kink coordinated by a magnesium ion (green sphere), the DC (h18, h44 and protein S12 from the small subunit and H69 from the large subunit) restricts the allowed geometry of the first two nucleotides of the codon. No such restraints are imposed on the third base pair. A near-cognate tRNA with G•U in the first or second position is forced to form Watson–Crick-like base pairs (middle panels). This creates repulsion or requires energy for tautomerization (shown in pink), which by itself can be the source of the tRNA discrimination. The right panels illustrate the impossible situation when standard wobble base pairs (shown in red) occur in either the first or second positions of the codon–anticodon duplexes (Demeshkina et al., 2012).

near-cognate tRNAs with A•A, C•A and U•U mismatches to the codon were predicted to dissociate from the ribosome owing to the instability of the absence of interactions between bases (Rozov et al., 2016). A wobble base pair, for example, G1•U36, cannot form at the first position because the decoding center prohibits shifting towards the minor groove. The decoding center also does not permit pyrimidine-pyrimidine mismatches (such as U1•U36) because the bases get close enough to hydrogen bond (Figure VI-4). They predicted that only G•U mismatches and cognate tRNAs can stably interact with the mRNA codons by the canonical base pair (Rozov et al., 2016). However, my data strongly disagree with their conclusion.

In my mammalian and yeast projects, I have observed G1•U36 (to Glu codon) and G2•U35 (to Arg codons) mismatches as well as U1•U36 (to stop codons) mismatches (Figure VI-5). Misreading of Glu codon GAG by tRNA_{UUU}^{Lys} involved mismatch of G1•U36 in HEK293 and 22RV1, occurring at the frequency of 2.5×10^{-4} and 2.1×10^{-4} , respectively. Though the error frequency of G1•U36 is the lowest in 22RV1, errors are higher in 22RV1 than in other three cell lines and are at the median frequency in HEK293 (Table VI-1). These data suggest that a G1•U36 mismatch can occur during decoding with a moderate error frequency. Mismatch G2•U35 occurred in both mammalian cells and yeast cells. Misreading of AGA and AGG by tRNA_{UUU}^{Lys}, and CGA and CGG by tRNA_{UUU}^{Gln} both involved G2•U35 mismatches, suggesting G2•U35 mismatch is very common since it is involved even in two different reporter systems. Indeed, our lab has not only observed G2•U35 mismatch in eukaryotes but also in prokaryotes with very high misreading frequency occurring (Kramer & Farabaugh, 2007; Manickam et al., 2014). Also, I have found U1•U36 (to stop codons), the type of mispairing that Rozov et al. proposed not to be allowed in the first position, was more frequently involved in misreading events than U1•G36

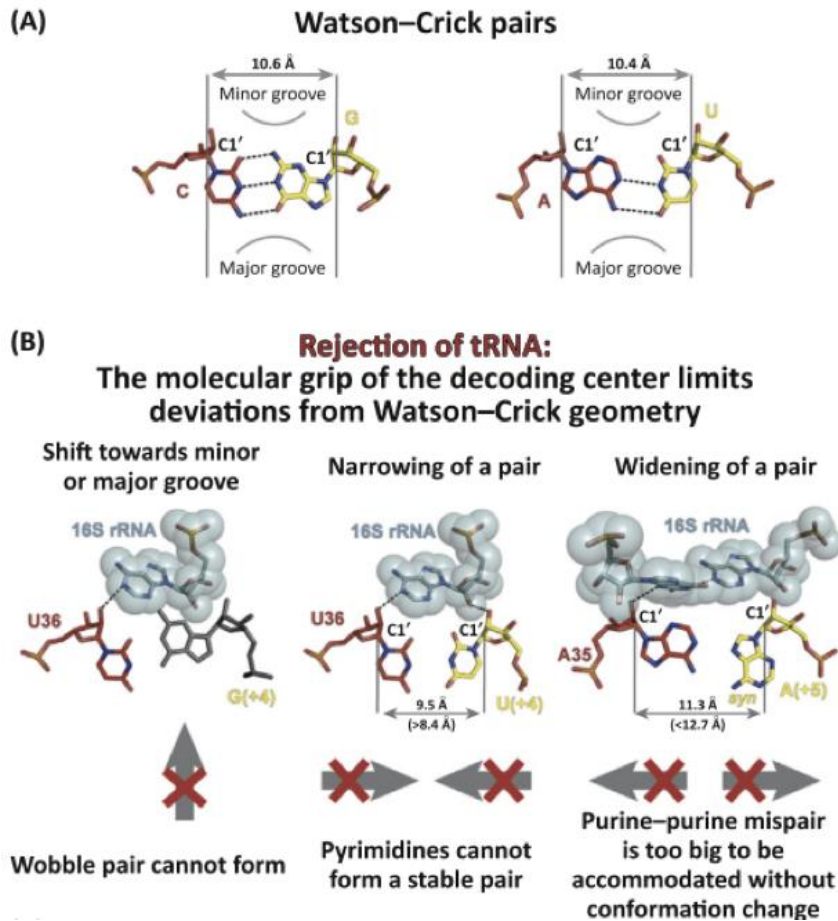


Figure VI–4. Mismatches leading to rejection of tRNA

(A) Canonical Watson–Crick pairs. (B) Mismatches leading to rejection of tRNA. The molecular grip of the decoding center limits deviations from the Watson–Crick geometry. The decoding center restrains the C10–C10 distances and minor groove surfaces in a way that permits only canonical Watson–Crick base pairing and the deviations incur severe energetic penalties. In particular, a ‘wobble’ base pair cannot form due to prohibited shift towards minor groove. Stable pairs inside pyrimidine–pyrimidine mismatches are not permitted, by not allowing the bases to get close enough. The purine–purine anti–anti base pairs can be accommodated only by enforcing syn/ anti-conformation change (Rozov et al., 2016).

	Mammalian cells	Yeast cells
	<pre> UUU AAA </pre>	<pre> GUU CAG </pre>
UAA/UAG (Stop)	<pre> UUU UAA </pre> U1•U36	<pre> GUU UAG </pre> U1•G36 *
GAA (Glu)	<pre> UUU GAA </pre> G1•U36 *	
CAG (Gln)	<pre> UUU CAA </pre> C1•U36 *	
AGA/AGG (Arg)	<pre> UUU AGA </pre> G2•U35	
CGA/CGG (Arg)		<pre> GUU • CGG </pre> G2•U35
AAC (Asn)	<pre> UUU AAC </pre> C3•U34	

Figure VI–5. Mismatches involved in mammalian cells and yeast cells

Cognate codons are shown in red square with codon-anticodon interactions. All observed error-prone codons in mammalian and yeast projects are listed on the left. Perfectly matched nucleotides are connected by solid lines while wobble geometry is represented by a filled circle.

Table VI-1. All possible error-prone codons in the four mammalian cell lines

Mismatch position	Amino acid	Codon	Misreading Frequency (x10 ⁻⁴)			
			HEK293	<i>HeLa</i>	22RV1	3T3
1st	Termination	<u>U</u> AA	<u>3.3</u>	1.5	<u>5.8</u>	<u>3.3</u>
		<u>U</u> AG	2.6	<u>1.1</u>	5.3	<u>1.2</u>
	Glutamine	<u>C</u> AG	-	3.9	-	-
	Glutamic acid	<u>G</u> AG	2.5	-	<u>2.1</u>	-
2nd	Arginine	<u>A</u> GA	1.8	3.5	2.6	2.1
		<u>A</u> GG	2.7	<u>5.3</u>	4.0	3.0
3rd	Asparagine	A <u>A</u> C	<u>1.5</u>	2.8	4.2	2.4

Highest and lowest error frequencies are in bold with underline

mismatch. The misreading frequency of the stop codon UAA by tRNA^{Lys}_{UUU} was as high as 5.8×10^{-4} per codon in 22RV1 cells, whereas the frequency of misreading UAA (U1•G36 mismatch) by tRNA^{Gln}_{UUG} was only 9.5×10^{-5} per codon in yeast, although the frequency of UAA was the highest in the Gln 625 reporter system. Rozov et al. (2016) seem to think that errors involve only U•G mismatches and downplay the U•U and other types of mispairs. Here my presented data suggests that several other types of mismatches could take place during decoding and the ribosome seems not to distinguish errors only by the mechanisms stated above.

4. Wobble errors occurred less frequently in eukaryotes than prokaryotes

Our lab has previously used a lysine reporter system to test all possible misreading events by tRNA^{Lys}_{UUU} in both *E. coli* and yeast (Kramer & Farabaugh, 2007; Kramer et al., 2010). Several conclusions came from these two studies. First, the background activity was no more than 3.1×10^{-4} error per codon in *E. coli*, and the frequency of errors varied over 10-fold. In yeast, protein translation seems more accurate, and the error frequency ranged from 8×10^{-5} to 6.9×10^{-4} per codon. Second, the variation of error frequency mostly results from tRNA competition between the cognate (correct) and near-cognate (incorrect) aa-tRNAs. Low abundance of tRNA^{Arg}_{CCU} led to slow decoding. Misreading at AGA and AGG in *E. coli* and AGG in yeast by tRNA^{Lys}_{UUU} would compete with the rare tRNA^{Arg}_{CCU}. Deletion of the gene encoding tRNA^{Arg}_{CCU} increased misreading significantly in yeast, whereas overexpression of the gene encoding this tRNA caused a reduction of misreading in *E. coli*. Third, weak cognate competition between tRNAs was not a major factor causing wobble mismatches; wobble errors did happen in *E. coli* at a high frequency despite the fact that the cognate tRNA is in a great abundance. However, my data presented here challenge the second and third conclusion. In our lab's previous study with tRNA^{Lys}_{UUU}, wobble errors occurred

at a rate of 1.6×10^{-3} per codon (AAU) in *E. coli* (Kramer & Farabaugh, 2007). Errors at the Asn AAU codon were only two-fold less than the most error-prone codon, AGA, which is in agreement with the previous study suggesting that wobble errors are frequent (Precup & Parker, 1987). However, in my study, I observed very low wobble errors in all the four mammalian cells with the Asn codon AAC the least frequently error-prone codon in HEK293 cell line. Indeed, I found that of all types of mismatches, U1•U36 (to stop codons), as well as G2•U35 (to Arg codons), had the most frequent errors. Neither of these two mismatches were wobble errors. Although functional replacement in the Gln 625 system blocked my measuring wobble errors in yeast by tRNA^{Gln}_{UUG}, in general, I observed very low wobble position frequencies in the mammalian system. This data is consistent with our lab's previous data in yeast (Kramer et al., 2010; K. Joshi, personal communication). In *E. coli*, by contrast, wobble errors were among the most frequent observed despite there being no limitation of cognate tRNAs for those codons.

5. Possible reasons for fewer wobble errors occurring in eukaryotes

a. Equal tRNA abundance may reduce the frequency of wobble errors in eukaryotes

Given the fact that tRNA abundance might play a role in the accuracy of decoding, I investigated the abundance of each tRNAs potentially involved in my studies (gtrnadb.ucsc.edu/). The database shows that the abundance of tRNA copy numbers for the cognate and near-cognate tRNAs are nearly the same, indicating that the cognate tRNA would compete with each other fiercely. In this scenario, the cognate tRNA would likely decode the correct codon and therefore results in a low wobble error frequency.

b. tRNA modification is important in decoding and may play a pivotal role in limiting wobble errors in eukaryotes

Alternatively, another possible explanation would be the fact that eukaryotic tRNA modifications restrict wobble errors. tRNA modifications either make tRNAs structurally more stable or are essential for tRNAs functioning normally during the decoding process. Lack of tRNA modifications at the wobble position can result in poorly functional tRNAs, tending to decode their cognate codons improperly. For example, human tRNA_{UUU}^{Lys} requires tRNA modifications 5-methoxycarbonylmethyl-2-thiouridine (mcm⁵s²U34) at the wobble position, 2-methylthio- N6-threonylcarbamoyladenine (ms²t⁶A37) at position 37 and pseudouridine (ψ 39) at position 39 to bind the cognate codons AAA and AAG, whereas unmodified tRNAs can barely bind to AAA and AAG. Critically, the mcm⁵s²U34•G3 base pair at the wobble position is in the canonical Watson-Crick geometry, which requires unusual hydrogen bonding to G so that the modified U34 must shift from the keto to enol form to base pair with G3. Post-transcriptional modifications are key factors for tRNAs functioning normally. Hence, the high abundance of tRNAs does not necessarily mean functional tRNAs and therefore tRNA modifications could play a critical role in limiting the occurrence of wobble errors.

6. Lack of some tRNA modifications facilitates more accurate protein translation in yeast cells

In yeast, the wobble position of tRNA_{UUG}^{Gln} also has the mcm⁵s²U modification (Björk et al., 2007). However, the activity of the CAU and CAC mutants were too high to measure wobble errors by tRNA_{UUG}^{Gln}, so we were not able to test the effect of tRNA modifications on wobble errors using this

system. However, lack of some tRNA modifications significantly decreased misreading events by tRNA^{Gln}_{UUG} of error-prone codons in yeast.

Modifications of tRNA anticodon nucleotides can affect decoding ability as well as affect translational fidelity. Eukaryotic cytoplasmic tRNAs often have a methoxycarbonylmethyl-2-thiouridine (mcm⁵) side chain and sometimes an additional 2-thio (s²) group. The mcm⁵s²U modifications are present in the wobble position uridine of four tRNA species, tRNA^{Arg}_{UCU}, tRNA^{Lys}_{UUU}, tRNA^{Gln}_{UUG}, and tRNA^{Glu}_{UUC} all of which decode codons in “split” codon boxes (Kalhor & Clarke, 2003; Lu et al., 2005). The presence of mcm⁵s² modification is pivotal in both decoding and maintaining translational accuracy (Johansson et al., 2008; Vendeix et al., 2012; Patil et al., 2012; Tükenmez et al., 2015). In yeast, the presence of the mcm⁵ side chain promotes reading of G-ending codons. Moreover, mcm⁵s² improves decoding of both A- and G-ending codons, which extends the decoding ability of tRNAs. Previous studies suggested that modification enhanced binding to A- and G-ending codons and prevented binding to U and C-ending codons (Durant et al., 2005; Johansson et al., 2008). These data suggest that tRNA modification should improve binding of the cognate codons (CAA and CAG) by the modified tRNA, and therefore the same effect may also occur for the A- or G-ending near-cognate codons. In my yeast project, the error prone codons, UAA, UAG, CGA, and CGG, are all A- or G- ending codons and the loss of mcm⁵ side group or s² decreased the frequency of misreading UAA, UAG, CGA and CGG by tRNA^{Gln}_{UUG} because there was less efficient binding of tRNA^{Gln}_{UUG} to these A- and G-ending codons.

7. Other factors may influence translational fidelity in both yeast and mammalian cells

Besides tRNA modifications, I have also studied other factors that may alter translational accuracy both in yeast cells and mammalian cells.

a. Paromomycin in yeast cells

Aminoglycoside antibiotics, such as neomycin and paromomycin, are potent drugs that can inhibit mRNA-tRNA translocation as well as subunit dissociation during ribosome recycling (Daniel N. Wilson, 2013). Previous studies have shown that aminoglycoside antibiotics did increase misreading errors both in *E. coli* and yeast (Stansfield et al., 1998; Kramer & Farabaugh, 2007; Kramer et al., 2010). As described below, my data agree with these earlier studies. The antibiotics induce translational misreading by stabilizing and promoting the binding of incorrect tRNAs to the mRNA. Aminoglycosides antibiotics were thought to interact with an internal loop of helix 44 at the decoding center of the 30S small subunit, stabilizing a 'flipped-out' conformation of A1492 and A1493 in the presence of incorrect tRNAs. Such conformational changes were thought to be the mechanism by which the ribosome distinguishes a cognate-tRNA from a near-cognate tRNA (Ogle et al., 2001; Ogle et al., 2002).

In yeast, I exposed cells to the aminoglycoside antibiotic paromomycin. In *E. coli*, antibiotics streptomycin and paromomycin increased the frequency of misreading of all error-prone codons significantly, which were UAA, UAG, AGA, AGG, AAU and AAC (Kramer & Farabaugh, 2007). Our lab has found that in yeast, paromomycin only increased misreading errors strongly at the stop codons UAA and UAG, and much weaker at an asparagine codon AAU. I have observed that paromomycin only affected misreading errors of UAG in the Gln 624 reporter system, and had no effect on either CGA or CGG, which are the other two error-prone codons.

b. G418 in mammalian cells

In mammalian cells, I also tested the effect of antibiotic G418 on misreading errors. G418, also known as geneticin, is an aminoglycoside related to Gentamicin and is usually used as a selective drug for stable transfection. Similar to paromomycin, G418 interferes with protein synthesis during elongation. My data showed that G418 increased misreading errors in all tested cell lines. The greatest effect of G418 is that it can induce readthrough of nonsense codons. Accordingly, scientists have found that G418 suppresses nonsense mutations in certain human genetic diseases (Sangkuhl et al., 2004; Azimov et al., 2008; Dranchak et al., 2011), suggesting that G418 might be used as a therapy for these diseases. Nevertheless, G418 also has the potential to promote errors and cause misfolded proteins (Silva et al., 2009). The significance of this study is to provide information about safe concentrations for treating these diseases since G418 can also promote misreading events and lead to protein misfolding. My data showed that G418 affected the frequency of misreading in a cell line-dependent manner. Different cell lines displayed various sensitivity to the drug (Table III-5). For example, 50 $\mu\text{g/ml}$ of G418 dramatically increased the frequency of misreading of a subset of near-cognate codons in HEK293, whereas 200 $\mu\text{g/ml}$ of G418 only affected a small subset of near-cognate codons in 3T3 cells. Hence, the effective concentration of G418 should be different to various target regions. My study aim on effects of G418 on misreading events provides information for further usage of G418 as a potential treatment.

c. Ribosomal protein 23 affected translational errors in yeast

Given the fact that ribosomal proteins strongly influence the accuracy of decoding, I measured the specific effect of mutations in ribosomal protein S23, which is known to alter protein translational fidelity, in both mammalian cells and yeast cells. Ribosomal protein S23 (rpS23 or rpS28) of the

40S small ribosomal subunit is required for translational accuracy. This protein is homologous to mammalian ribosomal protein S23 and bacterial S12.

Many mutations have been shown to affect translational accuracy in *Saccharomyces cerevisiae* (Alksne et al., 1993(a); Alksne et al., 1993(b); Anthony & Liebman, 1995). *SUP44* and *SUP46* encode ribosomal protein S4 and S13, which are homologs of *E. coli* S5 and S4 respectively (Ishiguro et al., 1981; All-Robyn et al., 1990; Vincent & Liebman, 1992). “Ribosomal ambiguity mutations” (*ram*) in S4 or S5 lead to a reduction of translational accuracy (Rosset & Gorini, 1969). Mutations in *SUP44* and *SUP46* result in an ‘omnipotent suppressor’ phenotype, which suppress all three nonsense mutations and increases sensitivity to paromomycin. These omnipotent suppressors have similar phenotypes to the *ram* mutations of *E. coli* (Wakem & Sherman, 1990).

Two studies identified mutations in the *RPS23* gene that affected the drug sensitivity associated with *SUP44* and *SUP46* mutations (Alksne et al., 1993; Anthony & Liebman, 1995). They showed that mutations in S23 either could increase accuracy (A113V) or can decrease accuracy (K62R). These studies introduced a mutant gene of *RPS23* into the wild-type strain or strains mutant for *SUP44* or *SUP46*. They determined that translational accuracy decreased by observing changes in suppression of nonsense alleles and changes in sensitivity to the aminoglycoside antibiotic paromomycin. However, they did not quantitatively test the mutations affecting translational accuracy. Instead, they did phenotype screening.

In yeast project, I used beta-Glo assay to quantitatively measure the alteration of translational accuracy and studied the effect of two mutations of *RPS23A* on translational fidelity (Figure IV-8). As I described above, mutation A113V is a hyperaccurate mutant, whereas the other one, K62R, is a hypoaccurate mutant. Both mutants affected the frequency of misreading as expected. The

hyperaccurate mutant A113V did result in a reduction of misreading the stop codon UAA, UAG, and CGG, whereas hypoaccurate mutant K62R increased misreading error frequency of UAA, UAG, CGA and CGG (Figure IV-8). All affected near-cognate codons are error-prone codons, directly supporting the idea that mutant forms of RPS23 can affect translational fidelity.

d. RPS23 did not affect translational fidelity in mammalian cells

Human RPS23 is 78% identical and 90% similar to the yeast RPS23. This high similarity led me to suspect that this human ribosomal protein may function similarly, and affect translational accuracy. Therefore, I introduced the same mutations to *RPS23* that changed Lysine 60 to arginine (hyperaccurate) and lysine 60 to threonine. The plasmids carrying either mutation were transfected into HEK293 cells and samples were collected 48-hours post-transfection. However, neither mutant form of RPS23 altered translational errors significantly. Indeed, the Fluc activity of each tested near-cognate codon was nearly the same under all three different background (wild type RPS23, K60R, and K60T).

One possibility for this result is that the mutant form of RPS23 is expressed at too low of a level since the introduced gene exists in the cell only for limited time and is not integrated into the genome. Hence, a transiently transfected plasmid is not able to pass from generation to generation during cell division. The transiently expressed transgene can generally be detected for 1 to 7 days, and transfected HEK293 cells were harvested 48-hour post-transfection. The expression of endogenous wild type RPS23 may overwhelm the expression of mutant forms of RPS23, causing the mutant form of RPS23 to not affect translational accuracy. Longer incubation time may produce more mutant forms of RPS23. However, genetic material may also be diluted out during cell division. One method to overcome this problem is to silence the expression of wild type RPS23.

Disruption of endogenous RPS23 protein expression should facilitate the influence of the mutant forms of RPS23. However, the mutation that carried by the plasmid is a point mutation. Because of that, knockdown of endogenous RPS23 expression by RNA interference is not feasible. Stable transfection is an alternative strategy and will be discussed in the future direction section.

B. Future direction

1. Investigation of the generality of translational accuracy in mammalian cells

To test the generality of misreading error frequency in mammalian cells in the future, measurement of misreading errors in more cell lines are necessary. These cell lines could be CHO, COS-7, and SK-BR3. The CHO cells, Chinese hamster ovary cells, are an epithelial cell line, which is derived from the ovary of the Chinese hamster. The COS-7 cell line was originally derived from the kidney tissue of the African green monkey, *Cercopithecus aethiops*. The cells are human fibroblast-like cells. Therefore, they are often called COS-7 monkey fibroblast. SK-BR3 is a human breast cancer cell line. This is also an epithelial cell line. Adding these three cell lines would allow a comparison of five epithelial cell lines (HEK293, *HeLa*, 22RV1, CHO, SK-BR3) derived from five different tissues, and two fibroblast cell lines (NIH 3T3 and COS-7) derived from two different tissues. Moreover, three of these lines are cancer cell lines, *HeLa*, 22RV1, and SK-BR3, which would enable testing the specificity of translational fidelity in cancer cell lines. These three additional cell lines will significantly broaden our insights on the question of misreading errors in mammalian systems.

Introducing the dual luciferase reporter system to an animal model would be the next step after a more comprehensive investigation of misreading errors in multiple mammalian cells. The plasmid carrying the dual luciferase system, pcDNA 3.1, has the CMV promoter, which is a strong

promoter and drives gene expression constitutively. The dual luciferase reporter system could be introduced into two transgenic strains, a normal mouse strain, and a strain with a high incidence of cancer. Mice from both strains would be sacrificed and dissected. Cells can be prepared from different organs and further be used for the dual luciferase assay. Therefore, this would enable us to compare the frequency of misreading *in vivo* and determine if variation in misreading frequencies are tissue-specific or if their frequency changes in cancerous cells.

2. Investigation of the effects of tRNA modifications on translational fidelity in mammalian cells

Exploring the effects of tRNA modifications on translational errors in general in mammalian cells, especially the influence of mcm^5s^2 , will be another interesting future direction. Loss of mcm^5s^2 or s^2 at the wobble position or ψ at position 38 all reduced the frequency of misreading of error-prone codons in yeast cells. Are these effects similar in yeast and mammalian cells? The human elongator complex, which is responsible for catalyzing mcm^5 group synthesis, is composed of Ikb kinase complex-associated protein [IKAP (yeast Elp1p)], Stat3-interacting protein [StIP1 (yeast Elp2p)], Elongator protein 3 homolog (ELP3), ELP4, and two unidentified polypeptides (Hawkes et al., 2002). Disruption of any of the identified proteins should eliminate the formation of mcm^5 . Transfection of the dual luciferase reporter system into either wild type or an mcm^5 modification deficient background would allow me to measure and compare the frequency of misreading, revealing the effects of mcm^5 and mcm^5s^2 on translational fidelity in mammalian cells.

To further explore the idea that tRNA modifications are also responsible for the low frequency of wobble errors in mammalian cells, I can eliminate wobble position modifications. To achieve this, I could knockout a gene that encodes the enzyme catalyzing the formation of modifications at the

wobble position. For example, in mammalian cells, ALKBH8 participates directly in the formation of mcm⁵s²U (Songe-Møller et al., 2010). Complete loss of uridine modification was not lethal in *Alkbh8*^{-/-} mice. Hence, I could either knock down its expression by using RNA interference or knock out the gene by CRISPR. Such that, tRNA_{UUU}^{Lys} should have an unmodified or hypomodified wobble uridine. If tRNA modifications at the wobble position are responsible for the low frequency of wobble errors in mammalian cells, the frequency of misreading errors at the wobble position should increase. Otherwise, the frequency would not be altered with or without the presence of tRNA modifications at the wobble position.

C. Summary

The primary purpose of my study is to measure every potential misreading event by tRNA_{UUU}^{Lys} in multiple mammalian cell lines, and by tRNA_{UUG}^{Gln} in yeast cells. All the results have contributed to a better understanding of misreading error and factors that can influence error frequency *in vivo*. This study has demonstrated that we can quantitatively measure the frequency of misreading errors in the mammalian system by a single tRNA. Moreover, a novel tRNA reporter system developed in yeast has provided another useful tool to test translational errors. Both projects allow us to study the effects of factors on the accuracy of decoding and of components that are essential in the translational machinery. Altogether, my research has broadened our knowledge of possible mismatches involved during the decoding process.

REFERENCES

- Abbott, J. A., Francklyn, C. S., & Robey-Bond, S. M. (2014). Transfer RNA and human disease. *Frontiers in Genetics*, 5, 158. <http://doi.org/10.3389/fgene.2014.00158>
- Acker, M. G., Shin, B. S., Dever, T. E., & Lorsch, J. R. (2006). Interaction between eukaryotic initiation factors 1A and 5B is required for efficient ribosomal subunit joining. *Journal of Biological Chemistry*, 281(13), 8469–8475. <http://doi.org/10.1074/jbc.M600210200>
- Agrawal, R. K., Penczek, P., Grassucci, R. a., & Frank, J. (1998). Visualization of elongation factor G on the Escherichia coli 70S ribosome: The mechanism of translocation. *Proceedings of the National Academy of Sciences*, 95(11), 6134–6138. <http://doi.org/10.1073/pnas.95.11.6134>
- Agris, P. F. (2004). Decoding the genome: A modified view. *Nucleic Acids Research*, 32(1), 223–38. <http://doi.org/10.1093/nar/gkh185>
- Agris, P. F., Vendeix, F. A. P., & Graham, W. D. (2007). tRNA's Wobble Decoding of the Genome: 40 Years of Modification. *Journal of Molecular Biology*, 366(1), 1–13. <http://doi.org/10.1016/j.jmb.2006.11.046>
- Ahel, I., Korencic, D., Ibba, M., & Söll, D. (2003). Trans-editing of mischarged tRNAs. *Proceedings of the National Academy of Sciences of the United States of America*, 100(26), 15422–7. <http://doi.org/10.1073/pnas.2136934100>
- Algire, M. A., Maag, D., & Lorsch, J. R. (2005). Pi release from eIF2, not GTP hydrolysis, is the step controlled by start-site selection during eukaryotic translation initiation. *Molecular Cell*, 20(2), 251–262. <http://doi.org/10.1016/j.molcel.2005.09.008>
- Alkalaeva, E. Z., Pisarev, A. V., Frolova, L. Y., Kisselev, L. L., & Pestova, T. V. (2006). In Vitro Reconstitution of Eukaryotic Translation Reveals Cooperativity between Release Factors eRF1 and eRF3. *Cell*, 125(6), 1125–1136. <http://doi.org/10.1016/j.cell.2006.04.035>
- Alksne, L. E., Anthony, R. A., Liebman, S. W., & Warner, J. R. (1993). An accuracy center in the ribosome conserved over 2 billion years. *Proceedings of the National Academy of Sciences of the United States of America*, 90(20), 9538–41. <http://doi.org/10.1073/pnas.90.20.9538>
- Alksne, L. E., Anthony, R. A., Liebman, S. W., & Warner, J. R. (1993). An accuracy center in the ribosome conserved, 90(October), 9538–9541.
- Alksne, L. E., Warner, J. R., Demeshkina, N., Jenner, L., Westhof, E., Yusupov, M., & Yusupova, G. (1993). A novel cloning strategy reveals the gene for the yeast homologue to Escherichia coli ribosomal protein S12. *Journal of Biological Chemistry*, 268(15), 10813–10819. <http://doi.org/10.1038/nature10913>
- All-Robyn, J. a, Brown, N., Otaka, E., & Liebman, S. W. (1990). Sequence and functional similarity between a yeast ribosomal protein and the Escherichia coli S5 ram protein. *Molecular and Cellular Biology*, 10(12), 6544–6553. <http://doi.org/10.1128/MCB.10.12.6544>. Updated

- Andersen, G. R., Nissen, P., & Nyborg, J. (2003). Elongation factors in protein biosynthesis. *Trends in Biochemical Sciences*. [http://doi.org/10.1016/S0968-0004\(03\)00162-2](http://doi.org/10.1016/S0968-0004(03)00162-2)
- Anderson, S. L., Coli, R., Daly, I. W., Kichula, E. A., Rork, M. J., Volpi, S. A., ... Rubin, B. Y. (2001). Familial Dysautonomia Is Caused by Mutations of the IKAP Gene. *The American Journal of Human Genetics*, *68*(3), 753–758. <http://doi.org/10.1086/318808>
- Angelini, M., Cannata, S., Mercaldo, V., Gibello, L., Santoro, C., Dianzani, I., & Loreni, F. (2007). Missense mutations associated with Diamond-Blackfan anemia affect the assembly of ribosomal protein S19 into the ribosome. *Human Molecular Genetics*, *16*(14), 1720–1727. <http://doi.org/10.1093/hmg/ddm120>
- Anger, A. M., Armache, J.-P., Berninghausen, O., Habeck, M., Subklewe, M., Wilson, D. N., & Beckmann, R. (2013). Structures of the human and Drosophila 80S ribosome. *Nature*, *497*(7447), 80–5. <http://doi.org/10.1038/nature12104>
- Anthony, R. A., & Liebman, S. W. (1995). Alterations in ribosomal protein RPS28 can diversely affect translational accuracy in *Saccharomyces cerevisiae*. *Genetics*, *140*(4), 1247–58. Retrieved from <http://www.pubmedcentral.nih.gov/articlerender.fcgi?artid=1206691&tool=pmcentrez&rendertype=abstract>
- Armache, J.-P., Jarasch, A., Anger, A. M., Villa, E., Becker, T., Bhushan, S., ... Beckmann, R. (2010a). Cryo-EM structure and rRNA model of a translating eukaryotic 80S ribosome at 5.5-Å resolution. *Proceedings of the National Academy of Sciences of the United States of America*, *107*(46), 19748–53. <http://doi.org/10.1073/pnas.1009999107>
- Armache, J.-P., Jarasch, A., Anger, A. M., Villa, E., Becker, T., Bhushan, S., ... Beckmann, R. (2010b). Localization of eukaryote-specific ribosomal proteins in a 5.5-Å cryo-EM map of the 80S eukaryotic ribosome. *Proceedings of the National Academy of Sciences of the United States of America*, *107*(46), 19754–9. <http://doi.org/10.1073/pnas.1010005107>
- Atkinson, G. C., Baldauf, S. L., & Haurlyliuk, V. (2008). Evolution of nonstop, no-go and nonsense-mediated mRNA decay and their termination factor-derived components. *BMC Evolutionary Biology*, *8*, 290. <http://doi.org/10.1186/1471-2148-8-290>
- Azimov, R., Abuladze, N., Sassani, P., Newman, D., Kao, L., Liu, W., ... Kurtz, I. (2008). G418-mediated ribosomal read-through of a nonsense mutation causing autosomal recessive proximal renal tubular acidosis. *American Journal of Physiology. Renal Physiology*, *295*(3), F633-41. <http://doi.org/10.1152/ajprenal.00015.2008>
- Baldwin, A. N., & Berg, P. (1966). Transfer ribonucleic acid-induced hydrolysis of valyladenylate bound to isoleucyl ribonucleic acid synthetase. *The Journal of Biological Chemistry*, *241*(4), 839–45. Retrieved from <http://www.ncbi.nlm.nih.gov/pubmed/5324173>
- Ban, N., Nissen, P., Hansen, J., Moore, P. B., & Steitz, T. A. (2000). The Complete Atomic Structure of the Large Ribosomal Subunit at 2.4 Å Resolution. *Science*, *289*(5481), 905–920. <http://doi.org/10.1126/science.289.5481.905>

- Barta, A., Steiner, G., Brosiustf, J., Nollert, H. F., & Kuechler, E. (1984). Identification of a site on 23S ribosomal RNA located at the peptidyl transferase center. *Biochemistry*, *81*, 3607–3611. Retrieved from <http://www.pnas.org/content/81/12/3607.long>
- Bebenek, K., & Kunkel, T. A. (1990). Frameshift errors initiated by nucleotide misincorporation. *Proceedings of the National Academy of Sciences of the United States of America*, *87*(13), 4946–50. <http://doi.org/10.1073/pnas.87.13.4946>
- Beckmann, R., Spahn, C. M. T., Eswar, N., Helmers, J., Penczek, P. A., Sali, A., ... Blobel, G. (2001). Architecture of the protein-conducting channel associated with the translating 80S ribosome. *Cell*, *107*(3), 361–372. [http://doi.org/10.1016/S0092-8674\(01\)00541-4](http://doi.org/10.1016/S0092-8674(01)00541-4)
- Bednářová, A., Hanna, M., Durham, I., VanCleave, T., England, A., Chaudhuri, A., & Krishnan, N. (2017). Lost in Translation: Defects in Transfer RNA Modifications and Neurological Disorders. *Frontiers in Molecular Neuroscience*, *10*, 135. <http://doi.org/10.3389/fnmol.2017.00135>
- Beebe, K., Merriman, E., & Schimmel, P. (2003). Structure-specific tRNA Determinants for Editing a Mischarged Amino Acid. *Journal of Biological Chemistry*, *278*(46), 45056–45061. <http://doi.org/10.1074/jbc.M307080200>
- Behrmann, E., Loerke, J., Budkevich, T. V., Yamamoto, K., Schmidt, A., Penczek, P. A., ... Spahn, C. M. T. (2015). Structural snapshots of actively translating human ribosomes. *Cell*, *161*(4). <http://doi.org/10.1016/j.cell.2015.03.052>
- Behura, S. K., & Severson, D. W. (2011). Coadaptation of isoacceptor tRNA genes and codon usage bias for translation efficiency in *Aedes aegypti* and *Anopheles gambiae*. *Insect Molecular Biology*, *20*(2), 177–87. <http://doi.org/10.1111/j.1365-2583.2010.01055.x>
- Ben-Shem, A., Garreau de Loubresse, N., Melnikov, S., Jenner, L., Yusupova, G., & Yusupov, M. (2011). The structure of the eukaryotic ribosome at 3.0 Å resolution. *Science (New York, N.Y.)*, *334*(6062), 1524–9. <http://doi.org/10.1126/science.1212642>
- Ben-Shem, A., Jenner, L., Yusupova, G., & Yusupov, M. (2010). Crystal structure of the eukaryotic ribosome. *Science (New York, N.Y.)*, *330*(6008), 1203–9. <http://doi.org/10.1126/science.1194294>
- Benveniste, R., & Davies, J. (1973). Structure-activity relationships among the aminoglycoside antibiotics: role of hydroxyl and amino groups. *Antimicrobial Agents and Chemotherapy*, *4*(4), 402–9. <http://doi.org/10.1128/AAC.4.4.402>. Updated
- Beringer, M. (2008). Modulating the activity of the peptidyl transferase center of the ribosome. *Rna*, *14*(5), 795–801. <http://doi.org/10.1261/rna.980308>
- Beringer, M., Bruell, C., Xiong, L., Pfister, P., Bieling, P., Katunin, V. I., ... Rodnina, M. V. (2005). Essential mechanisms in the catalysis of peptide bond formation on the ribosome. *Journal of Biological Chemistry*, *280*(43), 36065–36072. <http://doi.org/10.1074/jbc.M507961200>

- Bertram, G., Bell, H. A., Ritchie, D. W., Fullerton, G., & Stansfield, I. (2000). Terminating eukaryote translation: domain 1 of release factor eRF1 functions in stop codon recognition. *RNA (New York, N.Y.)*, *6*(9), 1236–47. Retrieved from <http://www.ncbi.nlm.nih.gov/pubmed/10999601>
- Biswas, D. K., & Gorini, L. (1972). Restriction, de-restriction and mistranslation in missense suppression. Ribosomal discrimination of transfer RNA's. *Journal of Molecular Biology*, *64*(1), 119–134. [http://doi.org/10.1016/0022-2836\(72\)90324-5](http://doi.org/10.1016/0022-2836(72)90324-5)
- Björk, G. R. (1995). Genetic dissection of synthesis and function of modified nucleosides in bacterial transfer RNA. *Progress in Nucleic Acid Research and Molecular Biology*, *50*, 263–338. Retrieved from <http://www.ncbi.nlm.nih.gov/pubmed/7538683>
- Björk, G. R., & Hagervall, T. G. Transfer RNA Modification: Presence, Synthesis, and Function. *EcoSal Plus*, *6*(1). <http://doi.org/10.1128/ecosalplus.ESP-0007-2013>
- Björk, G. R., Huang, B., Persson, O. P., & Byström, A. S. (2007). A conserved modified wobble nucleoside (mcm5s2U) in lysyl-tRNA is required for viability in yeast. *RNA (New York, N.Y.)*, *13*(8), 1245–55. <http://doi.org/10.1261/rna.558707>
- Blanchard, S. C., Gonzalez, R. L., Kim, H. D., Chu, S., & Puglisi, J. D. (2004a). tRNA selection and kinetic proofreading in translation. *Nature Structural & Molecular Biology*, *11*(10), 1008–14. <http://doi.org/10.1038/nsmb831>
- Blanchard, S. C., Gonzalez, R. L., Kim, H. D., Chu, S., & Puglisi, J. D. (2004b). tRNA selection and kinetic proofreading in translation. *Nature Structural & Molecular Biology*, *11*(10), 1008–1014. <http://doi.org/10.1038/nsmb831>
- Blanchet, S., Cornu, D., Argentini, M., & Namy, O. (2014). New insights into the incorporation of natural suppressor tRNAs at stop codons in *Saccharomyces cerevisiae*. *Nucleic Acids Research*, *42*(15), 10061–10072. <http://doi.org/10.1093/nar/gku663>
- Boniecki, M. T., Vu, M. T., Betha, A. K., & Martinis, S. A. (2008). CP1-dependent partitioning of pretransfer and posttransfer editing in leucyl-tRNA synthetase. *Proceedings of the National Academy of Sciences*, *105*(49), 19223–19228. <http://doi.org/10.1073/pnas.0809336105>
- Bouadloun, F., Donner, D., & Kurland, C. G. (1983). Codon-specific missense errors in vivo. *The EMBO Journal*, *2*(8), 1351–6. Retrieved from <http://www.ncbi.nlm.nih.gov/pubmed/10872330>
- Branchini, B. R., Magyar, R. a, Murtiashaw, M. H., Anderson, S. M., Helgerson, L. C., & Zimmer, M. (1999). Site-directed mutagenesis of firefly luciferase active site amino acids: a proposed model for bioluminescence color. *Biochemistry*, *38*(40), 13223–30. Retrieved from <http://www.ncbi.nlm.nih.gov/pubmed/10529195>
- Branchini, B. R., Murtiashaw, M. H., Magyar, R. a, & Anderson, S. M. (2000). The role of lysine 529, a conserved residue of the acyl-adenylate-forming enzyme superfamily, in firefly

- luciferase. *Biochemistry*, 39(18), 5433–40. Retrieved from <http://www.ncbi.nlm.nih.gov/pubmed/10820015>
- BRETSCHER, M. S. (1968). Translocation in Protein Synthesis: A Hybrid Structure Model. *Nature*, 218(5142), 675–677. <http://doi.org/10.1038/218675a0>
- Brimacombe, B. Y. R., Trupin, J., Leder, P., Bernfield, J., & Jaouni, T. (1965). RNA codewords and protein synthesis, VIII. Nucleotide sequences of synonym codons for arginine, valine, cysteine, and alanine. *Proc. Natl. Acad. Sci. USA*, 54, 954–960.
- Brown, C. M., Stockwell, P. A., Trotman, C. N., & Tate, W. P. (1990a). Sequence analysis suggests that tetra-nucleotides signal the termination of protein synthesis in eukaryotes. *Nucleic Acids Research*, 18(21), 6339–45. Retrieved from <http://www.ncbi.nlm.nih.gov/pubmed/2123028>
- Brown, C. M., Stockwell, P. A., Trotman, C. N., & Tate, W. P. (1990b). The signal for the termination of protein synthesis in procaryotes. *Nucleic Acids Research*, 18(8), 2079–86. Retrieved from <http://www.ncbi.nlm.nih.gov/pubmed/2186375>
- Budkevich, T., Giesebrecht, J., Altman, R. B., Munro, J. B., Mielke, T., Nierhaus, K. H., ... Spahn, C. M. T. (2011). Structure and dynamics of the mammalian ribosomal pretranslocation complex. *Molecular Cell*, 44(2), 214–224. <http://doi.org/10.1016/j.molcel.2011.07.040>
- Bulygin, K. N., Khairulina, Y. S., Kolosov, P. M., Ven'yaminova, A. G., Graifer, D. M., Vorobjev, Y. N., ... Karpova, G. G. (2010). Three distinct peptides from the N domain of translation termination factor eRF1 surround stop codon in the ribosome. *RNA (New York, N.Y.)*, 16(10), 1902–14. <http://doi.org/10.1261/rna.2066910>
- Burke, J. F., & Mogg, A. E. (1985). Suppression of a nonsense mutation in mammalian cells in vivo by the aminoglycoside anthiotics G–418 and paromomycin. *Nucleic Acids Research*, 13(17), 6265–6272. <http://doi.org/10.1093/nar/13.17.6265>
- Burke, J. F., & Mogg, A. E. (1985). Suppression of a nonsense mutation in mammalian cells in vivo by the aminoglycoside antibiotics G-418 and paromomycin. *Nucleic Acids Research*, 13(17), 6265–6272. Retrieved from <http://www.ncbi.nlm.nih.gov/pubmed/2995924>
- Carlberg, U., Nilsson, A., & Nygard, O. (1990). Functional properties of phosphorylated elongation factor 2. *Eur J Biochem*, 191(3), 639–645. <http://doi.org/10.1111/j.1432-1033.1990.tb19169.x>
- Carr-Schmid, A., Durko, N., Cavallius, J., Merrick, W. C., & Kinzy, T. G. (1999). Mutations in a GTP-binding motif of eukaryotic elongation factor 1A reduce both translational fidelity and the requirement for nucleotide exchange. *Journal of Biological Chemistry*, 274(42), 30297–30302. <http://doi.org/10.1074/jbc.274.42.30297>
- Carter, a P., Clemons, W. M., Brodersen, D. E., Morgan-Warren, R. J., Wimberly, B. T., & Ramakrishnan, V. (2000). Functional insights from the structure of the 30S ribosomal subunit and its interactions with antibiotics. *Nature*, 407(6802), 340–8. <http://doi.org/10.1038/35030019>

- Cate, J. H., Yusupov, M. M., Yusupova, G. Z., Earnest, T. N., & Noller, H. F. (1999). X-ray crystal structures of 70S ribosome functional complexes. *Science*, 285(5436), 2095–2104. <http://doi.org/10.1126/science.285.5436.2095>
- Chandramouli, P., Topf, M., Ménétret, J.-F., Eswar, N., Cannone, J. J., Gutell, R. R., ... Yusupov, M. (2008). Structure of the mammalian 80S ribosome at 8.7 Å resolution. *Structure (London, England : 1993)*, 16(4), 535–48. <http://doi.org/10.1016/j.str.2008.01.007>
- Charette, M., & Gray, M. W. (2000). Pseudouridine in RNA: what, where, how, and why. *IUBMB Life*, 49(5), 341–351. <http://doi.org/10.1080/152165400410182>
- Chen, C., Tuck, S., & Byström, A. S. (2009). Defects in tRNA modification associated with neurological and developmental dysfunctions in *Caenorhabditis elegans* elongator mutants. *PLoS Genetics*, 5(7). <http://doi.org/10.1371/journal.pgen.1000561>
- Chen, Y., Feng, S., Kumar, V., Ero, R., & Gao, Y.-G. (2013). Structure of EF-G-ribosome complex in a pretranslocation state. *Nature Structural & Molecular Biology*, 20(9), 1077–84. <http://doi.org/10.1038/nsmb.2645>
- Cheng, Z., Saito, K., Pisarev, A. V., Wada, M., Pisareva, V. P., Pestova, T. V., ... Song, H. (2009). Structural insights into eRF3 and stop codon recognition by eRF1. *Genes and Development*, 23(9), 1106–1118. <http://doi.org/10.1101/gad.1770109>
- Close, P., Hawkes, N., Cornez, I., Creppe, C., Lambert, C. A., Rogister, B., ... Chariot, A. (2006). Transcription Impairment and Cell Migration Defects in Elongator-Depleted Cells: Implication for Familial Dysautonomia. *Molecular Cell*, 22(4), 521–531. <http://doi.org/10.1016/j.molcel.2006.04.017>
- Cochella, L., Brunelle, J. L., & Green, R. (2007). Mutational analysis reveals two independent molecular requirements during transfer RNA selection on the ribosome. *Nat Struct Mol Biol.*, 14(1), 30–36. <http://doi.org/10.1038/nsmb1183>
- Cochella, L., & Green, R. (2005). An active role for tRNA in decoding beyond codon:anticodon pairing. *Science (New York, N.Y.)*, 308(5725), 1178–80. <http://doi.org/10.1126/science.1111408>
- Cogan, J., Weinstein, J., Wang, X., Hou, Y., Martin, S., South, A. P., ... Chen, M. (2014). Aminoglycosides restore full-length type VII collagen by overcoming premature termination codons: therapeutic implications for dystrophic epidermolysis bullosa. *Molecular Therapy : The Journal of the American Society of Gene Therapy*, 22(10), 1741–52. <http://doi.org/10.1038/mt.2014.140>
- Cox, E. C., White, J. R., & Flaks, J. G. (1964). STREPTOMYCIN ACTION AND THE RIBOSOME. *Proceedings of the National Academy of Sciences of the United States of America*, 51, 703–9. Retrieved from <http://www.pubmedcentral.nih.gov/articlerender.fcgi?artid=300143&tool=pmcentrez&rendertype=abstract>

- Crick, F. H., Barnett, L., Brenner, S., & Watts-Tobin, R. J. (1961). General nature of the genetic code for proteins. *Nature*, *192*, 1227–1232. <http://doi.org/10.1038/1921227a0>
- Crick, F. H. C. (1966). Codon—anticodon pairing: The wobble hypothesis. *Journal of Molecular Biology*, *19*(2), 548–555. [http://doi.org/10.1016/S0022-2836\(66\)80022-0](http://doi.org/10.1016/S0022-2836(66)80022-0)
- Czworkowski, J., Wang, J., Steitz, T. A., & Moore, P. B. (1994). The crystal structure of elongation factor G complexed with GDP, at 2.7 Å resolution. *The EMBO Journal*, *13*(16), 3661–3668. <http://doi.org/10.1016>
- Davies, J. E. (1964). STUDIES ON THE RIBOSOMES OF STREPTOMYCIN-SENSITIVE AND RESISTANT STRAINS OF ESCHERICHIA COLI. *Proceedings of the National Academy of Sciences of the United States of America*, *51*, 659–64. Retrieved from <http://www.pubmedcentral.nih.gov/articlerender.fcgi?artid=300136&tool=pmcentrez&rendertype=abstract>
- Davis, D. R. (1995). Stabilization of RNA stacking by pseudouridine. *Nucleic Acids Research*, *23*(24), 5020–5026. <http://doi.org/10.1093/nar/23.24.5020>
- Demeshkina, N., Jenner, L., Westhof, E., Yusupov, M., & Yusupova, G. (2012). A new understanding of the decoding principle on the ribosome. *Nature*, *484*(7393), 256–259. <http://doi.org/10.1038/nature10913>
- des Georges, A., Hashem, Y., Unbehaun, A., Grassucci, R. A., Taylor, D., Hellen, C. U. T., ... Frank, J. (2014). Structure of the mammalian ribosomal pre-termination complex associated with eRF1*eRF3*GDPNP. *Nucleic Acids Research*, *42*(5), 3409–3418. <http://doi.org/10.1093/nar/gkt1279>
- Dever, T. E., & Green, R. (2012). The elongation, termination, and recycling phases of translation in eukaryotes. *Cold Spring Harbor Perspectives in Biology*, *4*(7), a013706. <http://doi.org/10.1101/cshperspect.a013706>
- Dittmar, K. A., Goodenbour, J. M., & Pan, T. (2006). Tissue-specific differences in human transfer RNA expression. *PLoS Genetics*, *2*(12), e221. <http://doi.org/10.1371/journal.pgen.0020221>
- Donahue, T. . (2000). Genetic Approaches to Translation Initiation in *Saccharomyces cerevisiae*. In N. Sonenberg, J. W. B. Hershey, & M. B. Mathews (Eds.), *Translational Control of Gene Expression* (pp. 487–502). Cold Spring Harbor Laboratory Press.
- Dong, H., Nilsson, L., & Kurland, C. G. (1996). Co-variation of tRNA Abundance and Codon Usage in *Escherichia coli* at Different Growth Rates. *Journal of Molecular Biology*, *260*(5), 649–663. <http://doi.org/10.1006/jmbi.1996.0428>
- Doudna, J. A., & Sarnow, P. (2007). Translation Initiation by Viral Internal Ribosome Entry Sites. *Cold Spring Harbor Monograph Archive*, *48*, 129–153. <http://doi.org/10.1101/087969767.48.129>
- Dranchak, P. K., Di Pietro, E., Snowden, A., Oesch, N., Braverman, N. E., Steinberg, S. J., &

- Hacia, J. G. (2011). Nonsense suppressor therapies rescue peroxisome lipid metabolism and assembly in cells from patients with specific PEX gene mutations. *Journal of Cellular Biochemistry*, *112*(5), 1250–1258. <http://doi.org/10.1002/jcb.22979>
- Dunkle, J. A., Wang, L., Feldman, M. B., Pulk, A., Chen, V. B., Kapral, G. J., ... Cate, J. H. D. (2011). Structures of the bacterial ribosome in classical and hybrid states of tRNA binding. *Science (New York, NY)*, *332*(6032), 981–984. <http://doi.org/10.1126/science.1202692>
- Durant, P. C., Bajji, A. C., Sundaram, M., Kumar, R. K., & Davis, D. R. (2005). Structural effects of hypermodified nucleosides in the Escherichia coli and human tRNA^{Lys} anticodon loop: The effect of nucleosides s 2U, mcm5U, mcm5s2U, mnm 5s2U, t6A, and ms2t6A. *Biochemistry*, *44*(22), 8078–8089. <http://doi.org/10.1021/bi050343f>
- Edelmann, P., & Gallant, J. (1977). Mistranslation in E. coli. *Cell*, *10*(1), 131–7. Retrieved from <http://www.sciencedirect.com/science/article/pii/0092867477901477>
- El Yacoubi, B., Bailly, M., & de Crécy-Lagard, V. (2012). Biosynthesis and Function of Posttranscriptional Modifications of Transfer RNAs. *Annual Review of Genetics*, *46*(1), 69–95. <http://doi.org/10.1146/annurev-genet-110711-155641>
- Eldred, E. W., & Schimmel, P. R. (1972). Rapid deacylation by isoleucyl transfer ribonucleic acid synthetase of isoleucine-specific transfer ribonucleic acid aminoacylated with valine. *Journal of Biological Chemistry*, *247*(16), 2961–4. Retrieved from <http://www.jbc.org/content/247/9/2961.short>
- Englich, S., Englich, U., von der Haar, F., & Cramer, F. (1986). The proofreading of hydroxy analogues of leucine and isoleucine by leucyl-tRNA synthetases from E. coli and yeast. *Nucleic Acids Research*, *14*(19), 7529–39. Retrieved from <http://www.ncbi.nlm.nih.gov/pubmed/3534789>
- Erie, D. A., Yager, T. D., & von Hippel, P. H. (1992). The Single-Nucleotide Addition Cycle in Transcription: a Biophysical and Biochemical Perspective. *Annual Review of Biophysics and Biomolecular Structure*, *21*(1), 379–415. <http://doi.org/10.1146/annurev.bb.21.060192.002115>
- Esberg, A., Huang, B., Johansson, M. J. O., Byström, A. S., Yamaizumi, Z., Nishimura, S., ... al., et. (2006). Elevated levels of two tRNA species bypass the requirement for elongator complex in transcription and exocytosis. *Molecular Cell*, *24*(1), 139–48. <http://doi.org/10.1016/j.molcel.2006.07.031>
- Fan-Minogue, H., Du, M., Pisarev, A. V., Kallmeyer, A. K., Salas-Marco, J., Keeling, K. M., ... Bedwell, D. M. (2008). Distinct eRF3 Requirements Suggest Alternate eRF1 Conformations Mediate Peptide Release during Eukaryotic Translation Termination. *Molecular Cell*, *30*(5), 599–609. <http://doi.org/10.1016/j.molcel.2008.03.020>
- Feder, M., Pas, J., Wyrwicz, L. S., & Bujnicki, J. M. (2003). Molecular phylogenetics of the RrmJ/fibrillarin superfamily of ribose 2'-O-methyltransferases. *Gene*, *302*(1–2), 129–138. [http://doi.org/10.1016/S0378-1119\(02\)01097-1](http://doi.org/10.1016/S0378-1119(02)01097-1)

- Fersht, A. (1977). Editing Mechanisms in Protein Synthesis . Rejection of Valine by the isoleucyl-tRNA synthetase. *Amino Acid Recognition*, 16(5), 1025–1030.
- Fersht, A. R., & Dingwall, C. (1979). Evidence for the double-sieve editing mechanism in protein synthesis. Steric exclusion of isoleucine by valyl-tRNA synthetases. *Biochemistry*, 18(12), 2627–2631. <http://doi.org/10.1021/bi00579a030>
- Fletcher, C. M., Pestova, T. V, Hellen, C. U., & Wagner, G. (1999). Structure and interactions of the translation initiation factor eIF1. *The EMBO Journal*, 18(9), 2631–2637. <http://doi.org/10.1093/emboj/18.9.2631>
- Floquet, C., Deforges, J., Rousset, J.-P., & Bidou, L. (2011). Rescue of non-sense mutated p53 tumor suppressor gene by aminoglycosides. *Nucleic Acids Research*, 39(8), 3350–62. <http://doi.org/10.1093/nar/gkq1277>
- Floquet, C., Rousset, J.-P., & Bidou, L. (2011). Readthrough of premature termination codons in the adenomatous polyposis coli gene restores its biological activity in human cancer cells. *PLoS One*, 6(8), e24125. <http://doi.org/10.1371/journal.pone.0024125>
- Flygare, J., Aspesi, A., Bailey, J. C., Miyake, K., Caffrey, J. M., Karlsson, S., & Ellis, S. R. (2007). Human RPS19, the gene mutated in Diamond-Blackfan anemia, encodes a ribosomal protein required for the maturation of 40S ribosomal subunits. *Blood*, 109(3), 980–986.
- Fourmy, D., Recht, M. I., Blanchard, S. C., & Puglisi, J. D. (1996). Structure of the A Site of Escherichia coli 16S Ribosomal RNA Complexed with an Aminoglycoside Antibiotic. *Science*, 274(5291). Retrieved from <http://science.sciencemag.org/content/274/5291/1367/tab-pdf>
- Frank, J., & Agrawal, R. K. (2000). A ratchet-like inter-subunit reorganization of the ribosome during translocation. *Nature*, 406(6793), 318–22. <http://doi.org/10.1038/35018597>
- Frank, J., Gao, H., Sengupta, J., Gao, N., & Taylor, D. J. (2007). The process of mRNA-tRNA translocation. *Proceedings of the National Academy of Sciences of the United States of America*, 104(50), 19671–8. <http://doi.org/10.1073/pnas.0708517104>
- Frank, J., Sengupta, J., Gao, H., Li, W., Valle, M., Zavialov, A., & Ehrenberg, M. (2005). The role of tRNA as a molecular spring in decoding, accommodation, and peptidyl transfer. *FEBS Letters*, 579(4), 959–62. <http://doi.org/10.1016/j.febslet.2004.10.105>
- Frank, J., Zhu, J., Penczek, P., Li, Y., Srivastava, S., Verschoor, A., ... Agrawal, R. K. (1995). A model of protein synthesis based on cryo-electron microscopy of the E. coli ribosome. *Nature*, 376(6539), 441–444. <http://doi.org/10.1038/376441a0>
- Freier, S. M., Kierzek, R., Caruthers, M. H., Neilson, T., & Turner, D. H. (1986). Free energy contributions of G.U and other terminal mismatches to helix stability. *Biochemistry*, 25(11), 3209–13. Retrieved from <http://www.ncbi.nlm.nih.gov/pubmed/3730356>
- Freistroffer, D. V., Pavlov, M. Y., MacDougall, J., Buckingham, R. H., & Ehrenberg, M. (1997).

- Release factor RF3 in *E. coli* accelerates the dissociation of release factors RF1 and RF2 from the ribosome in a GTP-dependent manner. *EMBO Journal*, 16(13), 4126–4133. <http://doi.org/10.1093/emboj/16.13.4126>
- Freude, K., Hoffmann, K., Jensen, L.-R., Delatycki, M. B., des Portes, V., Moser, B., ... Ropers, H.-H. (2004). Mutations in the FTSJ1 gene coding for a novel S-adenosylmethionine-binding protein cause nonsyndromic X-linked mental retardation. *American Journal of Human Genetics*, 75(2), 305–9. <http://doi.org/10.1086/422507>
- Friedman, S., & Weinstein, I. (1964). Lack of fidelity in the translation of synthetic polyribonucleotides. ... *of the National Academy of Sciences ...*, 6(1960), 988–996. Retrieved from <https://www.ncbi.nlm.nih.gov/pmc/articles/PMC300383/pdf/pnas00184-0126.pdf>
- Frolova, L., Le Goff, X., Rasmussen, H. H., Cheperegin, S., Drugeon, G., Kress, M., ... Philippe, M. (1994). A highly conserved eukaryotic protein family possessing properties of polypeptide chain release factor. *Nature*. <http://doi.org/10.1038/372701a0>
- Frolova, L., Le Goff, X., Zhouravleva, G., Davydova, E., Philippe, M., & Kisselev, L. (1996). Eukaryotic polypeptide chain release factor eRF3 is an eRF1- and ribosome-dependent guanosine triphosphatase. *RNA (New York, N.Y.)*, 2(4), 334–41. Retrieved from <http://www.ncbi.nlm.nih.gov/pubmed/8634914>
- Frolova, L. Y., Tsivkovskii, R. Y., Sivolobova, G. F., Oparina, N. Y., Serpinsky, O. I., Blinov, V. M., ... Kisselev, L. L. (1999). Mutations in the highly conserved GGQ motif of class 1 polypeptide release factors abolish ability of human eRF1 to trigger peptidyl-tRNA hydrolysis. *RNA (New York, N.Y.)*, 5(8), 1014–1020. <http://doi.org/10.1017/S135583829999043X>
- Gao, H., Sengupta, J., Valle, M., Korostelev, A., Eswar, N., Stagg, S. M., ... Frank, J. (2003). Study of the structural dynamics of the *E. coli* 70S ribosome using real-space refinement. *Cell*, 113(6), 789–801. [http://doi.org/10.1016/S0092-8674\(03\)00427-6](http://doi.org/10.1016/S0092-8674(03)00427-6)
- Gehrke, C. W., & Kuo, K. C. (1989). Ribonucleoside analysis by reversed-phase high-performance liquid chromatography. *Molecular Cell*, 471, 3–36. Retrieved from [http://linkinghub.elsevier.com/retrieve/pii/S0021967300941529%5Cnfile:///Users/MartinB/Documents/PhD/Paper/Library.papers3/Files/A6/A606B7CD-534A-4144-B4C6-2D4DC9F29376.pdf%5Cnpapers3://publication/doi/10.1016/S0021-9673\(00\)94152-9](http://linkinghub.elsevier.com/retrieve/pii/S0021967300941529%5Cnfile:///Users/MartinB/Documents/PhD/Paper/Library.papers3/Files/A6/A606B7CD-534A-4144-B4C6-2D4DC9F29376.pdf%5Cnpapers3://publication/doi/10.1016/S0021-9673(00)94152-9)
- Giaever, G., Chu, A. M., Ni, L., Connelly, C., Riles, L., Véronneau, S., ... Johnston, M. (2002). Functional profiling of the *Saccharomyces cerevisiae* genome. *Nature*, 418(6896), 387–391. <http://doi.org/10.1038/nature00935>
- Giegé, R., Sissler, M., & Florentz, C. (1998). Universal rules and idiosyncratic features in tRNA identity. *Nucleic Acids Research*, 26(22), 5017–35. <http://doi.org/10.1093/nar/26.22.5017>
- Gietz, R. D., & Woods, R. A. (2002). Transformation of yeast by lithium acetate/single-stranded carrier DNA/polyethylene glycol method. *Methods in Enzymology*, 350, 87–96. Retrieved from <http://www.ncbi.nlm.nih.gov/pubmed/12073338>

- Gorini, L., & Kataja, E. (1964). PHENOTYPIC REPAIR BY STREPTOMYCIN OF DEFECTIVE GENOTYPES IN E. COLI. *Proceedings of the National Academy of Sciences of the United States of America*, *51*, 487–93. Retrieved from <http://www.pubmedcentral.nih.gov/articlerender.fcgi?artid=300100&tool=pmcentrez&rendertype=abstract>
- Green and, R., Noller, H. F., Green, R., & Noller, H. F. (1997). Ribosomes and translation. *Annual Review of Biochemistry*, *66*(1), 679–716. <http://doi.org/10.1146/annurev.biochem.66.1.679>
- Gromadski, K. B., & Rodnina, M. V. (2004a). Kinetic Determinants of High-Fidelity tRNA Discrimination on the Ribosome. *Molecular Cell*, *13*(2), 191–200. [http://doi.org/10.1016/S1097-2765\(04\)00005-X](http://doi.org/10.1016/S1097-2765(04)00005-X)
- Gromadski, K. B., & Rodnina, M. V. (2004b). Streptomycin interferes with conformational coupling between codon recognition and GTPase activation on the ribosome. *Nature Structural & Molecular Biology*, *11*(4), 316–322. <http://doi.org/10.1038/nsmb742>
- Grosjean, H. J., de Henau, S., & Crothers, D. M. (1978). On the physical basis for ambiguity in genetic coding interactions. *Proceedings of the National Academy of Sciences of the United States of America*, *75*(2), 610–614. <http://doi.org/10.1073/pnas.75.2.610>
- Gross, J. D., Moerke, N. J., Von Der Haar, T., Lugovskoy, A. A., Sachs, A. B., McCarthy, J. E. G., & Wagner, G. (2003). Ribosome loading onto the mRNA cap is driven by conformational coupling between eIF4G and eIF4E. *Cell*, *115*(6), 739–750. [http://doi.org/10.1016/S0092-8674\(03\)00975-9](http://doi.org/10.1016/S0092-8674(03)00975-9)
- Gustilo, E. M., Vendeix, F. A., & Agris, P. F. (2008). tRNA's modifications bring order to gene expression. *Current Opinion in Microbiology*, *11*(2), 134–40. <http://doi.org/10.1016/j.mib.2008.02.003>
- Guy, M. P., Young, D. L., Payea, M. J., Zhang, X., Kon, Y., Dean, K. M., ... Phizicky, E. M. (2014). Identification of the determinants of tRNA function and susceptibility to rapid tRNA decay by high-throughput in vivo analysis. *Genes & Development*, *28*(15), 1721–1732. <http://doi.org/10.1101/gad.245936.114>
- Hagervall, T. G., Pomerantz, S. C., & McCloskey, J. A. (1998). Reduced misreading of asparagine codons by Escherichia coli tRNA^{Lys} with hypomodified derivatives of 5-methylaminomethyl-2-thiouridine in the wobble position1. *Journal of Molecular Biology*, *284*(1), 33–42. <http://doi.org/http://dx.doi.org/10.1006/jmbi.1998.2162>
- Hale, S. P., Auld, D. S., Schmidt, E., & Schimmel, P. (1997). Discrete determinants in transfer RNA for editing and aminoacylation. *Science (New York, N.Y.)*, *276*(5316), 1250–2. <http://doi.org/10.1126/science.276.5316.1250>
- Han, L., Kon, Y., & Phizicky, E. M. (2015a). Functional importance of Ψ38 and Ψ39 in distinct tRNAs, amplified for tRNA^{Gln}(UUG) by unexpected temperature sensitivity of the s2U modification in yeast. *RNA (New York, N.Y.)*, *21*(2), 188–201. <http://doi.org/10.1261/rna.048173.114>

- Han, L., Kon, Y., & Phizicky, E. M. (2015b). Functional importance of Ψ 38 and Ψ 39 in distinct tRNAs, amplified for tRNA Gln(UUG) by unexpected temperature sensitivity of the s 2 U modification in yeast. *RNA*, *21*(2), 188–201. <http://doi.org/10.1261/rna.048173.114>
- Harding, C. V., Harding, D., McLimans, W. F., & Rake, G. (1956). Cytological changes accompanying the growth of poliomyelitis virus in cells of human origin (strain HeLa). *Virology*, *2*(1), 109–125. Retrieved from <http://www.ncbi.nlm.nih.gov/pubmed/13299706>
- Hawkes, N. A., Otero, G., Sebastiaan Winkler, G., Marshall, N., Dahmus, M. E., Krappmann, D., ... Svejstrup, J. Q. (2002). Purification and characterization of the human elongator complex. *Journal of Biological Chemistry*, *277*(4), 3047–3052. <http://doi.org/10.1074/jbc.M110445200>
- Heier, C. R., & DiDonato, C. J. (2009). Translational readthrough by the aminoglycoside geneticin (G418) modulates SMN stability in vitro and improves motor function in SMA mice in vivo. *Human Molecular Genetics*, *18*(7), 1310–22. <http://doi.org/10.1093/hmg/ddp030>
- Hendrickson, T. L., & Schimmel, P. (2003). Transfer RNA-dependent amino acid discrimination by aminoacyl-tRNA synthetases. In *Translation Mechanisms* (pp. 34–64).
- Hershey, J. W. B., Sonenberg, N., & Mathews, M. B. (2012). Principles of translational control: An overview. *Cold Spring Harbor Perspectives in Biology*, *4*(12). <http://doi.org/10.1101/cshperspect.a009829>
- Himeno, H., Hasegawa, T., Ueda, T., Watanabe, K., Miura, K., & Shimizu, M. (1989). Role of the extra G-C pair at the end of the acceptor stem of tRNA(His) in aminoacylation. *Nucleic Acids Research*, *17*(19), 7855–63. Retrieved from <http://www.ncbi.nlm.nih.gov/pubmed/2678006>
- Himeno, H., Hasegawa, T., Ueda, T., Watanabe, K., & Shimizu, M. (1990). Conversion of aminoacylation specificity from tRNA(Tyr) to tRNA(Ser) in vitro. *Nucleic Acids Research*, *18*(23), 6815–9. Retrieved from <http://www.ncbi.nlm.nih.gov/pubmed/2263446>
- Hinnebusch, A. G. (2011). Molecular Mechanism of Scanning and Start Codon Selection in Eukaryotes. *Microbiology and Molecular Biology Reviews*, *75*(3), 434–467. <http://doi.org/10.1128/MMBR.00008-11>
- Hirokawa, G., Nijman, R. M., Raj, V. S., Kaji, H., Igarashi, K., & Kaji, A. (2005). The role of ribosome recycling factor in dissociation of 70S ribosomes into subunits. *RNA (New York, N.Y.)*, *11*, 1317–1328. <http://doi.org/10.1261/rna.2520405>
- Holley, R. W., Everett, G. A., Madison, T., Zamir, A., & Madison, J. T. (1965). ARTICLE : Nucleotide Sequences in the Yeast Alanine Transfer Ribonucleic Acid Nucleotide Sequences in the Yeast Alanine Transfer Ribonucleic Acid *. *THE JOURNAL OF BUX, OORCX~ CHEMISTRY*, *240*(5), 2122–2129. Retrieved from <http://www.jbc.org/content/240/5/2122.full.pdf>
- Hopfield, J. J. (1974). Kinetic proofreading: a new mechanism for reducing errors in biosynthetic processes requiring high specificity. *Proceedings of the National Academy of Sciences*,

71(10), 4135–4139. <http://doi.org/10.1073/pnas.71.10.4135>

- Horos, R., Ijspeert, H., Pospisilova, D., Sendtner, R., Andrieu-Soler, C., Taskesen, E., ... von Lindern, M. (2012). Ribosomal deficiencies in Diamond-Blackfan anemia impair translation of transcripts essential for differentiation of murine and human erythroblasts. *Blood*, *119*(1), 262–72. <http://doi.org/10.1182/blood-2011-06-358200>
- Hou, Y. M., & Schimmel, P. (1989). Evidence that a major determinant for the identity of a transfer RNA is conserved in evolution. *Biochemistry*, *28*(17), 6800–4. Retrieved from <http://www.ncbi.nlm.nih.gov/pubmed/2684266>
- Hou, Y. M., Westhof, E., & Giegé, R. (1993). An unusual RNA tertiary interaction has a role for the specific aminoacylation of a transfer RNA. *Proceedings of the National Academy of Sciences of the United States of America*, *90*(14), 6776–80. Retrieved from <http://www.ncbi.nlm.nih.gov/pubmed/8341698>
- Huang, B., Johansson, M. J. O., & Byström, A. S. (2005). An early step in wobble uridine tRNA modification requires the Elongator complex. *RNA (New York, N.Y.)*, *11*(4), 424–36. <http://doi.org/10.1261/rna.7247705>
- Ibba, M., & Soll, D. (2001). The renaissance of aminoacyl-tRNA synthesis. *EMBO Reports*, *2*(5), 382–387. <http://doi.org/10.1093/embo-reports/kve095>
- Ibba, M., & Söll, D. (2004). Aminoacyl-tRNAs: setting the limits of the genetic code. *Genes & Development*, *18*(7), 731–8. <http://doi.org/10.1101/gad.1187404>
- Iizuka, N., Najita, L., Franzusoff, a, & Sarnow, P. (1994). Cap-dependent and cap-independent translation by internal initiation of mRNAs in cell extracts prepared from *Saccharomyces cerevisiae*. *Molecular and Cellular Biology*, *14*(11), 7322–7330. <http://doi.org/10.1128/MCB.14.11.7322>. Updated
- Ikemura, T. (1981). Correlation between the abundance of *Escherichia coli* transfer RNAs and the occurrence of the respective codons in its protein genes. *Journal of Molecular Biology*, *146*(1), 1–21. Retrieved from <http://www.ncbi.nlm.nih.gov/pubmed/6167728>
- Ishiguro, J., Ono, B. I., Masurekar, M., McLaughlin, C. S., & Sherman, F. (1981). Altered ribosomal protein S11 from the SUP46 suppressor of yeast. *Journal of Molecular Biology*, *147*(3), 391–397. [http://doi.org/10.1016/0022-2836\(81\)90491-5](http://doi.org/10.1016/0022-2836(81)90491-5)
- Ito, K., Ebihara, K., Uno, M., & Nakamura, Y. (1996). Conserved motifs in prokaryotic and eukaryotic polypeptide release factors: tRNA-protein mimicry hypothesis. *Proceedings of the National Academy of Sciences of the United States of America*, *93*(11), 5443–5448. <http://doi.org/10.1073/pnas.93.11.5443>
- Jackson, R. J. (2013). The current status of vertebrate cellular mRNA IRESs. *Cold Spring Harbor Perspectives in Biology*, *5*(2). <http://doi.org/10.1101/cshperspect.a011569>
- Jackson, R. J., Hellen, C. U. T., & Pestova, T. V. (2010). The mechanism of eukaryotic translation

- initiation and principles of its regulation. *Nature Reviews Molecular Cell Biology*, 11(2), 113–127. <http://doi.org/10.1038/nrm2838>
- Jainchill, J. L., Aaronson, S. A., & Todaro, G. J. (1969). Murine sarcoma and leukemia viruses: assay using clonal lines of contact-inhibited mouse cells. *Journal of Virology*, 4(5), 549–53. Retrieved from <http://www.ncbi.nlm.nih.gov/pubmed/4311790>
- Jakubowski, H. (1999). Misacylation of tRNA(Lys) with noncognate amino acids by Lysyl-tRNA synthetase. *Biochemistry*, 38(25), 8088–8093. <http://doi.org/10.1021/bi990629i>
- Jenner, L. B., Demeshkina, N., Yusupova, G., & Yusupov, M. (2010). Structural aspects of messenger RNA reading frame maintenance by the ribosome. *Nature Structural & Molecular Biology*, 17(5), 555–560. <http://doi.org/10.1038/nsmb.1790>
- Jenner, L., Demeshkina, N., Yusupova, G., & Yusupov, M. (2010). Structural rearrangements of the ribosome at the tRNA proofreading step. *Nature Structural & Molecular Biology*, 17(9), 1072–1078. <http://doi.org/10.1038/nsmb.1880>
- Johansson, M. J. O., Esberg, A., Huang, B., Bjork, G. R., & Bystrom, A. S. (2008). Eukaryotic Wobble Uridine Modifications Promote a Functionally Redundant Decoding System. *Molecular and Cellular Biology*, 28(10), 3301–3312. <http://doi.org/10.1128/MCB.01542-07>
- Johnson, R. E., Washington, M. T., Prakash, S., & Prakash, L. (2000). Fidelity of human DNA polymerase η . *The Journal of Biological Chemistry*, 275(11), 7447–50. <http://doi.org/10.1074/jbc.275.11.7447>
- Jørgensen, F., & Kurland, C. G. (1990). Processivity errors of gene expression in Escherichia coli. *Journal of Molecular Biology*, 215(4), 511–21. [http://doi.org/10.1016/S0022-2836\(05\)80164-0](http://doi.org/10.1016/S0022-2836(05)80164-0)
- Juers, D. H., Matthews, B. W., & Huber, R. E. (2012). LacZ β -galactosidase: structure and function of an enzyme of historical and molecular biological importance. *Protein Science: A Publication of the Protein Society*, 21(12), 1792–807. <http://doi.org/10.1002/pro.2165>
- Kalhor, H. R., & Clarke, S. (2003). Novel methyltransferase for modified uridine residues at the wobble position of tRNA. *Molecular and Cellular Biology*, 23(24), 9283–9292. <http://doi.org/10.1128/MCB.23.24.9283-9292.2003>
- Kapp, L. D., & Lorsch, J. R. (2004). The molecular mechanics of eukaryotic translation. *Annu. Rev. Biochem.*, 73, 657–704. <http://doi.org/10.1146/annurev.biochem.73.030403.080419>
- Karlsborn, T., Tükenmez, H., Mahmud, A. K. M. F., Xu, F., Xu, H., & Byström, A. S. (2014). Elongator, a conserved complex required for wobble uridine modifications in eukaryotes. *RNA Biology*, 11(12), 1519–28. <http://doi.org/10.4161/15476286.2014.992276>
- Kaul, G., Pattan, G., & Rafeequi, T. (2011). Eukaryotic elongation factor-2 (eEF2): Its regulation and peptide chain elongation. *Cell Biochemistry and Function*, 29(3), 227–234. <http://doi.org/10.1002/cbf.1740>

- Khatter, H., Myasnikov, A. G., Natchiar, S. K., & Klaholz, B. P. (2015). Structure of the human 80S ribosome. *Nature*, *520*(7549), 640–645. <http://doi.org/10.1038/nature14427>
- Khoshnevis, S., Gross, T., Rotte, C., Baierlein, C., Ficner, R., & Krebber, H. (2010). The iron–sulphur protein RNase L inhibitor functions in translation termination. *EMBO Reports*, *11*(3), 214–219. <http://doi.org/10.1038/embor.2009.272>
- Kim, S., Quigley, G., Suddath, F., & McPherson, A. (1972). The Three-Dimensional Structure of Yeast Phenylalanine Transfer RNA: Shape of the. *Proceedings of the National Academy of Sciences*, *69*(12), 3746–3750. Retrieved from <http://www.jstor.org/stable/1735681>
- Kimball, S. R. (1999). Eukaryotic initiation factor eIF2. *The International Journal of Biochemistry & Cell Biology*, *31*(1), 25–29. [http://doi.org/10.1016/S1357-2725\(98\)00128-9](http://doi.org/10.1016/S1357-2725(98)00128-9)
- Kisselev, L. (2003). NEW EMBO MEMBER’S REVIEW: Termination of translation: interplay of mRNA, rRNAs and release factors? *The EMBO Journal*, *22*(2), 175–182. <http://doi.org/10.1093/emboj/cdg017>
- Klassen, R., Ciftci, A., Funk, J., Bruch, A., Butter, F., & Schaffrath, R. (2016). TRNA anticodon loop modifications ensure protein homeostasis and cell morphogenesis in yeast. *Nucleic Acids Research*, *44*(22), 10946–10959. <http://doi.org/10.1093/nar/gkw705>
- Klassen, R., & Schaffrath, R. (2017). Role of Pseudouridine Formation by Deg1 for Functionality of Two Glutamine Isoacceptor tRNAs. *Biomolecules*, *7*(1). <http://doi.org/10.3390/biom7010008>
- Klinge, S., Voigts-Hoffmann, F., Leibundgut, M., Arpagaus, S., & Ban, N. (2011). Crystal structure of the eukaryotic 60S ribosomal subunit in complex with initiation factor 6. *Science (New York, N.Y.)*, *334*(6058), 941–8. <http://doi.org/10.1126/science.1211204>
- Klinge, S., Voigts-Hoffmann, F., Leibundgut, M., Ban, N., Ramakrishnan, V., Schmeing, T. M., ... al., et. (2012). Atomic structures of the eukaryotic ribosome. *Trends in Biochemical Sciences*, *37*(5), 189–98. <http://doi.org/10.1016/j.tibs.2012.02.007>
- Knudsen, C., Wieden, H. J., & Rodnina, M. V. (2001). The Importance of Structural Transitions of the Switch II Region for the Functions of Elongation Factor Tu on the Ribosome. *Journal of Biological Chemistry*, *276*(25), 22183–22190. <http://doi.org/10.1074/jbc.M102186200>
- Kobayashi, T., Irie, T., Yoshida, M., Takeishi, K., & Ukita, T. (1974). The primary structure of yeast glutamic acid tRNA specific to the GAA codon. *Biochimica et Biophysica Acta (BBA) - Nucleic Acids and Protein Synthesis*, *366*(2), 168–181. [http://doi.org/10.1016/0005-2787\(74\)90331-1](http://doi.org/10.1016/0005-2787(74)90331-1)
- Kochupurakkal, B. S., & Iglehart, J. D. (2013). Nourseothricin N-acetyl transferase: a positive selection marker for mammalian cells. *PloS One*, *8*(7), e68509. <http://doi.org/10.1371/journal.pone.0068509>
- Kolosov, P., Frolova, L., Seit-Nebi, A., Dubovaya, V., Kononenko, A., Oparina, N., ... Kisselev,

- L. (2005). Invariant amino acids essential for decoding function of polypeptide release factor eRF1. *Nucleic Acids Research*, 33(19), 6418–6425. <http://doi.org/10.1093/nar/gki927>
- Konecki, D. S., Aune, K. C., Tate, W., & Caskey, C. T. (1977). Characterization of reticulocyte release factor. *Journal of Biological Chemistry*, 252(13), 4514–4520.
- Kong, J., & Lasko, P. (2012). Translational control in cellular and developmental processes. *Nature Reviews Genetics*, 13(6), 383–394. <http://doi.org/10.1038/nrg3184>
- Kononenko, A. V., Mitkevich, V. A., Dubovaya, V. I., Kolosov, P. M., Makarov, A. A., & Kisselev, L. L. (2008). Role of the individual domains of translation termination factor eRF1 in GTP binding to eRF3. *Proteins: Structure, Function and Genetics*, 70(2), 388–393. <http://doi.org/10.1002/prot.21544>
- Kozak, M. (1991). Structural features in eukaryotic mRNAs that modulate the initiation of translation. *The Journal of Biological Chemistry*, 266(30), 19867–70. Retrieved from <http://www.ncbi.nlm.nih.gov/pubmed/1939050>
- Kramer, E. B., & Farabaugh, P. J. (2007). The frequency of translational misreading errors in *E. coli* is largely determined by tRNA competition. *RNA (New York, N.Y.)*, 13(1), 87–96. <http://doi.org/10.1261/rna.294907>
- Kramer, E. B., Vallabhaneni, H., Mayer, L. M., & Farabaugh, P. J. (2010). A comprehensive analysis of translational missense errors in the yeast *Saccharomyces cerevisiae*. *RNA (New York, N.Y.)*, 16(9), 1797–808. <http://doi.org/10.1261/rna.2201210>
- Krüger, M. K., Pedersen, S., Hagervall, T. G., & Sørensen, M. A. (1998). The modification of the wobble base of tRNA^{Glu} modulates the translation rate of glutamic acid codons in vivo. *Journal of Molecular Biology*, 284(3), 621–631. <http://doi.org/10.1006/jmbi.1998.2196>
- Kumar, R. K., & Davis, D. R. (1997). Synthesis and studies on the effect of 2-thiouridine and 4-thiouridine on sugar conformation and RNA duplex stability. *Nucleic Acids Research*, 25(6), 1272–80. Retrieved from <http://www.ncbi.nlm.nih.gov/pubmed/9092639>
- Kuntzel, B., Weissenbach, J., Wolff, R. E., Tumaitis-Kennedy, T. D., Lane, B. G., & Dirheimer, G. (1975). Presence of the methylester of 5-carboxymethyl uridine in the wobble position of the anticodon of tRNA^{III} Arg from brewer's yeast. *Biochimie*, 57(1), 61–70. Retrieved from <http://www.ncbi.nlm.nih.gov/pubmed/167871>
- Kurland, C. G. (1992). Translational accuracy and the fitness of bacteria. *Annual Review of Genetics*, 26(81), 29–50. <http://doi.org/10.1146/annurev.ge.26.120192.000333>
- Kurtz, D. (1975). The effect of ageing on in vitro fidelity of translation in mouse liver. *Biochimica et Biophysica Acta (BBA) Report*, 407, 479–484. Retrieved from <http://www.sciencedirect.com/science/article/pii/0005278775903020>
- Laurberg, M., Asahara, H., Korostelev, A., Zhu, J., Trakhanov, S., & Noller, H. F. (2008). Structural basis for translation termination on the 70S ribosome. *Nature*, 454(7206), 852–857.

<http://doi.org/10.1038/nature07115>

- Le Goff, X., Philippe, M., & Jean-Jean, O. (1997). Overexpression of human release factor 1 alone has an antisuppressor effect in human cells. *Molecular and Cellular Biology*, *17*(6), 3164–3172.
- Lecoite, F., Simos, G., Sauer, A., Hurt, E. C., Motorin, Y., & Grosjean, H. (1998). Characterization of Yeast Protein Deg1 as Pseudouridine Synthase (Pus3) Catalyzing the Formation of 38 and 39 in tRNA Anticodon Loop. *Journal of Biological Chemistry*, *273*(3), 1316–1323. <http://doi.org/10.1074/jbc.273.3.1316>
- Lee, J. W., Beebe, K., Nangle, L. A., Jang, J., Longo-Guess, C. M., Cook, S. A., ... Ackerman, S. L. (2006). Editing-defective tRNA synthetase causes protein misfolding and neurodegeneration. *Nature*, *443*(7107), 50–5. <http://doi.org/10.1038/nature05096>
- Lefebvre, A. K., Korneeva, N. L., Trutschl, M., Cvek, U., Duzan, R. D., Bradley, C. A., ... Rhoads, R. E. (2006). Translation initiation factor eIF4G-1 binds to eIF3 through the eIF3e subunit. *Journal of Biological Chemistry*, *281*(32), 22917–22932. <http://doi.org/10.1074/jbc.M605418200>
- Leidel, S., Pedrioli, P. G. A., Bucher, T., Brost, R., Costanzo, M., Schmidt, A., ... Peter, M. (2009). Ubiquitin-related modifier Urm1 acts as a sulphur carrier in thiolation of eukaryotic transfer RNA. *Nature*, *458*(7235), 228–232. <http://doi.org/10.1038/nature07643>
- Létoquart, J., van Tran, N., Caroline, V., Aleksandrov, A., Lazar, N., van Tilbeurgh, H., ... Graille, M. (2015). Insights into molecular plasticity in protein complexes from Trm9-Trm112 tRNA modifying enzyme crystal structure. *Nucleic Acids Research*, *43*(22), 10989–11002. <http://doi.org/10.1093/nar/gkv1009>
- Leyne, M., Mull, J., Gill, S. P., Cuajungco, M. P., Oddoux, C., Blumenfeld, A., ... Slaugenhaupt, S. A. (2003). Identification of the first non-Jewish mutation in familial Dysautonomia. *American Journal of Medical Genetics. Part A*, *118A*(4), 305–308. <http://doi.org/10.1002/ajmg.a.20052>
- Libby, R. T., & Gallant, J. A. (1991). The role of RNA polymerase in transcriptional fidelity. *Molecular Microbiology*. <http://doi.org/10.1111/j.1365-2958.1991.tb01872.x>
- Lim, V. I. (1994). Analysis of action of wobble nucleoside modification on Codon-anticodon pairing within the ribosome. *Journal of Molecular Biology*, *240*(1), 8–19. <http://doi.org/10.1006/jmbi.1994.1413>
- Ling, J., So, B. R., Yadavalli, S. S., Roy, H., Shoji, S., Fredrick, K., ... Ibba, M. (2009). Resampling and Editing of Mischarged tRNA Prior to Translation Elongation. *Molecular Cell*, *33*(5), 654–660. <http://doi.org/10.1016/j.molcel.2009.01.031>
- Lofffield, R. B., & Vanderjagt, D. (1972). The frequency of errors in protein biosynthesis. *The Biochemical Journal*, *128*(5), 1353–6. Retrieved from <http://www.ncbi.nlm.nih.gov/pubmed/4643706>

- Lorenz, W. W., McCann, R. O., Longiaru, M., & Cormier, M. J. (1991). Isolation and expression of a cDNA encoding *Renilla reniformis* luciferase. *Proceedings of the National Academy of Sciences of the United States of America*, 88(10), 4438–42. <http://doi.org/10.1073/pnas.88.10.4438>
- Lovmar, M., & Ehrenberg, M. (2006). Rate, accuracy and cost of ribosomes in bacterial cells. *Biochimie*, 88(8), 951–61. <http://doi.org/10.1016/j.biochi.2006.04.019>
- Lu, J., Huang, B., Esberg, A., Johansson, M. J. O., & Byström, A. S. (2005). The *Kluyveromyces lactis* gamma-toxin targets tRNA anticodons. *RNA*, 11(11), 1648–1654. <http://doi.org/10.1261/rna.2172105>
- Luce, M., & Bunn, C. (1989). Decreased accuracy of protein synthesis in extracts from aging human diploid fibroblasts. *Experimental Gerontology*, 24, 113–125. Retrieved from <http://www.sciencedirect.com/science/article/pii/0531556589900223>
- Lyko, F., & Tuorto, F. (2016). Genome recoding by tRNA modifications. <http://doi.org/10.1098/rsob.160287>
- Maag, D., Fekete, C. A., Gryczynski, Z., & Lorsch, J. R. (2005). A conformational change in the eukaryotic translation preinitiation complex and release of eIF1 signal recognition of the start codon. *Molecular Cell*, 17(2), 265–275. <http://doi.org/10.1016/j.molcel.2004.11.051>
- Majumdar, R., Chaudhuri, J., & Maitra, U. (2007). Reconstitution of Mammalian 48S Ribosomal Translation Initiation Complex. *Methods in Enzymology*. [http://doi.org/10.1016/S0076-6879\(07\)30008-6](http://doi.org/10.1016/S0076-6879(07)30008-6)
- Manickam, N., Joshi, K., Bhatt, M. J., & Farabaugh, P. J. (2016). Effects of tRNA modification on translational accuracy depend on intrinsic codon-anticodon strength. *Nucleic Acids Research*, 44(4), 1871–81. <http://doi.org/10.1093/nar/gkv1506>
- Manickam, N., Nag, N., Abbasi, A., Patel, K., & Farabaugh, P. J. (2014). Studies of translational misreading in vivo show that the ribosome very efficiently discriminates against most potential errors. *RNA (New York, N.Y.)*, 20(1), 9–15. <http://doi.org/10.1261/rna.039792.113>
- Manuvakhova, M., Keeling, K., & Bedwell, D. M. (2000). Aminoglycoside antibiotics mediate context-dependent suppression of termination codons in a mammalian translation system. *RNA*, 6(7), 1044–1055. Retrieved from <http://rnajournal.cshlp.org/content/6/7/1044.short>
- Marina V. Rodnina, Andreas Savelsbergh, V. I. K. & W. W. (1997). Hydrolysis of GTP by elongation factor G drives tRNA movement on the ribosome. *Nature*, 385(6611), 37–41. <http://doi.org/10.1038/385037a0>
- Marintchev, A., & Wagner, G. (2004). Translation initiation: structures, mechanisms and evolution. *Quarterly Reviews of Biophysics*, 37(3–4), 197–284. <http://doi.org/10.1017/S0033583505004026>
- Martin, R., Mogg, A. E., Heywood, L. A., Nitschke, L., & Burke, J. F. (1989). Aminoglycoside

- suppression at UAG, UAA and UGA codons in *Escherichia coli* and human tissue culture cells. *MGG Molecular & General Genetics*, 217(2–3), 411–418. <http://doi.org/10.1007/BF02464911>
- Martinis, S. A., & Boniecki, M. T. (2010, January 21). The balance between pre- and post-transfer editing in tRNA synthetases. *FEBS Letters*. <http://doi.org/10.1016/j.febslet.2009.11.071>
- Matthews, J. C., Hori, K., & Cormier, M. J. (1977). Purification and Properties of *Renilla reniformis* Luciferase. *Biochemistry*, 16(1), 85–91. <http://doi.org/10.1021/bi00620a014>
- McClain, W. H., & Foss, K. (1988). Changing the identity of a tRNA by introducing a G-U wobble pair near the 3' acceptor end. *Science (New York, N.Y.)*, 240(4853), 793–6. Retrieved from <http://www.ncbi.nlm.nih.gov/pubmed/2452483>
- Melnikov, S., Ben-Shem, A., Garreau de Loubresse, N., Jenner, L., Yusupova, G., & Yusupov, M. (2012). One core, two shells: bacterial and eukaryotic ribosomes. *Nature Structural & Molecular Biology*, 19(6), 560–7. <http://doi.org/10.1038/nsmb.2313>
- Menninger, J. R. (1976). Peptidyl transfer RNA dissociates during protein synthesis from ribosomes of *Escherichia coli*. *The Journal of Biological Chemistry*, 251(11), 3392–8. Retrieved from <http://www.ncbi.nlm.nih.gov/pubmed/776968>
- Merkulova, T. I., Frolova, L. Y., Lazar, M., Camonis, J., & Kisselev, L. L. (1999). C-terminal domains of human translation termination factors eRF1 and eRF3 mediate their in vivo interaction. *FEBS Letters*, 443(1), 41–47. [http://doi.org/10.1016/S0014-5793\(98\)01669-X](http://doi.org/10.1016/S0014-5793(98)01669-X)
- Merrick, W. C. (2004). Cap-dependent and cap-independent translation in eukaryotic systems. *Gene*. <http://doi.org/10.1016/j.gene.2004.02.051>
- Moazed, D., & Noller, H. F. (1987). Chloramphenicol, erythromycin, carbomycin and vernamycin B protect overlapping sites in the peptidyl transferase region of 23S ribosomal RNA. *Biochimie*, 69(8), 879–884. [http://doi.org/10.1016/0300-9084\(87\)90215-X](http://doi.org/10.1016/0300-9084(87)90215-X)
- Moazed, D., & Noller, H. F. (1989). Interaction of tRNA with 23S rRNA in the ribosomal A, P, and E sites. *Cell*, 57(4), 585–597. [http://doi.org/10.1016/0092-8674\(89\)90128-1](http://doi.org/10.1016/0092-8674(89)90128-1)
- Moazed, D., & Noller, H. F. (1989). Intermediate states in the movement of transfer RNA in the ribosome. *Nature*, 342(6246), 142–8. <http://doi.org/10.1038/342142a0>
- Mohr, D., Wintermeyer, W., & Rodnina, M. V. (2002). GTPase activation of elongation factors Tu and G on the ribosome. *Biochemistry*, 41(41), 12520–12528. <http://doi.org/10.1021/bi026301y>
- Moore, P. B., & Steitz, T. A. (2003). After the ribosome structures: how does peptidyl transferase work? *RNA (New York, N.Y.)*, 9(2), 155–159. <http://doi.org/10.1261/rna.2127103.RNA>
- Moore, V. G., Atchison, R. E., Thomas, G., Moran, M., & Noller, H. F. (1975). Identification of a ribosomal protein essential for peptidyl transferase activity. *Proceedings of the National*

- Academy of Sciences of the United States of America*, 72(3), 844–8. Retrieved from <http://www.ncbi.nlm.nih.gov/pubmed/1055382>
- Mori, N., Funatsu, Y., Hiruta, K., & Goto, S. (1985). Analysis of translational fidelity of ribosomes with protamine messenger RNA as a template. *Biochemistry*. Retrieved from <http://pubs.acs.org/doi/abs/10.1021/bi00326a027>
- Munro, J. B., Altman, R. B., O'Connor, N., & Blanchard, S. C. (2007). Identification of Two Distinct Hybrid State Intermediates on the Ribosome. *Molecular Cell*, 25(4), 505–517. <http://doi.org/10.1016/j.molcel.2007.01.022>
- Muramatsu, T., Nishikawa, K., Nemoto, F., Kuchino, Y., Nishimura, S., Miyazawa, T., & Yokoyama, S. (1988). Codon and amino-acid specificities of a transfer RNA are both converted by a single post-transcriptional modification. *Nature*, 336(6195), 179–181. <http://doi.org/10.1038/336179a0>
- Murphy Iv, F. V, Ramakrishnan, V., Malkiewicz, A., & Agris, P. F. (2004). The role of modifications in codon discrimination by tRNA Lys UUU. *NATURE STRUCTURAL & MOLECULAR BIOLOGY*, 11(12). <http://doi.org/10.1038/nsmb861>
- Newcombe, H. B., & Nyholm, M. H. (1950). The inheritance of streptomycin resistance and dependence in crosses of *Escherichia coli*. *Genetics*, 35(6), 603–11. Retrieved from <http://www.pubmedcentral.nih.gov/articlerender.fcgi?artid=1224325&tool=pmcentrez&rendertype=abstract>
- Nguyen, L., Humbert, S., Saudou, F., & Chariot, A. (2010). Elongator - an emerging role in neurological disorders. *Trends in Molecular Medicine*, 16(1), 1–6. <http://doi.org/10.1016/j.molmed.2009.11.002>
- Nierhaus, K. H., & Montejó, V. (1973). A protein involved in the peptidyltransferase activity of *Escherichia coli* ribosomes. *Proceedings of the National Academy of Sciences of the United States of America*, 70(7), 1931–5. Retrieved from <http://www.pubmedcentral.nih.gov/articlerender.fcgi?artid=433635&tool=pmcentrez&rendertype=abstract>
- Nilsson, K., Jäger, G., Björk, G. R., Tanaka, N., Sugawara, H., & Nishikawa, K. (2017). An unmodified wobble uridine in tRNAs specific for Glutamine, Lysine, and Glutamic acid from *Salmonella enterica* Serovar Typhimurium results in nonviability—Due to increased missense errors? *Plos One*, 12(4), e0175092. <http://doi.org/10.1371/journal.pone.0175092>
- Ninio, J. (1975). Kinetic amplification of enzyme discrimination. *Biochimie*, 57(5), 587–95. Retrieved from <http://www.ncbi.nlm.nih.gov/pubmed/1182215>
- Nirenberg, M., & Leder, P. (1964). RNA Codewords and Protein Synthesis. *Science*, 145(3639), 1399–1407. <http://doi.org/10.1073/pnas.53.5.1161>
- Nirenberg, M., Leder, P., Bernfield, M., Brimacombe, R., Trupin, J., Rottman, F., & O'Neal, C. (1965). RNA codewords and protein synthesis, VII. On the general nature of the RNA code.

- Proceedings of the National Academy of Sciences of the United States of America*, 53(5), 1161–8. Retrieved from <http://www.ncbi.nlm.nih.gov/pubmed/5330357>
- Nirenberg, M. W., & Matthaei, J. H. H. (1961). The dependence of cell-free protein synthesis in *E. coli* upon naturally occurring or synthetic polyribonucleotides. *Proceedings of the National Academy of Sciences of the United States of America*, 47(10), 1588–602. <http://doi.org/10.1021/ja7114579>
- Nishimura, S., Jones, D. S., & Khorana, H. G. (1965). Studies on polynucleotides. 48. The in vitro synthesis of a co-polypeptide containing two amino acids in alternating sequence dependent upon a DNA-like polymer containing two nucleotides in alternating sequence. *Journal of Molecular Biology*, 13(1), 302–24. Retrieved from <http://www.ncbi.nlm.nih.gov/pubmed/5323614>
- Nissen, P. (2000). The Structural Basis of Ribosome Activity in Peptide Bond Synthesis. *Science*, 289(5481), 920–930. <http://doi.org/10.1126/science.289.5481.920>
- Nissen, P., Hansen, J., Ban, N., Moore, P. B., Steitz, T. A., Nissen, P., ... Steitz, T. A. (2000). The Structural Basis of Ribosome Activity in Peptide Bond Synthesis, 289(5481), 920–930.
- Noller, H. F. (1991). Ribosomal RNA and translation. *Annual Review of Biochemistry*, 60, 191–227. <http://doi.org/10.1146/annurev.bi.60.070191.001203>
- Noller, H. F. (2005). RNA structure: Reading the ribosome. *Science*, 306(5702), 1783–1786.
- Noller, H. F. (2006). Biochemical characterization of the ribosomal decoding site. *Biochimie*, 88(8), 935–41. <http://doi.org/10.1016/j.biochi.2006.04.006>
- Noller, H. F., & Chaires, J. B. (1972). Functional modification of 16S ribosomal RNA by kethoxal. *Proceedings of the National Academy of Sciences of the United States of America*, 69(11), 3115–3118. <http://doi.org/10.1073/pnas.69.11.3115>
- Noller, H. F., Hoffarth, V., & Zimniak, L. (1992). Unusual Resistance of Peptidyl Transferase to Protein Extraction Procedures. *Source: Science, New Series Transplant. Bull. Ann. Surg. Br. Med. J*, 256(4), 1416–1419. <http://doi.org/10.1126/science.1604315>
- Noller, H. F., Yusupov, M. M., Yusupova, G. Z., Baucom, A., & Cate, J. H. D. (2002). Translocation of tRNA during protein synthesis. *FEBS Letters*, 514(1), 11–16. [http://doi.org/10.1016/S0014-5793\(02\)02327-X](http://doi.org/10.1016/S0014-5793(02)02327-X)
- Noma, A., Sakaguchi, Y., & Suzuki, T. (2009). Mechanistic characterization of the sulfur-relay system for eukaryotic 2-thiouridine biogenesis at tRNA wobble positions. *Nucleic Acids Research*, 37(4), 1335–52. <http://doi.org/10.1093/nar/gkn1023>
- Nureki, O., Niimi, T., Muramatsu, T., Kanno, H., Kohno, T., Florentz, C., ... Yokoyama, S. (1994). Molecular Recognition of the Identity-determinant Set of Isoleucine Transfer RNA from *Escherichia coli*. *Journal of Molecular Biology*, 236(3), 710–724. <http://doi.org/10.1006/jmbi.1994.1184>

- Nürenberg, E., & Tampé, R. (2013). Tying up loose ends: Ribosome recycling in eukaryotes and archaea. *Trends in Biochemical Sciences*. <http://doi.org/10.1016/j.tibs.2012.11.003>
- Ogle, J. M., Brodersen, D. E., Clemons, W. M., Tarry, M. J., Carter, A. P., & Ramakrishnan, V. (2001). Recognition of cognate transfer RNA by the 30S ribosomal subunit. *Science (New York, N.Y.)*, *292*(5518), 897–902. <http://doi.org/10.1126/science.1060612>
- Ogle, J. M., Carter, A. P., & Ramakrishnan, V. (2003). Insights into the decoding mechanism from recent ribosome structures. *Trends in Biochemical Sciences*, *28*(5), 259–66. [http://doi.org/10.1016/S0968-0004\(03\)00066-5](http://doi.org/10.1016/S0968-0004(03)00066-5)
- Ogle, J. M., Murphy, F. V., Tarry, M. J., & Ramakrishnan, V. (2002). Selection of tRNA by the ribosome requires a transition from an open to a closed form. *Cell*, *111*(5), 721–32. Retrieved from <http://www.ncbi.nlm.nih.gov/pubmed/12464183>
- Ogle, J. M., & Ramakrishnan, V. (2005). Structural insights into translational fidelity. *Annual Review of Biochemistry*, *74*(1), 129–77. <http://doi.org/10.1146/annurev.biochem.74.061903.155440>
- Olsson, M. O., & Isaksson, L. A. (1980). Analysis of rpsD mutations in Escherichia coli - IV. Accumulation of minor forms of protein S7(K) in ribosomes of rpsD mutant strains due to translational read-through. *MGG Molecular & General Genetics*, *177*(3), 485–491. <http://doi.org/10.1007/BF00271488>
- Ozaki, M., Mizushima, S., & Nomura, M. (1969). Identification and functional characterization of the protein controlled by the Streptomycin-resistant locus in E. coli. *Nature*, *222*(5191), 333–339. <http://doi.org/10.1038/222333a0>
- PALMER, E., WILHELM, J. M., SHERMAN, F., & EDWARD PALMER, J. M. W. & F. S. (1979). Phenotypic suppression of nonsense mutants in yeast by aminoglycoside antibiotics. *Nature*, *277*(5692), 148–150. <http://doi.org/10.1038/277148a0>
- Pang, Y. L. J., Poruri, K., & Martinis, S. A. (2014). tRNA synthetase: tRNA aminoacylation and beyond. *Wiley Interdisciplinary Reviews: RNA*, *5*(4), 461–480. <http://doi.org/10.1002/wrna.1224>
- Pape, T., Wintermeyer, W., & Rodnina, M. (1999). Induced fit in initial selection and proofreading of aminoacyl-tRNA on the ribosome. *The European Molecular Biology Organization Journal*, *18*(13), 3800–3807. Retrieved from <http://www.pubmedcentral.nih.gov/articlerender.fcgi?artid=1171457&tool=pmcentrez&rendertype=abstract>
- Pape, T., Wintermeyer, W., & Rodnina, M. V. (1998). Complete kinetic mechanism of elongation factor Tu-dependent binding of aminoacyl-tRNA to the A site of the E. coli ribosome. *The EMBO Journal*, *17*(24), 7490–7. <http://doi.org/10.1093/emboj/17.24.7490>
- Pape, T., Wintermeyer, W., & Rodnina, M. V. (2000). Conformational switch in the decoding region of 16S rRNA during aminoacyl-tRNA selection on the ribosome. *Nature Structural*

Biology, 7(2), 104–107. <http://doi.org/10.1038/72364>

- Parker, J., Johnston, T. C., Borgiag, P. T., Holtz, G., Remaut, E., & Fiersli, W. (1983). Codon Usage and Mistranslation IN VIVO BASAL LEVEL MISREADING OF THE MS2 COAT PROTEIN MESSAGE*. *THE JOURNAL OF BIOLOGICAL CHEMISTRY*, 258(16), 1–7. Retrieved from <http://www.jbc.org/content/258/16/10007.full.pdf>
- Parker, J. (1989). Errors and alternatives in reading the universal genetic code. *Microbiological Reviews*, 53(3), 273–98. Retrieved from <http://www.pubmedcentral.nih.gov/articlerender.fcgi?artid=372737&tool=pmcentrez&rendertype=abstract>
- Parker, J. (1992). Variations in reading the genetic code. In *Transfer RNA in Protein Synthesis* (pp. 191–267).
- Parker, J., & Friesen, J. D. (1980). “Two out of three” codon reading leading to mistranslation in vivo. *Molecular & General Genetics : MGG*, 177(3), 439–45. Retrieved from <http://www.ncbi.nlm.nih.gov/pubmed/6768967>
- Parker, J., & Holtz, G. (1984). Control of basal-level codon misreading in *Escherichia coli*. *Biochemical and Biophysical Research Communications*, 121(2), 487–92. Retrieved from <http://www.ncbi.nlm.nih.gov/pubmed/6375672>
- Parker, J., Pollard, J. W., Friesen, J. D., & Stanners, C. P. (1978). Stuttering: high-level mistranslation in animal and bacterial cells. *Proceedings of the ...*, 75(3), 1091–1095. Retrieved from <http://www.pubmedcentral.nih.gov/articlerender.fcgi?artid=411414&tool=pmcentrez&rendertype=abstract>
- Patil, A., Chan, C. T. Y., Dyavaiah, M., Rooney, J. P., Dedon, P. C., & Begley, T. J. (2012). Translational infidelity-induced protein stress results from a deficiency in Trm9-catalyzed tRNA modifications. *RNA Biology*, 9(7), 990–1001. <http://doi.org/10.4161/rna.20531>
- Paulin, F. E., Campbell, L. E., O’Brien, K., Loughlin, J., & Proud, C. G. (2001). Eukaryotic translation initiation factor 5 (eIF5) acts as a classical GTPase-activator protein. *Current Biology*, 11(1), 55–59. [http://doi.org/10.1016/S0960-9822\(00\)00025-7](http://doi.org/10.1016/S0960-9822(00)00025-7)
- Pel, H. J., Moffat, J. G., Ito, K., Nakamura, Y., & Tate, W. P. (1998). *Escherichia coli* release factor 3: resolving the paradox of a typical G protein structure and atypical function with guanine nucleotides. *RNA (New York, N.Y.)*, 4(1), 47–54.
- Percudani, R. (2001). Restricted wobble rules for eukaryotic genomes. *Trends in Genetics : TIG*, 17(3), 133–135. [http://doi.org/10.1016/S0168-9525\(00\)02208-3](http://doi.org/10.1016/S0168-9525(00)02208-3)
- Persson, B. C. (1993). Modification of tRNA as a regulatory device. *Molecular Microbiology*, 8(6), 1011–1016. <http://doi.org/10.1111/j.1365-2958.1993.tb01645.x>
- Peske, F., Rodnina, M. V., & Wintermeyer, W. (2005). Sequence of steps in ribosome recycling

- as defined by kinetic analysis. *Molecular Cell*, 18(4), 403–412. <http://doi.org/10.1016/j.molcel.2005.04.009>
- Pestova, T. V., & Kolupaeva, V. G. (2002). The roles of individual eukaryotic translation initiation factors in ribosomal scanning and initiation codon selection. *Genes and Development*, 16(22), 2906–2922. <http://doi.org/10.1101/gad.1020902>
- Pestova, T. V., Lorsch, J. R., & Hellen, C. U. T. (2007). The Mechanism of Translation Initiation in Eukaryotes. In M. B. Mathews, N. Sonenberg, & J. W. B. Hershey (Eds.), *Translational Control in Biology and Medicine* (pp. 87–128). Cold Spring Harbor Laboratory Press, New York.
- Phillips-Jones, M. K., Hill, L. S., Atkinson, J., & Martin, R. (1995). Context effects on misreading and suppression at UAG codons in human cells. *Molecular and Cellular Biology*, 15(12), 6593–6600. Retrieved from <http://www.pubmedcentral.nih.gov/articlerender.fcgi?artid=230912&tool=pmcentrez&rendertype=abstract>
- Phizicky, E. M., & Alfonzo, J. D. (2010). Do all modifications benefit all tRNAs? *FEBS Letters*, 584(2), 265–71. <http://doi.org/10.1016/j.febslet.2009.11.049>
- Phizicky, E. M., & Hopper, A. K. (2010). tRNA biology charges to the front. *Genes & Development*, 24(17), 1832–60. <http://doi.org/10.1101/gad.1956510>
- Phizicky, E. M., & Hopper, A. K. (2015). tRNA processing, modification, and subcellular dynamics: past, present, and future. *RNA (New York, N.Y.)*, 21(4), 483–5. <http://doi.org/10.1261/rna.049932.115>
- Pisarev, A. V., Skabkin, M. A., Pisareva, V. P., Skabkina, O. V., Rakotondrafara, A. M., Hentze, M. W., ... Pestova, T. V. (2010). The Role of ABCE1 in Eukaryotic Posttermination Ribosomal Recycling. *Molecular Cell*, 37(2), 196–210. <http://doi.org/10.1016/j.molcel.2009.12.034>
- Plant, E. P., Nguyen, P., Russ, J. R., Pittman, Y. R., Nguyen, T., Quesinberry, J. T., ... Dinman, J. D. (2007). Differentiating between near- and non-cognate codons in *Saccharomyces cerevisiae*. *PloS One*, 2(6), e517. <http://doi.org/10.1371/journal.pone.0000517>
- Polacek, N., & Mankin, A. S. (2005). The Ribosomal Peptidyl Transferase Center: Structure, Function, Evolution, Inhibition. *Critical Reviews in Biochemistry and Molecular Biology*, 40(5), 285–311. <http://doi.org/10.1080/10409230500326334>
- Powers, T., & Noller, H. F. (1990). Dominant lethal mutations in a conserved loop in 16S rRNA. *Proceedings of the National Academy of Sciences of the United States of America*, 87(3), 1042–6. <http://doi.org/10.1073/pnas.87.3.1042>
- Precup, J., & Parker, J. (1987). Missense misreading of asparagine codons as a function of codon identity and context. *The Journal of Biological Chemistry*, 262(23), 11351–5. Retrieved from <http://www.ncbi.nlm.nih.gov/pubmed/3112158>

- Prince, J. B., Taylor, B. H., Thurlow, D. L., Ofengand, J., & Zimmermann, R. a. (1982). Covalent crosslinking of tRNA^{1Val} to 16S RNA at the ribosomal P site: identification of crosslinked residues. *Proceedings of the National Academy of Sciences of the United States of America*, 79(September), 5450–5454. <http://doi.org/10.1073/pnas.79.18.5450>
- Rabl, J., Leibundgut, M., Ataide, S. F., Haag, A., & Ban, N. (2011). Crystal structure of the eukaryotic 40S ribosomal subunit in complex with initiation factor 1. *Science (New York, N.Y.)*, 331(6018), 730–6. <http://doi.org/10.1126/science.1198308>
- Rakwalska, M., & Rospert, S. (2004). The Ribosome-Bound Chaperones RAC and Ssb1 / 2p Are Required for Accurate Translation in *Saccharomyces cerevisiae* The Ribosome-Bound Chaperones RAC and Ssb1 / 2p Are Required for Accurate Translation in *Saccharomyces cerevisiae*, 24(20). <http://doi.org/10.1128/MCB.24.20.9186>
- Ramesh, M., Woolford, J. L., & Jr. (2016). Eukaryote-specific rRNA expansion segments function in ribosome biogenesis. *RNA (New York, N.Y.)*, 22(8), 1153–62. <http://doi.org/10.1261/rna.056705.116>
- Ramser, J., Winnepeninckx, B., Lenski, C., Errijgers, V., Platzer, M., Schwartz, C. E., ... Kooy, R. F. (2004). A splice site mutation in the methyltransferase gene FTSJ1 in Xp11.23 is associated with non-syndromic mental retardation in a large Belgian family (MRX9). *Journal of Medical Genetics*, 41(9), 679–83. <http://doi.org/10.1136/jmg.2004.019000>
- Ranjan, N., & Rodnina, M. V. (2016). tRNA wobble modifications and protein homeostasis. *Translation*, 4(1), e1143076. <http://doi.org/10.1080/21690731.2016.1143076>
- Rice, J. B., Libby, R. T., & Reeve, J. N. (1984). Mistranslation of the mRNA encoding bacteriophage T7 0.3 protein. *The Journal of Biological Chemistry*, 259(10), 6505–10. Retrieved from <http://www.ncbi.nlm.nih.gov/pubmed/6373759>
- Rodnina, M. V, Beringer, M., & Wintermeyer, W. (2007). How ribosomes make peptide bonds. *Trends in Biochemical Sciences*. <http://doi.org/10.1016/j.tibs.2006.11.007>
- Rodnina, M. V, Daviter, T., Gromadski, K., & Wintermeyer, W. (2002). Structural dynamics of ribosomal RNA during decoding on the ribosome. *Biochimie*, 84(8), 745–54. Retrieved from <http://www.ncbi.nlm.nih.gov/pubmed/12457562>
- Rodnina, M. V, Fricke, R., Kuhn, L., & Wintermeyer, W. (1995). Codon-dependent conformational change of elongation factor Tu preceding GTP hydrolysis on the ribosome. *The EMBO Journal*, 14(11), 2613–2619.
- Rodnina, M. V, Fricke, R., & Wintermeyer, W. (1994). Transient conformational states of aminoacyl-tRNA during ribosome binding catalyzed by elongation factor Tu. *Biochemistry*, 33(40), 12267–75. Retrieved from <http://www.ncbi.nlm.nih.gov/pubmed/7918447>
- Rodnina, M. V, Gromadski, K. B., Kothe, U., & Wieden, H.-J. (2005). Recognition and selection of tRNA in translation. *FEBS Letters*, 579(4), 938–42. <http://doi.org/10.1016/j.febslet.2004.11.048>

- Rodnina, M. V., & Wintermeyer, W. (2001). FIDELITY OF A MINOACYL -tRNA S ELECTION ON THE R IBOSOME : Kinetic and Structural Mechanisms.
- Rodnina, M. V., & Wintermeyer, W. (2001). Ribosome fidelity: tRNA discrimination, proofreading and induced fit. *Trends in Biochemical Sciences* , 26(2), 124–130. Retrieved from <http://www.ncbi.nlm.nih.gov/pubmed/11166571>
- Rodnina, M. V., & Wintermeyer, W. (2009). Recent mechanistic insights into eukaryotic ribosomes. *Current Opinion in Cell Biology*, 21(3), 435–43. <http://doi.org/10.1016/j.ceb.2009.01.023>
- Rodnina, M. V., & Wintermeyer, W. (2011). The ribosome as a molecular machine: the mechanism of tRNA–mRNA movement in translocation. *Biochemical Society Transactions*, 39(2). <http://doi.org/10.1042/BST0390658>
- Rogers, G. W., Lima, W. F., & Merrick, W. C. (2001). Further characterization of the helicase activity of eIF4A. Substrate specificity. *Journal of Biological Chemistry*, 276(16), 12598–12608. <http://doi.org/10.1074/jbc.M007560200>
- Rogers, G. W., Richter, N. J., Lima, W. F., & Merrick, W. C. (2001). Modulation of the Helicase Activity of eIF4A by eIF4B, eIF4H, and eIF4F. *Journal of Biological Chemistry*, 276(33), 30914–30922. <http://doi.org/10.1074/jbc.M100157200>
- Rosset, R., & Gorini, L. (1969). A ribosomal ambiguity mutation. *Journal of Molecular Biology*, 39(1), 95–112. [http://doi.org/10.1016/0022-2836\(69\)90336-2](http://doi.org/10.1016/0022-2836(69)90336-2)
- Rozov, A., Demeshkina, N., Khusainov, I., Westhof, E., Yusupov, M., & Yusupova, G. (2016). Novel base-pairing interactions at the tRNA wobble position crucial for accurate reading of the genetic code. *Nature Communications*, 7, 10457. <http://doi.org/10.1038/ncomms10457>
- Rozov, A., Demeshkina, N., Westhof, E., Yusupov, M., & Yusupova, G. (2015). Structural insights into the translational infidelity mechanism. *Nature Communications*, 6, 7251. <http://doi.org/10.1038/ncomms8251>
- Rozov, A., Demeshkina, N., Westhof, E., Yusupov, M., & Yusupova, G. (2016). New Structural Insights into Translational Miscoding. *Trends in Biochemical Sciences*, 41(9), 798–814. <http://doi.org/10.1016/j.tibs.2016.06.001>
- Russell, W. C., Graham, F. L., Smiley, J., & Nairn, R. (1977). Characteristics of a Human Cell Line Transformed by DNA from Human Adenovirus Type 5. *Journal of General Virology*, 36(1), 59–72. <http://doi.org/10.1099/0022-1317-36-1-59>
- Salas-Marco, J., & Bedwell, D. M. (2005). Discrimination between defects in elongation fidelity and termination efficiency provides mechanistic insights into translational readthrough. *Journal of Molecular Biology*, 348(4), 801–15. <http://doi.org/10.1016/j.jmb.2005.03.025>
- Scheidt, V., Jüdes, A., Bär, C., Klassen, R., & Schaffrath, R. (2014). Loss of wobble uridine modification in tRNA anticodons interferes with TOR pathway signaling. *Microbial Cell (Graz, Austria)*, 1(12), 416–424. <http://doi.org/10.15698/mic2014.12.179>

- Schluzen, F., Tocilj, A., Zarivach, R., Harms, J., Gluehmann, M., Janell, D., ... Yonath, A. (2000). Structure of Functionally Activated Small Ribosomal Subunit at 3.3 Å Resolution. *Cell*, 102(5), 615–623. [http://doi.org/10.1016/S0092-8674\(00\)00084-2](http://doi.org/10.1016/S0092-8674(00)00084-2)
- Schmeing, T. M., Huang, K. S., Kitchen, D. E., Strobel, S. A., & Steitz, T. A. (2005). Structural insights into the roles of water and the 2' hydroxyl of the P site tRNA in the peptidyl transferase reaction. *Molecular Cell*, 20(3), 437–448. <http://doi.org/10.1016/j.molcel.2005.09.006>
- Schmeing, T. M., Voorhees, R. M., Kelley, A. C., & Ramakrishnan, V. (2011). How mutations in tRNA distant from the anticodon affect the fidelity of decoding. *Nature Structural & Molecular Biology*, 18(4), 432–6. <http://doi.org/10.1038/nsmb.2003>
- Schmitt, E., Mechulam, Y., Fromant, M., Plateau, P., & Blanquet, S. (1997). Crystal structure at 1.2 Å resolution and active site mapping of Escherichia coli peptidyl-tRNA hydrolase. *EMBO Journal*, 16(15), 4760–4769. <http://doi.org/10.1093/emboj/16.15.4760>
- Schuette, J.-C., Murphy, F. V., Kelley, A. C., Weir, J. R., Giesebrecht, J., Connell, S. R., ... Spahn, C. M. T. (2009). GTPase activation of elongation factor EF-Tu by the ribosome during decoding. *The EMBO Journal*, 28(6), 755–65. <http://doi.org/10.1038/emboj.2009.26>
- Schuwirth, B. S., Borovinskaya, M. A., Hau, C. W., Zhang, W., Vila-Sanjurjo, A., Holton, J. M., & Cate, J. H. D. (2005). Structures of the bacterial ribosome at 3.5 Å resolution. *Science (New York, N.Y.)*, 310(5749), 827–34. <http://doi.org/10.1126/science.1117230>
- Selmer, M., Dunham, C. M., Murphy, F. V., Weixlbaumer, A., Petry, S., Kelley, A. C., ... Ramakrishnan, V. (2006). Structure of the 70S ribosome complexed with mRNA and tRNA. *Science (New York, N.Y.)*, 313(5795), 1935–42. <http://doi.org/10.1126/science.1131127>
- Senger, B., Auxilien, S., Englisch, U., Cramer, F., & Fasiolo, F. (1997). The modified wobble base inosine in yeast tRNA(Ile) is a positive determinant for aminoacylation by isoleucyl-tRNA synthetase. *Biochemistry*, 36(27), 8269–8275. <http://doi.org/10.1021/bi9702061>
- Shoemaker, C. J., & Green, R. (2011). Kinetic analysis reveals the ordered coupling of translation termination and ribosome recycling in yeast. *Proceedings of the National Academy of Sciences*, 108(51), E1392–E1398. <http://doi.org/10.1073/pnas.1113956108>
- Silva, R. M., Duarte, I. C. N., Paredes, J. A., Lima-Costa, T., Perrot, M., Boucherie, H., ... Santos, M. A. S. (2009). The yeast PNC1 longevity gene is up-regulated by mRNA mistranslation. *PLoS ONE*, 4(4). <http://doi.org/10.1371/journal.pone.0005212>
- Simonović, M., & Steitz, T. A. (2009). A structural view on the mechanism of the ribosome-catalyzed peptide bond formation. *Biochimica et Biophysica Acta - Gene Regulatory Mechanisms*. <http://doi.org/10.1016/j.bbagr.2009.06.006>
- Simpson, C. L., Lemmens, R., Miskiewicz, K., Broom, W. J., Hansen, V. K., van Vught, P. W. J., ... Al-Chalabi, A. (2009). Variants of the elongator protein 3 (ELP3) gene are associated with motor neuron degeneration. *Human Molecular Genetics*, 18(3), 472–481.

<http://doi.org/10.1093/hmg/ddn375>

- SINGH, A., URSIC, D., & DAVIES, J. (1979). Phenotypic suppression and misreading in *Saccharomyces cerevisiae*. *Nature*, 277(5692), 146–148. <http://doi.org/10.1038/277146a0>
- Slaugenhaupt, S. a, Blumenfeld, a, Gill, S. P., Leyne, M., Mull, J., Cuajungco, M. P., ... Gusella, J. F. (2001). Tissue-specific expression of a splicing mutation in the IKBKAP gene causes familial dysautonomia. *American Journal of Human Genetics*, 68(3), 598–605. <http://doi.org/10.1086/318810>
- Slaugenhaupt, S. a, & Gusella, J. F. (2002). Familial dysautonomia. *Current Opinion in Genetics & Development*, 12(3), 307–311. [http://doi.org/10.1016/S0959-437X\(02\)00303-9](http://doi.org/10.1016/S0959-437X(02)00303-9)
- Smith, C. J., Teh, H. S., Ley, A. N., & D'Obrenan, P. (1973). The nucleotide sequences and coding properties of the major and minor lysine transfer ribonucleic acids from the haploid yeast *Saccharomyces cerevisiae* S288C. *The Journal of Biological Chemistry*, 248(12), 4475–85. Retrieved from <http://www.ncbi.nlm.nih.gov/pubmed/4576137>
- Song, H., Mugnier, P., Das, A. K., Webb, H. M., Evans, D. R., Tuite, M. F., ... Barford, D. (2000). The crystal structure of human eukaryotic release factor eRF1--mechanism of stop codon recognition and peptidyl-tRNA hydrolysis. *Cell*, 100(3), 311–21. Retrieved from <http://www.ncbi.nlm.nih.gov/pubmed/10676813>
- Songe-Møller, L., van den Born, E., Leihne, V., Vågbø, C. B., Kristoffersen, T., Krokan, H. E., ... Klungland, A. (2010). Mammalian ALKBH8 possesses tRNA methyltransferase activity required for the biogenesis of multiple wobble uridine modifications implicated in translational decoding. *Molecular and Cellular Biology*, 30(7), 1814–27. <http://doi.org/10.1128/MCB.01602-09>
- Spahn, C. M. T. T., Beckmann, R., Eswar, N., Penczek, P. A., Sali, A., Blobel, G., & Frank, J. (2001). Structure of the 80S ribosome from *Saccharomyces cerevisiae* - tRNA-ribosome and subunit-subunit interactions. *Cell*, 107(3), 373–386. [http://doi.org/10.1016/S0092-8674\(01\)00539-6](http://doi.org/10.1016/S0092-8674(01)00539-6)
- Spiegel, P. C., Ermolenko, D. N., & Noller, H. F. (2007). Elongation factor G stabilizes the hybrid-state conformation of the 70S ribosome. *Rna*, 13(9), 1473–1482. <http://doi.org/10.1261/rna.601507>
- Spirin, A. S. (1968). How does the ribosome work? A hypothesis based on the two subunit construction of the ribosome. *Biosystems*, 2(3), 115–127. [http://doi.org/10.1016/0303-2647\(68\)90017-8](http://doi.org/10.1016/0303-2647(68)90017-8)
- Spirin, A. S. (2002). Ribosome as a molecular machine. In *FEBS Letters* (Vol. 514, pp. 2–10). [http://doi.org/10.1016/S0014-5793\(02\)02309-8](http://doi.org/10.1016/S0014-5793(02)02309-8)
- Spotts, C. R., & Stanier, R. Y. (1961). Mechanism of streptomycin action on bacteria: a unitary hypothesis. *Nature*, 192, 633–7. Retrieved from <http://www.ncbi.nlm.nih.gov/pubmed/13915908>

- Sprinzl, M., Horn, C., Brown, M., Loudovltch, A., & Steinberg, S. (1998). Compilation of tRNA sequences and sequences of tRNA genes. *Nucleic Acids Research*, 26(1), 148–153. <http://doi.org/10.1093/nar/26.1.148>
- Sprinzl, M., & Vassilenko, K. S. (2004). Compilation of tRNA sequences and sequences of tRNA genes. *Nucleic Acids Research*, 33(Database issue), D139–D140. <http://doi.org/10.1093/nar/gki012>
- Sramkoski, R. M., Pretlow, T. G., Giaconia, J. M., Pretlow, T. P., Schwartz, S., Sy, M.-S., ... Jacobberger, J. W. (1999). A new human prostate carcinoma cell line, 22Rv1. *In Vitro Cellular & Developmental Biology - Animal*, 35(7), 403–409. <http://doi.org/10.1007/s11626-999-0115-4>
- Stansfield, I., Jones, K. M., Herbert, P., Lewendon, a, Shaw, W. V., & Tuite, M. F. (1998). Missense translation errors in *Saccharomyces cerevisiae*. *Journal of Molecular Biology*, 282(1), 13–24. <http://doi.org/10.1006/jmbi.1998.1976>
- Stansfield, I., Jones, K. M., Ter-Avanesyan, M. D., & Tuite, M. F. (1995). The products of the SUP45 (eRF1) and SUP35 genes interact to mediate translation termination in *Saccharomyces cerevisiae*. *The EMBO Journal*, 14(17), 4365–4373. <http://doi.org/10.1016/j.biochi.2012.07.004>
- Stark, H., Rodnina, M. V., Wieden, H.-J., Zemlin, F., Wintermeyer, W., & van Heel, M. (2002). Ribosome interactions of aminoacyl-tRNA and elongation factor Tu in the codon-recognition complex. *Nature Structural Biology*, 9(11), 849–54. <http://doi.org/10.1038/nsb859>
- Steitz, T. a. (2008). A structural understanding of the dynamic ribosome machine. *Nature Reviews. Molecular Cell Biology*, 9(3), 242–253. <http://doi.org/10.1038/nrm2352>
- Strigini, P., & Brickman, E. (1973). Analysis of specific misreading in *Escherichia coli*. *Journal of Molecular Biology*, 75(4), 659–72. Retrieved from <http://www.ncbi.nlm.nih.gov/pubmed/4581523>
- Sun, J., Chen, M., Xu, J., & Luo, J. (2005). Relationships among stop codon usage bias, its context, isochores, and gene expression level in various eukaryotes. *Journal of Molecular Evolution*, 61(4), 437–444. <http://doi.org/10.1007/s00239-004-0277-3>
- Sundaram, M., Durant, P. C., & Davis, D. R. (2000). Hypermodified Nucleosides in the Anticodon of tRNA. *Biochemistry*, 12575–12584.
- Sundararajan, A., Michaud, W. A., Qian, Q., Stahl, G., & Farabaugh, P. J. (1999). Near-cognate peptidyl-tRNAs promote +1 programmed translational frameshifting in yeast. *Molecular Cell*, 4(6), 1005–15. Retrieved from <http://www.ncbi.nlm.nih.gov/pubmed/10635325>
- Sydow, J. F., & Cramer, P. (2009). RNA polymerase fidelity and transcriptional proofreading. *Current Opinion in Structural Biology*, 19(6), 732–739. <http://doi.org/10.1016/j.sbi.2009.10.009>

- T. Martin Schmeing, Rebecca M. Voorhees, Ann C. Kelley, Yong-Gui Gao, Frank V. Murphy IV, John R. Weir, V. R. (2009). The Crystal Structure of the Ribosome Bound to EF-Tu an Aminoacyl-tRNA. *Science*, 326, 688–694. <http://doi.org/10.1126/science.1178336>
- Takano, K., Nakagawa, E., Inoue, K., Kamada, F., Kure, S., Goto, Y. I., ... Wada, T. (2008). A loss-of-function mutation in the FTSJ1 gene causes nonsyndromic x-linked mental retardation in a Japanese family. *American Journal of Medical Genetics, Part B: Neuropsychiatric Genetics*, 147(4), 479–484. <http://doi.org/10.1002/ajmg.b.30638>
- Taylor, D. J., Nilsson, J., Merrill, a R., Andersen, G. R., Nissen, P., & Frank, J. (2007). Structures of modified eEF2·80S ribosome complexes reveal the role of GTP hydrolysis in translocation. *The EMBO Journal*, 26(9), 2421–2431. <http://doi.org/10.1038/sj.emboj.7601677>
- Ter-Avanesyan, M. D., Kushnirov, V. V., Dagkesamanskaya, A. R., Didichenko, S. A., Chernoff, Y. O., Inge-Vechtomov, S. G., & Smirnov, V. N. (1993). Deletion analysis of the SUP35 gene of the yeast *Saccharomyces cerevisiae* reveals two non-overlapping functional regions in the encoded protein. *Molecular Microbiology*, 7(5), 683–692. <http://doi.org/10.1111/j.1365-2958.1993.tb01159.x>
- Testa, S. M., Disney, M. D., Turner, D. H., & Kierzek, R. (1999). Thermodynamics of RNA-RNA duplexes with 2- or 4-thiouridines: Implications for antisense design and targeting a group I intron. *Biochemistry*, 38(50), 16655–16662. <http://doi.org/10.1021/bi991187d>
- Thompson, R. C., & Stone, P. J. (1977). Proofreading of the codon-anticodon interaction on ribosomes. *Proceedings of the National Academy of Sciences of the United States of America*, 74(1), 198–202. Retrieved from <http://www.pubmedcentral.nih.gov/articlerender.fcgi?artid=393225&tool=pmcentrez&rendertype=abstract>
- Tibshirani, R., Friedman, J. H., Mayeda, T. K., Lyons, T. W., Devlin, S. J., Rajagopalan, B., ... Verhoeven, M. (2011). The Structure of the Eukaryotic Ribosome at 3.0 Å Resolution. *Science*, (December), 1524–1529. <http://doi.org/10.1126/science.1212642>
- Tobe, R., Naranjo-Suarez, S., Everley, R. A., Carlson, B. A., Turanov, A. A., Tsuji, P. A., ... Hatfield, D. L. (2013). High error rates in selenocysteine insertion in mammalian cells treated with the antibiotic doxycycline, chloramphenicol, or geneticin. *The Journal of Biological Chemistry*, 288(21), 14709–15. <http://doi.org/10.1074/jbc.M112.446666>
- Toth, M. J., Murgola, E. J., & Schimmel, P. (1988). Evidence for a unique first position codon-anticodon mismatch in vivo. *Journal of Molecular Biology*, 201(2), 451–454. Retrieved from <http://www.ncbi.nlm.nih.gov/pubmed/3262166>
- Toth, M., Murgola, E., & Schimmel, P. (1988). Evidence for a unique first position codon-anticodon mismatch in vivo. *Journal of Molecular Biology*. Retrieved from <http://www.sciencedirect.com/science/article/pii/0022283688901520>
- Towns, W. L., & Begley, T. J. (2012). Transfer RNA methyltransferases and their corresponding modifications in budding yeast and humans: activities, predications, and potential roles in

- human health. *DNA and Cell Biology*, 31(4), 434–54. <http://doi.org/10.1089/dna.2011.1437>
- Triana-Alonso, F. J., Chakraborty, K., & Nierhaus, K. H. (1995). The elongation factor 3 unique in higher fungi and essential for protein biosynthesis is an E site factor. *Journal of Biological Chemistry*, 270(35), 20473–20478. <http://doi.org/10.1074/jbc.270.35.20473>
- Tsai, F., & Curran, J. F. (1998). tRNA(2Gln) mutants that translate the CGA arginine codon as glutamine in Escherichia coli. *RNA (New York, N.Y.)*, 4(12), 1514–22. Retrieved from <http://www.pubmedcentral.nih.gov/articlerender.fcgi?artid=1369722&tool=pmcentrez&rendertype=abstract>
- Tükenmez, H., Xu, H., Esberg, A., & Byström, A. S. (2015). The role of wobble uridine modifications in +1 translational frameshifting in eukaryotes. *Nucleic Acids Research*, 43(19), 9489–9499. <http://doi.org/10.1093/nar/gkv832>
- Uhlenbeck, O. C., Baller, J., & Doty, P. (1970). Complementary oligonucleotide binding to the anticodon loop of fMet-transfer RNA. *Nature*, 225(5232), 508–10. <http://doi.org/10.1038/225508a0>
- Unbehaun, A., Borukhov, S. I., Hellen, C. U. T., & Pestova, T. V. (2004). Release of initiation factors from 48S complexes during ribosomal subunit joining and the link between establishment of codon-anticodon base-pairing and hydrolysis of eIF2-bound GTP. *Genes and Development*, 18(24), 3078–3093. <http://doi.org/10.1101/gad.1255704>
- Urbonavičius, J., Qian, Q., Durand, J. M. B., Hagervall, T. G., & Björk, G. R. (2001). Improvement of reading frame maintenance is a common function for several tRNA modifications. *EMBO Journal*, 20(17), 4863–4873. <http://doi.org/10.1093/emboj/20.17.4863>
- Valle, M., Zavialov, A., Sengupta, J., Rawat, U., Ehrenberg, M., & Frank, J. (2003). Locking and unlocking of ribosomal motions. *Cell*, 114(1), 123–34. [http://doi.org/10.1016/S0092-8674\(03\)00476-8](http://doi.org/10.1016/S0092-8674(03)00476-8)
- Vendeix, F. A. P., Murphy, F. V., Cantara, W. A., Leszczyńska, G., Gustilo, E. M., Sproat, B., ... Agris, P. F. (2012). Human tRNA(Lys3)(UUU) is pre-structured by natural modifications for cognate and wobble codon binding through keto-enol tautomerism. *Journal of Molecular Biology*, 416(4), 467–85. <http://doi.org/10.1016/j.jmb.2011.12.048>
- Vester, B., & Garrett, R. A. (1988). The importance of highly conserved nucleotides in the binding region of chloramphenicol at the peptidyl transfer centre of Escherichia coli 23S ribosomal RNA. *The EMBO Journal*, 7(11), 3577–87. Retrieved from <http://www.ncbi.nlm.nih.gov/pubmed/3061800>
- Villa, E., Sengupta, J., Trabuco, L. G., LeBarron, J., Baxter, W. T., Shaikh, T. R., ... Frank, J. (2009). Ribosome-induced changes in elongation factor Tu conformation control GTP hydrolysis. *Proc Natl Acad Sci U S A*, 106(4), 1063–1068. <http://doi.org/10.1073/pnas.0811370106>
- Vincent, A., & Liebman, S. W. (1992). The yeast omnipotent suppressor SUP46 encodes a

- ribosomal protein which is a functional and structural homolog of the Escherichia coli S4 ram protein. *Genetics*, 132(2), 375–386.
- Wakem, L. P., & Sherman, F. (1990). Isolation and characterization of omnipotent suppressors in the yeast *Saccharomyces cerevisiae*. *Genetics*, 124(3), 515–522.
- Watson, J. D. (1964). The synthesis of proteins upon ribosomes. *Bull Soc Chim Biol (Paris)*, 46(June), 1399–1425. Retrieved from <http://www.ncbi.nlm.nih.gov/pubmed/14270536>
- Weinger, J. S., Parnell, K. M., Dorner, S., Green, R., & Strobel, S. a. (2004). Substrate-assisted catalysis of peptide bond formation by the ribosome. *Nature Structural & Molecular Biology*, 11(11), 1101–6. <http://doi.org/10.1038/nsmb841>
- Weisser, M., Voigts-Hoffmann, F., Rabl, J., Leibundgut, M., & Ban, N. (2013). The crystal structure of the eukaryotic 40S ribosomal subunit in complex with eIF1 and eIF1A. *Nature Structural & Molecular Biology*, 20(8), 1015–7. <http://doi.org/10.1038/nsmb.2622>
- Weixlbaumer, A., Jin, H., Neubauer, C., Voorhees, R. M., Petry, S., Kelley, A. C., & Ramakrishnan, V. (2008). Insights into Translational Termination from the Structure of RF2 Bound to the Ribosome. *Science*, 322(5903), 953–956. <http://doi.org/10.1126/science.1164840>
- Westhof, E., Yusupov, M., & Yusupova, G. (2014). Recognition of Watson-Crick base pairs: constraints and limits due to geometric selection and tautomerism. *F1000Prime Reports*, 6, 19. <http://doi.org/10.12703/P6-19>
- Williams, A. M., & Martinis, S. A. (2006). Mutational unmasking of a tRNA-dependent pathway for preventing genetic code ambiguity. *Proceedings of the National Academy of Sciences of the United States of America*, 103(10), 3586–91. <http://doi.org/10.1073/pnas.0507362103>
- Wilson, D. N. (2013). Ribosome-targeting antibiotics and mechanisms of bacterial resistance. *Nature Reviews Microbiology*, 12(1), 35–48. <http://doi.org/10.1038/nrmicro3155>
- Wilson, D. N., & Cate, J. H. D. (2012). The structure and function of the eukaryotic ribosome. *Cold Spring Harbor Perspectives in Biology*, 4(5), 5. <http://doi.org/10.1101/cshperspect.a011536>
- Wilson, D. N., & Nierhaus, K. H. (2006). The E-site story: the importance of maintaining two tRNAs on the ribosome during protein synthesis. *Cellular and Molecular Life Sciences : CMLS*, 63(23), 2725–37. <http://doi.org/10.1007/s00018-006-6125-4>
- Xu, J., McRae, M. A. ., Harron, S., Rob, B., & Huber, R. E. (2004). A study of the relationships of interactions between Asp-201, Na⁺ or K⁺, and galactosyl C6 hydroxyl and their effects on binding and reactivity of β -galactosidase. *Biochemistry and Cell Biology*, 82(2), 275–284. <http://doi.org/10.1139/o04-004>
- Yarian, C., Marszalek, M., Sochacka, E., Malkiewicz, A., Guenther, R., Miskiewicz, A., & Agris, P. F. (2000). Modified Nucleoside Dependent Watson–Crick and Wobble Codon Binding by

- tRNA Lys UUU Species †. *Biochemistry*, 39(44), 13390–13395. <http://doi.org/10.1021/bi001302g>
- Yarian, C., Townsend, H., Czestkowski, W., Sochacka, E., Malkiewicz, A. J., Guenther, R., ... Agris, P. F. (2002). Accurate translation of the genetic code depends on tRNA modified nucleosides. *Journal of Biological Chemistry*, 277(19), 16391–16395. <http://doi.org/10.1074/jbc.M200253200>
- Yokoyama, S., Watanabe, T., Muraot, K., Ishikurat, H., Yamaizumit, Z., Nishimurat, S., & Miyazawa, T. (1985). Molecular mechanism of codon recognition by tRNA species with modified uridine in the first position of the anticodon (post-transcriptional modification/base pair/conformation/NMR). *Biochemistry*, 82, 4905–4909. Retrieved from <https://www.ncbi.nlm.nih.gov/pmc/articles/PMC390466/pdf/pnas00355-0050.pdf>
- Yoshizawa, S. (1999). Recognition of the Codon-Anticodon Helix by Ribosomal RNA. *Science*, 285(5434), 1722–1725. <http://doi.org/10.1126/science.285.5434.1722>
- Young, D. J., Guydosh, N. R., Zhang, F., Hinnebusch, A. G., & Green, R. (2015). Rli1/ABCE1 Recycles Terminating Ribosomes and Controls Translation Reinitiation in 3'UTRs In Vivo. *Cell*, 162(4), 872–884. <http://doi.org/10.1016/j.cell.2015.07.041>
- Youngman, E. M., Brunelle, J. L., Kochaniak, A. B., & Green, R. (2004). The active site of the ribosome is composed of two layers of conserved nucleotides with distinct roles in peptide bond formation and peptide release. *Cell*, 117(5), 589–599. [http://doi.org/10.1016/S0092-8674\(04\)00411-8](http://doi.org/10.1016/S0092-8674(04)00411-8)
- Yuan, J., Martinez-Bilbaot, M., & Hubert, R. E. (1994). Substitutions for Glu-537 of -galactosidase from Escherichia coli cause large decreases in catalytic activity. *Biochem. J*, 299, 527–531. Retrieved from <https://www.ncbi.nlm.nih.gov/pmc/articles/PMC1138303/pdf/biochemj00089-0200.pdf>
- Yusupov, M. M., Yusupova, G. Z., Baucom, A., Lieberman, K., Earnest, T. N., Cate, J. H., & Noller, H. F. (2001). Crystal Structure of the Ribosome at 5.5 Å Resolution. *Science*, 292(5518), 883–896. <http://doi.org/10.1126/science.1060089>
- Yusupova, G., & Yusupov, M. (2014). High-Resolution Structure of the Eukaryotic 80S Ribosome. *Annual Review of Biochemistry*, 83(1), 467–486. <http://doi.org/10.1146/annurev-biochem-060713-035445>
- Yusupova, G. Z., Yusupov, M. M., Cate, J. H. D., & Noller, H. F. (2001). The path of messenger RNA through the ribosome. *Cell*, 106(2), 233–241. [http://doi.org/10.1016/S0092-8674\(01\)00435-4](http://doi.org/10.1016/S0092-8674(01)00435-4)
- Zaher, H. S., & Green, R. (2009). Quality control by the ribosome following peptide bond formation. *Nature*, 457(7226), 161–6. <http://doi.org/10.1038/nature07582>
- Zhang, Z., Shah, B., & Bondarenko, P. V. (2013). G/U and certain wobble position mismatches as possible main causes of amino acid misincorporations. *Biochemistry*, 52(45), 8165–8176.

<http://doi.org/10.1021/bi401002c>

Zhouravleva, G., Frolova, L., Le Goff, X., Le Guellec, R., Inge-Vechtomov, S., Kisselev, L., & Philippe, M. (1995). Termination of translation in eukaryotes is governed by two interacting polypeptide chain release factors, eRF1 and eRF3. *The EMBO Journal*, *14*(16), 4065–72. [http://doi.org/10.1016/S1097-2765\(02\)00691-3](http://doi.org/10.1016/S1097-2765(02)00691-3)

